PERFORMANCE ANALYSIS OF COOPERATIVE SPECTRUM SENSING NETWORK OVER VARIOUS FADING CHANNELS

Submitted in partial fulfilment of the requirements

for the award of the degree of

Doctor of Philosophy

by

M. Ranjeeth

(Roll No. 701424)

Supervisor

Dr. S. Anuradha

Associate Professor, Dept. of ECE

Department of Electronics & Communication Engineering

NATIONAL INSTITUTE OF TECHNOLOGY WARANGAL – 506004, T.S, INDIA

July-2018

APPROVAL SHEET

This thesis entitled "**Performance Analysis of Cooperative Spectrum Sensing Network over Various Fading Channels**" by Mr. **M. Ranjeeth** is approved for the degree of **Doctor of Philosophy**.

Examiners

_____

_____

Supervisor

_____

Dr. S. Anuradha

Associate Professor, Electronics and Communication Engineering Department,

NIT WARANGAL

Chairman

_____

Prof. N. Bheema Rao

Head, Electronics and Communication Engineering Department,

NIT WARANGAL

Date:

Place:

DECLARATION

I hereby declare that the matter embodied in this thesis entitled "**Performance Analysis of Cooperative Spectrum Sensing Network over Various Fading Channels**" is based entirely on the results of the investigations and research work carried out by me under the supervision of **Dr. S. Anuradha**, Department of Electronics and Communication Engineering, National Institute of Technology Warangal. I declare that this work is original and has not been submitted in part or full, for any degree or diploma to this or any other University.

I declare that this written submission represents my ideas in my own words and where others ideas or words have not been included. I have adequately cited and referenced the original sources. I also declare that I have adhered to all principles of academic honesty and integrity and have not misrepresented or fabricated or falsified any idea/date/fact/source in my submission. I understand that any violation of the above will be cause for disciplinary action by the institute and can also evoke penal action from the sources which have thus not been properly cited or from whom proper permission has not been taken when needed.

M.Ranjeeth

Roll No: 701424

Date:

Place: Warangal

Department of Electronics and Communication Engineering
National Institute of Technology
Warangal – 506 004, Telangana, India

CERTIFICATE

This is to certify that the dissertation work entitled **"Performance Analysis of Cooperative Spectrum Sensing Network over Various Fading Channels"**, which is being submitted by Mr. M. Ranjeeth (Roll No.701424), is a bonafide work submitted to National Institute of Technology Warangal in partial fulfilment of the requirement for the award of the degree of *Doctor of Philosophy in Electronics and Communication Engineering.*

To the best of our knowledge, the work incorporated in this thesis has not been submitted elsewhere for the award of any degree.

Dr. S. Anuradha
Supervisor
Department of ECE
National Institute of Technology
Warangal – 506004

Dedicated to My Family,

For their unconditional Love and Support

Contents

ACKNOWLEDGEMENTS

I am grateful to many people who made this work possible and helped me during my Ph.D. studies. I am greatly indebted to my research supervisor Dr. S. Anuradha for giving me excellent support during my research activity at NIT Warangal. She encouraged me in choosing my research topic, her vision in my research area leads to successful investigations. I am very much thankful for giving research freedom and guidance, support in non-academic matters and for the humanity shown to me. With her inimitable qualities as a good teacher, she chiseled my path towards perfection. Ever since I met her, she has been an eternal source of motivation, inspiration, encouragement and enlightenment. She is responsible for making the period of my research work as an educative and enjoyable learning experience. The thesis would not have seen the light of the day without her insistent support and cooperation.

I am also grateful to Prof. N. Bheema Rao, Head of the Department, Dept. of Electronics and Communication Engineering, for his valuable suggestions and support that he shared during my research tenure.

I take this privilege to thank all my Doctoral Scrutiny Committee members, Prof. M. Sydulu, Department of Electrical Engineering, Prof. L. Anjaneyulu, Professor, Department of Electronics and Communication Engineering, Dr. D.Vakula, Associate Professor, Department of Electronics and Communication Engineering for their detailed review, constructive suggestions and excellent advice during the progress of this research work.

I am grateful to the former Head of the ECE department Prof. T. Kishore Kumar for his continuous support and encouragement. I would also appreciate the encouragement from teaching, non-teaching members and fraternity of Dept. of E.C.E. of N.I.T. Warangal. They have always been encouraging and supportive.

I take this opportunity to convey my regards to my closest friends for being always next to me. Thanks to B. Shravan Kumar, Sudha Elison, D. Pavan, D. Santhosh, D. Kiran, K. Shriram Tej, and V. Sandeep Kumar Department of Electronics and Communication Engineering for their motivation and support throughout my work.

I acknowledge my gratitude to all my teachers and colleagues at various places for supporting and cooperating me to complete this work.

I would like to thank my family members (my father Mr. M. Satyanarayana, mother Mrs. M. Chandrakala and my sister's families) for giving me mental support and inspiration. They have motivated and helped me to complete my thesis work successfully.

Finally, I thank God, for filling me every day with new hopes, strength, purpose and faith.

M. Ranjeeth

ABSTRACT

The demand for radio spectrum has dramatically increased over the past decade due to the proliferation of wireless services and applications. According to current static spectrum allocation policy, almost all frequency bands of radio spectrum has allocated and that there is a shortage of spectrum for new wireless services. On the other hand, actual measurements of radio spectrum usage have shown that most of the licensed spectrum is largely underutilized. Cognitive radio (CR) technology is considered as a promising technology to increase the efficiency of spectrum usage by allowing the secondary (unlicensed) users to opportunistically access the allocated spectrum of primary (licensed) users. To enable the secondary users (SUs) and to utilize the underutilized spectrum, they need to make the necessary observations about their surrounding radio environment. Therefore, spectrum sensing (SS) is required by the SUs to learn about the activities of primary users (PUs). However, the performance of spectrum sensing is limited due to multipath fading and shadowing effects present in the nature which are the fundamental characteristics of wireless channels. To overcome these challenges, cooperation among SUs is required to perform the spectrum sensing which is known as cooperative spectrum sensing (CSS) technique. The aim of this thesis is to increase the detection probability value and efficient utilization of radio spectrum using different techniques in cooperative spectrum sensing network when it is affected by various fading environments.

The influence of fading effect limits the detection probability of PU. So, soft data fusion rules called diversity techniques are used to improve the detection performance when CSS network is affected by various fading effects. Diversity techniques improve the received signal SNR and uses the multiple antennas to receive the signal strength. Initially, average detection probability values are calculated using different diversity techniques at fusion center (FC) when CSS network is affected by various fading environment to know which diversity technique gives higher detection probability. The detection probability values are calculated using various diversity techniques such as selection combining (SC), square law combining (SLC), square law selection (SLS), maximal ratio combining (MRC), and equal gain combining (EGC) over different fading environments like Rayleigh, Rician, Nakagami-*m*, Weibull, and Hoyt fading effects. The performance is evaluated using the conventional energy detector (CED) and single antenna at each CR in CSS network.

Next, due to the fading effect in the environment, some of the CR users are deeply affected, and sensing information associated with these CRs are not transferred to the FC accurately. So, it is better to eliminate these CR users; this can be done with the help of censoring schemes (Rank based and Threshold based censoring schemes). Two censoring schemes are used individually in reporting channel of CSS network when it is affected by Rician, Hoyt, and Weibull fading environments. The novel expressions for estimation error, its mean, and variance expressions are derived under various fading effects. The missed detection probability and total error values are calculated in various fading environments using the censoring schemes in CSS network.

Further, the performance is evaluated with proposed CSS network which is equipped with multiple antennas and an improved energy detector (IED) scheme at each CR over various fading channels. Selection combining scheme is also used at each CR to receive the binary decisions about the PU from an IED technique using multiple antennas and selects the better detection value of PU. The sensing information about the PU is passed to FC through the reporting channel (R-channel). Final decision is made at FC using different fusion rules such as *OR-Rule*, *AND-Rule*. The novel expressions of missed detection probability using multiple antennas and an IED scheme at each CR for different fading channels are derived. The optimized performance of proposed CSS network is achieved by optimizing its network parameters such as a number of CR users (N), the threshold value (λ), and arbitrary power of received signal (p). The novel optimized expressions of CSS network parameters such as number CR users (N_{opt}), threshold value (λ_{opt}), and arbitrary power of received signal (p_{opt}) are also derived for various fading channels using single and multiple antennas at each CR.

Finally, average channel throughput (C_{avg}) and network utility network utility function (NUF) performances are evaluated using the proposed CSS network over Rayleigh and Weibull fading channels. The performance is evaluated using the different fusion rules such as $k=1+n$ and $k=N-n$ rules at FC. An optimal number CRs are calculated to maximize the average channel throughput value for different fusion rules. C_{avg} and NUF performances are improved by using multiple antennas and an IED scheme at each CR in the proposed CSS network.

List of Figures

List of Tables

Nomenclature

AWGN	Additive White Gaussian Noise
BPF	Band Pass Filter
BPSK	Binary Phase Shift Keying
CDF	Cumulative Distributive Function
CED	Conventional Energy Detector
CFD	Cyclostationary Feature Detection
CR	Cognitive Radio
CROC	Complementary Receiver Operating Characteristics
CSI	Channel State Information
CSS	Cooperative Spectrum Sensing
DSA	Dynamic Spectrum Access
EGC	Equal Gain Combining
FC	Fusion Center
FCC	Federal Communications Commission
FSK	Frequency Shift Keying
IBD	Interference-Based Detection
IED	Improved Energy Detector
IEEE	Institute of Electrical and Electronics Engineering
IFFT	Inverse Fast Fourier Transform
I.I.D	Independent and Identical Distributed
LoS	Line of Sight
MAC	Medium Access Control
MFD	Matched Filter Detection
MMSE	Minimum Mean Square Estimation
MRC	Maximal Ratio Combining

NLOS	Non-Line of Sight
NUF	Network Utility Function
PDF	Probability Density Function
PU	Primary User
QAM	Quadrature Amplitude Modulation
R-Channel	Reporting Channel
R-links	Radio links
S-Channel	Sensing Channel
SC	Selection Combining
SDR	Software Defined Radio
SLC	Square Law Combining
SLS	Square Law Selection
SS	Spectrum Sensing
SU	Secondary User
TV Band	Television Band
WRAN	Wireless Region Area Network

Notations

${}_1F_1(\,)$	Confluent Hypergeometric Function
${}_2F_1(\,)$	Gaussian Hypergeometric Function
$G_{a,b}^{m,n}(\,)$	Meijer's G Function
$I_n(\,)$	*n*-th order modified first kind Bessel's Function
$I_0(\,)$	Zeroth order modified first kind Bessel's Function
$L_n(\,)$	Laguerre polynomial of degree-*n*
Q_u	Marccum-Q Function
$\gamma(\,,\,)$	Lower Incomplete Gamma Function
$\Gamma(\,,\,)$	Upper Incomplete Gamma Function
$\Gamma(\,)$	Complete Gamma Function

Chapter-1

Introduction

1.1. Introduction

Radio spectrum is a very precious resource that available in the nature. As an important resource, radio spectrum has to be carefully managed to mitigate the interference, and efficiently utilized for the proper application. According to federal communications commission (FCC) spectrum policy task force statistics, only 15% to 85% of total allocated radio spectrum is properly utilized, and the remaining part of the radio spectrum is underutilized [1]. So, new technologies have to be introduced for efficient utilization of radio spectrum and to meet the present requirements.

Dynamic spectrum access (DSA) policy is considered as a key technology for efficient utilization of radio spectrum [2-4]. According to the DSA model, some parts of the radio spectrum are assigned to one or more licensed users called primary users (PUs), these PUs have a license to access the radio spectrum. Whenever the PUs become inactive, secondary users (SUs) called cognitive radio (CR) users can access the radio spectrum. By doing this, the radio spectrum can be reused for other applications. Cognitive radio technology is considered as a promising technology for efficient utilization of radio spectrum and it is a key technology to enable of DSA policy. The important features of CR technology are radio environment awareness and spectrum intelligence. Spectrum intelligence can be achieved by adopting transmission parameters. An ultimate goal of cognitive radio technology is to improve the detection probability of primary user [5, 6].

The concept of spectrum sensing (SS) is a useful task to monitor the radio spectrum continuously [7]. In SS technique, a single CR is present and it continuously observes the activity of radio spectrum. There are various detection techniques are addressed in the literature

to identify vacant bands present in the radio spectrum such as conventional energy detector (CED), matched filter detector (MFD), and cyclostationary feature detection (CFD) techniques. Among all detection techniques, CED scheme is most commonly used detection technique because of less complexity and non-coherent in nature. It measures the received signal strength with a non-linear device called squaring device. Whereas MFD technique is coherent in nature so it requires synchronization between transmitter and receiver to detect the vacant bands of radio spectrum. Cyclostationary detection technique utilizes the cyclic (periodic) properties of the signal in the frequency domain which are robust to the noise, with this complexity of the network is increases [8-12].

The detection performance using SS technique is limited because of shadowing, fading effects in the nature, time-varying nature of the channel, and also due to a single CR in the network. So, new techniques have to be introduced to improve the detection performance. The detection performance can be improved by introducing the concept of cooperative spectrum sensing (CSS) network. In CSS network, multiple CRs are present and they exchange and share the information among them so that detection performance can be improved. The CSS network performs better even in the presence of shadowing and fading effects because of cooperation among multiple CRs. The CSS network also eliminates the hidden terminal problem [13].

The CSS network consists of multiple CRs, a primary user (PU), and a fusion center (FC). The channel present between CRs and PU is called as sensing channel and the channel present between CRs and FC is called as reporting channel. In CSS network, the final decision about PU can be made at FC using hard decision rules and soft data fusion rules individually. The channels present in the CSS network are affected by different fading environments [14-16].

The detection performance can be further improved by using an improved energy detection (IED) scheme. An IED scheme overcomes the drawbacks present in the conventional energy detection technique. Using an IED scheme and multiple antennas at each CR in the CSS network will further improve the detection performance [17-19].

Finally, the key features of the implementation of CSS network are to improve the detection performance of primary user and efficient utilization of radio spectrum in the presence of various fading effects.

1.2. Motivation

The concept of cooperative spectrum sensing has been introduced to improve the detection probability even in the presence of shadowing, multipath fading effects, and it also eliminates the hidden terminal problem. This has motivated us to evaluate the detection performance of primary user using CSS network over various fading channels.

As mentioned above, the detection performance can be reduced due to the influence of fading effect. So, soft data fusion rules called diversity techniques are used to improve the detection performance when CSS network is affected by various fading effects [20-22]. Diversity techniques improve the received signal SNR and use the multiple antennas to increase the received signal strength. This has motivated us to evaluate the detection performance of PU using various diversity techniques at FC when CSS network is affected by different fading environments.

Next, due to the fading effect in the environment, some of the CR users are deeply affected, and the information associated with these CRs are not transferred to the FC accurately. Hence, these radio links are to be eliminated to reduce the complexity of the system and to improve the detection probability. This can be done using censoring schemes in reporting channel of CSS network. This has motivated us to evaluate the detection performance using the censoring schemes (Rank based and Threshold based censoring schemes) in the reporting channel of CSS network when it is affected by various fading environments [23-25].

The detection performance of PU can be further improved by considering multiple antennas and an IED scheme as detection technique at each CR in CSS network. In certain cases, it is required to optimize the performance of CSS network by optimizing its network parameters to achieve better performance with a minimum number of components and to reduce the system complexity. This has motivated us to evaluate the optimized performance of the proposed CSS network by optimizing the CSS network parameters using the multiple antennas and an IED scheme at each CR in CSS network over various fading channels [26-29].

Sometimes, PUs may not be identified accurately due to the fading effect in sensing and reporting channels which can cause severe interference problem of SUs with PUs. This issue can be resolved and PUs are exactly identified if the sensing time of each secondary user is increased, but this will reduce the throughput value of the network. Hence, average channel throughput value will be increased by performing sensing and transmission simultaneously

[30]. This has inspired us to evaluate the average channel throughput performance using CSS network over various fading channels.

From the above discussion, it can be concluded that the detection performance using spectrum sensing network can be improved with multiple CRs. As the number of CRs increases in the network, the resources used in the CSS network become more and more, which may cause a delay in deciding the PU activity and inefficient utilization of radio spectrum, this issue can be balanced by network utility function (NUF) [31]. The network utility function is used to improve the spectrum utilization. This has motivated us to evaluate the performance of NUF using CSS network over various fading channels.

1.3. Research Objectives

The research objectives of our proposed work are to improve the detection performance of primary user (PU), an efficient utilization of radio spectrum with the help cooperative spectrum sensing (CSS) network when it is affected by various fading environments. An influence of fading effect limits the detection performance using the spectrum sensing network. Hence, the concept of CSS network has been introduced to improve the detection probability of PU.

1. Initially, the influence of fading effect limits the detection performance using the spectrum sensing network. Hence, the concept of CSS network has been introduced to improve the detection probability of PU. The detection performance is evaluated using soft data techniques (selection combining (SC), square law combining (SLC), square law selection (SLS), maximal ratio combining (MRC), and equal gain combining (EGC)) at FC over various fading channels (Rayleigh, Rician, Nakagami-*m*, Weibull, and Hoyt fading channel) in CSS network. The detection performance is analyzed using the CED scheme and a single antenna at each CR in CSS network.

2. Rank based censoring scheme and Threshold based censoring scheme are used individually to eliminate the heavily faded radio links in the reporting channel of CSS network. The CSS network consists of a single antenna and CED scheme as detection technique at each CR in CSS network. The majority logic and MRC rules are applied individually at FC to decide the PU activity. The performance comparison between perfect and imperfect channel estimation also described. The performance is evaluated when CSS network is affected by various fading effects. For both the above objectives,

CSS network consists of a single antenna and CED scheme as detection technique at each CR.

Later on, we came to know from the available literature is that the detection probability value can be further improved if an IED scheme and multiple antennas at each CR in the CSS network are used instead of CED scheme and a single antenna.

3. In the next two objectives, we have proposed the CSS network, it consists of multiple antennas at each CR, selection combining scheme, and an IED scheme as detection technique at each CR. The optimized performance of the proposed CSS network is achieved by optimizing the CSS network parameters such as a number of CR users (N), the threshold value (λ), and arbitrary power of received signal (p). The optimized CSS network performance is analyzed over various fading channels. The novel analytical expressions of missed detection probability for different fading channels are derived. The novel analytical optimized expressions for number of CR users (N_{opt}), threshold value (λ_{opt}), and an arbitrary power of received signal (p_{opt}) are derived in various fading channels using single and multiple antennas at each CR.

4. An average channel throughput and network utility function performances are evaluated using multiple antennas at each CR with an IED scheme in the proposed CSS network over Rayleigh and Weibull fading channels.

Finally, our main aim of objectives are to significant improvement in the detection probability value and an efficient utilization radio spectrum using the multiple antennas at each CR, selection combining scheme, and an IED scheme as detection technique at each CR in the proposed CSS network.

1.4. Thesis Contribution

The main aim of this work is to improve the detection performance of the primary user, efficient utilization of radio spectrum, and to improve the spectral efficiency using CSS network. This thesis focusses on the performance evaluation of CSS network when various fading environments are affect the radio spectrum.

Initially, to improve the detection probability of PU and to mitigate the fading effects, diversity techniques are used in CSS network when it is influenced by various fading environments. Next, due to the fading effect, some of the CRs are heavily faded, and the

information received from these CRs at FC is erroneous. So, heavily faded links are eliminated by using the censoring schemes with which complexity of the network reduces.

The above mentioned two techniques (diversity techniques and censoring schemes) are used in traditional CSS network has a single antenna at each CR and CED scheme as a detection technique. The performance is evaluated when CSS network is affected by various fading channels.

Later, we proposed a CSS network which is equipped with multiple antennas, selection combining technique, and an IED scheme at each CR. Using the proposed CSS network, the detection performance is improved compared to traditional CED technique. The optimized performance of proposed CSS network is achieved by optimizing its network parameters with which total error rate is minimized and the network complexity also reduced.

The novel expressions of missed detection probability for various fading channels are derived using an IED scheme and multiple antennas at each CR in the proposed CSS network. Finally, an average channel throughput and network utility function analysis are evaluated using multiple antennas at each CR with an IED scheme in the proposed CSS network.

The main objectives of this work are to improve the detection performance and an efficient utilization radio spectrum using the proposed CSS network, highlighted the strength and weakness points. All the performances are described with the help of MATLAB simulations which are drawn with the strong support of analytical expressions. All the simulation results are perfectly in accordance with theoretical results.

1.5. Thesis Organization

The thesis is organized into seven chapters. This section gives the summary of all chapters.

Chapter 1: Gives the introduction, background, and reasons for choosing the problem.

Chapter 2: The second chapter begins with the importance of radio spectrum and an overview of the traditional SS technique. The basic principle of SS technique and various detection scheme which are used to identify the existence of PU are described clearly. The importance of CSS network and the reason for choosing it are described in detail. The concept of multipath fading and different fading channels are discussed clearly. The usefulness of fusion rules such as hard decision rules and soft data fusion rules are clearly discussed in this chapter.

Chapter 3: In this chapter, the detection performance of PU is evaluated using the soft data techniques in CSS network over various fading channels. The importance of using soft data rules, how they are used to overcome the fading effects, and various soft data rules are explained clearly. Soft data techniques such as SC, SLC, MRC, EGC, and SLS are used at FC to make a final decision about the PU. The detection performance is calculated using these diversity techniques over various fading channels such as Rayleigh, Rician, Nakagami-*m*, Weibull, and Hoyt fading channels. The closed form of detection probability expressions is derived for each diversity technique over various fading effects. Finally, the performance is evaluated with the help of sensing channel SNR versus detection probability curves and complementary receiver operating characteristic (CROC) curves using the CED scheme and a single antenna at each CR in CSS network over various fading environments.

Chapter 4: The importance of choosing censoring schemes in CSS network are clearly explained in this chapter. The complete details about the various censoring (Rank based and Threshold based) techniques are provided in this chapter. In CSS network, two different censoring techniques are used individually in reporting channel when it is affected by various fading effects. The final decision about the PU is made at FC using the hard decision logic called majority logic and soft data fusion logic called MRC Rule respectively. The performance is evaluated with the help of missed detection probability and total error rate curves.

Chapter 5: In this chapter, how the optimized performance of proposed CSS network can be achieved is explained in detail. The CSS network parameters such as a number of CR users (N), arbitrary power of received signal (p), and the threshold value (λ) are optimized when CSS network is effected by various fading environments. The performance is evaluated using the proposed CSS network which consists of multiple antennas and an IED scheme as detection technique at each CR. The novel analytical expressions of missed detection probability for different fading channels are derived. The novel analytical optimized expressions of number of CR users (N_{opt}), threshold value (λ_{opt}), and an arbitrary power of received signal (p_{opt}) are derived for various fading channels using single and multiple antennas at each CR. The performance is evaluated with the help of complementary receiver operating characteristics (CROC) and total error rate curves.

Chapter 6: This chapter describes the importance of average channel throughput (C_{avg}) analysis and network utility function (NUF) performances and reason for choosing it are provided in detail. The performance is analyzed using the proposed CSS network which is equipped with

multiple antennas and an IED scheme as detection technique at each CR. Two different fusion rules (k=1+n and k=N-n) are used at FC individually to get the C_{avg} and NUF performances. The novel analysis of average channel throughput and NUF performances are evaluated using MATLAB simulations over Rayleigh and Weibull fading channels. The optimal number of CR users are also calculated to maximize the average channel throughput over these fading channels.

Chapter 7: This chapter presents a summary of the results and conclusions from work carried out in the earlier chapters. The scope for future research is also indicated.

Chapter-2

Literature Survey

2.1. Introduction

Radio spectrum is a natural resource which is available in nature. The utilization of radio frequency spectrum has grown tremendously in the last few years. As a precious resource, the radio spectrum must be carefully managed to minimize the interference, and to maximize the utilization. The regulatory agencies are allocated the chunks of radio spectrum to different wireless services. Fig.2.1 shows the allocation of specific frequency bands of radio spectrum for different radio transmissions and applications.

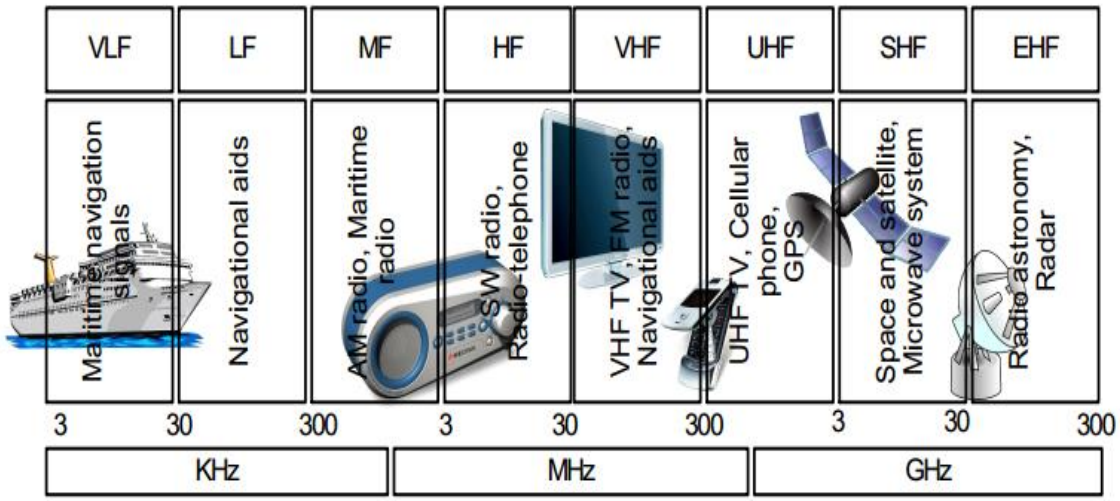

Fig.2.1. Allocation of radio spectrum for different applications.

The current static spectrum allocation policy allocates the radio spectrum exclusively to specific wireless services and they are working very well in mitigating interferences among the wireless services. Currently, uses of radio spectrum have become crowded due to increase

in the number of communication networks and services. The emerging and relentless growth of wireless services increases the demand for radio spectrum which results in spectrum scarcity. From the United States frequency allocation chart [32], it can be seen that almost all the frequency bands of radio spectrum has allocated for different applications. It also shows that there is a serious shortage of spectrum for new wireless services or expanding existing ones because of the rapid growth of wireless applications. According to the survey conducted by federal communication commissions (FCC) spectrum policy task force reported that only 15% to 85% of radio spectrum is efficiently utilized and most of the radio spectrum is underutilized [1]. It shows that the allocated spectrum experiences a low spectrum utilization rate when the statistics are noted for different time periods and geographical locations. Figure 2.2 shows the utilization of radio spectrum for a particular period given by FCC and it gives the information about utilized and underutilized frequency bands of radio spectrum. To meet the present requirements of wireless services and to improve the spectral efficiency, these underutilized frequency bands of radio spectrum should be identified and allocated for different applications by secondary transmitter and receiver.

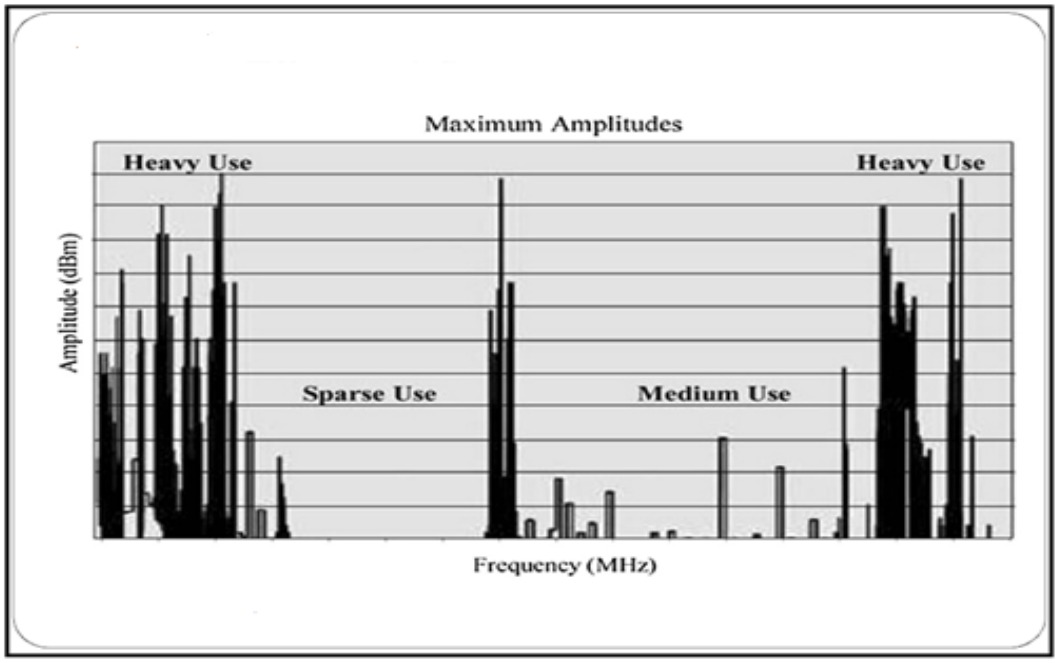

Fig.2.2. Utilization of radio spectrum.

To cater the increase in demand of radio spectrum for wireless services, radio spectrum must be efficiently utilized [3]. Hence, new technologies have to be introduced for an efficient utilization radio spectrum. This motivates the introduction of dynamic spectrum access (DSA) technique, which allows some wireless services to dynamically access the radio spectrum with

licensed wireless services [2-4]. The DSA technique offers the potential to increase the efficiency of spectrum usage dramatically and meets the growing demand for wireless services. The DSA policy is considered as a key technology for efficient utilization of radio spectrum. To support DSA, secondary users (SUs) are required to sense the radio spectrum environment, and the SUs with such a cognition capability is called as cognitive radio (CR). The cognitive radio is a new concept that utilizes the licensed spectrum in an unlicensed manner [5, 6]. The important features of CR technology are radio environment awareness and spectrum intelligence. As an intelligent wireless communication system, CR technology is aware of its surrounding environment through learning, and changes its operating parameters according to the environment, is the enabling technology for DSA. The cognitive radio concept is a better solution for efficient utilization of available radio spectrum.

According to the DSA model, some portion of the radio spectrum is allocated to one or more users called licensed users; these licensed users have a license to access the radio spectrum whenever they require. The licensed users also called primary users (PUs). To improve the spectral efficiency, unlicensed users called secondary users can utilize the licensed radio spectrum without interfering PU operation when PUs are inactive, and these SUs terminates their operations when PUs became active. By doing this, the same frequency bands of the radio spectrum are reused for other applications. The opportunistic access of PU resources by SUs have described as dynamic spectrum access. To access the spectrum dynamically, SUs are required to monitor the radio spectrum continuously. The cognitive radio is a key technology that allows a cognitive wireless terminal to access the available spectral opportunities dynamically. The term cognitive radio was first coined by Joseph Mitola. The unique features of CR technology are cognition capability and reconfigurability; these features are helpful to interact with the radio environment. The intelligence of SU is achieved by learning its surrounding radio environment with which it can determine how the SU can utilize the spectrum. The existing opportunities and emerging technologies of CR technology are to enable and support a wide variety of wireless applications, ranging from the smart grid, public safety and broadband cellular, to medical applications are discussed in [33]. In [34], synopsis of the commonly used platforms and test beds, discussion of what has been achieved in the last decade of experimentation, and analysis of CR technology is provided. The software defined radio (SDR) technique provides an ideal platform for the realization of cognitive radio technology [35]. CR technology is used in smart grid networks, public safety networks, cellular networks, CR mesh networks, leased networks, military networks, and emergency networks.

2.2. Spectrum Sensing

Spectrum sensing (SS) technique is an important task that continuously monitors the radio spectrum to identify the spectrum holes or vacant bands present in it in opportunistic spectrum access (OSA) manner. The spectrum hole is defined as spectrum bands that are usable by SUs without interfering the PU's operation. Hence, identification of spectrum hole is a useful task in CR system. After identifying the spectrum holes successfully, they may be used for secondary communication by the secondary transmitter and secondary receiver [2, 9].

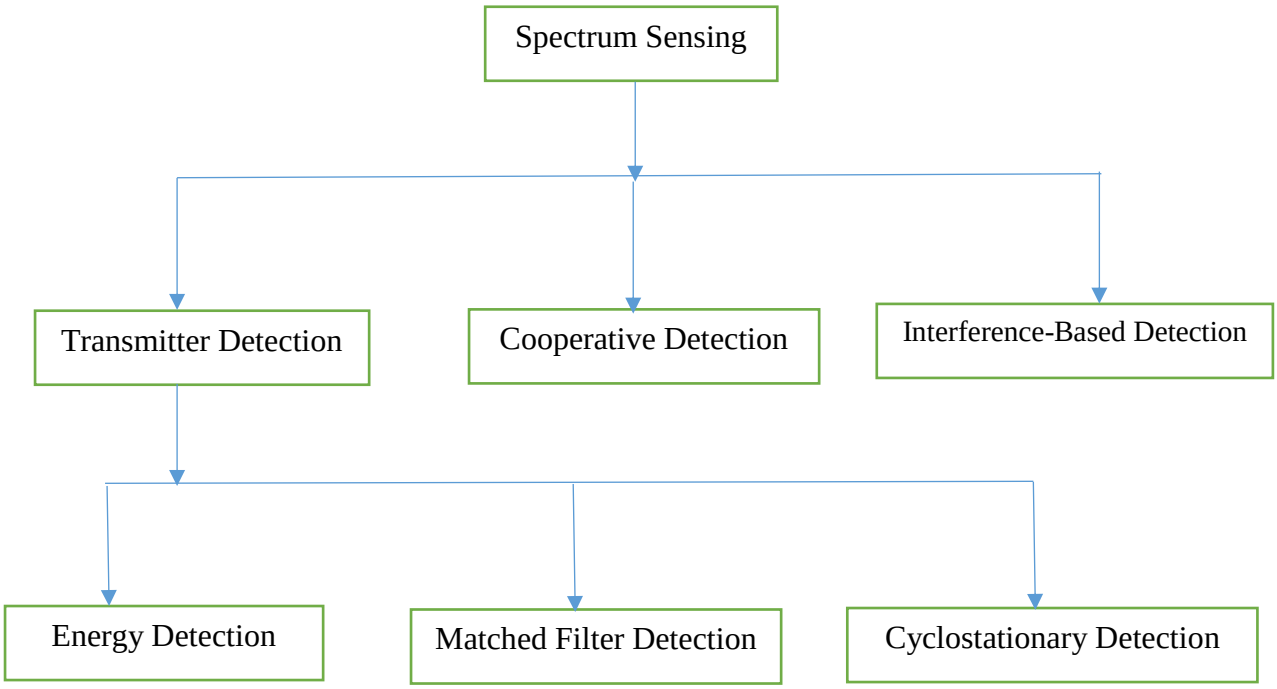

Fig.2.3. Classification of spectrum sensing technique.

Two key performance metrics associated with spectrum sensing are the probability of detection and probability of false alarm. A lower probability of false alarm increases the spectrum reuse efficiency by the SUs, which in turn, increases their throughput. A higher detection probability value will result in the PU is less likely to be interfered by the SUs. Hence, there is a vast research interest in spectrum sensing algorithms in recent years to improve the detection performance using less time and low complexity [8, 9, 36–38]. In literature, three different ways are addressed for the detection of spectrum holes such as transmitter detection, cooperative detection, and interference-based detection [2, 36] as shown in Fig.2.3. The most efficient way to detect the spectrum holes is to detect the PUs that are receiving the data within the communication range of SUs.

2.2.1. Transmitter Detection

The transmitter detection technique detects the spectrum holes by detecting whether any PU transmitter is operating or not. In transmitter detection scheme if the PU exists, then the received signal at the receiver consists of signal and noise. Otherwise, if PU is absent, only noise is present at the receiver. The Basic hypothesis model for transmitter detection can be defined as follows [10];

$$x(t) = \begin{cases} n(t) & : H_0 \\ h * s(t) + n(t) & : H_1 \end{cases} \tag{2.1}$$

In the above expression, $x(t)$ is the output of the detector, $s(t)$ represents the received signal at the input of receiver, $n(t)$ is the noise value, h is the fading coefficient which occurs due to fading effect in the channel. H_0 and H_1 are the decision statistics which represents the absence and presence of PU. Three schemes are generally used for the transmitter detection according to the hypothesis model [39] such as energy detection, matched filter detection, and cyclostationary detection.

A. Energy detection

In this technique, received signal energy is calculated and compared with a pre-defined threshold value to decide the presence or absence of PU [10, 11]. The energy detection (ED) scheme is most commonly used detection technique because of low complexity and non-coherent in nature. It does not need prior information about the PU. It may not distinguish the signal type, but it can determine the existence of signal components. One inherent drawback of ED is that its performance gets degraded at higher levels of noise and interference.

B. Matched filter detection

The matched filter detection (MFD) is an optimal detection technique when prior knowledge of PU signal is known to SUs [40, 41]. In this technique, the correlation between transmitter and receiver is present so that it maximizes the received signal SNR value. The main advantage of MFD is that it requires less time to achieve the desired detection performance. However, the matched filter requires perfect knowledge of PU signals which is hardly available to the SUs. It requires prior knowledge of PU signals such as modulation type and order, pulse shape, and packet format. Hence, if this information is not accurate, then matched filter performs poorly. However, most of the wireless network systems have a pilot,

preambles, and synchronization word or spreading codes; these can be used for the coherent detection.

C. Cyclostationary detection

The cyclostationary feature detection (CFD) exploits the periodicity in the received primary signal to identify the presence of PUs [42]. The periodicity is commonly embedded in sinusoidal carriers, pulse trains, spreading codes, hopping sequences, and cyclic prefixes of the primary signals. Due to the periodicity, these cyclostationary signals exhibit the features of periodic statistics and spectral correlation, which is not found in stationary noise and interference. Thus, CFD is robust to noise uncertainties and performs better than energy detection in low SNR regions. Although it requires a priori knowledge of the signal characteristics, CFD is capable of distinguishing the CR transmissions from various types of PU signals [7, 43]. This eliminates the synchronization requirement of energy detection in cooperative sensing. Moreover, CR users may not be required to keep silent during cooperative sensing which improves the overall CR throughput. This method requires high computational complexity and long sensing time. Due to these issues, this detection method is less common than energy detection in cooperative sensing.

2.2.2. Cooperative Detection

Due to the deep fading effect in the environment, the CRs are not able to detect the PU accurately which leads to the hidden terminal problem in spectrum sensing technique. Though line-of-sight (LoS) is present between PU and SU, identification of PUs become limited because of shadowing uncertainty. If the CR user experiences a hidden terminal problem or shadowing uncertainty, the transmitter detection cannot detect the PU's presence. These problems can be overcome and uncertainty caused by the single SU detection is reduced with the cooperation of multiple SUs. Using multiple sensing nodes, cooperative sensing can exploit spatial diversity. Shadowing and multipath fading effects are main factors that deteriorate the performance of a single SU detection i.e. spectrum sensing technique. The cooperative spectrum detection technique provides more accurate performance compared to the spectrum sensing technique because of cooperation among multiple SUs [44]. However, it requires an additional operation and overhead traffic to communicate with CR users. Hence, there can be an effect on the performance of resource-constrained networks.

2.2.3. Interference-Based Detection

A new model for measuring interference is referred as interference temperature has been introduced by FCC [45]. In this technique, an interference level at the PU receivers is measured to protect them from interference. The CR user can access the spectrum bands as long as its interference at the primary receiver does not exceed PU's interference temperature limit, which is the maximum amount of interference that the receiver can tolerate.

The interference temperature T_I is defined as [46];

$$T_I\left(f_c, B\right) = \frac{P_I\left(f_c, B\right)}{kB} \tag{2.2}$$

where $P_I(f_c, B)$ is the average interference power in Watts centred at f_c, covering bandwidth *B*, and *k* is Boltzmann's constant.

2.3. IEEE 802.22 WRAN Standard

As discussed above, radio spectrum is divided into a number of subbands, and each subband is allocated for different applications. The frequency range from 54MHz to 862 MHz of radio spectrum is allowed for television (TV) broadcasting which is used by different TV operators [2]. The frequency bands which are not being used by the operators are called spectrum holes. FCC has permitted to use of these spectrum holes of TV band frequencies by the unlicensed users called SUs. The IEEE 802.22 standard has been released with medium access control (MAC) and physical layer specifications for a wireless regional area network (WRAN), allowing the use of the cognitive radio technique on a non-interfering basis [47-49]. The standards requirement on the receiver parameters for IEEE 802.22 is provided in [50]. According to it, signals are classified into three types such as analog TV, digital TV, and wireless microphone signals.

Parameter	Analog TV	Digital TV	Wireless Microphone
Probability of false alarm	90%	90%	90%
Probability of detection	10%	10%	10%
Channel detection time	≤2sec	≤2sec	≤2sec

Table. 2.1. Receiver parameters of 802.22 WRAN.

2.4. Cooperative Spectrum Sensing

Reliable primary user detection is one of the most challenging and difficult tasks with the spectrum sensing technique because of single SU present in the network [51, 52]. Moreover, selecting the best available frequency bands in radio spectrum and reducing or eliminating the interference with PUs are also essential [2, 53], all these requirements depend on the spectrum sensing technique. To meet the above mentioned IEEE 802.22 WRAN spectrum sensing specifications can be a tough task because of shadowing, multipath fading effect, and time-varying nature wireless channel. When a single CR based CED technique [54] employed in the system, it might be facing a hidden terminal problem and thereby limiting its performance due to shadowing and fading effects.

To overcome these drawbacks, to improve the detection probability, and to meet the present requirements, a new technique called cooperative spectrum sensing (CSS) network [14] has been introduced, in which multiple SUs are present as shown in Fig. 2.4. These multiple SUs have individually sensed the PU's activity and send their sensing information to the fusion center (FC). The sharing and exchange of sensing information among the multiple SUs are present so that detection performance will be improved. The random spatial distribution of the cooperative nodes helps to reduce the impact of the hidden terminal problem. The CSS network gives better detection probability values though shadowing and fading effects present [15]. As discussed above, sensing information from multiple SUs is passed to the FC and final decision about the PU will be made at FC. The CSS network consists of sensing channel (S-channel), reporting channel (R-channel), a PU, an FC, and multiple SUs in it. The S-channel is present between PU and SUs and R-channel lies between SUs and FC. Various detection schemes are used at each CR in CSS network. If the sensing information in the form of binary decisions (either 0 or 1) from each SU is passed to the FC through the R-channel, then hard decision fusion rules such as OR-Rule, AND-Rule, and Majority logic are used at FC to make a final decision about PU. If the sensing information in the form of data (energy values) from each SU is passed to the FC through the R-channel, then soft data fusion rules called diversity techniques are used at FC to decide the activity of PU. In data fusion, each cooperative node simply amplifies the received signal from the PU and forwards to the FC [13, 16, 55]. In decision fusion, each cooperative node makes its own hard decision about the PU activity, and the individual decisions are reported to the FC.

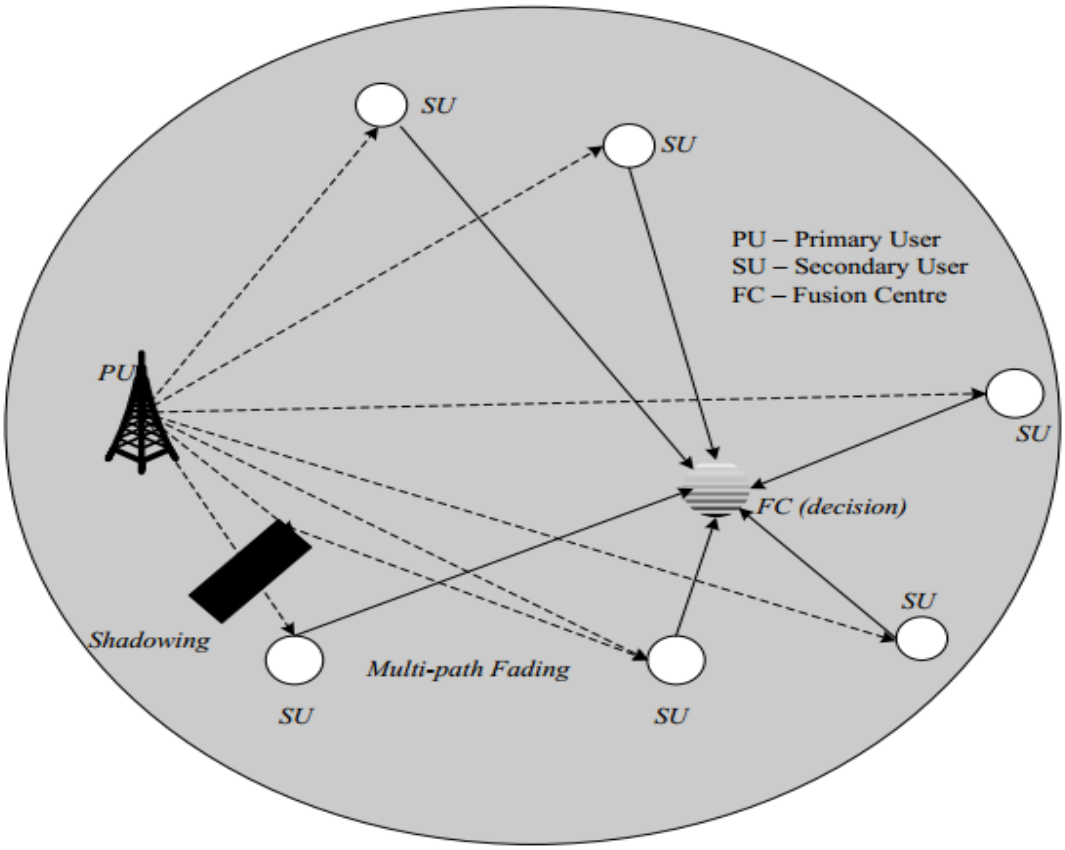

Fig. 2.4. Cooperative spectrum sensing network.

The performance analysis of spectrum sensing based energy detection technique in cognitive radio networks over generalized fading channels is discussed in [56]. The detection performance using spectrum sensing technique is limited due to multipath fading and shadowing effects which are the fundamental characteristics of wireless channels is discussed in [57]. To overcome these challenges, cooperation among SUs is required to perform spectrum sensing which is proposed in [58]. By exploiting the advantages of spatial and multiuser diversities, cooperative spectrum sensing technique has been introduced to improve the reliability of spectrum sensing. It has been proven in [59] that CSS technique can alleviate the noise uncertainty problems and CSS technique also decreases the required amount of sensing time [60, 61]. Therefore, CSS technique will have an important role in the implementation of cognitive radio networks (CRNs) under the OSA model.

An improved energy detection (IED) scheme [17] is introduced to improve the detection probability and to overcome the limitations present in the CED scheme. More precisely, the detection performance can be further improved significantly by replacing CED with an IED at each CR in CSS network [18]. An IED scheme measures the received signal amplitude (i.e., PU's transmitted signal) with an arbitrary positive power (p) rather than

squaring device used in CED scheme. In [62], an experimental approach of IED based spectrum sensing for CR network is proposed.

2.5. Shadowing and Fading Channels

In this section, various fading models and shadowing effects are described clearly. The multipath fading effect is due to the constructive and destructive combination of randomly reflected, scattered, and diffracted signal components. This type of fading effect is relatively fast and responsible for short-term signal variations. Depending on the nature of the radio propagation environment, different models are describing the statistical behavior of the multipath fading envelope [63, 64].

A. Shadowing effect

In terrestrial and satellite land-mobile systems, the radio link present between transmitter and receiver is affected by slow variations of signal level due to the shadowing from multiple objects, trees, and buildings present in the environment. Based on mathematical approach, this shadowing effect can be modeled by log-normal distribution and its probability density function (PDF) is given in [63-65] as;

$$f_{\gamma}(\gamma) = \frac{\zeta}{\sqrt{2\pi}\sigma\gamma} \exp\left(-\frac{\left(10\log_{10}\gamma - \mu\right)^2}{2\sigma^2} \right) \tag{2.3}$$

where ζ =$10/ln10$, μ and σ are mean and standard deviations in dB, γ-is instantaneous SNR.

B. Rayleigh fading

The Rayleigh channel model is a fading channel, which is commonly used to describe the statistical time-varying nature of the received envelope of a signal or the envelope of individual multipath components. It is often used to describe when the direct path between transmitter and receiver does not exist, such as in mobile links, ionospheric and tropospheric scattering, and ship to ship radio links. The PDF of Rayleigh fading channel is given in [63-65] as;

$$f_{\gamma}(\gamma) = \frac{1}{\bar{\gamma}} \exp\left(\frac{\gamma}{\bar{\gamma}} \right) \qquad \gamma \geq 0 \tag{2.4}$$

where γ is instantaneous SNR of PU signal at the SU.

C. Rician fading

When a dominant stationary signal is present between transmitter and receiver such as a line-of-sight (LoS) propagation path, then the small-scale fading envelope distribution is Rician distribution. Mostly, it is used in the analysis of urban and suburban mobile radio links, pico-cellular indoor radio links, and satellite links. The PDF of Rician fading channel is given in [64] as;

$$f_\gamma(\gamma) = \frac{(1+K)}{\bar{\gamma}} \exp\left(-\frac{(1+K)\gamma}{\bar{\gamma}}\right) I_0\left(2\sqrt{\frac{K(1+K)\gamma}{\bar{\gamma}}}\right) \qquad \gamma \geq 0 \tag{2.5}$$

where $I_0(z)$ is zeroth order of modified Bessel function of first kind and *K*-is Rician fading parameter. The Rayleigh distribution is a special case for Rician distribution when *K* approaches to zero.

D. Nakagami-*m* fading

Nakagami-*m* channel model is a general multipath fading model. It is used to model the attenuation of signals traversing in multiple paths. It is often used to describe the fading in both indoor and outdoor mobile radio links as well as in ionospheric radio links. The PDF of Nakagami-*m* fading channel is given in [10, 64] as;

$$f_\gamma(\gamma) = \frac{1}{\Gamma(m)}\left(\frac{m}{\bar{\gamma}}\right)^m \gamma^{m-1} \exp\left(-\frac{m\gamma}{\bar{\gamma}}\right) \qquad \gamma \geq 0 \tag{2.6}$$

where *m*-is Nakagami fading parameter.

Rayleigh fading channel is a special case for Nakagami-*m* fading channel when *m* equals to 1. If $m \rightarrow +\infty$, Nakagami-*m* fading channel converges to AWGN channel [64].

E. Weibull fading

Weibull fading has been employed in modeling multipath waves propagating in non-homogeneous environments. It is very flexible and has been shown to provide adequate fitting to empirical results from wireless channel measurements in both indoor and outdoor communication scenarios. It includes special cases such as well-known Rayleigh and exponential distributions for $V = 2$ and $V = 1$ respectively. The PDF of Weibull fading channel is given in [66, 117] as;

$$f_{\gamma}(\gamma) = c\left[\frac{\Gamma\left(1+\frac{2}{c}\right)}{\bar{\gamma}}\right]\gamma^{c-1}\exp\left(-\left[\frac{\gamma\Gamma\left(1+\frac{2}{V}\right)}{\bar{\gamma}}\right]^{c}\right) \qquad \gamma \geq 0 \tag{2.7}$$

where $c = V/2$ and V-is Weibull fading parameter.

F. Hoyt (Nakagami-*q*) fading

Hoyt or Nakagami-q fading distribution is generally used to characterize the fading environments that are more severe than Rayleigh fading. Satellite links with strong ionospheric scintillation can be modeled with this distribution, and its PDF is given in [67] as;

$$f_{\gamma}(\gamma) = \frac{1}{\sqrt{p\bar{\gamma}}}\exp\left(-\frac{\gamma}{p\bar{\gamma}}\right)I_0\left(\frac{\gamma\sqrt{1-p}}{p\bar{\gamma}}\right) \qquad \gamma \geq 0 \tag{2.8}$$

where $p = 4q^2/\left(1+q^2\right)^2$ and q-is Hoyt fading parameter which ranges from $(0 < q < 1)$. For $q = p = 1$, hoyt distribution reduces to Rayleigh distribution and for $q = p = 0$, it represents the one-sided Gaussian PDF.

2.6. Fusion Rules

In CSS network, multiple SUs are individually sensed the PU activity and stores the sensing information with them. The sensing information associated with each SU is transferred to the FC through the reporting channel of CSS network. The final decision is made at FC using different fusion rules such as hard decision fusion rules and soft data fusion rules. The detailed information about the different fusion rules are discussed in following sections.

2.6.1. Hard Decision Fusion Rules

As discussed above, hard decision fusion rules are used when the sensing information associated with each SU is passed to the FC in the form of binary decisions (either 0 or 1) to make a final decision about the PU. Assuming that the energy observations at each SU is independent and identically distributed (i.i.d.). The overall false alarm probability (Q_f) and over all probability of detection (Q_d) are the detection performance metrics in CSS network. These can be calculated for different hard decision fusion rules as [68, 69];

A. OR-Rule

The OR-Rule decides that a primary signal is present (H_0 or H_1) when any of the secondary user detects a signal. The Q_f and Q_d expressions using OR-Rule can be formulated as follows;

$$Q_f = 1-\left(1-P_f\right)^N \tag{2.9}$$

$$Q_d = 1-\left(1-P_d\right)^N \tag{2.10}$$

where P_f and P_d are the probability false alarm and detection probability of an individual SU. H_0 and H_1 are the final decision statistics of absence or presence of PU. *N*-is number of SUs in the network.

B. AND-Rule

The AND-Rule decides that a primary signal is present (H_0 or H_1) when all the secondary users are detects a signal. The Q_f and Q_d expressions using AND-Rule can be formulated as follows;

$$Q_f = \left(P_f\right)^N \tag{2.11}$$

$$Q_d = \left(P_d\right)^N \tag{2.12}$$

C. Majority logic

The Majority logic decides that a primary signal is present (H_0 or H_1) when at least *k* out of *N* secondary users detects a signal. The Q_f and Q_d expressions using Majority logic can be formulated as follows;

$$Q_f = \sum_{l=k}^{N}\binom{N}{l}\left(P_f\right)^l\left(1-P_f\right)^{N-l} \tag{2.13}$$

$$Q_d = \sum_{l=k}^{N}\binom{N}{l}\left(P_d\right)^l\left(1-P_d\right)^{N-l} \tag{2.14}$$

In the above expression, if we substitute *k*=1, it gives the expression for OR-Rule, and if we substitute *k*=*N*, it gives the expression for AND-Rule.

2.6.2. Soft Data Fusion Rules

The soft data fusion rules are used when the sensing information associated with each SU is passed to the FC in the form of energy values to make a final decision about the PU. The fusion center combines the forwarded observations and compares the aggregated energy value with a pre-defined threshold value. Assuming that the energy observations at each SU is independent and identically distributed (i.i.d.). The Q_f and Q_d expressions can be calculated as;

$$Q_f = P\{Y > \lambda \mid \mathrm{H}_0\} \tag{2.15}$$

$$Q_d = P\{Y > \lambda \mid \mathrm{H}_1\} \tag{2.16}$$

where *Y*-is combined value of all decision statistics from each diversity branch and λ is a pre-defined threshold value.

2.7. Diversity Techniques

Antenna diversity techniques are known to improve the signal reception by exploiting the advantage of the spatial dimensions at the receiver. Receiving the multiple replicas of the fading signal via different antenna branches and by combining them improves the overall received SNR [64]. These diversity techniques are used to combat the effect of multipath fading since different diversity branches may not concurrently go into deep fading and the branches with better SNR quality can compensate even if the signals in other branches are in deep fade. The ED performance has been shown to significantly improve the detection performance through the use of multiple antennas in [11], [12], [70], [71]. There are two different types of diversity techniques are addressed in the literature such as coherent diversity techniques and non-coherent diversity techniques. The signal may be received at multiple antennas and combined in different manners. There are five different classical diversity techniques are discussed briefly in this section as follows;

A. Selection combining

It is a non-coherent detection technique which processes a single branch instead of using all branches. It selects the one branch which is having highest SNR value out of the total number of branches present in it. Since the output of selection combining (SC) scheme is equal to the signal value of one branch so, the coherent sum of the individual branch signals is not

required. Therefore, SC scheme is used in conjunction with differentially coherent and non-coherent modulation techniques since it does not require knowledge of the signal phases on each branch. SC scheme is easy to implement, using this technique system complexity reduces, and it does not require processing of signals coming from each branch [10, 64]. This scheme requires continuous monitoring of signals which are coming from each branch.

B. Square law combining

Square law combining (SLC) scheme is a non-coherent combining scheme in which the received signal at each branch is squared before combining [11]. This scheme is particularly useful for non-coherent operation without any channel state information (CSI). In this scheme, each diversity branch has a square law device which performs the square and integrates operation. The combiner is implemented after the square law operation [72]. The energy detector receives the sum of all branches decision statistics. The output of the square law combing is the sum of all branches decision statistics and that yields a new decision statistics.

C. Square law selection

In square law selection (SLS), each diversity branch has a square law device and the branch with the maximum decision statistic is selected [72]. It is also a non-coherent detection technique. The sensing information from all SUs is collected at FC in the form of energy values, using SLS scheme at FC, the branch with highest energy value will be selected instead of the sum of all diversity branches like SLC diversity scheme.

D. Equal gain combining

Equal gain combiner (EGC) is a coherent detection technique and it does not require estimation of fading amplitudes so, its system complexity reduces compared to the other coherent techniques [64, 72]. However, EGC is often limited in practice to coherent modulations with equal energy symbols such as M-ary PSK signals. In many wireless applications, the phase of the received signal is not identified accurately, in that case, coherent detection scheme may not be possible to perform. In such cases, communication systems must rely on non-coherent detection techniques such as an envelope or square-law detection of frequency shift keying (FSK) signals.

E. Maximal ratio combining

Maximal ratio combining (MRC) is also a coherent combining scheme which requires channel state information (CSI) and it requires the estimation of both amplitude and phase of the received signal. At the receiver, the received signals are weighted by their respective channel coefficients before combining [64]. This scheme gives optimal performance. Signals with unequal energy symbols such as M-QAM modulation schemes, MRC scheme should be used to achieve better performance [73]. The requirement of complete CSI being a trade-off regarding cost and complexity.

In [15], authors considered that S-channel of CSS network is affected by different fading environments like Rayleigh, Lognormal shadowing, and R-channel is considered as an ideal channel. The hard decision fusion rules are considered at FC to know the PU activity over different fading environments [15, 69]. The average detection probability value is calculated with ED scheme over α-μ generalized fading channels using SC diversity technique in CSS network is discussed in [74]. In [10], authors provided the detection probability expressions for Rayleigh, Nakagami fading channels and also for various diversity techniques such as EGC, SC, and switch and stay combining (SSC) techniques. The soft data fusion techniques such as MRC, likelihood ratio test (LRT), and EGC rules are applied at FC to know the PU activity in [70, 75]. In [75], LRT soft data fusion rule is considered at FC in case of wireless sensor networks. In [76], authors have used neyman-pearson (NP) criterion at FC, and their proposed scheme works as EGC scheme at higher SNR range of values and reduces to MRC scheme at lower range of SNR values. The detection probability value also improved by considering multiple antennas at each CR user is described in [70].

In [77], authors provided the performance analysis and comparison between hard decision (HD) and soft data (SD) fusion rules based CSS network in the presence of error rates in R-channel. The effect of channel errors is incorporated in the analysis through the bit error probability (BEP). A general expression for the detection probability with *K*-out-of-*N* fusion rule has been derived using HD fusion rule with the error rate in R-channel. Furthermore, it is shown that SD based CSS network gives better performance even if the error rates are considered in the R-channel [77, 78], the impact of error detection and error correction performance also shown. The performance of sequential detection scheme at each CR of CSS network with an error rate in R-channel is evaluated in [79]. Two novel quantization schemes are used to improve the sensing performance considering SD fusion rule in CSS network is

discussed in [80]. In [81], authors considered the effect of imperfect R-channel on decision logic. In [21], authors proposed a new soft data fusion scheme which simplifies the analysis of data at FC. However, CSS network can incur cooperation overhead regarding extra sensing time, delay, energy, and operations devoted to cooperative sensing. The detail information regarding these issues is addressed in [2], which specifically addresses the issues of cooperation method, cooperative gain, and cooperation overhead.

2.8. Censoring Schemes

However, most of the literature work exists on CSS network by assuming a noiseless R-channel and noisy S-channel [15, 69, 76, 82]. But, in many practical situations, R-channel of CSS network may be affected by noise, shadowing, and multipath fading effects [21, 83, 84]. The presence of fading or shadowing in R-channel is likely to affect the sensing information sent by CR users so that the information received at FC is erroneous. If this is the case, it is better to interrupt the transmission of sensing information from such CR users; this can be done by censoring schemes. The heavily faded R-channel CR links can be eliminated by using the censoring schemes such as Rank based and Threshold based censoring schemes to improve the detection probability and to reduce the system complexity.

Although all the CR users detect the PU's activity using ED technique, some of the CR users are censored, and some are allowed to transmit on the basis of R-channel quality. Censoring decision is taken by the FC using the estimation techniques on the R-channel fading coefficients. Minimum mean square estimation (MMSE) is frequently applied on fading coefficients of R-channels because it gives the least value of error rate. The FC selects a subset of CR users among all the available CR users (say P out of N) which have the highest channel coefficients, i.e., the CR users associated with best-estimated channel coefficients are selected, this approach is referred as Rank based censoring [25]. In Threshold based censoring, whose R-channel fading coefficients exceeds a pre-defined threshold value are selected to transmit the information to the FC [85].

Initially censoring concept is used in sensor networks, later it is applied to the CSS network. An idea of censoring scheme is applied to CSS with the aid of CR network in 2007 [86]. The R-channel is considered as noisy and Rayleigh faded in context of a sensor network where sensors report their decision to the FC [87, 88]. Censoring of sensors are proposed in [89, 90] and channel aware censoring of sensors is discussed in [91], and these can be well applied in the context of CSS network. The censoring of CRs is necessary to improve the

detection performance using the CSS network. More precisely, the goal of censoring technique is to decide which CRs should transmit their observations to the FC, to achieve the best tradeoff between energy efficiency and detection probability. Censoring of CRs can be done on the basis of channel state information of estimated R-channel coefficients for both perfect and imperfect channel estimations is discussed in [92, 93]. In [85, 94], threshold based censoring scheme is used in CSS network over Rayleigh fading using majority logic and MRC rule at FC. In [24], CSS network performance with Rank based and Threshold based censoring schemes is evaluated over Rayleigh and Nakagami-*m* fading channels using majority logic and MRC Rule at FC. In [95], censoring scheme is used to overcome the drawback of overhead traffic problem at FC.

2.9. Optimization of CSS Network Parameters

Sometimes, it is required to optimize the CSS network parameters to achieve better performance with a minimum number of components and to minimize the complexity of the network. The optimal spectrum sensing network performance under data fusion scheme is investigated in [96]. In [97], authors discussed that the optimum performance can be achieved with the cooperation of a certain number of SUs present in the network and with the highest PU signal SNR. The optimal sensing throughput trade-off was studied in [30]. Optimization of CSS parameters with CED technique in CR network over fading and non-fading environments is discussed in [26]. In [98], CSS network parameters are optimized using the CED technique in non-fading environment. It is shown in [99, 100] that the performance of a CR network can be improved by utilizing an IED scheme at each CR. In [27], optimized performance of CSS network is evaluated by using a single antenna at each CR with an IED scheme over imperfect R-channel. In [28], optimized performance of CSS network is analyzed using the multiple antennas at each CR with an IED scheme over Rayleigh fading channel. The CSS network with an IED scheme is considered in [29] which uses optimization techniques to minimize the total error rate which is the sum of missed detection and false alarm probabilities.

2.10. Average Channel Throughput and Network Utility Function

It is also important to maximize the average channel throughput and network utility function to improve the detection performance of PUs and for efficient utilization of radio spectrum. Due to the fading effect in the environment sometimes PUs have not detected accurately, this may cause severe interference problem of SUs with PUs. This issue can be overcome and PUs are accurately identified if the sensing time of each SU is increased. An

increase in the sensing duration will improve the sensing performance, but data transmission time of the SUs also increases which results in reduced throughput. Such a problem is addressed in [30] to find the optimal sensing duration by maximizing throughput under sufficient protection to the PU. Hence, there is a trade-off between sensing time and throughput value of the network [30]. Throughput value can be increased if the sensing time decreases, but it degrades the accurate detection of PUs. Hence, average channel throughput value will be increased by performing sensing and transmission simultaneously [101]. In [102], throughput maximization is considered over erroneous control channel using the CED scheme. In [97], it is shown that joint optimization of sensing duration and fusion parameter increases the throughput of the secondary network. In [103], fusion parameter is optimized by maximizing the throughput under a constraint on the miss detection probability at FC. Number of SUs are optimized by maximizing secondary network throughput under a constraint on the detection probability at FC for OR-Rule is studied in [104]. Optimal voting rule is used at FC with an erroneous control channel in CSS network over non-fading environment is discussed in [105]. Similarly, network utility function should be maximized to improve the detection performance of PUs and to improve the spectral efficiency. The network utility function can be maximized by using an optimal number of SUs is addressed in [31].

2.11. Conclusions

In this chapter, relevant background theories of wireless communications are presented. Initially, allocation of frequency bands of radio spectrum for different applications, its utilization, and an issue of spectrum scarcity are described in detail. Next, the concept of spectrum sensing (SS) and overview of traditional SS technique are discussed. The basic principle of SS technique and various detection schemes that are used to identify the vacant bands of the radio spectrum are explained clearly. Further, importance of cooperative spectrum sensing (CSS) network and the reason for choosing it are described in detail. The concept of shadowing, multipath fading effect, and different fading channels are discussed. The usefulness of fusion rules such as hard decision rules and soft data fusion rules are properly summarized along with their probability distribution functions. Finally, the brief introduction about the censoring schemes, optimization of CSS network parameters, average channel throughput, the concept of network utility function, and an importance of choosing these techniques in CSS network are provided in this chapter.

Chapter-3

Performance Analysis of CSS Network using Diversity Techniques

3.1. Introduction

Spectrum sensing (SS) technique is an important task that monitors the radio spectrum continuously to identify the vacant bands present in it. The identification of vacant bands using the SS technique is limited due to multipath fading, shadowing effects, time-varying nature of wireless channels, and also single cognitive radio (CR) is present in the network. Hence, new techniques have to be introduced to overcome these drawbacks and to improve the detection performance. The detection performance can be improved and fading effects are mitigated by introducing the concept of cooperative spectrum sensing (CSS) network. In CSS network, multiple CRs are present, they sense the primary user (PU) activity individually, and they share and exchange the information among them so that detection performance can be improved. The CSS network performs better even in the presence of shadowing and fading effects due to cooperation among multiple CRs. The CSS network also eliminates the hidden terminal problem [106].

To overcome the influence of fading effect and to improve the detection probability of PU, various fusion rules such as hard decision and soft data fusion rules are used at fusion center (FC). If the sensing information from individual CRs is transferred to FC in the form of binary decisions (0 or 1), then hard decision fusion rules (OR-Rule, AND-Rule, and Majority-Rule) are used at FC. Similarly, if the sensing information from individual CRs is transferred to FC in the form of energy values [68, 69], then soft data fusion rules called diversity techniques are used at FC to make a final decision about the PU. Various diversity techniques such as selection combining (SC), square law combining (SLC), square law selection (SLS),

maximal ratio combing (MRC), and equal gain combiner (EGC) are addressed in the literature [10, 11]. The detection performance is more with soft data fusion rules compared to the hard decision fusion rules [64, 72].

In this chapter, we have evaluated the performance of CSS network under different soft data combining techniques in various fading environments. The performance is analyzed using the conventional energy detection (CED) scheme and a single antenna at each CR in CSS network. To evaluate the detection performance, we have assumed that sensing channel of CSS network is affected by various fading environments and reporting channel of CSS network is considered as a non-faded channel. The performance is evaluated using different diversity techniques (SC, SLC, SLS, MRC, and EGC) at FC when CSS network is influenced by various fading environments (Rayleigh, Rician, Nakagami-*m*, Weibull, and Hoyt fading). Our main aim in this chapter is to identify which diversity technique gives higher average detection probability ($\overline{Q_d}$) value when CSS network is affected by various fading environments. For this, we have gathered all the detection probability expressions that are available in the literature for various diversity techniques over different fading environments. The performance is described using simulations which are drawn between sensing channel SNR versus average detection probability curves and complimentary receiver operating characteristics (CROC) curves. With the help of MATLAB simulations, average detection probability performance comparison among various diversity techniques over different fading channels is provided.

3.2. System Model

Fig.3.1 shows the system model of CED technique. The received signal is passed through the bandpass filter (BPF) to eliminate the noise components present in it [10]. The average energy of the received signal (*Y*) is calculated from the square law device and integrator blocks of CED scheme. The output of integrator block is compared with a predefined threshold (λ) value to decide the absence or presence of PU.

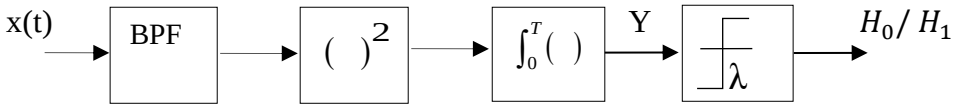

Fig.3.1. Block diagram of conventional energy detector.

Two hypotheses are defined in the literature to decide the absence and presence of PU as H_0 and H_1 respectively. The received signal at *j*-th CR user can be written as [10];

$$x_j(\mathrm{t}) = \begin{cases} n_j(t) & : H_0 \\ h_j * s(t) + n_j(t) & : H_1 \end{cases} \tag{3.1}$$

In the above expression, $s(t)$ represents the received signal at the input of CED and $n_j(t)$ is the noise value at *j*-th CR. AWGN noise (Additive white Gaussian noise) is considered in the network which is uniformly distributed over each CR. h_j is the fading coefficient which occurs due to fading effect in the channel. The test statistics are given by

$$Y = \sum_{j=1}^{N} \left| x_j(t) \right|^2 \tag{3.2}$$

The energy value (*Y*) is compared with a pre-defined threshold (λ) value to make a final decision about the PU. The expressions for probability of false alarm (P_f), probability of detection (P_d), and missed detection probability (P_m) over AWGN channels are given in [10] as;

$$P_d = (\mathrm{Y} > \lambda \mid \mathrm{H}_1) = Q_u(\sqrt{2\gamma}, \sqrt{\lambda}) \tag{3.3}$$

$$P_f = \left(\mathrm{Y} > \lambda \mid \mathrm{H}_0\right) = \frac{\Gamma\left(\mathrm{u}, \frac{\lambda}{2}\right)}{\Gamma(\mathrm{u})} \tag{3.4}$$

$$P_m = 1 - P_d \tag{3.5}$$

In Eq.(3.3), Q_u is marcum-Q function [107], in Eq.(3.4), $\Gamma(,)$ represents the incomplete gamma function, and $\Gamma()$ is complete gamma function [108].

Fig.3.2 shows the CSS network model with *N* number of SUs, an FC, and a PU. The channel present between PU and SUs is called as sensing channel (S-channel), in this channel each CR senses and stores the information about the PU. The sensing information associated with each CR is transferred to FC through the reporting channel (R-channel). The R-channel lies between SUs and FC in the CSS network. We are assuming that S-channel is affected by various fading environments and R-channel as a non-faded channel. Complete information in the form of energy values from all CRs are collected at FC, and the final decision is made at FC using soft data fusion rules such as (SC, SLC, SLS, MRC, and EGC). Each CR in the CSS network uses the CED scheme and single antenna at each CR to sense the activity of the PU [22].

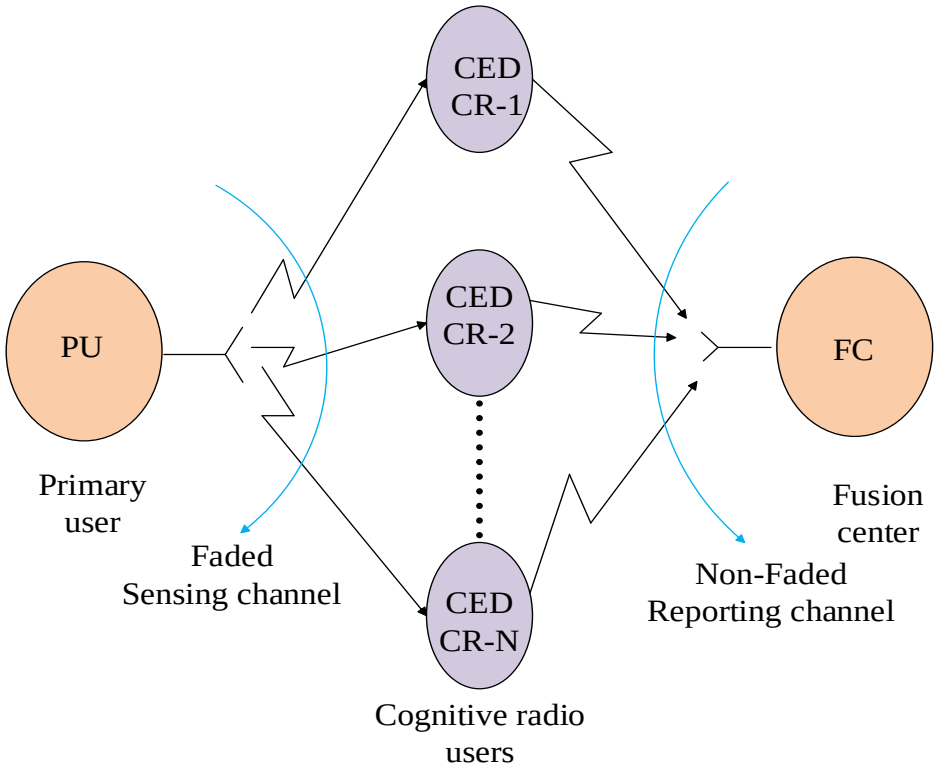

Fig.3.2. Cooperative spectrum sensing network.

3.3. Diversity Techniques

Multipath fading, shadowing effects, and time-varying wireless channels are degraded the detection performance. These distortions can be mitigated and detection probability value by using diversity combining techniques. In diversity combining, the same information-bearing signal is received by multiple antennas. In this section, various diversity techniques such as SC, SLC, SLS, EGC, and MRC are discussed in detail. The average detection probability expressions for each diversity technique over various fading environments are provided. We are assuming that all the CRs are identically independent distributed (i.i.d.) over the fading channels.

3.3.1. Square Law Combining (SLC) Diversity Technique

The square law combining (SLC) scheme is a non-coherent diversity technique [11, 72]. These non-coherent combining schemes are used to exploits the diversity gain in the absence of channel state information (CSI). In SLC scheme, each diversity branch has a square law device which performs the square and integrates operation. The output of the square-law device is the sum of all branches decision statistics which yields to a new decision statistics.

A. Expression for average detection probability in Non-fading environment

In this scheme, the output of the square-law device is the sum of all diversity branches (N) statistics. A new decision statistic Y_{SLC} appeares at the output SLC scheme. Y_{SLC} is represented by $Y_{SLC}=\sum_{i=1}^{N} Y_i$, where Y_i is the test statistic of i-th branch. In case of Non-fading environment (AWGN channel), the expressions for overall false alarm probability (Q_f) and overall detection probability (Q_d) under the SLC scheme are provided in [72] as;

$$Q_{f,SLC} = \frac{\Gamma\left(Nu, \lambda/2\right)}{\Gamma\left(Nu\right)} \tag{3.6}$$

$$Q_{d,SLC} = Q_{Nu}\left(\sqrt{2\gamma_{SLC}}, \sqrt{\lambda}\right) \tag{3.7}$$

where $\gamma_{SLC}=\sum_{i=1}^{N} \gamma_i$, and γ_i is the SNR in the i-th CR, and u-is time band width product (u=TW).

B. Expression for average detection probability in Rayleigh fading environment

If the signal experiences fading effect over N channels, the average false alarm probability value remains the same because it is independent of S-channel SNR but, the average detection probability value will vary. Under fading scenario, the average detection probability ($\overline{Q_d}$) value can be calculated as [64];

$$\overline{Q_d} = \int_0^{\infty} Q_d\left(\gamma, \lambda\right) f_{\gamma}\left(\gamma\right) d\gamma \tag{3.8}$$

where $f_{\gamma}(\gamma)$ indicates the probability density function (PDF) of the signal to noise ratio (γ) under fading and it depends on the type of fusion scheme. The average false alarm probability $\left(\overline{Q_f}\right)$ expressions remains the same for different fading schemes. Assuming N i.i.d. number of Rayleigh faded S-channels, the average detection probability ($\overline{Q_d}$) expression is obtained as [109, 110];

$$\overline{Q_d} = \sum_{n=0}^{\infty} \frac{\Gamma\left(Nu+n, \lambda/2\right)}{\Gamma\left(Nu+n\right)n!} \frac{\Gamma\left(N+n\right)}{\Gamma\left(N\right)} \left(\frac{\bar{\gamma}}{1+\bar{\gamma}}\right)^n \tag{3.9}$$

where $\Gamma(\,,)$ is incomplete gamma function, $\Gamma(\,)$ represents the complete gamma function, and $\bar{\gamma}$ is average S-channel SNR.

C. Expression for average detection probability in Rician fading environment

If S-channel of CSS network is affected by Rician fading environment, the final expression for average detection probability ($\overline{Q_d}$) is given in [110] as;

$$\overline{Q_d} = \left(\frac{1+K}{1+K+\bar{\gamma}}\right)^N \exp(-NK) \sum_{n=0}^{\infty} \frac{\Gamma\left(Nu+n, \lambda/2\right)}{\Gamma(Nu+n)n!} \frac{\Gamma(N+n)}{\Gamma(N)} \left(\frac{\bar{\gamma}}{1+K+\bar{\gamma}}\right)^n {}_1F_1\left[n+N; N; \frac{NK(1+K)}{1+K+\bar{\gamma}}\right] \tag{3.10}$$

where *K*-is Rician fading parameter and ${}_1F_1(\,;\,;\,)$ represents the confluent hypergeometric function [115, section 8.970].

D. Expression for average detection probability in Nakagami-*m* fading environment

In case of Nakagami-*m* fading environment, the average detection probability ($\overline{Q_d}$) expression is given in [109, 111] as;

$$\overline{Q_d} = 1 - B\left(Nu, Nm, N\bar{\gamma}\right) \tag{3.11}$$

where $B(\alpha,\beta,x) \triangleq \left(\frac{\beta}{\beta+x}\right)^{\beta} \sum_{n=0}^{\infty} \frac{\gamma\left(n+\alpha, \frac{\lambda}{2}\right)(\beta)_n}{\Gamma(n+\alpha)n!} \left(\frac{x}{\beta+x}\right)^n$, $(\beta)_n = \Gamma(\beta+n)/\Gamma(\beta)$, and

m-is Nakagami fading parameter.

E. Expression for average detection probability in Hoyt fading environment

If S-channel of CSS network is affected by Hoyt fading environment, the average detection probability ($\overline{Q_d}$) expression is given as in [112];

$$\overline{Q_d} = \left(\frac{rq}{r+q}\right)^N \sum_{n=0}^{\infty} \frac{\Gamma\left(Nu+n, \lambda/2\right)}{\Gamma(Nu+n)n!} \frac{\Gamma(n+N)}{\Gamma(N)} \left(\frac{q}{r+q}\right) {}_2F_1\left[\frac{N}{2}, n+N; N; \frac{r(1-q^2)}{r+q}\right] \tag{3.12}$$

Where $r = (1+q^2)/2q\bar{\gamma}$, *q*-is Hoyt fading parameter, and ${}_2F_1(\,,\,;\,;)$ is Gaussian hypergeometric function [115, section 9.100].

F. Expression for average detection probability in Weibull fading environment

The expression for average detection probability using SLC diversity technique at FC when S-channel of CSS network is affected by Weibull fading environment is given in [112] as;

$$\overline{Q_d} = \frac{(2\pi)^{\frac{1-c}{2}}}{\Gamma(N)\left(E\bar{\gamma}\right)^{Nc}} \sum_{n=0}^{\infty} c^{n+Nc+\frac{1}{2}} \frac{\Gamma\left(Nu+n, \lambda/2\right)}{\Gamma(Nu+n)n!} G_{1,c}^{c,1}\left[\frac{\left(E\bar{\gamma}\right)^{c}}{c^{c}}\middle| \begin{matrix} 1 \\ \frac{n+Nc}{c},.....,\frac{n+Nc+c-1}{c} \end{matrix}\right] \quad (3.13)$$

Where $E = \Gamma(N)/\Gamma\left(N+1/c\right)$, $G_{p,q}^{m,n}\left(x\middle|\begin{matrix} a_1,...,a_p \\ b_1,...,b_p \end{matrix}\right)$ denotes the Meijer's G function [115, section 9.301], $c = V/2$, and *V*-is Weibull fading parameter.

3.3.2. Selection Combining (SC) Diversity Technique

The selection combining (SC) scheme is also a non-coherent diversity technique. In SC diversity technique, the branch with highest SNR value will be selected from all the available number of branches. The output of the SC combiner is equal to one branch which has the highest value of SNR instead of the coherent sum of all individual branch signals [64, 72].

A. Expression for average detection probability in Non-fading environment

In this scheme, the branch with the highest value of S-channel SNR will be selected from a total number of available diversity branches (*N*). In case of Non-fading environment (AWGN channel), the expressions for false alarm (Q_f) and detection probabilities (Q_d) under the SC scheme are provided in [72] as;

$$Q_{f,SC} = \frac{\Gamma\left(u, \lambda/2\right)}{\Gamma(u)} \quad (3.14)$$

$$Q_{d,SC} = Q_u\left(\sqrt{2\gamma_{SC}}, \sqrt{\lambda}\right) \quad (3.15)$$

where $\gamma_{SC} = max(\gamma_1, \gamma_2, ... \gamma_N)$.

B. Expression for average detection probability in Rayleigh fading environment

Assuming *N* i.i.d. number of Rayleigh faded S-channels, the average detection probability ($\overline{Q_d}$) expression using SC diversity technique at FC is obtained as [10];

$$\overline{Q_d} = N\sum_{i=0}^{N-1}\frac{(-1)^i}{i+1}\binom{N-1}{i}\left\{\left(\frac{1+i}{1+i+\bar{\gamma}}\right)\sum_{n=0}^{u-2}\frac{e^{-\frac{\lambda}{2}}}{n!}\left(\frac{\lambda}{2}\right)^n + \left[\frac{1+i+\bar{\gamma}}{(1+i)}\right]^{u-1}\left[e^{-\frac{\lambda(1+i)}{2\left(1+i+\bar{\gamma}\right)}} - e^{-\frac{\lambda}{2}}\sum_{n=0}^{u-2}\frac{1}{n!}\frac{\lambda\bar{\gamma}}{2\left(1+i+\bar{\gamma}\right)}\right]\right\} \quad (3.16)$$

C. Expression for average detection probability in Rician fading environment

If S-channel of CSS network is affected by Rician fading environment, the final expression for average detection probability ($\overline{Q_d}$) is given in [110] as;

$$\overline{Q_d} = C\int_0^{\Pi/2} Q_u\left(\sqrt{2\tan\theta},\sqrt{\lambda}\right)\exp\left(-\frac{(1+K)\tan\theta}{\bar{\gamma}}\right)I_0\left(2\sqrt{\frac{K(1+K)\tan\theta}{\bar{\gamma}}}\right)\left[1-Q_1\left(\sqrt{2K},\sqrt{\frac{2(1+K)\tan\theta}{\bar{\gamma}}}\right)\right]\sec^2\theta d\theta \tag{3.17}$$

where $C = N(1+K)\exp(-\mathrm{K})/\bar{\gamma}$, $\gamma_{sc} = \tan\theta$, and $d\gamma_{sc} = \sec^2\theta d\theta$.

D. Expression for average detection probability in Nakagami-*m* fading environment

In case of Nakagami-*m* fading environment, the average detection probability ($\overline{Q_d}$) expression is given in [111, 113] as;

$$\overline{Q_d} = 1 - N\sum_{k=0}^{N-1}(-1)^k\binom{N-1}{k}\sum_{j=0}^{k(m-1)}b_j^k\left(\frac{m}{\bar{\gamma}}\right)^{m+j}\left\{\left(\frac{\bar{\gamma}}{\bar{\gamma}+m(1+k)}\right)^{n+m+j}\sum_{n=0}^{\infty}\frac{\gamma(n+u,\lambda/2)(m)_{n+j}}{\Gamma(n+u)n!}\right\} \tag{3.18}$$

where $b_j^k = \frac{1}{j}\sum_{s=1}^{J}b_{j-s}^k\frac{j(l+1)-k}{j!}$ and $J = \min(k, m-1)$.

E. Expression for average detection probability in Hoyt fading environment

If S-channel of CSS network is affected by Hoyt fading environment, the average detection probability ($\overline{Q_d}$) expression is given in [112] as;

$$\overline{Q_d} = \frac{N}{\sqrt{p}\bar{\gamma}}\int_0^{\pi/2} Q_u\left(\sqrt{2\tan\theta},\sqrt{\lambda}\right)\exp\left(\frac{-\tan\theta}{p\bar{\gamma}}\right)I_o\left(\frac{\tan\theta\sqrt{1-p}}{p\bar{\gamma}}\right)\left[1+\exp\left(\frac{-\tan\theta}{p\bar{\gamma}}\right)I_o\left(\frac{\tan\theta\sqrt{1-p}}{p\bar{\gamma}}\right)-2Q_1(m_1,n_1)\right]^{N-1}\sec^2\theta d\theta \tag{3.19}$$

where $I_n(.)$ is *n*-th order modified fist kind Bessel function [115],

$\{m_1, n_1\} = \sqrt{\left(1\mp\sqrt{p}\right)\tan\theta/\left(p\bar{\gamma}\right)}$ and $p = 4q^2/\left(1+q^2\right)^2$.

F. Expression for average detection probability in Weibull fading environment

The expression for average detection probability using SC diversity technique at FC when the S-channel of CSS network is affected by Weibull fading environment is given in [112] as;

$$\overline{Q_d} = Nc\left[\frac{\Gamma(p)}{\bar{\gamma}}\right]^c \int_0^{\pi/2} Q_u\left(\sqrt{2\tan\theta}, \sqrt{\lambda}\right) \tan\theta^{c-1} \exp\left[-\left\{\frac{\tan\theta\Gamma(p)}{\bar{\gamma}}\right\}^c\right]\left(1-\exp\left[-\left\{\frac{\tan\theta\Gamma(p)}{\bar{\gamma}}\right\}^c\right]\right)^{N-1} \sec^2\theta d\theta \quad (3.20)$$

where $p = 1 + {}^{1}/_{C}$ and $C = {}^{V}/_{2}$.

3.3.3. Square Law Selection (SLS) Diversity Technique

The square law selection (SLS) scheme is a non-coherent diversity technique. In SLS diversity technique, each diversity branch has a square law device, and the branch with highest decision statistic will be selected f0rom all the available number of diversity branches (*N*) [64, 72].

A. Expression for average detection probability in Non-fading environment

In this scheme, the output of square law selection device is the branch with highest test statistic value, i.e. $Y_{SLS} = \max(Y_1, Y_2 \ldots . Y_N)$. In case of Non-fading environment (AWGN channel), expressions for false alarm (Q_f) and detection probabilities (Q_d) under the SLS scheme are given in [72] as;

$$Q_{f,SLS} = 1 - \left[1 - \frac{\Gamma\left(u, {}^{\lambda}/_{2}\right)}{\Gamma(u)}\right]^N \quad (3.21)$$

$$Q_{d,SLS} = 1 - \prod_{k=1}^{N}\left[1 - Q_u\left(\sqrt{2\gamma_k}, \sqrt{\lambda}\right)\right] \quad (3.22)$$

B. Expression for average detection probability in Rayleigh fading environment

Assuming *N* i.i.d. number of Rayleigh faded S-channels, the average detection probability ($\overline{Q_d}$) expression using SLS diversity technique at FC is obtained as [110];

$$\overline{Q_d} = 1 - \prod_{k=1}^{N}\left(1 - \sum_{n=0}^{\infty} \frac{\Gamma\left(u+n, {}^{\lambda}/_{2}\right)}{\Gamma(u+n)n!}\left(\frac{\overline{\gamma_k}}{1+\overline{\gamma_k}}\right)^{n+1}\right) \quad (3.23)$$

C. Expression for average detection probability in Rician fading environment

If S-channel of CSS network is affected by Rician fading environment, the final expression for average detection probability ($\overline{Q_d}$) is given in [110] as;

$$\overline{Q_d} = 1 - \prod_{k=1}^{N}\left(1 - \frac{1+K}{\overline{\gamma_k}}\exp(-K)\sum_{n=0}^{\infty}\frac{\Gamma\left(u+n,\lambda/2\right)}{\Gamma(u+n)n!}\left(\frac{\overline{\gamma_k}}{1+K+\overline{\gamma_k}}\right)^{n+1}{}_1F_1\left[n+1;1;\frac{K(1+K)}{1+K+\overline{\gamma_k}}\right]\right) \quad (3.24)$$

D. Expression for average detection probability in Nakagami-*m* fading environment

In case of Nakagami-*m* fading environment, the average detection probability ($\overline{Q_d}$) expression is given in [112] as;

$$\overline{Q_d} = 1 - \prod_{k=1}^{N}\left(1 - A_1\sum_{n=1}^{u-1}\frac{(\lambda/2)^n}{n!}{}_1F_1(m;n+1;B) + C\left[\sum_{i=0}^{m-2}\left(\frac{m}{m+\overline{\gamma_k}}\right)^i L_i(-B) + DL_{m-1}(-B)\right]\right) \quad (3.25)$$

$A = \exp(-\lambda/2)\Big/\left(m/m+\overline{\gamma_k}\right)^m$, $B = \overline{\gamma_k}\lambda/2\left(m+\overline{\gamma_k}\right)$, $C = \overline{\gamma_k}\Big/\left(m+\overline{\gamma_k}\right)\exp(-B)$,

$D = \left(m+\overline{\gamma_k}/\overline{\gamma_k}\right)\left(m/m+\overline{\gamma_k}\right)^{m-1}$.

E. Expression for average detection probability in Hoyt fading environment

If S-channel of CSS network is affected by Hoyt fading environment, the average detection probability ($\overline{Q_d}$) expression is obtained as [112];

$$\overline{Q_d} = 1 - \prod_{k=1}^{N}\left(1 - \frac{1}{\sqrt{p\overline{\gamma_k}}}\sum_{n=0}^{\infty}\frac{\Gamma(u+n,\lambda/2)}{\Gamma(u+n)}\left(\frac{p\overline{\gamma_k}}{1+p\overline{\gamma_k}}\right)^{n+1}{}_2F_1\left[\frac{n+2}{2},\frac{n+1}{2};1;\frac{1-p}{\left(1+p\overline{\gamma_k}\right)^2}\right]\right) \quad (3.26)$$

F. Expression for average detection probability in Weibull fading environment

The expression for average detection probability using SLS diversity technique at FC when S-channel of CSS network is affected by Weibull fading environment is given in [112] as;

$$\overline{Q_d} = 1 - \prod_{k=1}^{N}\left(1 - (2\pi)^{\frac{1-c}{2}}\left[\frac{\Gamma(p)}{\overline{\gamma_k}}\right]^c\sum_{n=0}^{\infty}c^{n+c+\frac{1}{2}}\frac{\Gamma\left(u+n,\lambda/2\right)}{\Gamma(u+n)n!}G_{1,c}^{c,1}\left[\frac{1}{\left\{c\Gamma(p)/\overline{\gamma_k}\right\}^c}\middle|\begin{matrix}\frac{n+c}{c},\ldots\ldots,\frac{n+2c-1}{c}\\ \end{matrix}\right]\right) \quad (3.27)$$

3.3.4. Maximal Ratio Combining (MRC) Diversity Technique

The maximal ratio combining (MRC) scheme is a coherent detection technique which needs the channel state information. The need of channel state information in MRC diversity technique may increase the design complexity. The MRC receiver combines all diversity branches weighted with their corresponding complex fading gains. The instantaneous SNR of MRC combiner output is sum of the SNRs of all *N* i.i.d. diversity branches [64, 72].

A. Expression for average detection probability in Non-fading environment

In MRC scheme, all CRs send their sensing information of PU in the form of energy values with an appropriate weighting to FC. The weights are proportional to the received instantaneous S-channel SNR of each CR. The output of MRC combiner is the sum of the SNRs of all diversity branches (*N*). A new decision statistic Y_{MRC} occurs at the output of MRC scheme. Y_{MRC} is represented by $Y_{MRC}=\sum_{i=1}^{N} Y_i w_i$, where Y_i is the test statistic of the *i*-th branch and $w_i = \frac{\gamma_i}{\gamma_1+\gamma_2 \ldots \gamma_N}$ is the weighting factor appropriate to each branch. In case of Non-fading environment (AWGN channel), the expressions for false alarm (Q_f) and detection probabilities (Q_d) under the MRC scheme are provided in [72] as;

$$Q_{f,\mathrm{MRC}} = \frac{\Gamma\left(u, \lambda/2\right)}{\Gamma\left(u\right)} \tag{3.28}$$

$$Q_{d,\mathrm{MRC}} = Q_u\left(\sqrt{2\gamma_{MRC}}, \sqrt{\lambda}\right) \tag{3.29}$$

where $\gamma_{MRC}=\sum_{i=1}^{N} \gamma_i$, and γ_i denotes the instantaneous SNR at the output of MRC combiner.

B. Expression for average detection probability in Rayleigh fading environment

Assuming *N* i.i.d. number of Rayleigh faded S-channels, the average detection probability ($\overline{Q_d}$) expression using MRC diversity technique at FC is obtained as [110];

$$\overline{Q_d} = \sum_{n=0}^{\infty} \frac{\Gamma\left(u+n, \lambda/2\right)}{\Gamma\left(u+n\right) n!} \frac{\Gamma\left(N+n\right)}{\Gamma\left(N\right)} \left(\frac{\bar{\gamma}}{1+\bar{\gamma}}\right)^n \tag{3.30}$$

C. Expression for average detection probability in Rician fading environment

If S-channel of CSS network is affected by Rician fading environment, the final expression for average detection probability ($\overline{Q_d}$) is given in [110] as;

$$\overline{Q_d} = \left(\frac{1+K}{\bar{\gamma}+1+K} \right)^N \exp(-NK) \sum_{n=0}^{\infty} \frac{\Gamma\left(u+n, \lambda/2\right)}{\Gamma(u+n)n!} \frac{\Gamma(N+n)}{\Gamma(N)} \left(\frac{\bar{\gamma}}{1+K+\bar{\gamma}} \right)^n {}_1F_1\left[n+N; \mathrm{N}; \frac{NK(1+K)}{1+K+\bar{\gamma}} \right] \tag{3.31}$$

D. Expression for average detection probability in Nakagami-*m* fading environment

In case of Nakagami-*m* fading environment, the average detection probability ($\overline{Q_d}$) expression is obtained as [112];

$$\overline{Q_d} = \left(\frac{m}{m+\bar{\gamma}} \right)^{Nm} \sum_{n=1}^{u-1} \frac{\lambda^n \exp(-\lambda/2)}{n!2^n} {}_1F_1\left[Nm; n+1; \frac{\lambda\bar{\gamma}}{2\left(m+\bar{\gamma}\right)} \right] \frac{\bar{\gamma}}{m+\bar{\gamma}} \exp\left[-\frac{\lambda m}{m+\bar{\gamma}} \right] \left[\sum_{j=0}^{Nm-2} \left(\frac{m}{m+\bar{\gamma}} \right)^j L_j\left[-\frac{\lambda\bar{\gamma}}{2(m+\bar{\gamma})} \right] + \left(\frac{m+\bar{\gamma}}{\bar{\gamma}} \right) \left(\frac{m}{\bar{\gamma}+m} \right)^a L_{Nm-1}\left[-\frac{\lambda\bar{\gamma}}{2(m+\bar{\gamma})} \right] \right] \tag{3.32}$$

$L_n(.)$ is Laguerre polynomial of degree *n* [115, section 8.970].

E. Expression for average detection probability in Hoyt fading environment

If S-channel of CSS network is affected by Hoyt fading environment, the average detection probability ($\overline{Q_d}$) expression is given in [112] as;

$$\overline{Q_d} = \left(\frac{rq}{r+q} \right)^N \sum_{n=0}^{\infty} \frac{\Gamma(u+n, \lambda/2)}{\Gamma(u+n)n!} \frac{\Gamma(N+n)}{\Gamma(N)} \left(\frac{q}{r+q} \right)^n {}_2F_1\left[\frac{N}{2}, n+N; N; \frac{r\left(1-q^2\right)}{(r+q)} \right] \tag{3.33}$$

F. Expression for average detection probability in Weibull fading environment

The expression for average detection probability using MRC diversity technique at FC when S-channel of CSS network is affected by Weibull fading environment is [112];

$$\overline{Q_d} = \frac{(2\pi)^{\frac{1-c}{2}}}{\Gamma(N)\left(E\bar{\gamma}\right)^{Nc}} \sum_{n=0}^{\infty} c^{nN+c+\frac{1}{2}} \frac{\Gamma\left(u+n, \lambda/2\right)}{\Gamma(u+n)n!} G_{1,c}^{c,1}\left[\frac{\left(E\bar{\gamma}\right)^c}{c^c} \middle| \begin{matrix} 1 \\ \frac{\mathrm{n}+Nc}{c}, \ldots\ldots, \frac{\mathrm{n}+Nc+c-1}{c} \end{matrix} \right] \tag{3.34}$$

3.3.5. Equal Gain Combining (EGC) Diversity Technique

The equal gain combining (EGC) scheme is also a coherent detection technique which the needs channel state information. The EGC requires only the knowledge of the phase of a received signal which reduces the system complexity. In EGC scheme, the receiver combines all diversity branches weighted with their phase [64, 72].

A. Expression for average detection probability in Non-fading environment

In EGC, the measured energies are summed together with equal weights. The test statistics of EGC follows a central square or a non-central square distribution under H_0 and H_1 respectively. In case of Non-fading environment (AWGN channel), the expressions for false alarm (Q_f) and detection probabilities (Q_d) under the EGC scheme are provided in [72] as;

$$Q_{f,\mathrm{EGC}} = \frac{\Gamma\left(u, \lambda/2\right)}{\Gamma\left(u\right)} \tag{3.35}$$

$$Q_{d,\mathrm{EGC}} = Q_u\left(\sqrt{2\gamma_{EGC}}, \sqrt{\lambda}\right) \tag{3.36}$$

where γ_{EGC}=$\sum_{i=1}^{N}\gamma_i$, and γ_i denotes the instantaneous SNR at the output of EGC combiner.

B. Expression for average detection probability in Rayleigh fading environment

Assuming *N* i.i.d number of Rayleigh faded S-channels, the average detection probability ($\overline{Q_d}$) expression using EGC diversity technique at FC is derived as [114, Eq.(5.4)];

$$\overline{Q_{d,Ray}}\left(N, m, \bar{\gamma}, \lambda\right) = P_{d,Nak}\left(N, Nm, Nm\bar{\gamma}, N\lambda\right) \tag{3.37}$$

C. Expression for average detection probability in Rician fading environment

If S-channel of CSS network is effected by Rician fading environment, the final expression for average detection probability ($\overline{Q_d}$) is given in [113] as;

$$\overline{Q_{d|u=1}} = Q_N\left(\sqrt{\frac{2NK\bar{\gamma}}{1+K+\bar{\gamma}}}, \sqrt{\frac{\lambda\left(1+K\right)}{1+K+\bar{\gamma}}}\right) \tag{3.38}$$

D. Expression for average detection probability in Nakagami-*m* fading environment

In case of Nakagami-*m* fading environment, the average detection probability ($\overline{Q_d}$) expression is obtained as [113];

$$\overline{Q_d} = \alpha\left[A_1 + \beta\sum_{n=1}^{Nu-1}\frac{\left(\lambda/2\right)^n}{n!}{}_1F_1\left(mN; \mathrm{n}+1; \lambda\bar{\gamma}/2\left(m+\bar{\gamma}\right)\right)\right] \tag{3.39}$$

where α, β, and G_1 are given by

$$\alpha = \frac{1}{2^{Nm-1}\Gamma(Nm)}\left(\frac{m}{\bar{\gamma}}\right)^{Nm},\ \beta = \Gamma(Nm)\left(\frac{2\bar{\gamma}}{m+\bar{\gamma}}\right)^{Nm} e^{-\lambda/2},\ \varepsilon_n = \begin{cases} 1 & n < Nm-1 \\ 1+\dfrac{m}{\bar{\gamma}} & n < Nm-1 \end{cases}$$

$$G_1 = \left[2^{Nm-1}(Nm-1)!\left(\frac{\bar{\gamma}}{m}\right)^{Nm}\frac{\bar{\gamma}}{m+\bar{\gamma}}\exp\left(\frac{-\lambda m}{2(m+\bar{\gamma})}\right)\sum_{n=0}^{Nm-1}\varepsilon_n\left(\frac{m}{m+\bar{\gamma}}\right)L_n\left(\frac{-\lambda\bar{\gamma}}{2(m+\bar{\gamma})}\right)\right]$$

$L_n(.)$ is Laguerre polynomial of degree n [115, section 8.970].

The closed form of average detection probability expressions for Weibull and Hoyt fading channels using MRC diversity technique is complex to derive.

3.4. Results and Discussions

In this section, simulation results are drawn to calculate the average detection probability values using the complementary receiver operating characteristics (CROC) curves and average detection probability versus sensing channel SNR curves. The conventional energy detector and single antenna are used at each CR in the CSS network to analyze the performance. The average detection probability value is calculated using diversity techniques (SC, SLC, SLS, MRC, and EGC) in CSS network over different fading channels (Rayleigh, Rician, Nakagami-*m*, Weibull, and Hoyt).

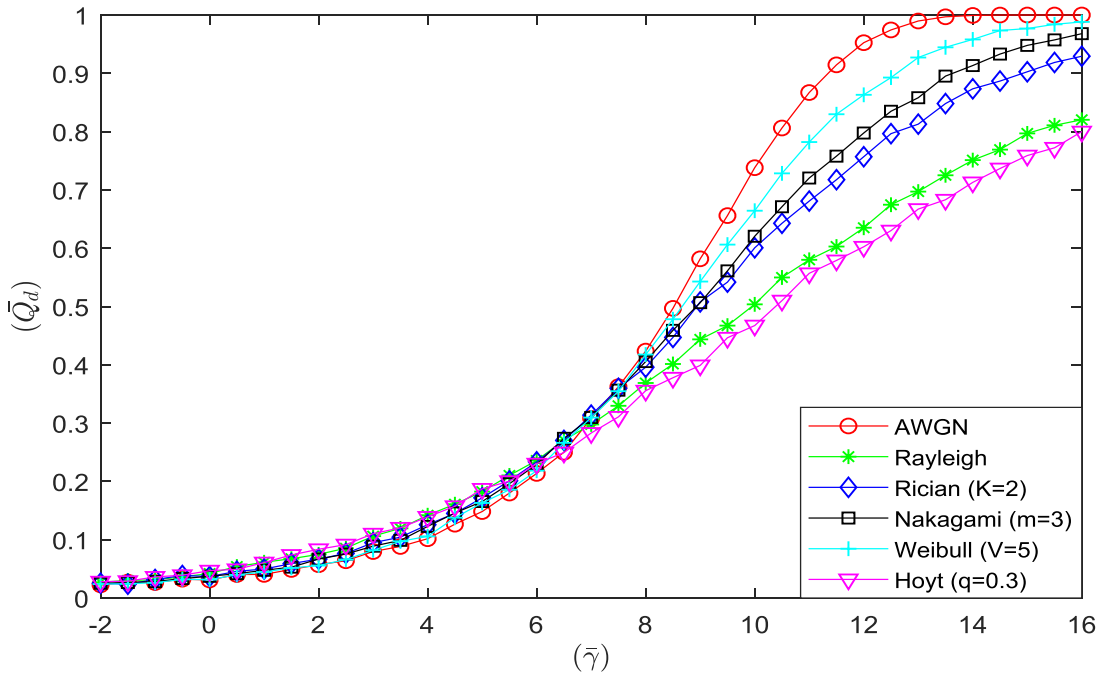

Fig.3.3. $\overline{Q_d}$ versus $\bar{\gamma}$ graphs for different fading channels using SC diversity technique.

In Fig.3.3, performance is drawn between average detection probability ($\overline{Q_d}$) and average sensing channel SNR ($\bar{\gamma}$) using selection combining (SC) diversity technique at FC when CSS network is affected by various fading environments. $\overline{Q_d}$ value increases with the increment of S-channel SNR because the increased $\bar{\gamma}$ value increases the signal strength and decreases the noise value present in S-channel. $\overline{Q_d}$ value is more with Non-fading environment and it decreases by introducing the fading effect. The network parameters such as time band width product u=10, probability of false alarm P_f=0.01, number of diversity branches N=3, various fading parameters such as Rician fading parameter K=2, Nakagami-m fading parameter m=3, Weibull fading parameter V=5, and Hoyt fading parameter q=0.3 are used in the simulation. As S-channel SNR value increases from $\bar{\gamma}$=8dB to $\bar{\gamma}$=10dB, $\overline{Q_d}$ value increases by 54.2% in Non-fading environment, it increases by 49.3% in Weibull fading channel, and it increases by 33.6% in Hoyt fading channel. From the above lines it can be concluded that the average detection probability value is more in Weibull fading and less in Hoyt fading environment in case of fading effect, whereas Non-fading environment achieves higher value of $\overline{Q_d}$ compared to the fading environment.

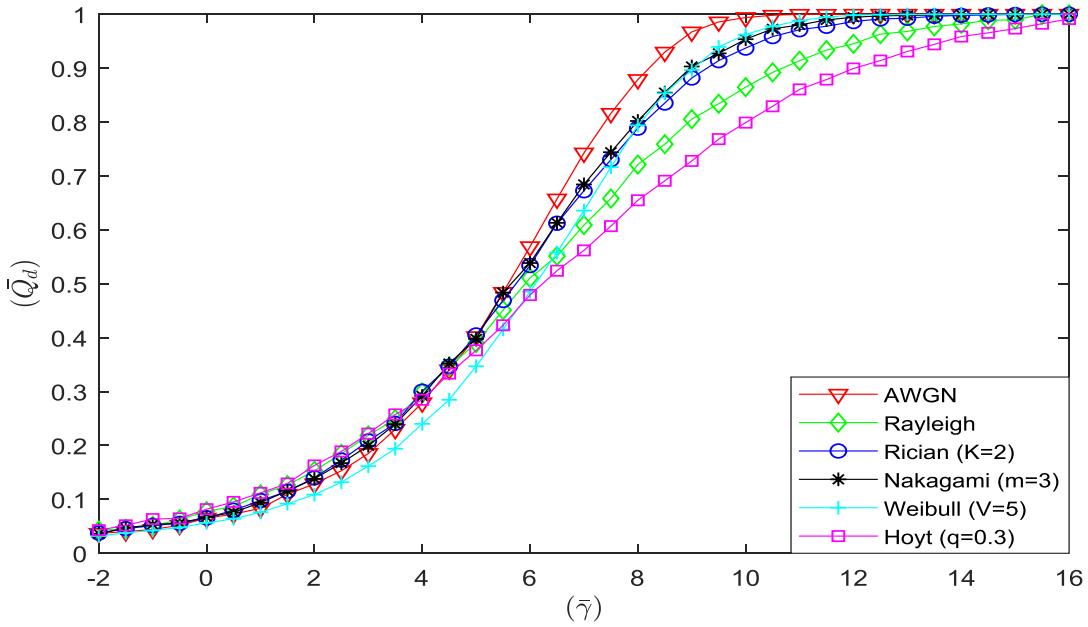

Fig.3.4. $\overline{Q_d}$ versus $\bar{\gamma}$ graphs for different fading channels using SLC diversity technique.

In Fig.3.4, the performance statistic is drawn between $\overline{Q_d}$ and $\bar{\gamma}$ curves using square law combining (SLC) diversity technique at FC over various fading environments. The network parameters such as u=10, P_f=0.01, N=3, various fading parameters such as K=2, m=3, V=5, and q=0.3 are used in the simulation. As S-channel SNR value increases from $\bar{\gamma}$=8dB to

$\bar{\gamma}$=10dB, $\overline{Q_d}$ value increases by 64.6% in Non-fading environment, it increases by 60.7% in Weibull fading channel, and it increases by 45.1% in Hoyt fading channel. In this case also, detection probability value is more in Weibull fading and less in Hoyt fading environment, where as Non-fading environment achieves higher value of $\overline{Q_d}$ compared to the fading environment, and a similar phenomenon is observed with other diversity techniques also.

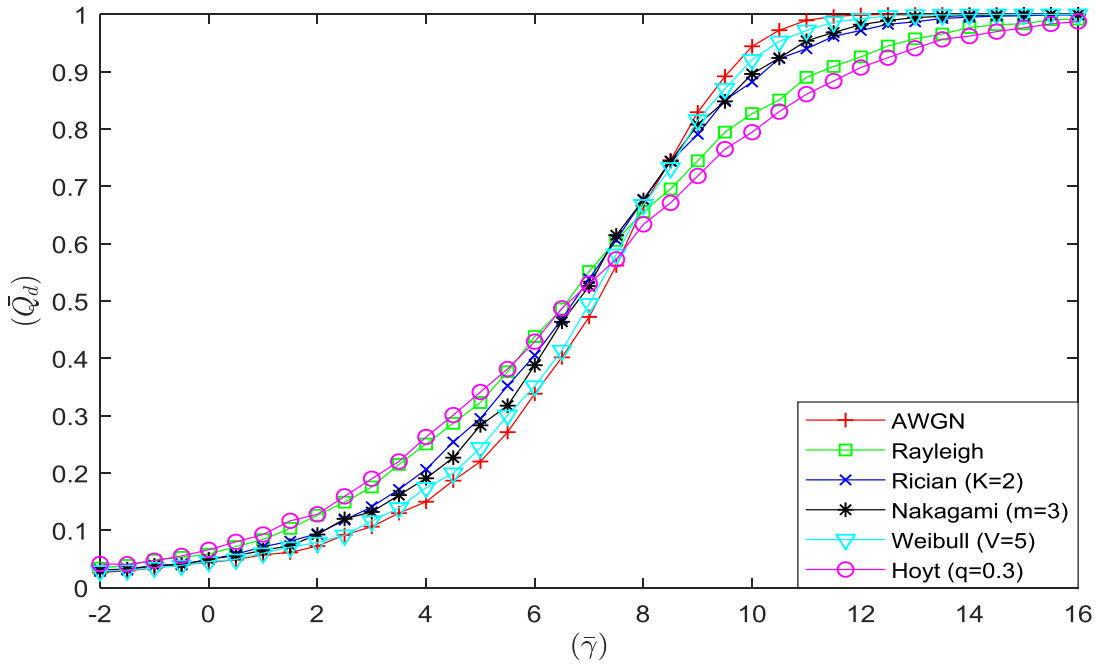

Fig.3.5. $\overline{Q_d}$ versus $\bar{\gamma}$ graphs for different fading channels using SLS diversity technique.

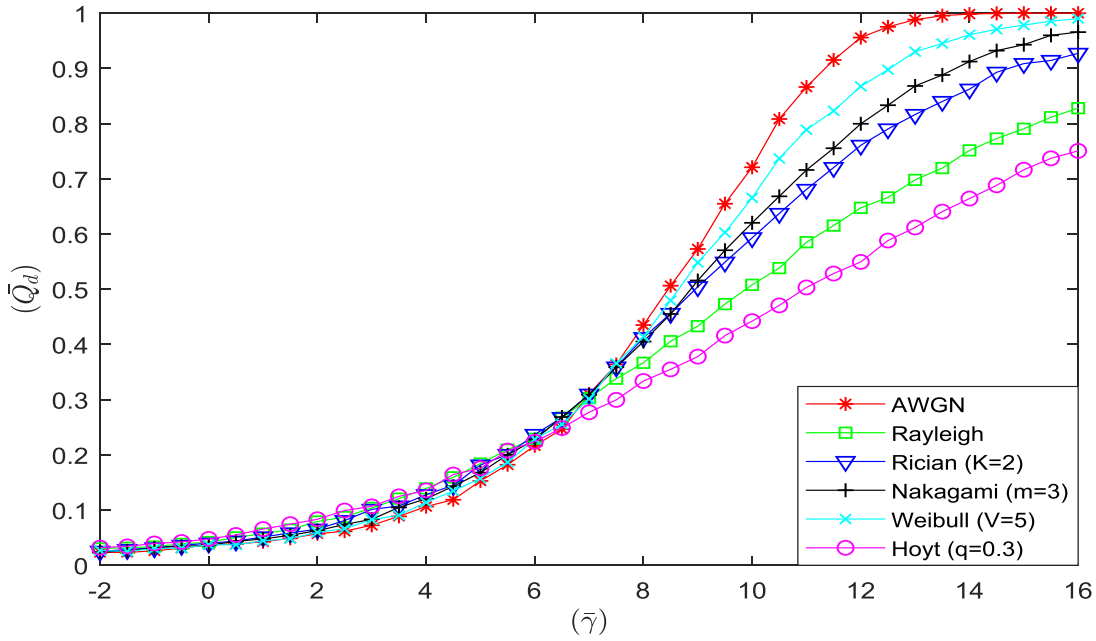

Fig.3.6. $\overline{Q_d}$ versus $\bar{\gamma}$ graphs for different fading channels using MRC diversity technique.

A similar performance ($\overline{Q_d}$ vs $\bar{\gamma}$) is evaluated in Fig.3.5 also using the square law selection (SLS) combining diversity technique at FC when CSS network is affected by various fading environments. The network parameters such as u=10, P_f=0.01, N=3, various fading parameters such as K=2, m=3, V=5, and q=0.3 are used in the simulation. Due to the high probability of false alarm in SLS diversity technique, for lower values of S-channel SNRs, detection probability value is less, and $\overline{Q_d}$ value increases at higher S-channel SNRs. As S-channel SNR value increases from $\bar{\gamma}$=8dB to $\bar{\gamma}$=10dB, $\overline{Q_d}$ value increases by 60.7% in Non-fading environment, it increases by 54.5% in Weibull fading channel, and it increases by 37.2% in Hoyt fading channel.

In Fig.3.6, $\overline{Q_d}$ vs average S-channel SNR performance is evaluated using maximal ratio combining (MRC) diversity technique at FC over different fading environments. The network parameters such as u=10, P_f=0.01, N=3, various fading parameters such as K=2, m=3, V=5, and q=0.3 are used in the simulation. As S-channel SNR value increases from $\bar{\gamma}$=8dB to $\bar{\gamma}$=10dB, $\overline{Q_d}$ value increases by 73.2% in Non-fading environment, it increases by 64.2% in Weibull fading channel, and it increases by 52.3% in Hoyt fading environment.

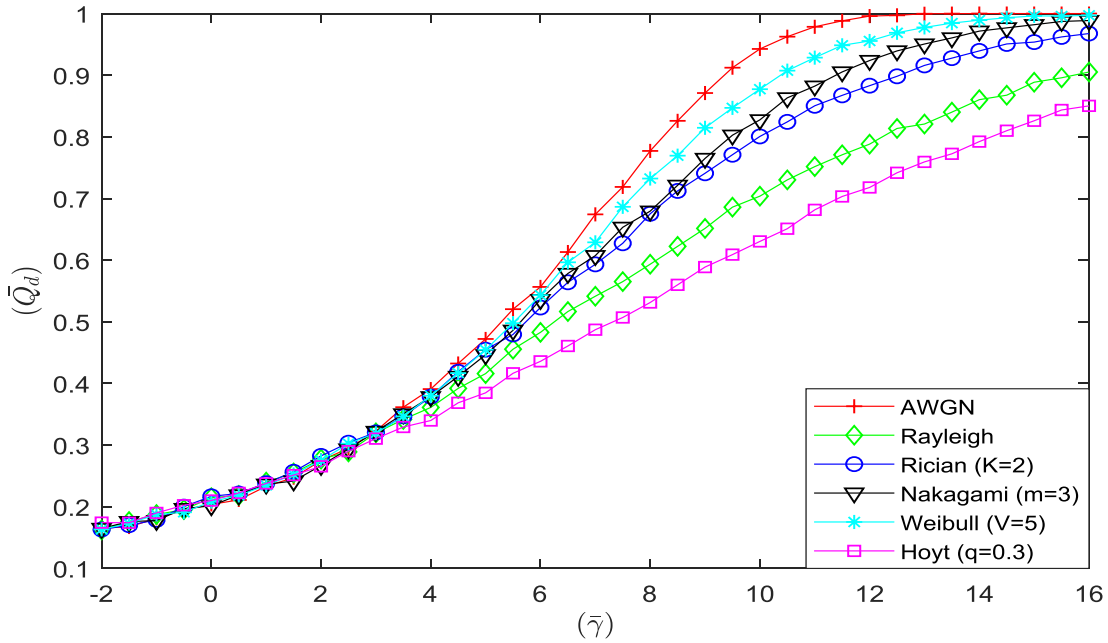

Fig.3.7. $\overline{Q_d}$ versus $\bar{\gamma}$ graphs for different fading channels using EGC diversity technique.

In Fig.3.7, $\overline{Q_d}$ vs average S-channel SNR performance is evaluated using equal gain combining (EGC) diversity technique at FC over different fading environments. The network parameters such as u=10, P_f=0.01, N=3, various fading parameters such as K=2, m=3, V=5,

and q=0.3 are used in the simulation. As S-channel SNR value increases from $\bar{\gamma}$=8dB to $\bar{\gamma}$=10dB, $\overline{Q_d}$ value increases by 76.1% in Non-fading environment, it increases by 67.1% in Weibull fading channel, and it increases by 54.3% in Hoyt fading environment.

In Fig.3.8, performance is analyzed with CROC curves which are drawn between average missed detection probability ($\overline{Q_m}$) and average probability of false alarm ($\overline{Q_f}$) using SC diversity technique at FC over various fading environments. As $\overline{Q_f}$ value increases, $\overline{Q_m}$ value decreases. The network parameters such as u=10, $\bar{\gamma}$=5dB, 6dB and 7dB, N=3, various fading parameters such as K=2, m=3, V=5, and q=0.3 are used in the simulation. $\overline{Q_m}$ value is more in Hoyt fading and less in Weibull fading environment, where as Non-fading environment achieves lower value of $\overline{Q_m}$ compared to fading environment. As the average probability of false alarm value increases from $\overline{Q_f}$=0.1 to $\overline{Q_f}$=0.2, $\overline{Q_m}$ value decreases by 32.2% in Weibull fading channel, it decreases by 19.9% in Hoyt fading channel, and it decreases by 38.4% in Non-fading environment. From the above lines it can be concluded that $\overline{Q_m}$ value increases with fading effect.

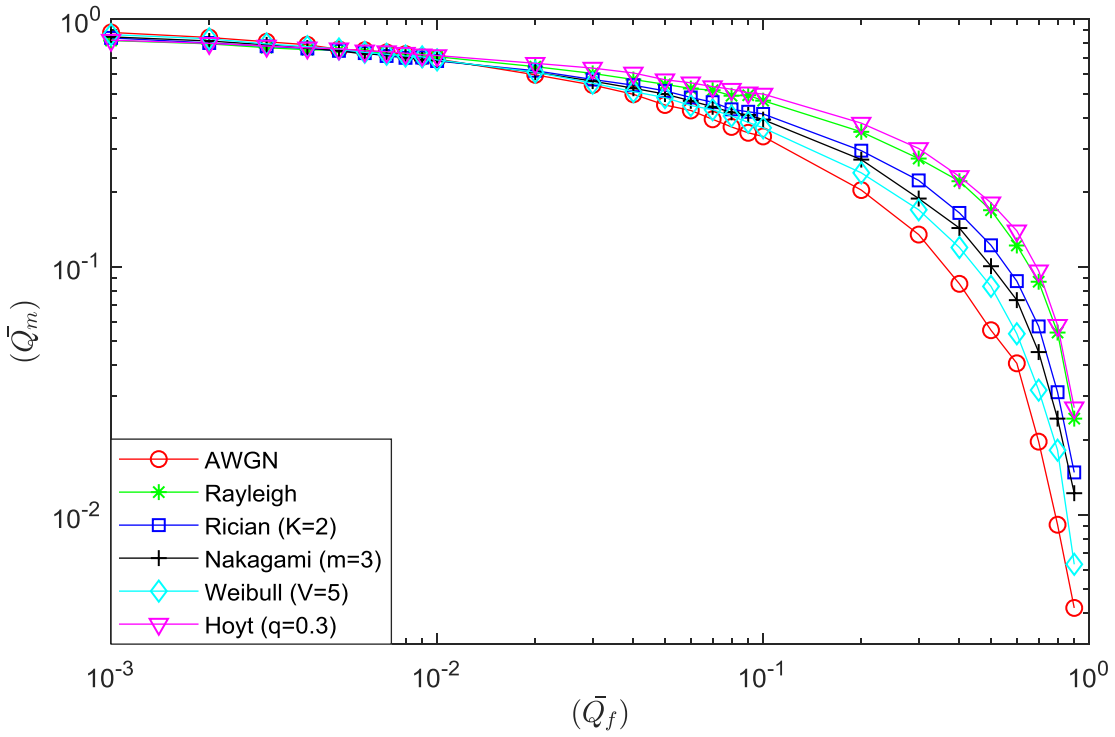

Fig.3.8. CROC graphs for different fading channels using SC diversity technique.

In Fig.3.9, performance is drawn between $\overline{Q_m}$ and $\overline{Q_f}$ values using SLC diversity technique at FC over various fading environments. As the average probability of false alarm value increases, average missed detection probability value decreases. The network parameters

such as u=10, $\bar{\gamma}$=5dB, 6dB and 7dB, N=3, various fading parameters such as K=2, m=3, V=5, and q=0.3 are used in the simulation. $\overline{Q_m}$ value is more in Hoyt fading and less in Weibull fading environment in case of fading while Non-fading environment achieves lower value of $\overline{Q_m}$ compared to fading environment, and a similar phenomenon is observed with other diversity techniques also. As the average probability of false alarm value increases from $\overline{Q_f}$=0.1 to $\overline{Q_f}$=0.2, $\overline{Q_m}$ value decreases by 47.5% in Weibull fading channel, it decreases by 22.9% in Hoyt fading channel, and it decreases by 59.8% in Non-fading environment. $\overline{Q_m}$ value less in Non-fading environment compared to fading environment.

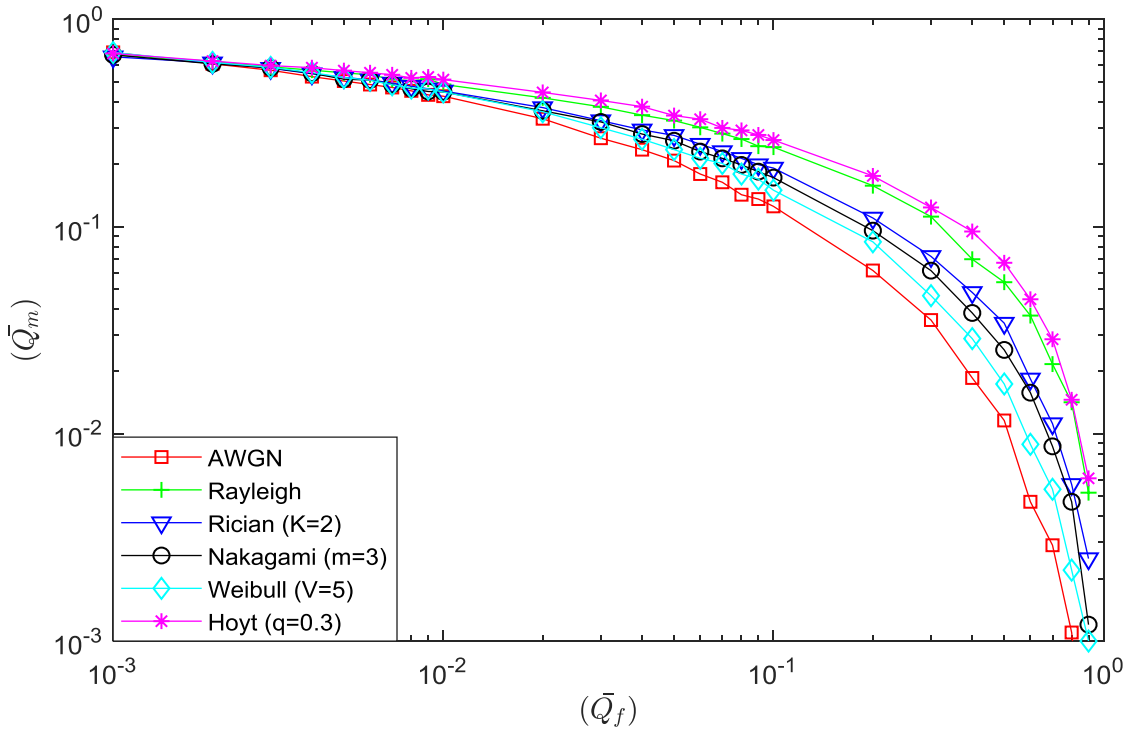

Fig.3.9. CROC graphs for different fading channels using SLC diversity technique.

In Fig.3.10, simulation is drawn to calculate average missed detection probability value using SLS diversity technique at FC over various fading environments. As the average probability of false alarm value increases, average missed detection probability value decreases. The network parameters such as u=10, $\bar{\gamma}$=5dB, 6dB and 7dB, N=3, various fading parameters such as K=2, m=3, V=5, and q=0.3 are used in the simulation. As the average probability of false alarm value increases from $\overline{Q_f}$=0.1 to $\overline{Q_f}$=0.2, $\overline{Q_m}$ value decreases by 42.2% in Weibull fading channel, it decreases by 21.6% in Hoyt fading channel, and it decreases by 51.7% in Non-fading environment.

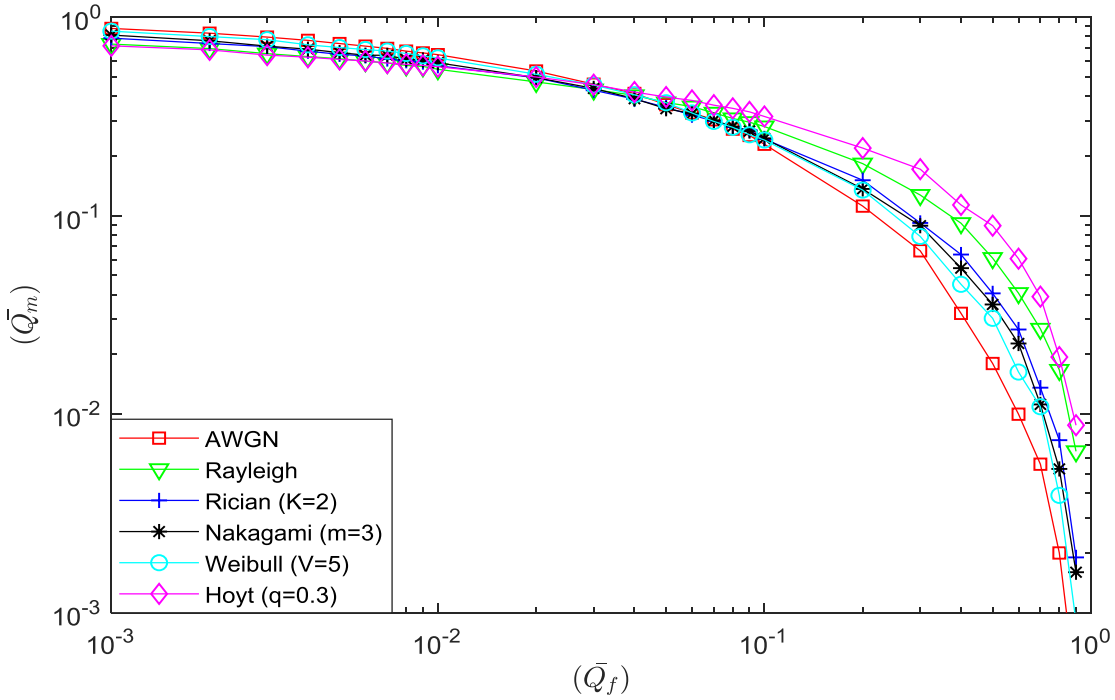

Fig.3.10. CROC graphs for different fading channels using SLS diversity technique.

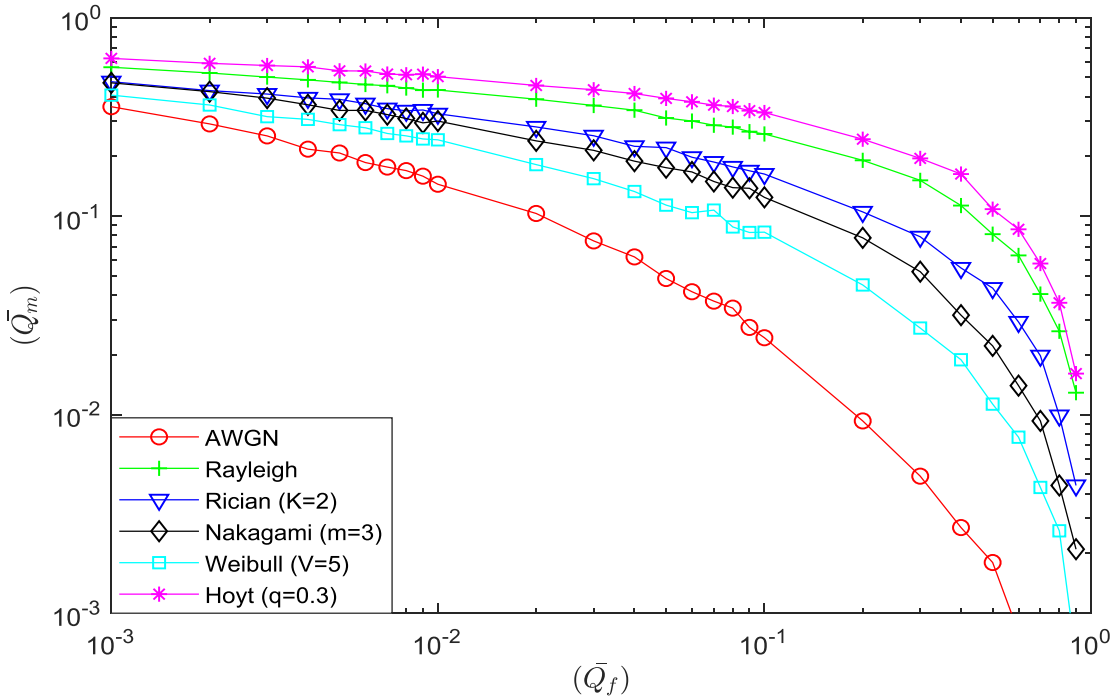

Fig.3.11. CROC graphs for different fading channels using MRC diversity technique.

Similar performance ($\overline{Q_m}$ vs $\overline{Q_f}$) is evaluated in Fig.3.11 also using MRC diversity technique at FC over various fading environments. As the average probability of false alarm value increases, average missed detection probability value decreases. The network parameters

such as u=10, $\bar{\gamma}$=5dB, 6dB and 7dB, N=3, various fading parameters such as K=2, m=3, V=5, and q=0.3 are used in the simulation. As the average probability of false alarm value increases from $\overline{Q_f}$=0.1 to $\overline{Q_f}$=0.2, $\overline{Q_m}$ value decreases by 49.7% in Weibull fading channel, it decreases by 26.6% in Hoyt fading channel, and it decreases by 61.8% in Non-fading the environment.

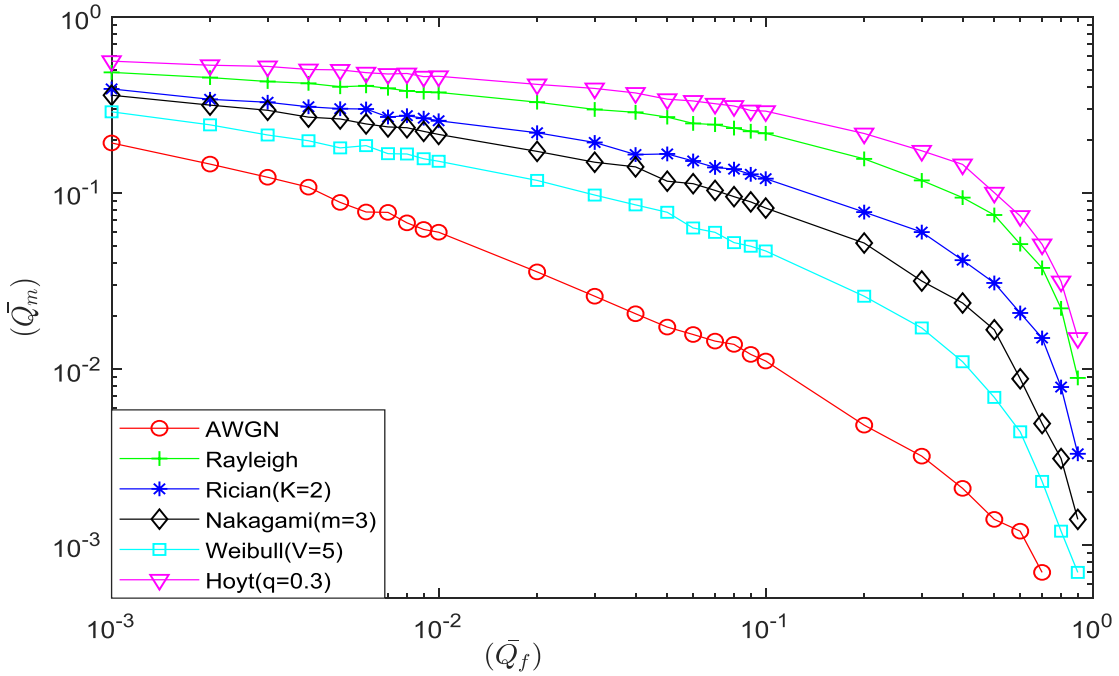

Fig.3.12. CROC graphs for different fading channels using EGC diversity technique.

Similar performance ($\overline{Q_m}$ vs $\overline{Q_f}$) is evaluated in Fig.3.12 also using EGC diversity technique at FC over various fading environments. As the $\overline{Q_f}$ value increases, $\overline{Q_m}$ value decreases. The network parameters such as u=10, $\bar{\gamma}$=7dB, N=3, and various fading parameters such as K=2, m=3, V=5, and q=0.3 are used in the simulation. As the average probability of false alarm value increases from $\overline{Q_f}$=0.1 to $\overline{Q_f}$=0.2, $\overline{Q_m}$ value decreases by 54.6% in Weibull fading channel, it decreases by 31.3% in Hoyt fading channel, and it decreases by 65.7% in Non-fading environment.

In table 3.1, average detection probability values are noted from simulations which are drawn for various diversity techniques over different fading environments. The network parameters such as u=10, P_f=0.1, N=3, various fading parameters such as K=2, m=3, V=5, and q=0.3 are used in the simulation. From table 3.1, we can conclude that SC diversity gives lower $\overline{Q_d}$ value and EGC diversity gives higher $\overline{Q_d}$ value. The average detection probability value decreases with fading effect present in the environment.

Diversity techniques	Non-fading environment (AWGN)	Rayleigh fading	Rician fading	Nakagami-*m* fading	Weibull fading	Hoyt fading
	Average detection probability ($\overline{Q_d}$) values					
SC	0.6639	0.5312	0.5857	0.6069	0.6358	0.5014
SLS	0.7911	0.7189	0.7328	0.757	0.7789	0.6841
SLC	0.8748	0.7407	0.8084	0.8277	0.8502	0.7184
MRC	0.9756	0.7583	0.8371	0.8757	0.9170	0.6675
EGC	0.9889	0.782	0.8796	0.918	0.9532	0.7087

Table.3.1. $\overline{Q_d}$ values for various diversity techniques in different fading environments.

3.5. Conclusions

In this chapter, we have evaluated the performance of the cooperative spectrum sensing (CSS) network under different soft data combining techniques in various fading environments. The performance is analyzed using complementary receiver operating characteristics (CROC) curves and sensing channel SNR versus average detection probability curves. The average detection probability ($\overline{Q_d}$) and average missed detection probability ($\overline{Q_m}$) values are calculated using different diversity techniques such as SC, SLC, SLS, MRC, and EGC over various fading channels like Rayleigh, Rician, Nakagami-*m*, Hoyt, and Weibull fading environments in CSS network. To draw the simulations, a numerical framework for CSS network with soft data schemes in a wide variety of fading scenarios is presented.

The average detection probability values are calculated using different diversity techniques over various fading environments to identify which diversity technique gives higher detection probability value. It is observed from the simulations that detection performance is improved with soft data techniques in the presence of fading environments. From the simulation, we can conclude that selection combining diversity gives lower $\overline{Q_d}$ value and equal gain combining diversity technique gives higher $\overline{Q_d}$ value. The Non-fading environment gives higher $\overline{Q_d}$ value and its value decreases by introducing the fading effect. In case of fading environment, $\overline{Q_d}$ value is higher in Weibull fading environment and lower in Hoyt fading environment.

Chapter-4

Performance Analysis of CSS Network using Censoring Schemes

4.1. Introduction

The cooperative spectrum sensing (CSS) network has been proposed to overcome the drawbacks present in spectrum sensing network and to improve the detection probability when fading and shadowing effects are present. With the cooperation of multiple SUs in the CSS network, detection probability increases and hidden terminal problem also eliminated. The final decision about the PU is made at FC using various fusion rules. The conventional energy detector (CED) scheme is frequently used to identify the vacant bands of the spectrum because it is easy to implement, system complexity is less, and non-coherent [10, 54]. In [15], authors showed that improvement in detection performance using CSS network in different fading channels. Most of the literature dealt while sensing channel (S-channel) is faded with different fading environments and reporting channel (R-channel) is considered as an ideal channel [57-61]. In practice, both S-channel and R-channel are faded and noisy. Though the CSS network improves the detection performance even in the presence of shadowing and fading effects, due to heavily faded radio links in R-channel, the information received at the FC is likely to be erroneous. So, it is better to eliminate these heavily faded CRs in R-channel to improve the detection probability.

The censoring schemes [95] are used to eliminate the heavily faded radio links in R-channel. Two different types of censoring schemes are available in the literature such as Rank based censoring scheme and Threshold based censoring scheme [24]. These censoring techniques are used to eliminate the heavily faded CR links so that complexity of the network

is reduced and detection probability of PU is improved. Censoring techniques are also used to eliminate the trade-off between energy efficiency and detection probability.

In this chapter, we discuss the performance evaluation of missed detection probability and total error probability using the censoring techniques in R-channel of CSS network when it is affected by different fading environments such as Rician, Weibull, and Hoyt fading effects. The performance is evaluated using the conventional energy detection (CED) scheme and a single antenna at each CR in CSS network with perfect and imperfect reporting channel estimations. We have considered both S-channel and R-channel of CSS network are affected by Rician, Weibull, and Hoyt fading channels respectively. The Rank based and Threshold based censoring schemes are used to eliminate the heavily faded R-channel links in CSS network. The final decision about the primary user is made at fusion center using the hard decision fusion rule (Majority logic) and soft data fusion rule (MRC Rule) individually.

Furthermore, the performance of soft decision-based fusion rule is compared with hard decision-based fusion rule under the impact of channel nature (perfect/imperfect). Estimation techniques are used on fading coefficients to characterize the channel present between CRs and FC. The closed-form of expression for the estimation error in the imperfect R-channel is derived for various fading channels such as Rician, Weibull, and Hoyt fading environments. The mean and variance expressions of estimation error are derived for each fading channels. Simulations are carried out to know the missed detection probability (Q_m) and total error probability $\left(Q_m + Q_f\right)$ performance for both perfect and imperfect channel estimations by varying the network parameters such as sensing channel SNR, reporting channel SNR, false alarm probability (P_f), Rician fading parameter (K), Hoyt fading parameter (q), number of CR users (N), and censoring threshold value (C_{th}).

4.2. System Model

Figure 4.1 shows the system model of conventional energy detection (CED) technique. The complete description about the CED scheme is provided in section 3.2.

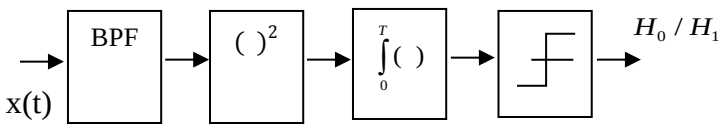

Fig 4.1. Block diagram of conventional energy detector.

The expressions for probability of false alarm (P_f), probability of detection (P_d), and missed detection probability (P_m) over AWGN channel are given in [10] as;

$$P_d = (\mathrm{Y} > \lambda \,|\, \mathrm{H}_1) = Q_u(\sqrt{2\gamma}, \sqrt{\lambda}) \tag{4.1}$$

$$P_f = (\mathrm{Y} > \lambda \,|\, \mathrm{H}_0) = \frac{\Gamma\left(\mathrm{u}, \frac{\lambda}{2}\right)}{\Gamma(\mathrm{u})} \tag{4.2}$$

$$P_m = 1 - P_d \tag{4.3}$$

In Eq.(4.1), Q_u represents the marcum-Q function [107], in Eq.(4.2), $\Gamma(\,,)$ represents incomplete gamma function, and $\Gamma(\,)$ represents the upper complete gamma function [108].

Figure 4.2 shows the cooperative spectrum sensing (CSS) network model. Using this network, PU is detected by the cooperation of multiple CRs. This network consists of sensing channel (S-channel), reporting channel (R-channel), multiple CRs, a PU, and an FC. Due to the deep fading effect in R-channel, radio links present in CSS network are heavily faded so that information associated with CRs is corrupted. The information received from these CRs at FC is erroneous. Hence, censoring schemes are applied to eliminate these CRs to improve the detection probability and to reduce the system complexity.

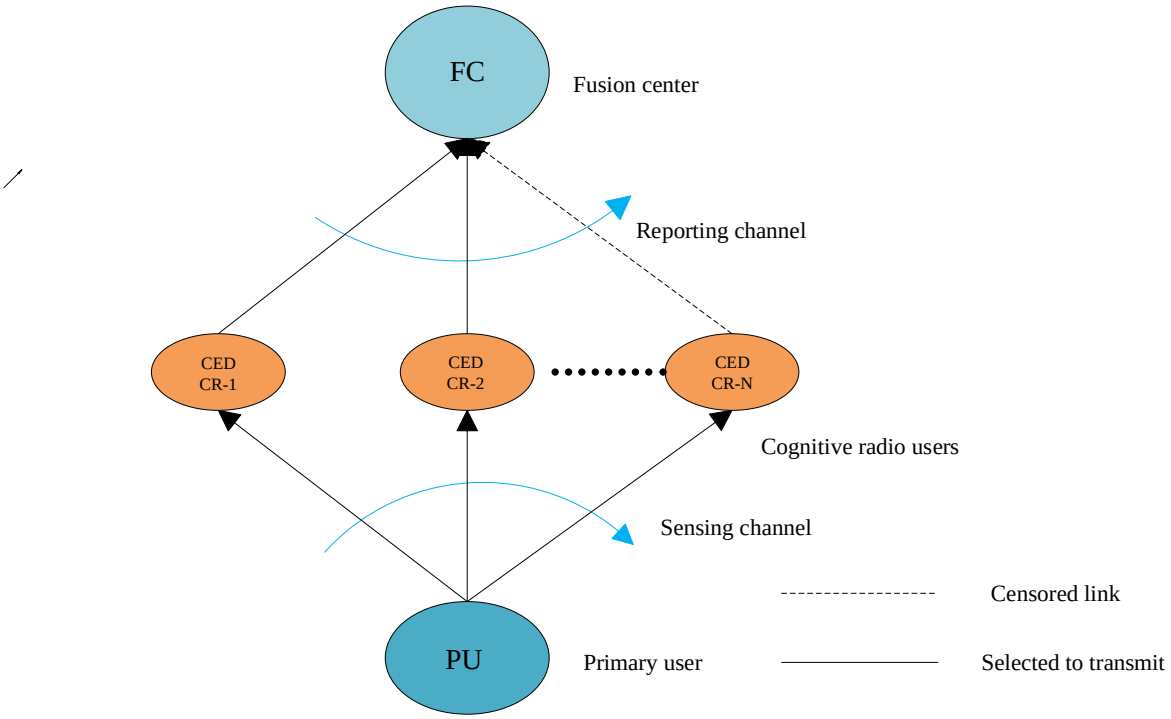

Fig 4.2. Cooperative spectrum sensing network model with censored CRs.

4.2.1. Rician Fading Channel

We have considered the Rician fading in both the channels of CSS network. If the signal present in a channel follows a Rician distribution, then all the fading coefficients also follows a Rician fading effect. The PDF of Rician fading is given in [10, 64] as;

$$f(y)=\frac{K+1}{\bar{\gamma}}\exp\left(-K-\frac{(K+1)y}{\bar{\gamma}}\right)*I_0\left(2\sqrt{\frac{K(1+\mathrm{K})y}{\bar{\gamma}}}\right) \tag{4.4}$$

where $\bar{\gamma}$ is average S-channel SNR and *K*-is Rician fading parameter. The average detection probability for Rician channel $(P_{d,Ric})$ is given in [10] as;

$$\bar{P}_{d,Ric}\,|_{u=1}=Q\left(\sqrt{\frac{2K\bar{\gamma}}{k+1+\bar{\gamma}}},\sqrt{\frac{\lambda(K+1)}{k+1+\bar{\gamma}}}\right) \tag{4.5}$$

4.2.2. Hoyt Fading Channel

If both the channels of CSS network are affected by Hoyt fading, then the entire fading coefficients follows a Hoyt distribution. The PDF of Hoyt distribution is given by [64, 67];

$$f_\alpha(\alpha)=\frac{(1+\mathrm{q}^2)\alpha}{q\Omega}\exp\left(-\frac{(1+\mathrm{q}^2)^2\alpha^2}{4q^2\Omega}\right)I_0\left(\frac{(1-\mathrm{q}^4)\alpha^2}{4q^2\Omega}\right)\quad \alpha\geq 0 \tag{4.6}$$

where $I_0(.)$ is the zeroth-order modified Bessel function of the first kind and *q* represents the Hoyt fading parameter which ranges from 0 to 1. If we substitute *q*= 1 in Eq. (4.6), PDF of Hoyt distribution reduces to Rayleigh distribution expression.

Let's consider $\sigma_1=\sqrt{\frac{\Omega q^2}{1+q^2}}$ and $\sigma_2=\sqrt{\frac{\Omega}{1+q^2}}$, then Eq.(4.6) reduces to

$$f_\alpha(\alpha)=\frac{\alpha}{\sigma_1\sigma_2}\exp\left(-\frac{\alpha^2}{4}\left(\frac{1}{\sigma_1^2}+\frac{1}{\sigma_2^2}\right)\right)I_0\left(\frac{\alpha^2}{4}\left(\frac{1}{\sigma_1^2}-\frac{1}{\sigma_2^2}\right)\right)\alpha\geq 0 \tag{4.7}$$

Missed detection probability expression for Hoyt fading channel is [67];

$$P_m=\frac{1}{16}\left[1+\exp(-\mathrm{A}\,\lambda^{2/p})\,\mathrm{I}_0(\mathrm{B}\,\lambda^{2/p})-2\,\mathrm{Q}(\mathrm{u}_1,\mathrm{v}_1)\right] \tag{4.8}$$

where

$$A=\left(\frac{1}{4}\right)\left(\frac{1}{\sigma_2^2}+\frac{1}{\sigma_1^2}\right),\ B=\left(\frac{1}{4}\right)\left(\frac{1}{\sigma_2^2}-\frac{1}{\sigma_1^2}\right),\ u_1=\sqrt{\left(A-\sqrt{A^2-B}^2\right)\lambda^{2/p}},V_1=\sqrt{\left(A+\sqrt{A^2-B}^2\right)\lambda^{2/p}}$$

4.2.3. Weibull Fading Channel

If both the channels of CSS network are affected by Weibull faded, then the entire fading coefficients follows a Weibull distribution. The PDF of Weibull distribution is given by [116];

$$f_{\gamma}(\gamma) = c\left[\frac{\Gamma(\mathrm{P})}{\bar{\gamma}}\right]^{c} \gamma^{c-1} \exp\left[-\left\{\frac{\gamma\Gamma(\mathrm{P})}{\bar{\gamma}}\right\}^{c}\right] \qquad \gamma \geq 0 \tag{4.9}$$

where $= {}^{V}/_{2}$, $P = 1 + {}^{1}/_{C}$, and *V*- is weibull fading parameter.

The average detection probability for Weibull channel $\left(P_{d,Wei}\right)$ is given in [117] as;

$$\overline{P_{d,wei}} = \sum_{n=0}^{u-1} \frac{\lambda^{l} e^{\lambda/2}}{2^{l}\, \mathrm{l}!} + \sum_{n=0}^{\infty} \frac{(-1)^{\mathrm{l}} \lambda^{u} A^{l}}{2^{u} \bar{\gamma}^{\frac{lv}{2}} u!\mathrm{l}! e^{\lambda/2}} \Gamma\left(\frac{lV}{2}+1\right) {}_{1}F_{1}\left(\frac{lV}{2}+1, u+1, \frac{\lambda}{2}\right) \tag{4.10}$$

where $A = \left[\Gamma\left(1+\frac{2}{V}\right)\right]^{V/2}$.

4.3. Fusion Rules

4.3.1. Majority Logic Fusion Rule

Majority logic is a hard decision fusion rule. If FC receives sensing information in the form of one-bit data (either 0 or 1) from all CRs, then the final decision about the PU can be made at FC using majority logic. Because of censoring schemes in the R-channel, out of *P* CRs in the network only *k* numbers of CRs are selected to transmit the data to FC through R-channel. The received decision is denoted as [87];

$$u_{k} = \begin{cases} 1 & \textit{if the received decision is} \quad H_{1} \\ 0 & \textit{if the received decision is} \quad H_{0} \end{cases} \tag{4.11}$$

where $k \in \{1,2,.....P\}$. Finally, majority logic can be applied at FC with the help of following expression [87];

$$u_{0} = \Gamma\left(u_{1} \ldots .. u_{p}\right) = \begin{cases} H_{1} & \text{if } \sum_{k=1}^{\mathrm{P}} u_{k} \geq \frac{\mathrm{P}}{2}+1 \\ H_{0} & \text{if } \sum_{k=1}^{\mathrm{P}} u_{k} < \frac{\mathrm{P}}{2}+1 \end{cases} \tag{4.12}$$

4.3.2. Maximal Ratio Combining (MRC) Rule

The MRC rule is a soft decision fusion rule. If FC receives the sensing information in the form of energy values, then the final decision about the PU can be made using MRC Rule. The expression for selecting the CRs using MRC logic is given in [91] as;

$$\wedge = \prod_{k=1}^{P} \frac{f\left(y_{k,d} \mid H_1\right)}{f\left(y_{k,d} \mid H_0\right)} \tag{4.13}$$

$$= \prod_{k=1}^{P} \frac{P_{d_k} + \left(1 - P_{d_k}\right) e^{\frac{-4\sqrt{E_b}}{\sigma_w^2} \mathrm{Re}\left(y_{k,d}\, h_k^*\right)}}{P_{d_k} + \left(1 - P_{f_k}\right) e^{\frac{-4\sqrt{E_b}}{\sigma_w^2} \mathrm{Re}\left(y_{k,d}\, h_k^*\right)}} \tag{4.14}$$

where $$\sigma_w^2 = E_b \sigma_{\tilde{h}}^2 + \sigma_n^2 = \frac{E_b \sigma_n^2}{E_b + \sigma_n^2} + \sigma_n^2 \tag{4.15}$$

For the perfect channel, the variance of estimated channel coefficient ($\sigma_{\tilde{h}}^2$) value is zero. Then, Eq. (4.15) reduces to $\sigma_w^2 = \sigma_n^2$.

Applying *logarithm* on both sides to Eq. (4.14), after simplification, it reduces to

$$\wedge_1 = \log(\wedge) = \frac{2\sqrt{E_b}}{\sigma_w^2} \sum_{k=1}^{K} (\mathrm{P}_{d_k} - \mathrm{P}_{f_k})\, \mathrm{Re}(\mathrm{y}_{\mathrm{k,d}}\, h_k^*) \tag{4.16}$$

If the selected CRs have identical local performances, then $\wedge_1$ can be further simplified as follows

$$\wedge_{MRC} = \sum_{k=1}^{K} \mathrm{Re}\left(y_{k,d}\, h_k^*\right) \tag{4.17}$$

h_k^* is the complex conjugate of h_k. At FC decision can be taken in favor of H_0 or H_1 by comparing $\wedge_{MRC}$ with the threshold value.

4.4. Censoring in Reporting Channel

The decision about the PU is passed to the FC in the form of BPSK signal through the fading environment of R-channel. The signal received from *k-th* CR at FC is

$$y_k = h_k m_k + n_k \tag{4.18}$$

where m_k is BPSK signal, m_k ε $(\sqrt{E_b}, -\sqrt{E_b})$ for H_1 and H_0 respectively. Let us assume that n_k and h_k are mutually independent. The fading coefficients (h_k) present in the R-channel are estimated by minimum mean square estimation (MMSE) strategy as follows [91];

$$\hat{h_k} = E\left[h_k / y_k\right] = y_k \frac{\sqrt{E_b}}{E_b + \sigma_n^2} \tag{4.19}$$

substituting Eq. (4.18) in Eq. (4.19)

$$\hat{h_k} = \frac{E_b}{E_b + \sigma_n^2} h_k + \frac{\sqrt{E_b}}{E_b + \sigma_n^2} n_k \tag{4.20}$$

In the above equation, $\hat{h_k}$ represents the estimated value of fading coefficient (h_k) after using MMSE estimation and E_b represents the bit energy of R-channel radio link. Finally, the channel estimation error ($\tilde{h_k}$) can be calculated as;

$$\tilde{h_k} = h_k - \hat{h_k} \tag{4.21}$$

We have assumed that the estimation error has zero mean complex Gaussian random variable and variance value is [91]

$$\sigma_{\tilde{h}}^2 = \left(\frac{E_b}{\sigma_n^2} + 1 \right)^{-1} \tag{4.22}$$

4.4.1. Estimation Error in Rician Fading Channel

For *k*-th Rician faded R-channel, the actual fading coefficient h_k can be expressed in terms of in-phase h_{kI} and quadrature h_{kQ} components as;

$$h_k = \left(h_{kI} + j h_{kQ} \right)^{1/2} \tag{4.23}$$

The mean and variance of h_k, when it follows Rician distribution are [64];

$$\mu_{h,Rice} = E\left[h_k\right] = \sigma \sqrt{\frac{\pi}{2}} L_{1/2}\left(-v^2 / 2\sigma^2 \right) \tag{4.24}$$

$$\sigma_{h,Rice}^2 = 2\sigma^2 + v^2 - \frac{(\Pi \sigma^2)}{2} L_{1/2}^2(-v^2 / (2\sigma^2)) \tag{4.25}$$

Estimated *k*-th Rician faded R-channel coefficient ($\hat{h_k}$) can be calculated by substituting Eq. (4.23) in Eq. (4.20);

$$\hat{h}_k = \frac{E_b}{E_b + \sigma_n^2}\left(h_{kI} + jh_{kQ}\right)^{1/2} + \frac{\sqrt{E_b}}{E_b + \sigma_n^2} n_k \tag{4.26}$$

Estimation error for *k*-th R-channel fading coefficient can be calculated by substituting Eq. (4.26) in Eq. (4.21);

$$\tilde{h}_k = h_k - \left[\frac{E_b}{E_b + \sigma_n^2} h_k + \frac{\sqrt{E_b}}{E_b + \sigma_n^2} n_k \right] \tag{4.27}$$

$$\tilde{h}_k = \left[1 - \frac{E_b}{E_b + \sigma_n^2} \right] h_k - \frac{\sqrt{E_b}}{E_b + \sigma_n^2} n_k \tag{4.28}$$

Substituting Eq. (4.23) in Eq. (4.28) gives the estimation error expression for Rician faded R-channel;

$$\tilde{h}_k = \frac{\sigma_n^2}{E_b + \sigma_n^2}\left(h_{kI} + jh_{kQ}\right)^{1/2} - \frac{\sqrt{E_b}}{E_b + \sigma_n^2} n_k \tag{4.29}$$

The mean and variance of $\tilde{h}_k$ can be evaluated by using Eq.(4.24) and Eq.(4.25) as

$$\mu_{\tilde{h}_k, rice} = E\left[\tilde{h}_k\right] = E\left[\frac{\sigma_n^2}{E_b + \sigma_n^2}\left(h_{kI} + jh_{kQ}\right)^{1/2} - \frac{\sqrt{E_b}}{E_b + \sigma_n^2} n_k \right] \tag{4.30}$$

$$\mu_{\tilde{h}_k, rice} = E\left[\tilde{h}_k\right] = \frac{\sigma_n^2}{E_b + \sigma_n^2} E\left[\left(h_{kI} + jh_{kQ}\right)^{1/2}\right] - \frac{\sqrt{E_b}}{E_b + \sigma_n^2} E\left[n_k\right] \tag{4.31}$$

We have assumed that mean value of noise component is zero, then Eq. (4.31) reduces to

$$\mu_{\tilde{h}_k, rice} = E\left[\tilde{h}_k\right] = \sigma\sqrt{\frac{\pi}{2}} L_{1/2}\left(-v^2 / 2\sigma^2\right) \frac{1}{1+\overline{\gamma_r}} \tag{4.32}$$

Similarly, final expression for the variance of estimation error ($\sigma^2_{\tilde{h}, Rice}$) is

$$\sigma^2_{\tilde{h}, Rice} = \frac{1}{\left(1+\overline{\gamma_r}\right)^2}\left[\overline{\gamma_r} + \sigma^2_{h, Rice}\right] \tag{4.33}$$

4.4.2. Estimation Error in Hoyt Fading Channel

For *k*-th Hoyt faded R-channel, the actual fading coefficient h_k can be expressed in terms of in-phase h_{kI} and quadrature h_{kQ} components as;

$$h_k = \left(h_{kI} + jh_{kQ}\right)^{1/2} \tag{4.34}$$

The in-phase h_{kI} and quadrature h_{kQ} components for Hoyt fading can be generated as

$$h_{kI} \sim (0, \sigma_1^2), \;\; h_{kQ} \sim (0, \sigma_2^2) \tag{4.35}$$

where $\sigma_1 = \sqrt{\frac{\Omega q^2}{1+q^2}}$, $\sigma_1 = \sqrt{\frac{q^2}{1+q^2}}$, and q-is Hoyt fading parameter.

The mean expression for Hoyt fading channel is [67];

$$\mu_{h,\text{Hoyt}} = E[h_k] = \frac{4*\Gamma\left(\frac{3}{2}\right)}{A}\Omega F\left(\frac{3}{4}, \frac{5}{4}; 1; \frac{B^2}{A^2}\right) \tag{4.36}$$

where $\Omega = \sigma_1^2 + \sigma_2^2$, $q = \frac{\sigma_2^2}{\sigma_1^2}$, $A = \frac{(1+q^2)^2}{q^2}$, and $B = \frac{(1-q^4)}{q^2}$.

The variance expression for Hoyt fading channel is

$$\sigma_{h,Rice}^2 = \Omega\left(1 - \left(\frac{4*\Gamma\left(\frac{3}{2}\right)}{A}\mathrm{F}\left(\frac{3}{4}, \frac{5}{4}; 1; \frac{B^2}{A^2}\right)\right)^2\right) \tag{4.37}$$

The estimated k-th Hoyt faded R-channel coefficient (h_k) can be calculated using the procedure given in section 4.4.1.The mean and variance expressions of estimation error Hoyt faded R-channel coefficient are

$$\mu_{\tilde{h},\text{Hoyt}} = E\left[\tilde{h}_k\right] = \frac{4*\Gamma\left(\frac{3}{2}\right)}{A}\Omega F\left(\frac{3}{4}, \frac{5}{4}; 1; \frac{B^2}{A^2}\right)\frac{1}{1+\overline{\gamma_r}} \tag{4.38}$$

$$\sigma_{\tilde{h},Hoyt}^2 = \frac{1}{\left(1+\overline{\gamma_r}\right)^2}\left[\overline{\gamma_r} + \sigma_{h,Hoyt}^2\right] \tag{4.39}$$

4.4.3. Estimation Error in Weibull fading Channel

For k-th Weibull faded R-channel, the actual fading coefficient h_k can be expressed in terms of in-phase h_{kI} and quadrature h_{kQ} components as [22];

$$h_k = \left(h_{kI} + jh_{kQ}\right)^{2/V} \tag{4.40}$$

The estimated *k*-th Weibull faded R-channel coefficient ($\hat{h}_k$) can be calculated as;

$$\hat{h}_k = \frac{E_b}{E_b + \sigma_n^2}\left(h_{kI} + jh_{kQ}\right)^{2/V} + \frac{\sqrt{E_b}}{E_b + \sigma_n^2} n_k \tag{4.41}$$

The estimation error for *k*-th R-channel coefficient can be calculated as;

$$\tilde{h}_k = \frac{\sigma_n^2}{E_b + \sigma_n^2}\left(h_{kI} + jh_{kQ}\right)^{2/V} - \frac{\sqrt{E_b}}{E_b + \sigma_n^2} n_k \tag{4.42}$$

4.5. Censoring Techniques

With the help of censoring schemes, heavily faded radio links of R-channel in CSS network are removed. There are two different types of censoring techniques are addressed in the literature namely Rank based censoring scheme and Threshold based censoring scheme.

4.5.1. Rank Based Censoring Scheme

Rank based censoring scheme is applied to the estimated channel coefficients. All the fading coefficients are arranged Rank wise, then FC selects the *k* CRs, whose R-channel fading coefficients having highest estimated channel coefficient amplitude. All these estimated channel coefficients are gathered at FC and the fusion rules are applied to identify the presence of PU activity [24].

4.5.2. Threshold Based Censoring Scheme

In threshold based censoring scheme, a particular CR can be transmitted if the amplitude of estimated R-channel coefficient is greater than censoring threshold (C_{th}). The probability of selecting a CR for different faded R-channel coefficients is [24]

$$p = \Pr\left(\left|\hat{h}_k\right| > C_{th}\right) \tag{4.43}$$

Using the binomial distribution, the probability of selecting *k* CRs from *P* CRs can be calculated as follows

$$P(k) = \binom{P}{k} p^k \left(1-p\right)^{(P-k)} \tag{4.44}$$

In Eq. (4.44), *P(k)* represents the probability of selecting *k* CRs, *P* is a total number of CR users, and *k* represents the number of CRs which are gathered at FC.

4.6. Results and Discussions

In this section, simulation results are drawn to evaluate the performance of missed detection probability and total error probability using the censoring schemes in CSS network. The performance comparison between MRC Rule and majority logic is provided. The performance is also evaluated with perfect and imperfect channel estimations. Two censoring schemes are applied individually in CSS network when it is affected by Rician, Weibull, and Hoyt fading effects respectively.

The performance evolution of missed detection probability (Q_m) as a function of number of CR users (N) is shown in Fig.4.3. To evaluate this performance two different R-channel SNR values (namely -9dB and -7dB), S-channel SNR=15dB, probability of false alarm P_f=0.05, and Rician fading parameter K=3 are considered as network parameters. The performance comparison between perfect and imperfect channel estimation is provided in Fig.4.3 using majority logic at fusion center (FC) over Rician fading channel. Particularly, R-channel SNR is considered as variable parameter (-9dB and-7dB) to show the effect of R-channel SNR on Q_m value. As R-channel SNR value increases from -9dB to -7dB, Q_m value decreases with both perfect and imperfect channel estimations. As R-channel SNR value increases, noise level reduces in the channel. Furthermore, according to Eq. (4.22), as R-channel SNR value increases, estimation error variance value decreases and this makes further a reduction of average estimation error. Hence, this reduces estimation error reduces the missed detection probability. It can also be observed from Fig.4.3 that Q_m value is more with imperfect channel estimation compared to perfect channel estimation; this is due to the estimation error present in the channel. Q_m value becomes constant with perfect channel estimation after N=15 which is due to FC choosing the CRs which are having lowest probability of getting rejected. For an instant, at N=8 and R-channel SNR increases from -9dB to -7dB, Q_m value decreases by 26.1% with perfect channel estimation and it decreases by 25.7% with imperfect channel estimation. If the channel is considered as perfect channel instead of imperfect channel, then Q_m value decreases by 28.8% at R-channel SNR=-9dB, N=10, and using majority logic at FC. The performance comparison between Rayleigh and Rician fading channels are also provided in Fig.4.3. Q_m value is 42.7% less with perfect channel estimation in Rician fading compared to Rayleigh fading channel at R-channel SNR=-9dB and N=10.

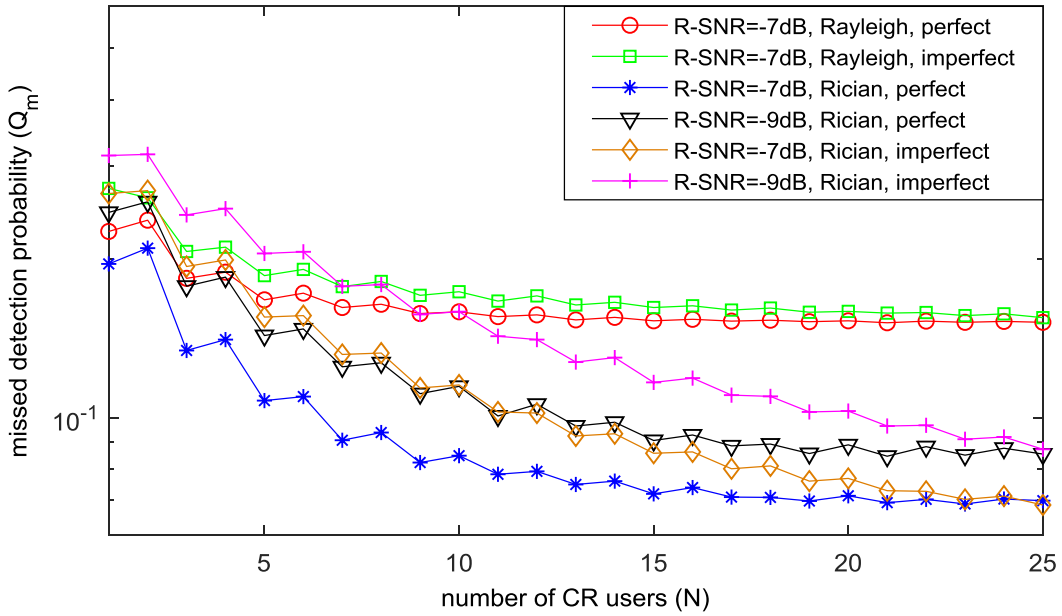

Fig.4.3. Q_m versus N graphs for different R-channel SNRs using Majority logic at FC.

In Fig.4.4, the effect of S-channel SNR on Q_m value as a function of N is discussed. It can be observed from the graph that as N value increases, Q_m value decreases because cooperation among the users increases. S-channel SNR is considered as variable parameter to show the effect of S-channel SNR on Q_m is observed by using majority logic at FC. The performance is evaluated with perfect and imperfect channel estimations and comparison between them also provided.

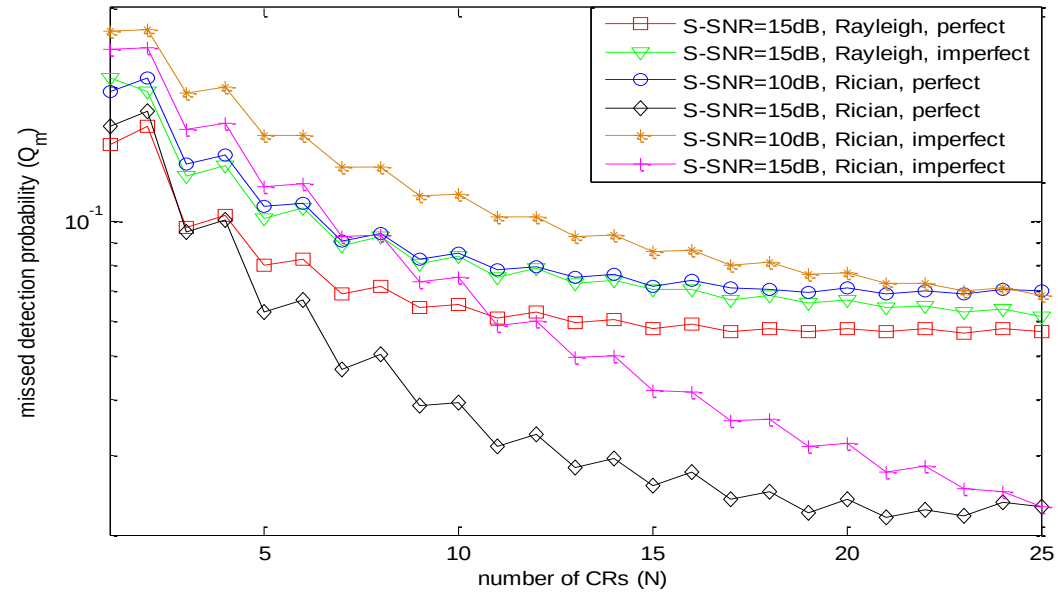

Fig.4.4. Q_m versus N graphs for different S-channel SNRs using Majority logic at FC.

The network parameters such as S-channel SNR=10dB and 15dB, R-channel SNR=-7dB, P_f=0.05, and K=3 are used to simulate this graph. As S-channel SNR value increases, fading effect decreases and signal strength increases in S-channel this leads to improve the sensing information about the PU. For a particular case, N=10 and S-channel SNR value increases from 10dB to 15dB, Q_m value decreases by 53.7% with perfect channel estimation and it decreases by 34.9% with imperfect channel estimation. If the channel is considered as perfect channel instead of imperfect channel, then Q_m value decreases by 47.6% at S-channel SNR=15dB and N=10 using majority logic at FC. The performance comparison between Rayleigh and Rician fading channels are also provided. Q_m value is 40.1% less with perfect channel estimation in Rician fading compared to Rayleigh fading channel at S-channel SNR=15dB and N=10.

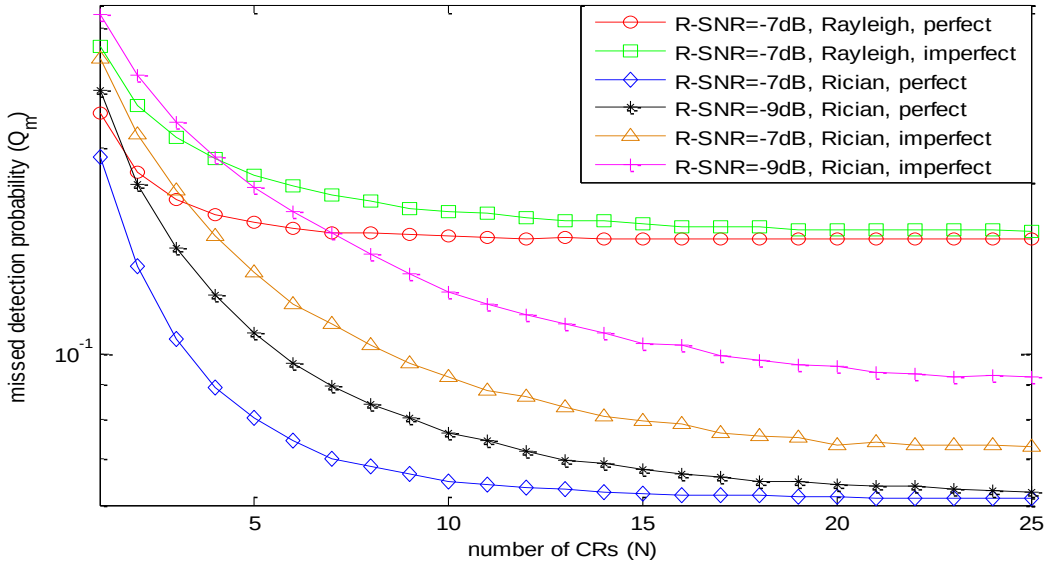

Fig.4.5. Q_m versus N graphs for different R-channel SNRs using MRC Rule at FC.

In Fig.4.5, Q_m performance is shown as a function of N. MRC rule is used at FC to decide the PU activity in Rician fading with perfect and imperfect channel estimation. In Fig.4.5, performance comparison between Rayleigh channel and Rician channel is also provided for various values of R-channel SNRs. It can also observed from the graph that Q_m value is more with imperfect channel estimation compared to perfect channel estimation. The R-channel SNR is considered as variable parameter (-9dB and -7dB), S-channel SNR=15dB, P_f=0.05, and K=3 are chosen as network parameters to simulate this graph. For a particular value of N=10 and R-channel SNR increases from -9dB to -7dB, Q_m value decreases by 24.9% with perfect channel estimation and it decreases by 12.8% with imperfect channel estimation.

If the channel is considered as perfect channel instead of imperfect channel, then Q_m value decreases by 29.8% at R-channel SNR=-7dB and *N*=10 using MRC rule at FC. Q_m value is 56.2% less with perfect channel estimation in Rician fading compared to Rayleigh fading channel at R-channel SNR=-7dB and *N*=10. Q_m values are less with MRC rule compared to majority logic.

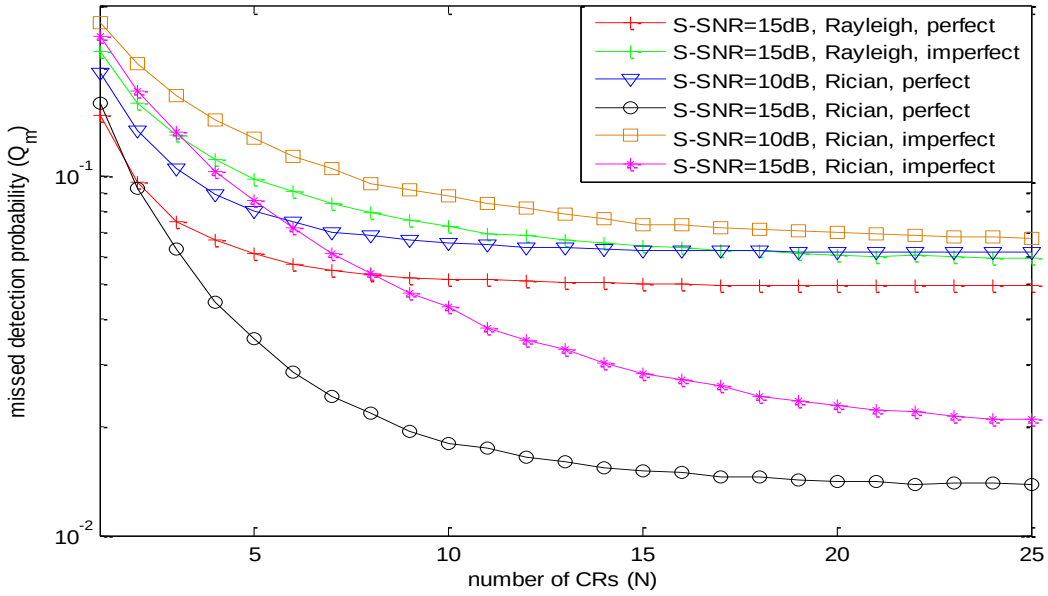

Fig.4.6. Q_m versus *N* graphs for different S-channel SNRs using MRC Rule at FC.

Fig.4.6 is drawn between Q_m and *N* considering S-channel SNR as variable parameter with perfect and imperfect channel estimation in Rician fading using MRC rule at FC. As S-channel SNR increases, Q_m value decreases in both perfect and imperfect channel estimation. The network parameters used in the simulation to get Fig.4.6 are R-channel SNR=-7dB, S-channel SNR=10dB and 15dB, P_f=0.05, and *K*=3. As S-channel SNR value increases from 10dB to 15dB, Q_m value decreases by 72.1% with perfect channel estimation and it decreases by 50.9% with imperfect channel estimation at *N*=10. Q_m value with perfect channel is 58.1% lower than imperfect channel at *N*=8 and S-channel SNR=15dB. Q_m value is 65.1% less with perfect channel estimation in Rician fading compared to Rayleigh fading channel at S-channel SNR=15dB and *N*=10.

Fig 4.7 is drawn between Q_m and *N* using majority logic at FC in Hoyt fading channel. The performance comparison between both perfect and imperfect channels as a function of R-channel SNR is provided. We have considered two different R-channel SNR values (-9dB and -7dB), S-channel SNR=15dB, P_f=0.05, and Hoyt fading parameter *q*=0.5 as network

parameters. As R-channel SNR increases, Q_m value decreases. For a particular case, at N=10 and R-channel SNR value increases from -9dB to -7dB, Q_m value decreases by 11.8% with perfect channel estimation and it decreases by 9.1% with imperfect channel estimation. We can also observe that after a particular value of N=17, Q_m value becomes constant in case of perfect channel because FC may select the CRs which are having lower probability of getting rejected. Q_m value is more with imperfect channel compared to perfect channel estimation. The comparison between Hoyt fading and Rayleigh fading channels are also provided in Fig.4.7. Q_m value is 17.6% more with perfect channel estimation in Hoyt fading channel compared to Rayleigh fading channel at R-channel SNR=-9dB and N=10.

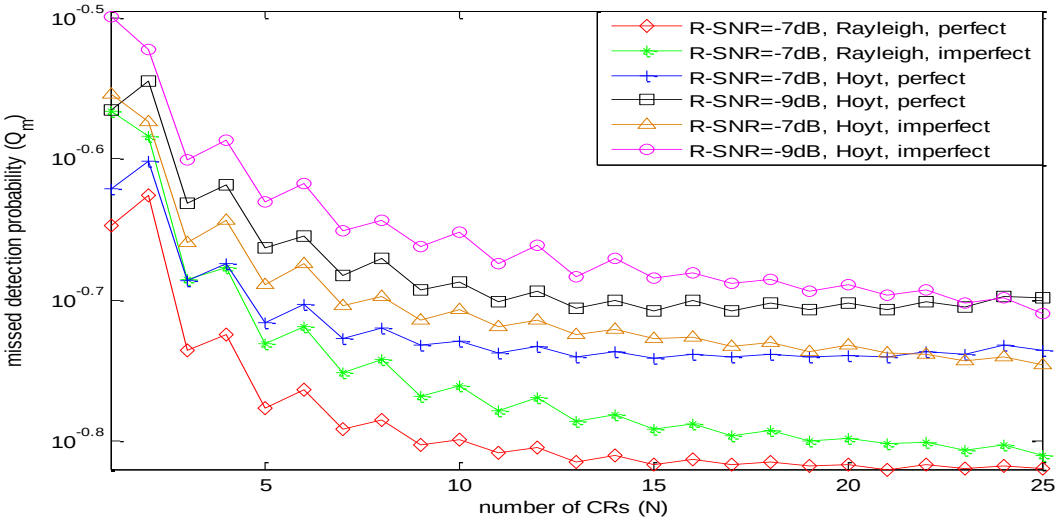

Fig.4.7. Q_m versus N graphs for different R-channel SNRs using Majority logic at FC.

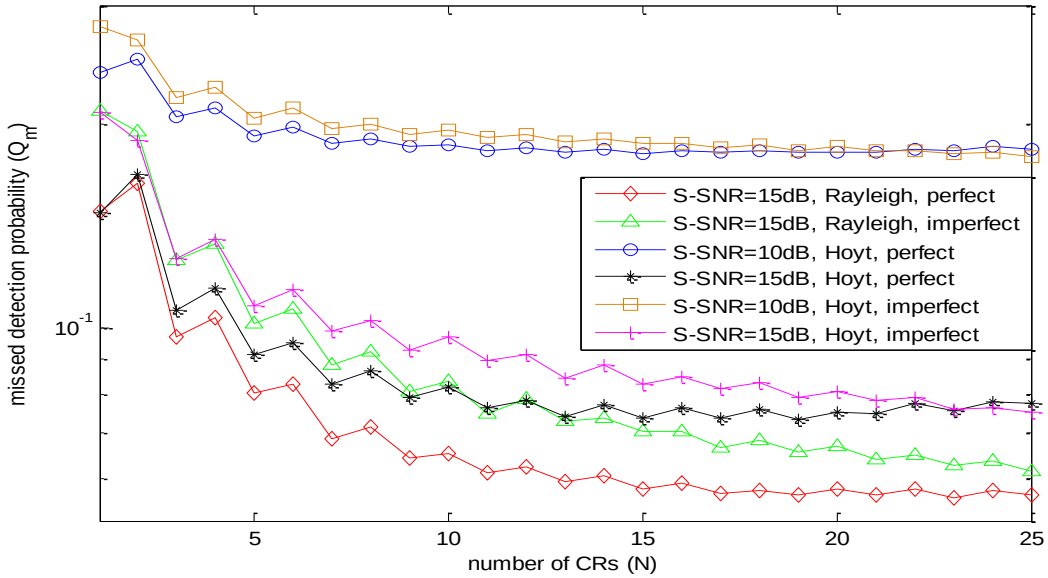

Fig.4.8. Q_m versus N graphs for different S-channel SNRs using Majority logic at FC.

Fig.4.8 describes the effect of S-channel SNR on Q_m using majority logic at FC in Hoyt fading channel. The performance comparison between perfect and imperfect channel estimation is provided. We have considered R-channel SNR=-7dB, S-channel SNR=10dB and 15dB, P_f=0.05, and q=0.5 to simulate this graph. As S-channel SNR value increases from 10dB to 15dB, Q_m value decreases by 56.1% with perfect channel estimation and it decreases by 50.6% with imperfect channel estimation at N=10. Q_m value decreases by 15.4% when the nature of the channel changes from imperfect to perfect channel estimation at S-channel SNR=15dB and N=10. The performance comparison between Rayleigh and Hoyt fading channels are also provided. Q_m value is 20.1% more with perfect channel estimation in Hoyt fading channel compared to Rayleigh fading channel at S-channel SNR=15dB and N=10.

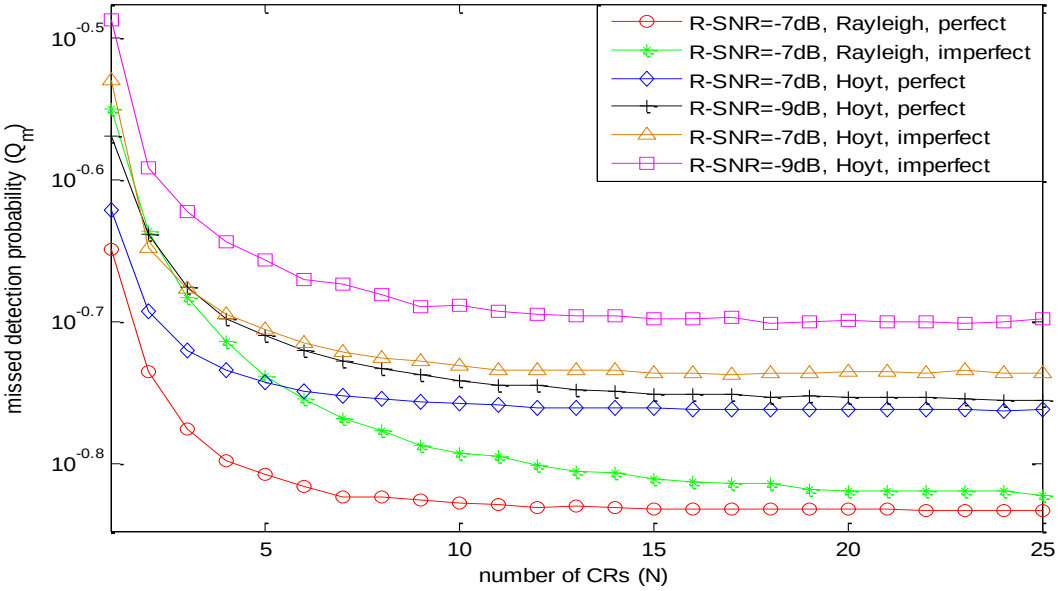

Fig.4.9. Q_m versus N graphs for different R-channel SNRs using MRC Rule at FC.

In Fig.4.9, Q_m performance is shown as a function of N. MRC rule is used at FC to decide the PU activity in Hoyt fading with perfect and imperfect channel estimation. In Fig.4.9, performance comparison between Rayleigh channel and Hoyt channel is provided for various values of R-channel SNRs. The R-channel SNR is considered as variable parameter (-9dB and -7dB), S-channel SNR=15dB, P_f=0.05, and q=0.5 are chosen as network parameters to simulate this graph. For a particular value of N=10 and R-channel SNR value increases from -9dB to -7dB, Q_m value decreases by 9.5% with perfect channel estimation and it decreases by 3.5% with imperfect channel estimation. If the channel is considered as perfect channel instead of imperfect channel, then Q_m value decreases by 5.8% at R-channel SNR=-7dB and N=10.

Q_m value is 17.6% more with perfect channel estimation in Hoyt fading channel compared to Rayleigh fading channel at R-channel SNR=-7dB and *N*=10. Q_m values are less with MRC rule compared to majority logic.

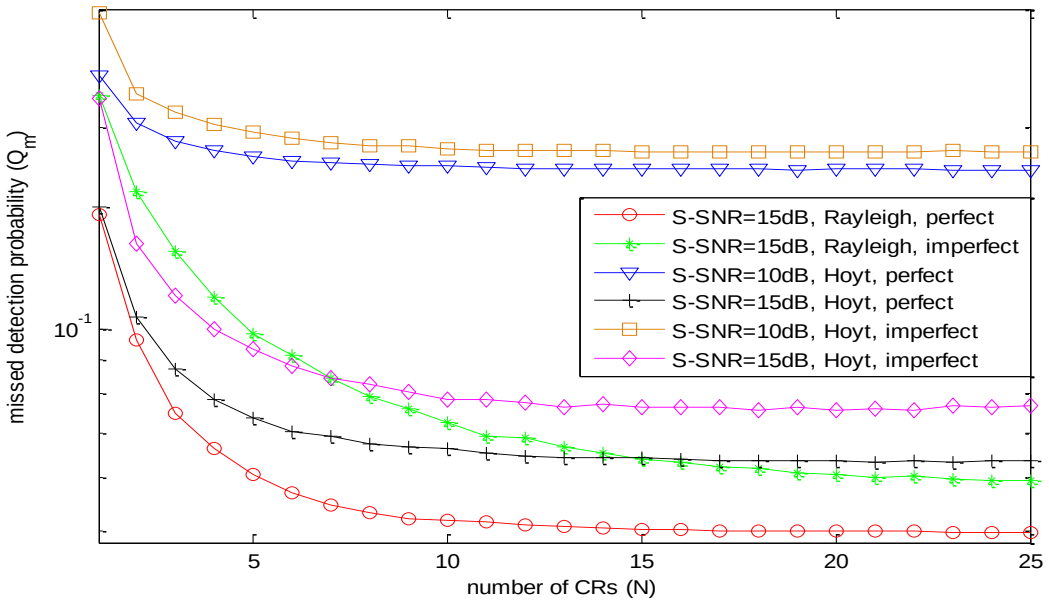

Fig.4.10. Q_m versus *N* graphs for different S-channel SNRs using MRC Rule at FC.

Figure 4.10 is drawn between Q_m and *N* considering S-channel SNR as variable parameter with perfect and imperfect channel estimation in Hoyt fading using MRC rule at FC. The R-channel SNR=-7dB, S-channel SNR =10dB and 15dB, P_f=0.05, and *q*=0.5 are considered asss network parameters. As S-channel SNR value increases from 10dB to 15dB, Q_m value decreases by 62.1% with perfect channel estimation and it decreases by 57.6% with imperfect channel estimation at *N*=10. Q_m value with perfect channel is 15.6% lower than imperfect channel at *N*=8 and S-channel SNR=15dB. Q_m value is 21.6% more with perfect channel estimation in Hoyt fading compared to Rayleigh fading channel at S-channel SNR=15dB and *N*=10.

Figure 4.11 is drawn between Q_m and *N* using majority logic at FC in Weibull fading channel. The performance comparison between both perfect and imperfect channels as a function of R-channel SNR is provided. We have considered two different R-SNR values (-9dB and-7dB), S-channel SNR=15dB, P_f=0.05, and Weibull fading parameter *V*=5 as network parameters. For a particular case, *N*=10 and R-channel SNR value increases from -9dB to -7dB, Q_m value decreases by 48.2% with perfect channel estimation and it decreases by 39.9% with imperfect channel estimation. Q_m value is more with imperfect channel compared to

perfect channel estimation. The performance comparison between Weibull fading and Rayleigh fading channels are also provided. Q_m value is 50.8% less with perfect channel estimation in Weibull fading channel compared to Rayleigh fading channel at R-channel SNR=-9dB and *N*=10.

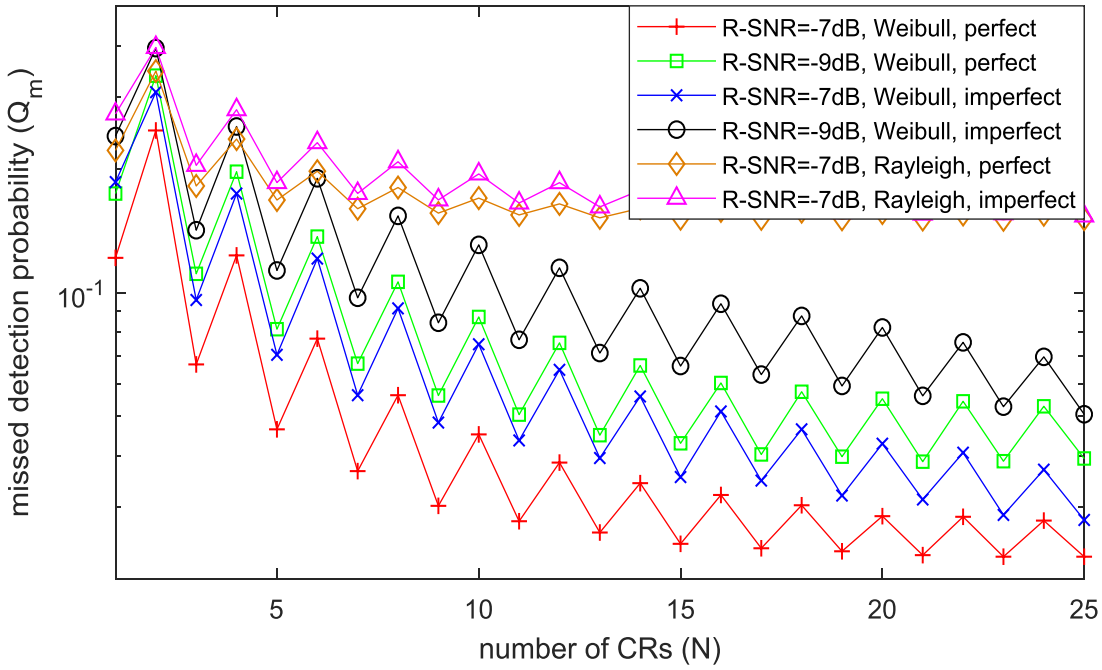

Fig.4.11. Q_m versus *N* graphs for different R-channel SNRs using Majority logic at FC.

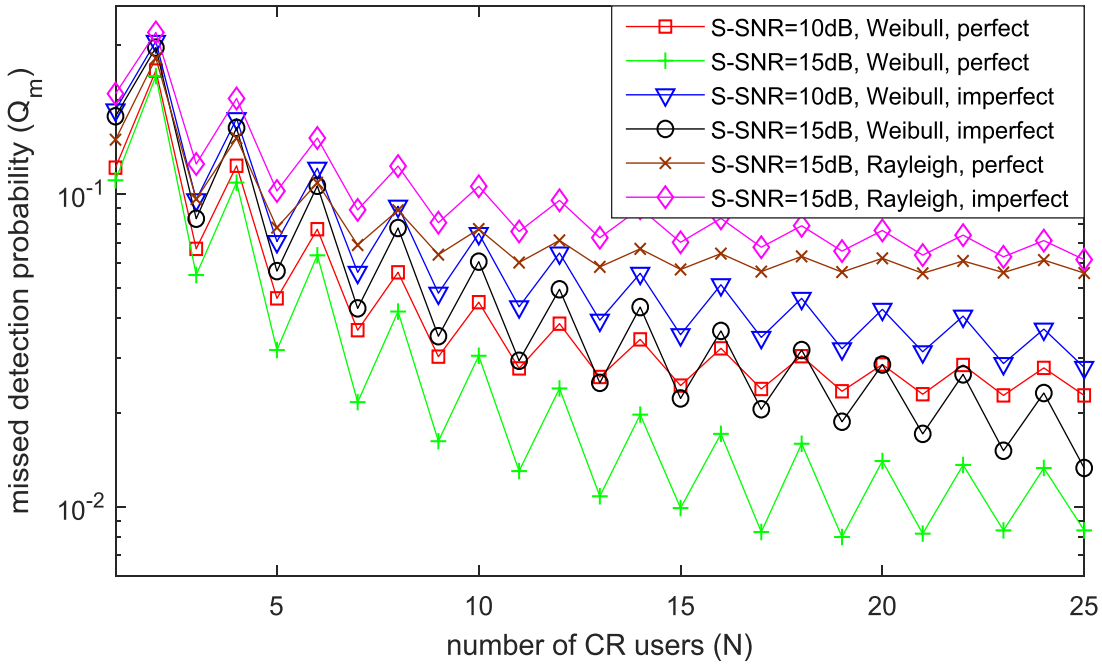

Fig.4.12. Q_m versus *N* graphs for different S-channel SNRs using Majority logic at FC.

Figure 4.12 is drawn between Q_m and N using majority logic at FC in Weibull fading channel. The performance comparison between both perfect and imperfect channels as a function of S-channel SNR is provided. We have considered two different S-channel SNR values (10dB and 15dB), R-channel SNR=-7dB, P_f=0.05, and V=5 as network parameters. For a particular case, N=10 and S-channel SNR value increases from 10dB to 15dB, Q_m value decreases by 32.5% with perfect channel estimation and it decreases by 17.9% with imperfect channel estimation. The performance comparison between Weibull fading and Rayleigh fading channels are also provided. Q_m value is 39.4% less with perfect channel estimation in Weibull fading channel compared to Rayleigh fading channel at S-channel SNR=10dB and N=10.

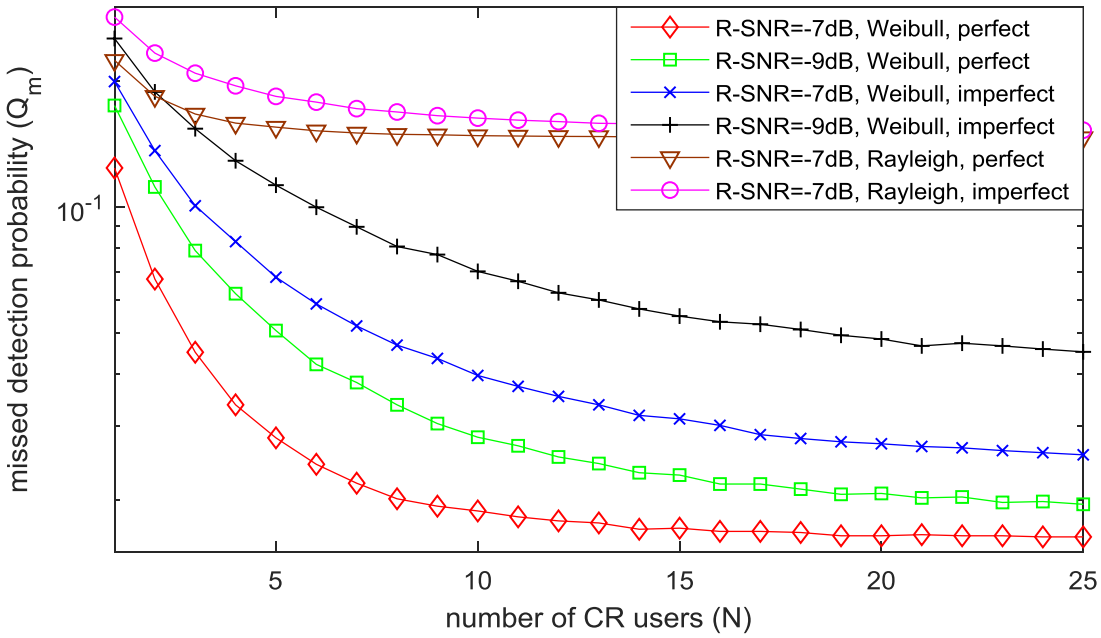

Fig.4.13. Q_m versus N graphs for different R-channel SNRs using MRC Rule at FC.

In Fig.4.13, Q_m performance is shown as a function of N. MRC rule is used at FC to decide the PU activity in Weibull fading with perfect and imperfect channel estimation. In Fig.4.13, comparison between Rayleigh channel and Weibull channel is also provided for various values of R-channel SNRs. The R-channel SNR is considered as variable parameter (-9dB and -7dB), S-channel SNR=15BdB, P_f=0.05, and V=5 are chosen as network parameters to simulate this graph. For a particular value of N=10 and R-channel SNR increases from -9dB to -7dB, Q_m value decreases by 33.3% with perfect channel estimation and it decreases by 28.4% with imperfect channel estimation. If the channel is considered as perfect channel instead of imperfect channel, then Q_m value decreases by 35.8% at R-channel SNR=-7dB and

N=10. Q_m values are less with MRC rule compared to majority logic. Q_m value is 7.86% less with perfect channel estimation in Weibull fading channel compared to Rayleigh fading channel at R-channel SNR=-7dB and N=10.

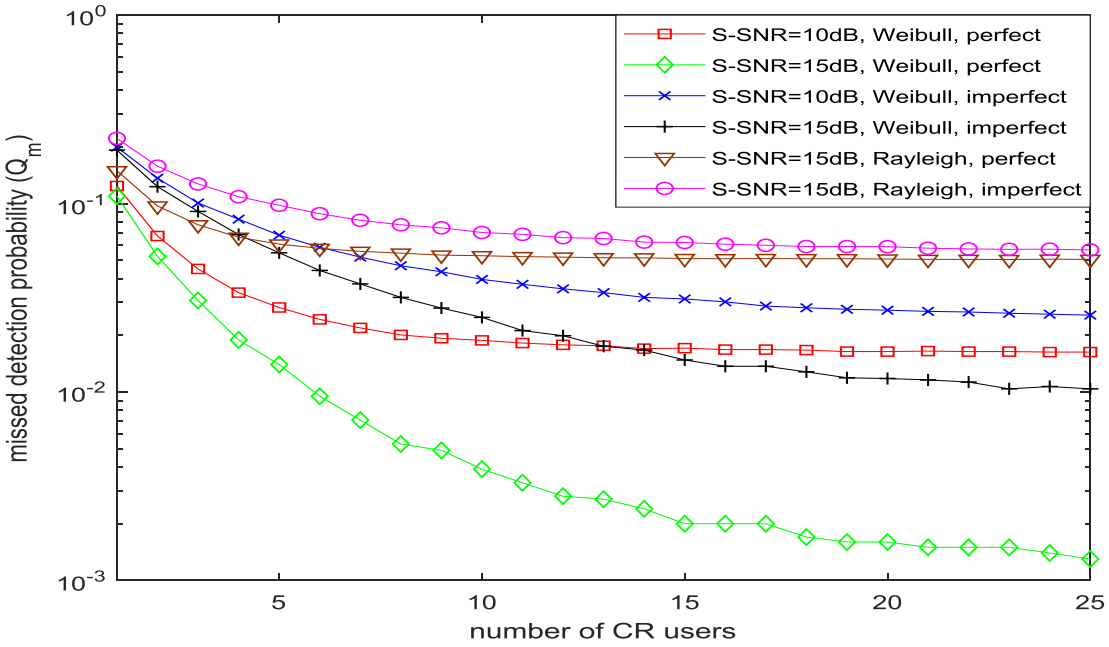

Fig.4.14. Q_m versus N graphs for different values of S-channel SNRs using MRC Rule at FC.

In Fig.4.14, Q_m performance is shown as a function of N. MRC rule is used at FC to decide the PU activity in Weibull fading with perfect and imperfect channel estimation. In Fig.4.14, comparison between Rayleigh channel and Weibull channel is also provided for various values of S-channel SNRs. The S-channel SNR is considered as variable parameter (10dB and 15dB), R-channel SNR=-9BdB, P_f=0.05, and V=5 are chosen as network parameters to simulate this graph. For a particular value of N=10 and S-channel SNR increases from 10dB to 15dB, Q_m value decreases by 79.2% with perfect channel estimation and it decreases by 37.1% with imperfect channel estimation.

From Fig.4.3 to Fig.4.14 missed detection probability (Q_m) performances are evaluated using Rank based censoring scheme as a function of number of CRs (N). Now, from Fig.4.15 to Fig.4.22 missed detection probability (Q_m) performances are evaluated using Threshold based censoring scheme as a function of censoring thresholds (C_{th}).

Figure 4.15 is drawn between missed detection probability (Q_m) and censoring threshold value (C_{th}) with perfect channel estimation using threshold based censoring scheme. The network parameters such as N=30, P_f=0.05, K=3, S-channel SNR=15dB, and R-channel

SNR=-9dB and -7dB are used to simulate this graph in Rician fading. It can be observed from the graph that as C_{th} increases, Q_m reaches minimum value for an optimal C_{th} level, thereafter it increases with the threshold value there after it attaining constant value. Two fusion rules namely majority logic and MRC rules are performed separately at FC and performance comparison between these two fusions rules are provided. Q_m value decreases with the increment of R-channel SNR using MRC rule and majority logic at FC. As R-channel SNR increases, fading effect in R-channel decreases, so that more number of CR users get selected using censoring scheme and all these selected CRs pass their sensing information to the FC. After a certain value of C_{th}, Q_m becomes constant with perfect channel estimation because FC select the best R-channel links which are having lowest probability of getting rejected.

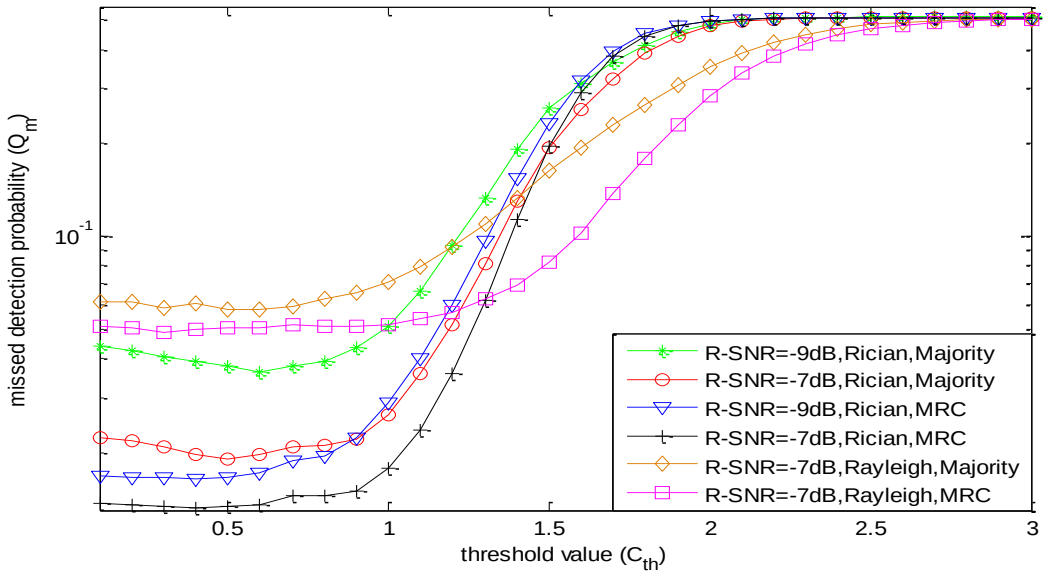

Fig.4.15. Q_m versus C_{th} graphs for different R-channel SNRs with perfect channel estimation.

At C_{th}=0.8, R-channel SNR=-7dB, and if MRC rule is used at FC instead of majority logic, then Q_m value reduces by 31.4%, this implies that MRC rule achieves lower value of missed detection probability than majority logic. If we consider higher value of C_{th}, no other CR is selected to transmit and Q_m reaches a constant value approximately 0.5 for both majority and MRC rules. If R-channel SNR increases from -9dB to -7dB, Q_m value decreases by 26.7% with majority logic and it decreases by 46.1% with MRC rule at C_{th}=0.8. The performance comparison between Rayleigh and Rician channels are also provided. Q_m value is 66.5% less with majority logic and it is 71.6% less with MRC Rule in Rician channel compared to Rayleigh channel at R-channel SNR=-7dB and C_{th}= 0.8.

Figure 4.16 shows the performance comparison between MRC rule and majority logic with perfect channel estimation using Q_m versus C_{th} curves as a function of S-channel SNR in Rician fading. Network parameters such as N=30, P_f=0.05, R-channel SNR=-7dB, K=3, and S-channel SNR=10dB and 15dB are used to simulate this graph. MRC rule achieves lower value of Q_m compared to majority logic. For a particular value of C_{th}= 0.8 and S-channel SNR increases from 10dB to 15dB, Q_m value decreases by 68.2% with majority logic and it decreases by 76.1% with MRC rule respectively. For a particular value of S-channel SNR=15dB and C_{th}=0.8, Q_m value reduces by 31.4% with MRC rule compared to majority logic rule. Q_m value is 57.5% less with Majority logic and it is 58.9% less with MRC Rule in Rician channel compared to Rayleigh channel at S-channel SNR=10dB and C_{th}= 0.8.

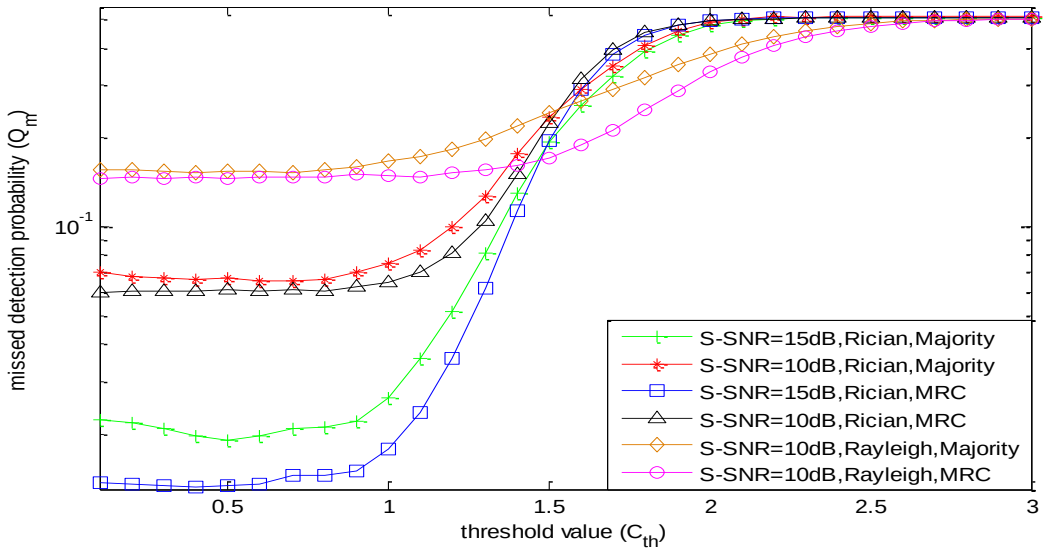

Fig.4.16. Q_m versus C_{th} graphs for different S-channel SNRs with perfect channel estimation.

Figure 4.17 shows the performance of Q_m with imperfect channel estimation in Rician fading channel for two different R-channel SNRs (-9dB and -7dB). The performance is analyzed by considering two fusion rules namely majority logic rule and MRC rule individually at FC. We have considered network parameters such as N=30, P_f=0.05, S-channel SNR=15dB, R-channel SNR= -9dB and -7dB, and K=3 to simulate this graph. For a particular case, C_{th}=1.0 and R-channel SNR value increases from -9dB to -7dB, Q_m value decreases by 46.2% with majority logic and it decreases by 47.1% with MRC rule. In case of imperfect channel also MRC rule achieves lower values of Q_m compared to majority logic. For a particular value of R-channel SNR=-9dB, $Q_m$value reducs by 28.4% if MRC rule is considered instead of majority logic at C_{th}=1.0. Q_m value is 57.2% less with majority logic and it is 61.8% less with MRC Rule in Rician channel compared to Rayleigh channel at R-channel SNR=-7dB and C_{th}= 0.8.

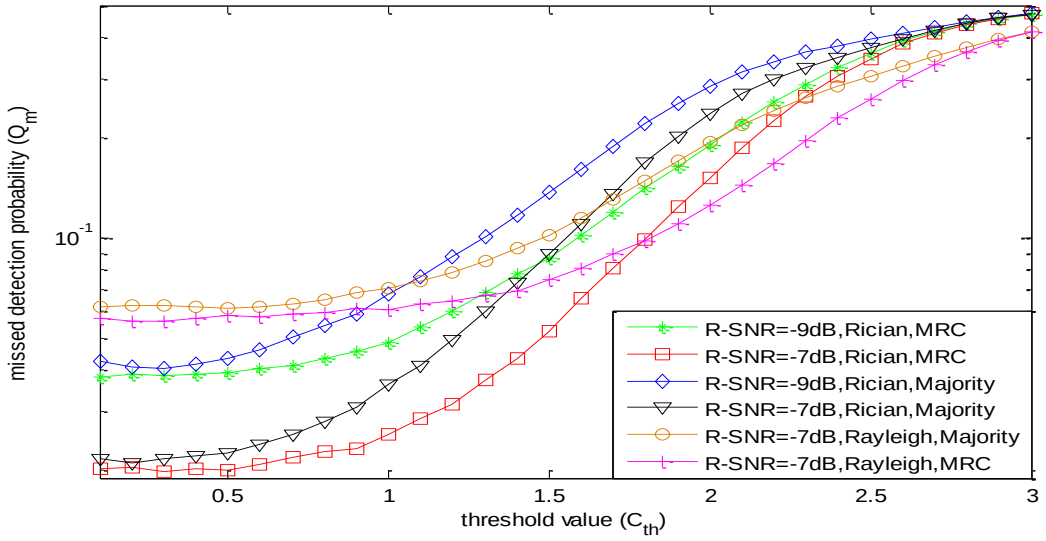

Fig.4.17. Q_m versus C_{th} graphs for different R-channel SNRs with imperfect channel estimation.

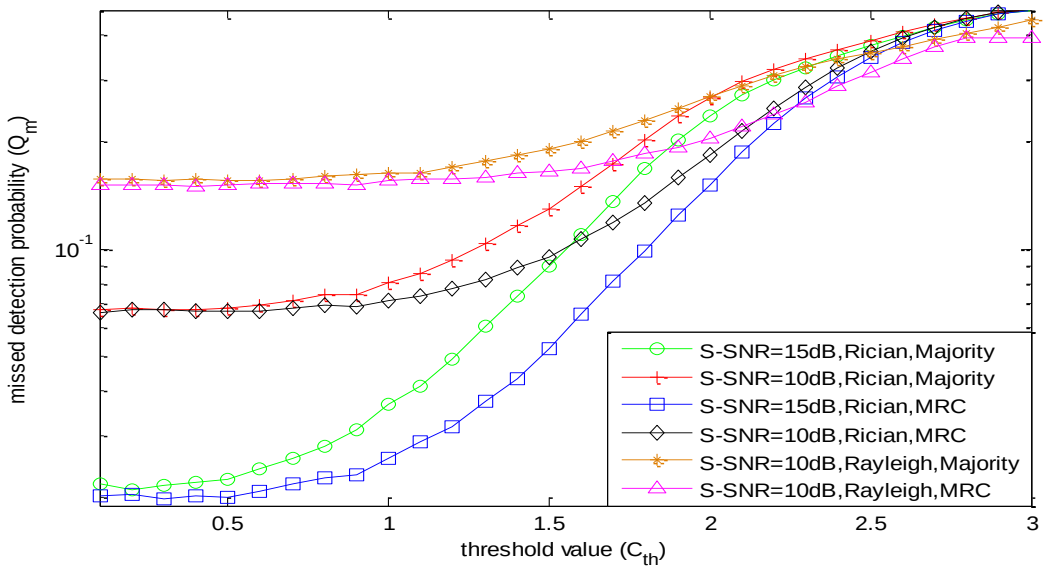

Fig.4.18. Q_m versus C_{th} curvs for different S-channel SNRs with imperfect channel estimation.

Effect of S-channel SNR on Q_m is shown in Fig.4.18 with imperfect channel estimation. We have considered two different S-channel SNR values namely 10dB and 15dB, N=30, P_f=0.05, R-channel SNR=-7dB, and K=3 to evaluate this simulation. The performance comparison between MRC rule and majority logic fusion for different S-channel SNRs is provided. If S-channel SNR value increases from 10dB to 15dB, Q_m value decreases by 62.2% with majority logic and it decreases by 67.2% with MRC rule at C_{th}= 0.8. For a particular value of S-channel SNR=15dB, Q_m value reduces by 29.5% if MRC rule is used at FC instead of

majority logic. Q_m value is 53.6% less with majority logic and it is 54.4% less with MRC Rule in Rician channel compared to Rayleigh channel at S-channel SNR=10dB and C_{th}= 0.8.

Figure 4.19 is drawn between Q_m and C_{th} with perfect channel estimation in Hoyt fading channel. The network parameters such as N=30, P_f=0.05, q=0.5, S-channel SNR=15dB, and R-channel SNR=-9dB and -7dB are used in the simulation. Two fusion rules namely majority logic and MRC rule have been performed separately at FC and performance comparison between them also provided.

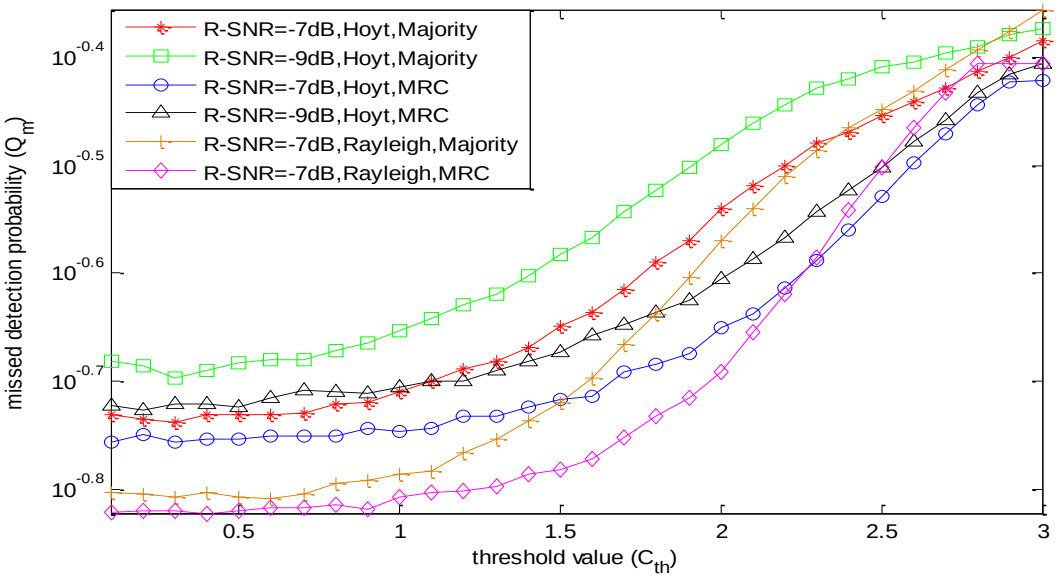

Fig.4.19. Q_m versus C_{th} graphs for different R-channel SNRs with perfect channel estimation.

For a particular value of C_{th}=0.8, R-channel SNR=-7dB and MRC logic rule is used at FC instead of majority logic, then Q_m value reduces by 6.4%, this indicates that MRC rule achieves lower value of Q_m value than majority logic. If R-channel SNR increases from -9dB to -7dB, Q_m value decreases by 3.8% with majority logic and it decreases by 8.7% with MRC rule at C_{th}=0.8. The performance comparison between Rayleigh and Hoyt channels are also provided. The Q_m value is 17.5% more with majority logic and it is 16.7% more with MRC rule in Hoyt channel compared to Rayleigh channel at R-channel SNR=-7dB and C_{th}= 0.8.

The effect of S-channel SNR on Q_m is shown in Fig.4.20 with imperfect channel estimation in Hoyt fading channel. Two different S-channel SNR values namely 10dB and 15dB, N=30, P_f=0.05, R-channel SNR=-7dB, and q=0.5 to evaluate this simulation. The performance comparison between MRC rule and majority logic fusions are provided. As S-

channel SNR value increases from 10dB to 15dB, Q_m value decreases by 52.2% with majority logic and it decreases by 59.6% with MRC rule at C_{th}= 0.8.

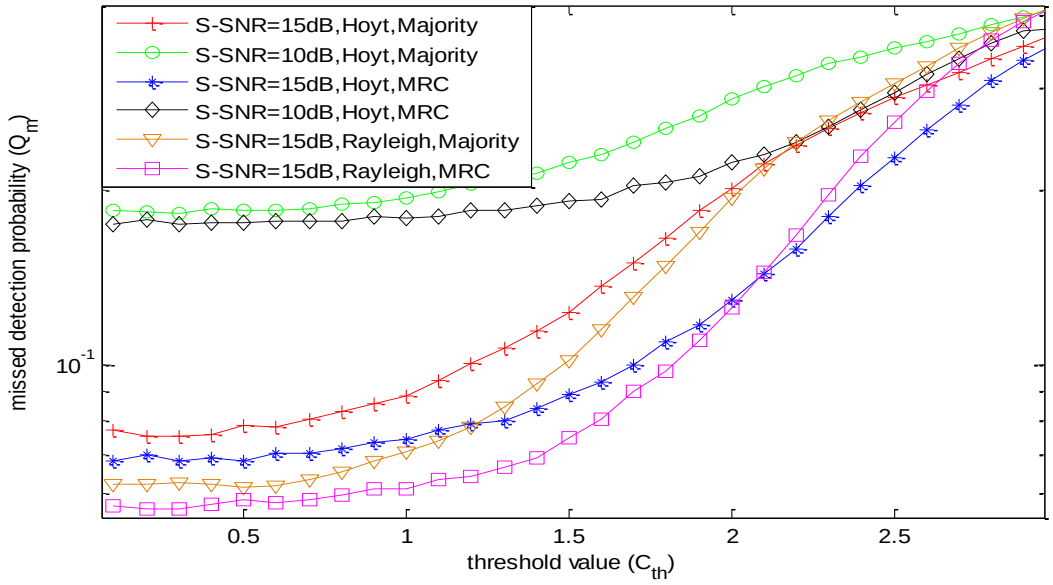

Fig.4.20. Q_m versus C_{th} graphs for different S-channel SNRs with imperfect channel estimation.

If MRC Rule is used at FC instead of majority logic then Q_m value reduces by 13.6% at S-channel SNR=10dB and C_{th}= 0.8. Q_m value is 26.7% more with majority logic and it is 19.9% more with MRC Rule in Hoyt channel compared to Rayleigh channel at S-channel SNR=15dB and C_{th}= 0.8.

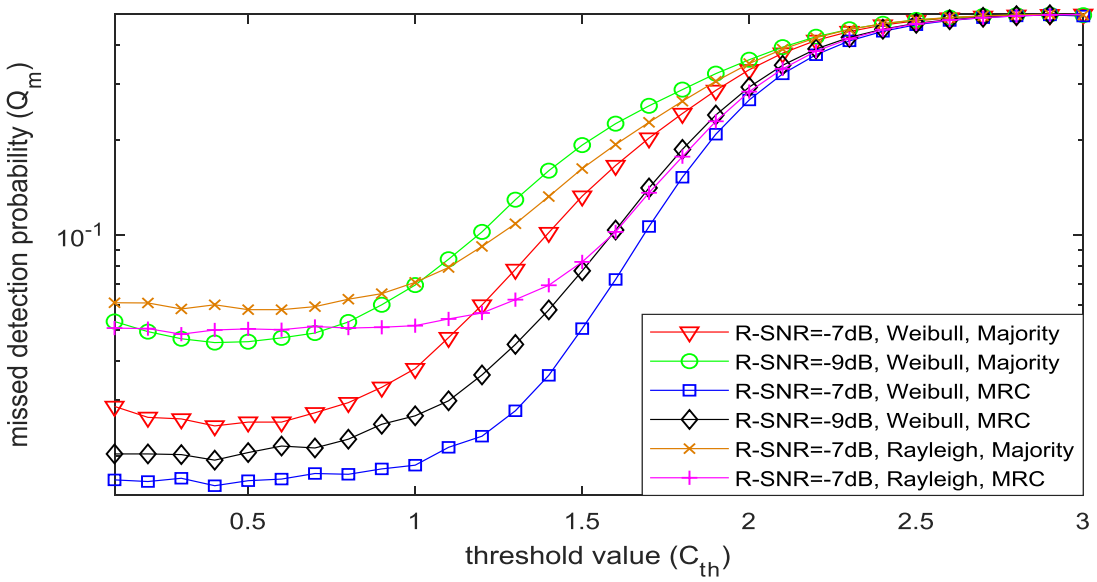

Fig.4.21. Q_m versus C_{th} graphs for different R-channel SNRs with perfect channel estimation.

Figure 4.21 is drawn between Q_m and C_{th} with perfect channel estimation in Weibull fading channel. The network parameters such as N=30, P_f=0.05, V=5, S-channel SNR=15dB, and R-channel SNR=-9dB & -7dB are used in the simulation. Two fusion rules namely majority logic and MRC rule are used separately at FC and performance comparison between them also provided. At C_{th}=0.8, R-channel SNR=-7dB, and MRC logic rule is used at FC instead of majority logic, then Q_m value reduces by 40.6%. If R-channel SNR increases from -9dB to -7dB, Q_m value decreases by 21.5% with majority logic and it decreases by 44.4% with MRC rule at C_{th}=0.8. The performance comparison between Rayleigh and Weibull channels also provided. Q_m value is 15.8% less with majority logic and it is 21.7% less with MRC rule in Weibull channel compared to Rayleigh channel at R-channel SNR=-7dB and C_{th}= 0.8.

The effect of S-channel SNR on Q_m is shown in Fig.4.22 with imperfect channel estimation in Weibull fading channel. Two different S-channel SNR values namely 10dB and 15dB, N=30, P_f=0.05, R-channel SNR=-7dB, and V=5 are used to evaluate this simulation. The performance comparison between MRC rule and majority logic fusions for different S-channel SNRs is also provided. As S-channel SNR value increases from 10dB to 15dB, Q_m value decreases by 43.6% with majority logic and it decreases by 57.4% with MRC rule at C_{th}= 0.8. If MRC rule is used at FC instead of majority logic, then Q_m value reducs by 23.6% at S-channel SNR=10dB and C_{th}= 0.8.

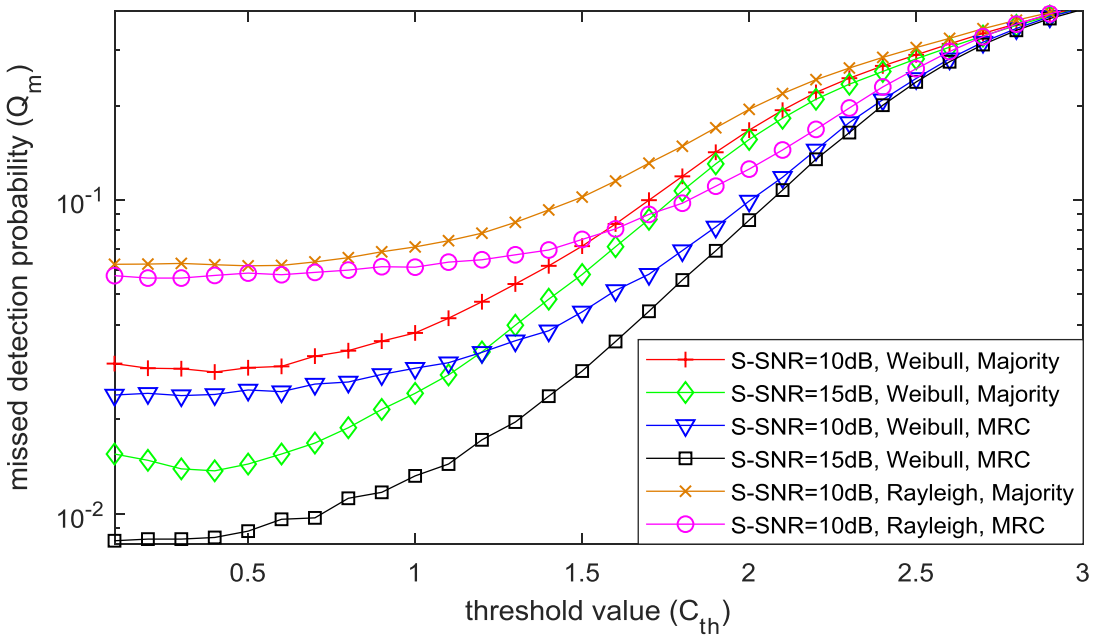

Fig.4.22. Q_m versus C_{th} graphs for different S-channel SNRs with imperfect channel estimation.

From Fig.4.23 to Fig.4.30 represents the performance analysis of total error probability ($Q_m + Q_f$) is discussed in Rician, Weibull, and Hoyt fading channels using Rank based and Threshold based censoring schemes.

In Fig 4.23, the effect on total error probability ($Q_m + Q_f$) for various values of probability of false alarm (P_f) with perfect channel estimation as a function of number of CR users (N) is described. The performance comparison between perfect channel estimation and imperfect channel estimation is shown over Rician fading using majority logic at FC. The probability of false alarm is considered as variable parameter, two P_f values namely 0.0005 and 0.05, S-channel SNR=15dB, R-SNR=-5dB, and K=3 are used in the simulation. As P_f value increases, ($Q_m + Q_f$) value decreases with both perfect and imperfect channel estimation. This figure itself shows that as N value increases, ($Q_m + Q_f$) value decreases due to the cooperation among the CRs.

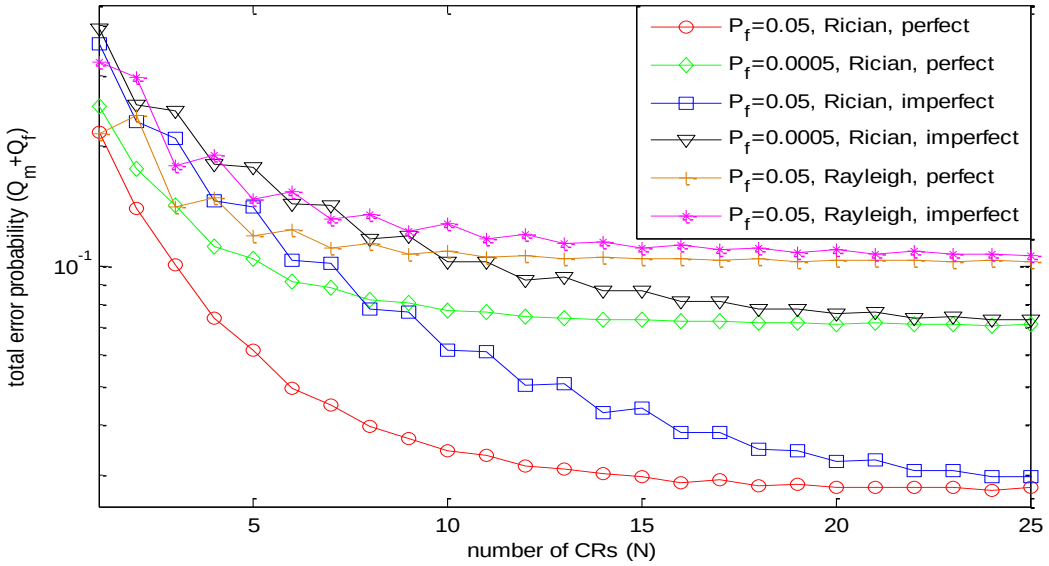

Fig.4.23. $Q_m + Q_f$ versus N graphs for different R-channel SNRs using Majority logic at FC.

For a particular instance, at N=8 and P_f value increases from 0.0005 to 0.05, ($Q_m + Q_f$) value decreases by 51.7% with perfect channel estimation and it decreases by 33.4% with imperfect channel estimation. ($Q_m + Q_f$) value is more with imperfect channel estimation compared to perfect channel estimation. The total error probability is constant after a certain number of CRs (N=13) because FC may select the CRs have less probability to reject. As the nature of the channel changes from imperfect to perfect, ($Q_m + Q_f$) value decreases by 49.1% at P_f=0.05 and N=8. The performance comparison between Rayleigh and Rician fading

channels are also provided. $(Q_m + Q_f)$ value is 64.9% less with perfect channel estimation and it is 39% less with imperfect channel estimation in Rician fading compared to Raleigh fading at P_f=0.05 and N=8.

Figure 4.24 is drawn between $(Q_m + Q_f)$ and P_f using MRC Rule at FC. The performance comparison between perfect channel estimation and imperfect channel estimation is shown over Rician fading. Two P_f values namely 0.0005 and 0.05, S-channel SNR=15dB, R-channel SNR=-5dB, and K=3 are used in the simulation. For a particular instance, at N=8 and P_f value increases from 0.0005 to 0.05, $(Q_m + Q_f)$ value decreases by 61.3% with perfect channel estimation and it decreases by 51.5% with imperfect channel estimation.

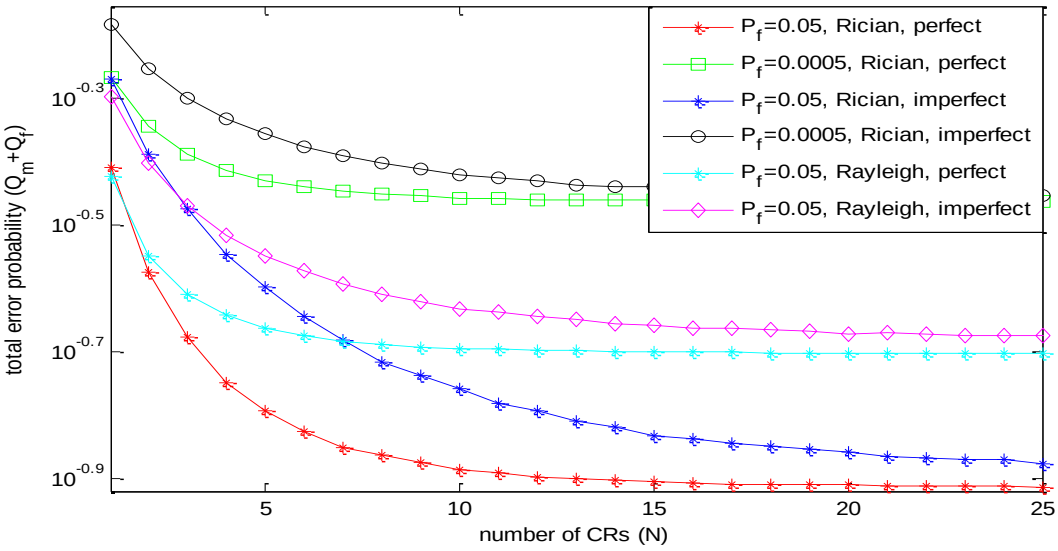

Fig.4.24. $Q_m + Q_f$ versus N graphs for different P_f values using MRC Rule at FC.

As the nature of the channel changes from imperfect to perfect channel estimation, $(Q_m + Q_f)$ value decreases by 28.7% at P_f=0.05 and N=8. $(Q_m + Q_f)$ value is 33.3% less with perfect channel and it is 21.9% less with imperfect channel in Rician fading compared to Rayleigh fading channel at P_f=0.05 and N=8.

Figure 4.25 is drawn between $(Q_m + Q_f)$ and Hoyt fading parameter (q) using majority logic at FC. The performance comparison between perfect channel estimation and imperfect channel estimation is shown over Hoyt fading. Two different q values namely 0.5 and 0.3, S-channel SNR=15dB, R-SNR=-7dB, and P_f=0.05 are used in the simulation. As q-value increases, $(Q_m + Q_f)$ value decreases with perfect and imperfect channel estimation. As fading parameter increases, fading effect decreases. For a particular instance, at N=8 and q-value

increases from 0.3 to 0.5, $(Q_m + Q_f)$ value decreases by 18.3% with perfect channel estimation and it decreases by 9.5% with imperfect channel estimation. As the nature of the channel changes from imperfect to perfect channel estimation, $(Q_m + Q_f)$ value decreases by 34.7% at P_f=0.05 and N=8. The performance comparison between Rayleigh and Hoyt fading channels are also provided. $(Q_m + Q_f)$ value is 34.7% more with perfect channel and it is 26.7% more with imperfect channel in Hoyt channel compared to Rayleigh channel at N=8.

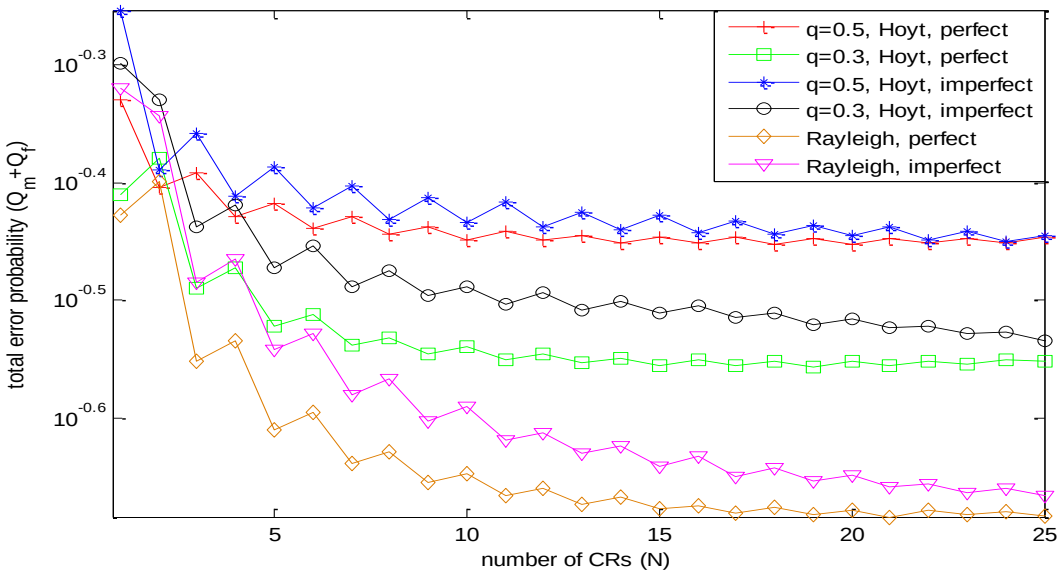

Fig.4.25. $Q_m + Q_f$ versus N graphs for different Hoyt fading parameters using Majority logic at FC.

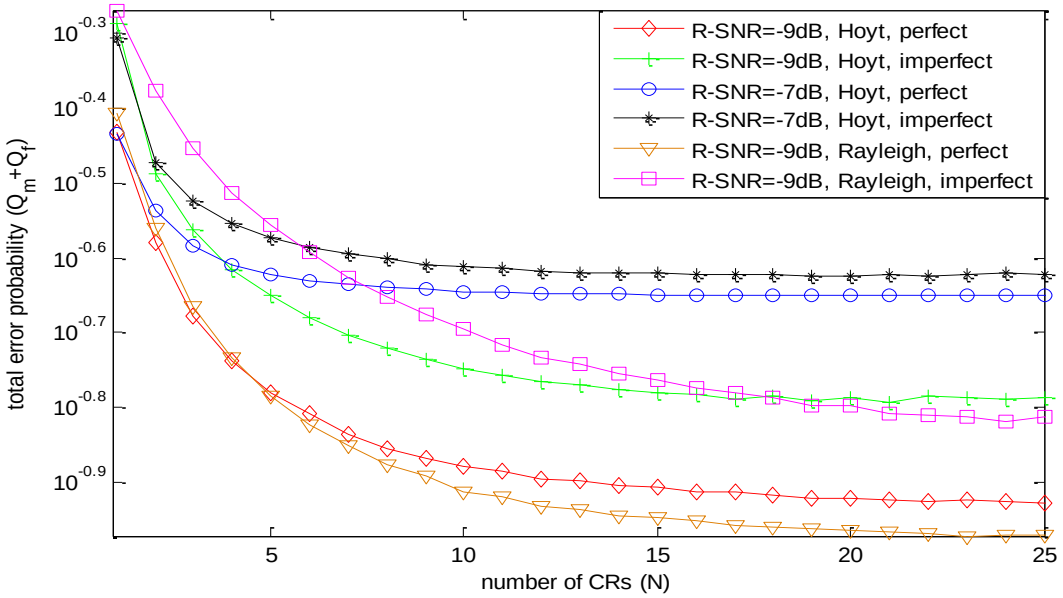

Fig.4.26. $Q_m + Q_f$ versus N graphs for different R-channel SNRs using MRC Rule at FC.

Figure 4.26 is drawn between $(Q_m + Q_f)$ and N using MRC Rule at FC. The performance comparison between perfect channel estimation and imperfect channel estimation is shown over Hoyt fading. Two different R-channel SNR values namely -9dB and -7dB, S-channel SNR=15dB, q=0.5, and P_f=0.05 are used in the simulation. For a particular instance, at N=8 and R-SNR=-9dB, if the channel nature changes from imperfect to perfect, $(Q_m + Q_f)$ value decreases by 26.6% in Rayleigh fading and it decreases by 8.5% in Hoyt fading. $(Q_m + Q_f)$ value is 14.9% more with perfect channel and it is 4.5% more with imperfect channel in Hoyt fading compared to Rayleigh fading at R-SNR=-9dB and N=8.

In Fig.4.27, we have considered K and N as variable parameters to evaluate the performance of $(Q_m + Q_f)$ as a function of C_{th} with perfect channel estimation in Rician fading. Two different fusion rule are individually used at FC to make a final decision about the PU and the performance comparison between them also provided. As K value increases, fading effect present in the channel decreases which increases the detection probability. As N value decreases, cooperation among the CRs are decreases so that detection probability value decreases.

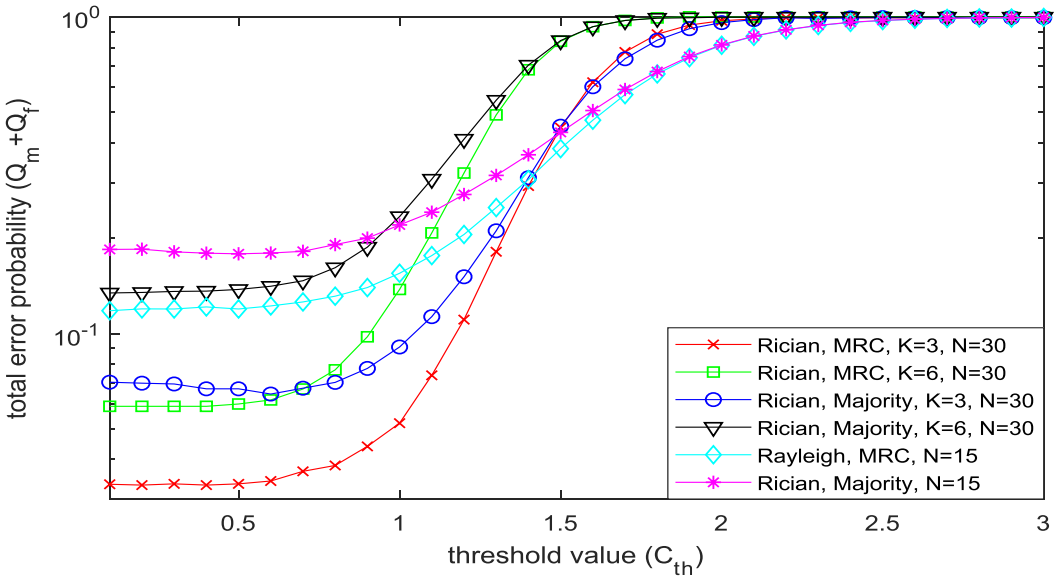

Fig. 4.27. $Q_m + Q_f$ versus C_{th} as a function of K and N with perfect channel estimation.

As K value increases from 3 to 6 and N value decreases from 30 to 15, $(Q_m + Q_f)$ value decreases by 61.2% with majority logic and it decreases by 62.2% with MRC rule with perfect channel estimation. Similarly, $(Q_m + Q_f)$ value decreases by 53% with majority logic and it decreases by 57.4% with MRC rule with imperfect channel for same conditions. Though K

value increases and *N* value decreases, $(Q_m + Q_f)$ value increases because cooperation among the users decreases. MRC rule achieves lower value of total error compared to majority logic. For a particular value of *K*=3, *N*=30, and MRC rule used at FC instead of majority rule, $(Q_m + Q_f)$ value reduces by 42.5% with perfect channel estimation and it reduces by 28.9% with imperfect channel estimation respectively at C_{th}=1.0. $(Q_m + Q_f)$ value is 5.8% less with majority logic and it is 11% less with MRC rule when fading effect changes from Rayleigh to Rician fading at *N*=15 and C_{th}=1.0.

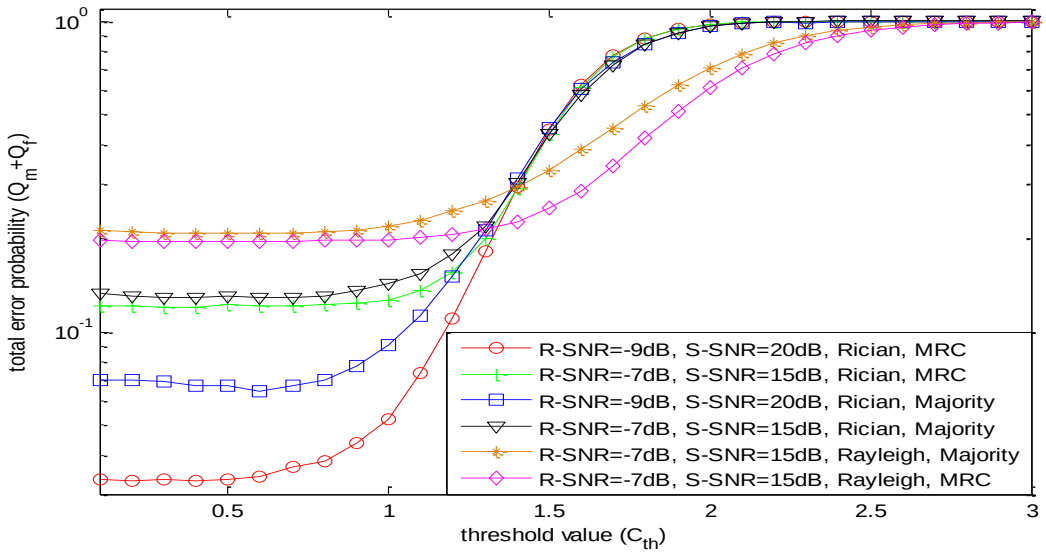

Fig. 4.28 $Q_m + Q_f$ versus C_{th} as a function of R-SNRs and S-SNRs with perfect channel estimation.

Figure 4.28 shows the effect on $(Q_m + Q_f)$ for various values of R-channel SNR and S-channel SNR values with perfect channel estimation in Rician fading. The performance comparison between MRC rule and majority logic is provided in Fig.4.28. As R-channel SNR value increases from -9dB to -7dB and S-channel SNR value decreases from 20dB to 15dB, $(Q_m + Q_f)$ value decreases by 36.5% with majority logic and it decreases by 58.8% with MRC logic at C_{th}=1.0. For a particular value of R-channel SNR=-9dB, S-channel SNR=20dB, and MRC rule is used at FC instead of majority logic, $(Q_m + Q_f)$ value reduces by 45.3% at C_{th}=0.8. The network parameters such as P_f= 0.05, S-channel SNR= 20dB and 15dB, R-channel SNR=-7dB and -9dB, *K*=3, and *N*=30 are used in the simulation. For a particular value of R-SNR=-7dB and S-SNR=15dB, as the fading environment changes from Rayleigh to Rician channel, $(Q_m + Q_f)$ value decreases by 34.7% with majority logic and it decreases by 36.1% with MRC Rule at C_{th}=1.0.

Figure 4.29 is drawn between (Q_m+Q_f) and C_{th} with imperfect channel estimation in Hoyt fading channel. The network parameters such as *N*=30, P_f=0.05, *q*=0.5, S-channel SNR=15dB and 20dB, and R-channel SNR=-7dB are used in the simulation. The performance comparison between two fusion rules are provided. For a particular value of C_{th}=1.0, S-channel SNR = 15dB, and MRC rule is used at FC instead of majority logic, (Q_m+Q_f) value reduces by 11%. Similarly, as S-channel SNR value increases from 15dB to 20dB, (Q_m+Q_f) value decreases by 40.5% with majority logic and it decreases by 46.2% with MRC rule at C_{th}=1.0. (Q_m+Q_f) value is 5.6% more with majority logic and it is 13.5% more with MRC Rule in Hoyt channel compared to Rayleigh channel at S-channel SNR=20dB and C_{th}= 1.0.

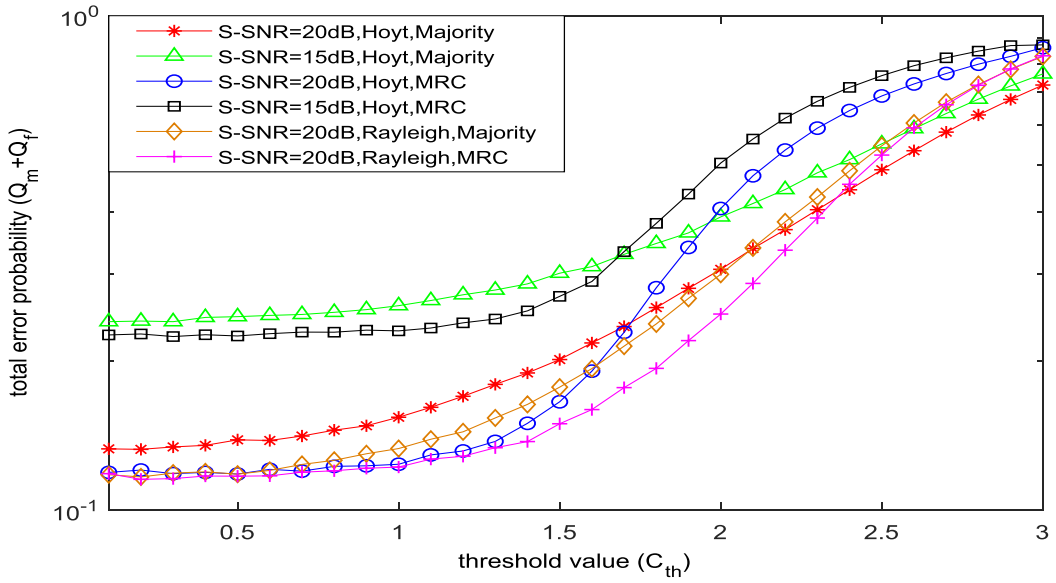

Fig.4.29. $Q_m + Q_f$ versus C_{th} graphs for different S-channel SNRs with imperfect channel estimation.

Figure 4.30 shows the effect on ($Q_m + Q_f$) for various values of R-channel SNR with perfect channel estimation in Weibull fading. The performance comparison between MRC rule and majority logic is provided in Fig.4.30. As R-channel SNR increases from -9dB to -7dB, ($Q_m + Q_f$) value decreases by 12.7% with majority logic and it decreases by 30.4% with MRC rule at C_{th}=0.8. For a particular value of R-channel SNR=-9dB, S-channel SNR=15dB, and MRC logic rule used at FC instead of majority logic, ($Q_m + Q_f$) value reduces by 34.3% at C_{th}=0.8. The network parameters P_f= 0.05, S-channel SNR= 15dB, R-channel SNR=-7dB and -9dB, *V*=5, and *N*=30 are used in the simulation.

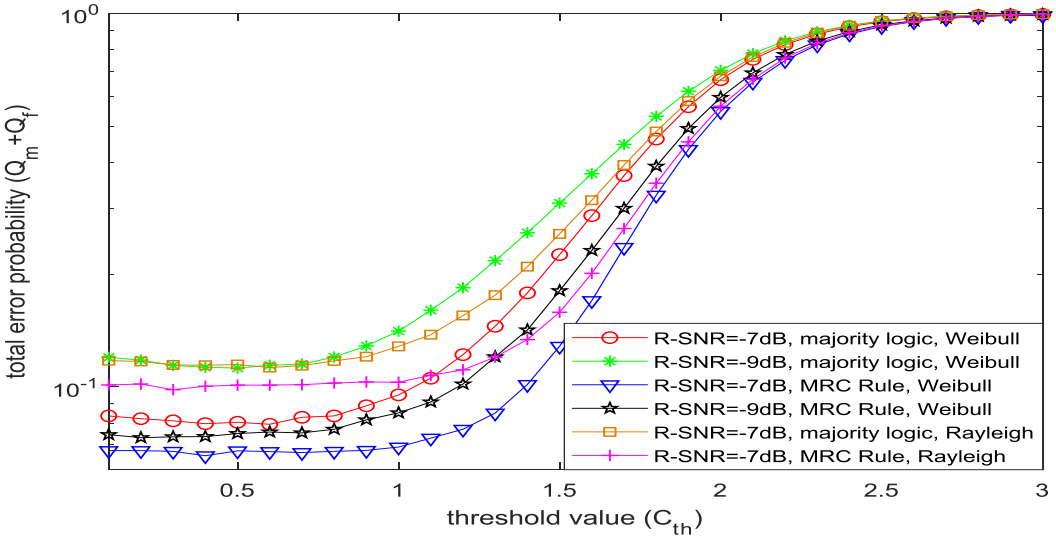

Fig. 4.30 $Q_m + Q_f$ versus C_{th} as a function of R-channel SNRs with perfect channel estimation.

Network parameters	Rayleigh fading (Existing)		Rician fading (Proposed)		Hoyt fading (Proposed)		Weibull fading (Proposed)	
	Perfect channel	Imperfect channel	Perfect channel	Imperfect channel	Perfect channel	Imperfect channel	Perfect channel	Imperfect channel
R-SNR=-9dB (Majority)	0.1775	0.1995	0.1155	0.1589	0.2057	0.2228	0.0872	0.1246
R-SNR=-9dB (MRC)	0.1535	0.1863	0.0764	0.1233	0.1812	0.2052	0.0282	0.0602
R-SNR=-7dB (Majority)	0.1589	0.1733	0.0849	0.1175	0.1868	0.1965	0.0451	0.0748
R-SNR=-7dB (MRC)	0.1485	0.1612	0.0653	0.0926	0.1747	0.1855	0.0188	0.0396
S-SNR=15dB (Majority)	0.0655	0.0849	0.0393	0.0751	0.0823	0.0972	0.0304	0.0608
S-SNR=15dB (MRC)	0.0519	0.0726	0.0181	0.0433	0.0662	0.0785	0.0039	0.0249
S-SNR=10dB (Majority)	0.0745	0.0923	0.0849	0.1155	0.1868	0.1965	0.0451	0.0733
S-SNR=10dB (MRC)	0.0586	0.0775	0.0652	0.0883	0.1747	0.1855	0.0188	0.0396

Table 4.1 Missed detection probability (Q_m) values for different fading channels using Rank based censoring scheme.

Network parameters	Rayleigh fading (Existing)		Rician fading (Proposed)		Hoyt fading (Proposed)		Weibull fading (Proposed)	
	Perfect channel	Imperfect channel	Perfect channel	Imperfect channel	Perfect channel	Imperfect channel	Perfect channel	Imperfect channel
R-SNR=-9dB (Majority)	0.1002	0.1018	0.0517	0.0679	0.1101	0.1208	0.0409	0.0268
R-SNR=-9dB (MRC)	0.0596	0.0831	0.0288	0.0486	0.0720	0.0972	0.0168	0.0323
R-SNR=-7dB (Majority)	0.0709	0.0832	0.0264	0.0365	0.0791	0.0883	0.0254	0.0316
R-SNR=-7dB (MRC)	0.0507	0.0611	0.0178	0.0257	0.0640	0.0745	0.0127	0.0191
S-SNR=15dB (Majority)	0.1655	0.1835	0.0753	0.0804	0.1822	0.1948	0.0553	0.0604
S-SNR=15dB (MRC)	0.1485	0.1557	0.0651	0.0715	0.1719	0.1820	0.0451	0.0515
S-SNR=10dB (Majority)	0.0709	0.0832	0.0264	0.0365	0.0791	0.0883	0.0164	0.0265
S-SNR=10dB (MRC)	0.0517	0.0611	0.0178	0.0257	0.0640	0.0745	0.0078	0.0157

Table 4.2 Missed detection probability (Q_m) values for different fading channels using Threshold based censoring scheme.

In table.4.1 and table.4.2, missed detection probability (Q_m) values are provided using Rank based censoring scheme and Threshold based censoring schemes individually in R-channel of CSS network. The performance is evaluated with perfect and imperfect channel estimation and comparison between them also provided. These Q_m values are calculated for different network parameters such as R-channel SNR, S-channel SNRs using majority logic and MRC rule at fusion center in different fading environments (Rician, Weibull, and Hoyt fading channels). All the Q_m values are calculated at number of CRs N=10 in Rank based censoring scheme and threshold value C_{th}=0.8 in Threshold based censoring scheme. In each case, missed detection probability values are more with imperfect channel estimation compared to perfect channel estimation because estimation error is present in imperfect channel. Q_m performance with MRC rule is better compared to majority logic rule. The MRC rule achieves lower Q_m values with both perfect and imperfect channel.

4.7. Conclusions

In this chapter, we have investigated the performance analysis of cooperative spectrum sensing (CSS) network using the censoring schemes (Rank based and Threshold based) over various fading channels (Rician, Weibull, and Hoyt fading channels). The CED scheme and a single antenna are used at each CR in the CSS network. The performance is evaluated using the hard decision fusion rule (majority logic) and soft data fusion rule (MRC rule) at the fusion center. The performance has been analyzed in a comparative way, considering meaningful performance metrics and evaluating the impact of several network parameters. Our simulation results shows that CSS network with censoring of CRs using the CED scheme achieves the lowest probability of missed detection with MRC rule compared to the majority logic under similar conditions for different fading channels with perfect and imperfect channel estimations. The novel expressions for estimation error is derived and its mean and variance are also calculated for different fading channels in imperfect reporting channel.

Our simulation results shows that as R-channel SNR value increases, missed detection probability (Q_m) value decreases with both perfect and imperfect channel estimation. The perfect channel estimation gives lower value of Q_m than imperfect channel estimation. Censoring threshold value is used to select the less fading reporting channel radio links, hence missed detection probability varies according to censoring threshold value. Censoring scheme is useful to reduce the system complexity, to eliminate traffic overhead communication problem, and to eliminate the heavily faded channel coefficients.

Chapter-5

Performance Analysis using an Optimization of CSS Network Parameters

5.1. Introduction

Spectrum sensing (SS) technique is used to monitor the radio spectrum continuously. The vacant bands or spectrum holes of radio spectrum can be identified with the help of detection techniques. Various detection techniques are addressed in the literature such as conventional energy detection (CED), cyclostationary detection, and matched filter detection. The CED scheme [10] is a frequently used detection method due to low complexity compared to other detection methods and it is an optimal detection technique when SUs do not have any information about PU signals. The detection performance using SS technique is limited due to a single CR present in the network, fading, and multipath shadowing effects. To overcome these drawbacks, the multiple number of CR users are used to sense the spectrum; this concept is called as a cooperative spectrum sensing (CSS) technique [2, 14, 15]. The CSS network provides better immunity to fading and shadowing effects and it consists of a single antenna and CED scheme at each CR to mitigate the fading effect and to improve the detection probability value. The detection performance can be further improved by using an improved energy detector (IED) scheme in the CSS network [17, 18]. An IED measures the received signal amplitude with an arbitrary positive power (p) instead of squaring device used in CED. Using an IED scheme and multiple antennas at each CR in the CSS network will further improve the detection probability value. Sometimes, it is required to optimize the performance of CSS network by optimizing its network parameters to reduce the complexity of the network and to achieve better performance with minimum number of components.

In this chapter, we have evaluated the optimized performance of proposed CSS network by optimizing its network parameters over various fading channels. The performance is evaluated using multiple antennas and an IED scheme at each CR in the proposed CSS network when it is affected by various fading channels such as Rayleigh, Rician, Hoyt, and Weibull fading channels. We have derived the novel expressions of missed detection probability (P_m) considering multiple antennas (M) at each CR for different fading channels. Selection combining (SC) diversity scheme is used at each CR to select the maximum value of antenna among all antennas present at each CR. The binary symmetric channel (BSC) having an error probability rate (r) is assumed between CRs and FC. The closed form of optimal expressions for CSS network parameters such as optimal number of CR users (N_{opt}), optimal value of threshold value (λ_{opt}), optimal value of arbitrary the power of received signal (p_{opt}) are derived in various fading environments. The simulations are drawn to find out the optimal values of network parameters and to calculate the minimum value of total error rate for various fading channels. The network parameters such as threshold value (λ), arbitrary power of received signal (p), error rate (r), and multiple antennas at each CR are considered as simulation parameters. The performance comparison between CED and IED schemes, comparison among various fading channels are also provided for different cases.

5.2. System Model

There are various detection schemes are addressed in the literature to decide the primary user activity. Among all detection schemes, conventional energy detection (CED) scheme is frequently used because of less complex and non-coherent in nature. To further improvement in detection probability of primary user an improved energy detector (IED) scheme is used. Fig.5.1 shows the system model of IED technique. According to it, the received signal is passed through the bandpass filter (BPF) to eliminate the noise components present in it. Further, the received signal is passed through the non-linear device which having arbitrary power p to calculate the energy present in the received signal. If p=2, in the non-linear device it becomes CED scheme. For an IED scheme value of p should be more than two i.e. p>2.

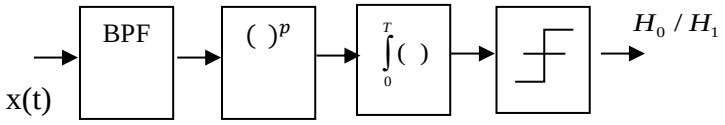

Fig. 5.1. Block diagram of an improved energy detector.

The integrator block is used to calculate the energy for a particular duration of time. Finally, output of the integrator block is compared with the pre-defined threshold value to decide the primary user activity (i.e. absence or presence of PU). *p*- is arbitrary power of the received signal, it is an integer value like *p*=2, 3, 4. For *p*=2, an IED scheme becomes to CED scheme hence it is a unit less quantity.

Figure 5.2 shows the proposed model of CSS network with *N* number of SUs, an FC, and a PU. The channel present between PU and SUs is called as sensing channel (S-channel); in this channel each CR senses and stores the information about the PU. The sensing information associated with each CR is transferred to the FC through reporting channel (R-channel) and S-channel is assumed as an error-free channel. The R-channel lies between SUs and FC in the proposed network and error rate (r) is considered in it. The complete information from all CRs are collected at FC and the final decision made at FC using the fusion rules such as *OR-Rule* and *AND-Rue*. Each CR uses an IED scheme and SC diversity technique to get the binary decision about the PU.

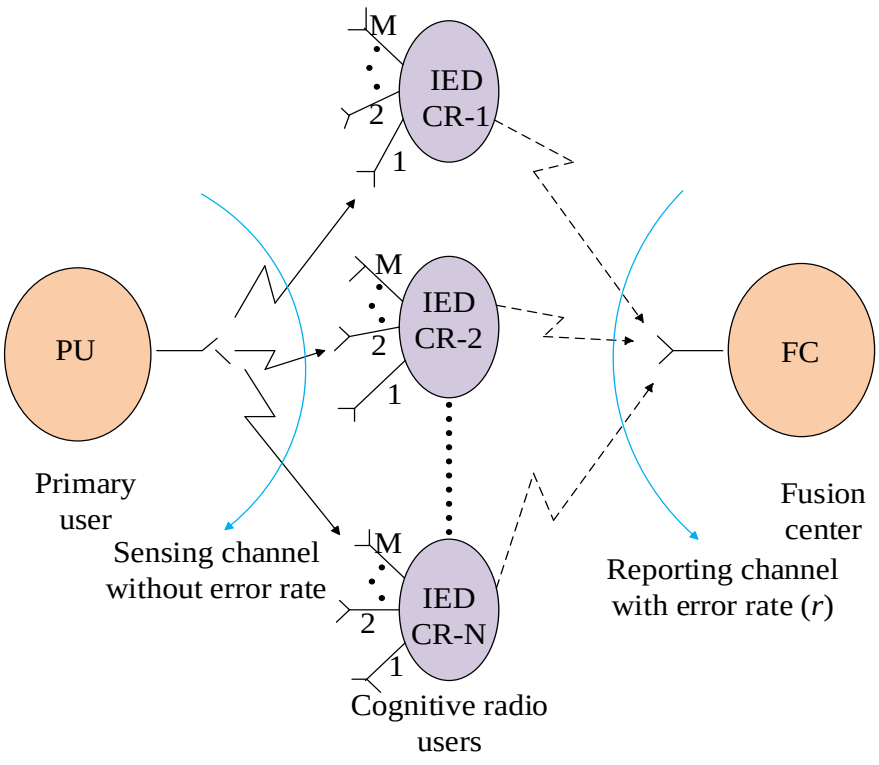

Fig. 5.2. Proposed model of cooperative spectrum sensing network.

Two hypotheses are defined in the literature to decide the absence and presence of PU as H_0 and H_1 respectively. The received signal at *j*-th CR can be written as [10];

$$y_j(\mathrm{t}) = \begin{cases} n_j(t) & : H_0 \\ h_j * s(t) + n_j(t) & : H_1 \end{cases} \tag{5.1}$$

In the above expression, $s(t)$ represents the received signal at the input of IED and $n_j(t)$ is the noise value at *j*-th CR. AWGN noise (Additive white Gaussian noise) is considered in the network which is uniformly distributed over each CR. h_j is the fading coefficient which occurs due to fading effect in the channel.

The expression for *i*-th antenna to make a local decision about the PU is given by [18]

$$W_i = y_i^{\,p} \; ; \qquad p > 0 \tag{5.2}$$

For an IED scheme, *p*-value should be more than 2, i.e., (*p*> 2) to achieve better detection probability than CED scheme.

Each CR uses an IED technique to get the decision statistics from all antennas (*i*= 1….*M*). With the help of SC diversity technique, the largest value of w_i can be selected from all available w_i values and it is denoted as *Z*. The final decision about the PU is obtained by comparing *Z* value with detection threshold (λ) is calculated as [28];

$$Z \geq \lambda \; : H_1 \;\; \& \;\; \mathrm{Z} < \lambda \; : H_0 \tag{5.3}$$

Where λ can be obtained from the expression

$$\lambda = \lambda_n \sigma_n^p \tag{5.4}$$

where λ_n represents the normalized detection threshold value and σ_n^2 is the noise power for *p*=2.

5.3. Missed Detection Probability Calculation for Different Fading Channels

In this section, missed detection probability (P_m) expression for AWGN, Rayleigh, Rician, Weibull, and Hoyt fading channels are derived using multiple antennas (*M*) and an IED scheme at each CR in CSS network.

5.3.1. Missed Detection Probability Expression for AWGN Channel

The missed detection probability expression for non-fading channel (AWGN channel) can be calculated using the PDF given in [100, 64];

$$f_{y_i|H_1}(y) = \frac{2y^{\frac{1-p}{p}}}{p\sqrt{2\pi(E_s\sigma_h^2+\sigma_n^2)}}\exp\left(-\frac{y^{2/p}}{2(E_s\sigma_h^2+\sigma_n^2)}\right) \tag{5.5}$$

Steps for the calculation of P_m expression for AWGN are provided in Appendix A.1. Finally, P_m expression for AWGN channel using multiple (M) antennas and an IED scheme at each CR is obtained as;

$$P_{m,AWGN} = \left[\frac{1}{\sqrt{\pi}}\gamma\left(\frac{1}{2},\frac{\lambda^{(2/p)}}{2(E_s\sigma_h^2+\sigma_n^2)}\right)\right]^M \tag{5.6}$$

5.3.2. Missed Detection Probability Expression for Rayleigh Fading Channel

The missed detection probability expression for Rayleigh fading channel can be calculated using the PDF given in [28];

$$f_{y_i|H_1}(y) = \frac{2y^{\frac{2-p}{p}}}{p(E_s\sigma_h^2+\sigma_n^2)}\exp\left(-\frac{y^{2/p}}{(E_s\sigma_h^2+\sigma_n^2)}\right) \tag{5.7}$$

Steps for the calculation of P_m expression for Rayleigh fading channel are provided in Appendix A.2. Finally, P_m expression for Rayleigh fading channel using multiple antennas and an IED scheme at each CR is obtained as;

$$P_{m,Ray} = \left(1-\exp\left(-\lambda^{2/p}/(1+\bar{\gamma})\sigma_n^2\right)\right)^M \tag{5.8}$$

where $\gamma = E_s\sigma_h^2/\sigma_n^2$ is S-channel SNR.

5.3.3. Missed Detection Probability Expression for Rician Fading Channel

The missed detection probability expression for Rician fading channel can be calculated using the PDF given in [10, 64];

$$f_{w_i|H_1}(y) = \frac{2y^{(2/p)-1}(K+1)}{p(E_s\sigma_h^2+\sigma_n^2)}\exp\left(-K-\frac{(K+1)y^{2/p}}{(E_s\sigma_h^2+\sigma_n^2)}\right)I_0\left(2\sqrt{\frac{K(1+K)y^{2/p}}{(E_s\sigma_h^2+\sigma_n^2)}}\right) \tag{5.9}$$

where K is Rician fading parameter.

Steps for the calculation of P_m expression for Rician fading channel are provided in Appendix A.3. Finally, P_m expression for Rician fading channel using multiple antennas and an IED scheme at each CR is obtained as;

$$P_{m,Ric} = \left[1 - Q\left(\sqrt{2K}, \lambda^{1/P}\sqrt{\frac{2(1+K)}{\sigma_n^2(1+\bar{\gamma})}}\right)\right]^M \tag{5.10}$$

where $\gamma = E_s\sigma_h^2/\sigma_n^2$ is S-channel SNR.

5.3.4. Missed Detection Probability Expression for Weibull Fading Channel

The missed detection probability expression for Weibull fading channel can be calculated using the PDF given in [112];

$$f_{w_i|\mathrm{H}_1}(\mathrm{y}) = \frac{2y^{(2/p)-1}C}{p}\left[\frac{\Gamma(P)}{(E_s\sigma_h^2+\sigma_n^2)}\right]\left(\mathrm{y}^{2/p}\right)^{\mathrm{C}-1}\exp\left(-\left\{\frac{\mathrm{y}^{2/p}\Gamma(P)}{(E_s\sigma_h^2+\sigma_n^2)}\right\}^C\right) \tag{5.11}$$

where $C = V/2$, $P = 1 + 1/C$, and V is Weibull fading parameter.

Steps for the calculation of P_m expression for Weibull fading channel are provided in Appendix A.4. Finally, P_m expression for Weibull fading channel using multiple antennas and an IED scheme at each CR is obtained as;

$$P_{m,\mathrm{Wei}} = \left[1 - \exp\left(-\left\{\frac{\lambda^{2/p}\Gamma(P)}{\sigma_n^2(1+\bar{\gamma})}\right\}^C\right)\right]^M \tag{5.12}$$

where $\gamma = E_s\sigma_h^2/\sigma_n^2$ is S-channel SNR.

5.3.5. Missed Detection Probability Expression for Hoyt Fading Channel

The missed detection probability expression for Hoyt fading channel can be calculated using the PDF given in [67];

$$f_{y_i|\mathrm{H}_1}(\mathrm{y}) = \frac{\mathrm{y}^{2/p-1}}{p\sigma_1\sigma_2}\exp\left(-\left(\frac{y^{2/p}}{4}\right)\left(\frac{1}{\sigma_2^2}+\frac{1}{\sigma_1^2}\right)\right)I_0\left(\left(\frac{y^{2/p}}{4}\right)\left(\frac{1}{\sigma_2^2}-\frac{1}{\sigma_1^2}\right)\right) \tag{5.13}$$

where $\sigma_1^2 = \frac{E_s\sigma_I^2+\sigma_n^2}{2}$, $\sigma_2^2 = \frac{E_s\sigma_q^2+\sigma_n^2}{2}$, $\sigma_I = \sqrt{\frac{\Omega q^2}{1+q^2}}$, $\sigma_q = \sqrt{\frac{\Omega}{1+q^2}}$, and q is the Hoyt fading parameter which ranges from 0 to 1.

Steps for the calculation of P_m expression for Hoyt fading channel are provided in Appendix A.5. Finally, P_m expression for Hoyt fading channel using multiple antennas and an IED scheme at each CR is obtained as;

$$P_{m,Hoyt} = \frac{1}{16}\left[1 + exp(-A\lambda^{2/p})\,\mathrm{I}_0(B\lambda^{2/p}) - 2Q(u_1, v_1)\right]^M \tag{5.14}$$

where

$$A = \left(\frac{1}{4}\right)\left(\frac{1}{\sigma_2^2} + \frac{1}{\sigma_1^2}\right),\ B = \left(\frac{1}{4}\right)\left(\frac{1}{\sigma_2^2} - \frac{1}{\sigma_1^2}\right),\ u_1 = \sqrt{\left(A - \sqrt{A^2 - B}^2\right)\lambda^{2/p}}\ , v_1 = \sqrt{\left(A - \sqrt{A^2 - B}^2\right)\lambda^{2/p}}$$

Expression for P_m is different for various fading channels because it depends on S-channel SNR value. Similarly, expression for probability false alarm (P_f) using multiple antennas and an IED scheme at each CR is provided in [28], which is independent of S-channel SNR. The expression for probability of false alarm is given as [28];

$$P_f = 1 - \left(1 - \exp\left(-\lambda^{2/p}/\sigma_n^2\right)\right)^M \tag{5.15}$$

Setting a threshold value in IED scheme is more important to decide the presence or the absence of a PU. It also helps to get the complementary receiver operating characteristics (CROC) curves for the proposed network. The closed form of expression for threshold value at each CR can be derived by using Eq. (5.15) as;

$$\lambda = \left\{\sigma_n^2 \ln\left[\frac{1}{1 - \exp(\ln(1 - P_f)/M)}\right]\right\}^{\frac{p}{2}} \tag{5.16}$$

5.4. Total Error Rate Calculation for Different Fading Channels

To calculate the total error probability ($Q_m + Q_f$) value in different fading channels, initially, we require probability of false alarm (P_f) and probability of missed detection (P_m) expressions for each CR. Later, we can calculate Q_m and Q_f values using the expressions below which are missed detection and false alarm probabilities of all CRs. Q_m and Q_f expressions with an error rate (r) in R-channel are given as [27];

$$\begin{aligned} Q_f &= 1 - [(1 - P_f)(1 - r) + rP_f]^N \\ Q_m &= [P_m(1 - r) + r(1 - P_m)]^N \end{aligned} \tag{5.17}$$

Finally, total error rate *Z(N)* is calculated by taking the sum of Q_m and Q_f is [27]

$$Z(p, \lambda, N) \cong Q_f + Q_m \tag{5.18}$$

$$\Rightarrow 1 - [(1 - P_f)(1 - r) + rP_f]^N + [P_m(1 - r) + r(1 - P_m)]^N \tag{5.19}$$

Expressions for Q_m and Q_f with perfect R-channel (r=0) when *OR-logic* is used at FC [118] are;

$$\begin{aligned} Q_f &= 1-[(1-P_f)]^N \\ Q_m &= [P_m]^N \end{aligned} \tag{5.20}$$

Similarly, expressions for Q_m and Q_f with perfect R-channel (r=0) when *AND-logic* is used at FC [118] are;

$$\begin{aligned} Q_m &= 1-[(1-P_m)]^N \\ Q_f &= [P_f]^N \end{aligned} \tag{5.21}$$

5.5. Optimization of CSS Network Parameters in Various Fading Channels

In this section, we have provided the procedure for calculating the optimal values of network parameters such as N, λ, and p.

5.5.1. Calculation of an Optimal Number of CRs (N_{opt})

In the proposed CSS network, if the number of CR users increases, there is a chance to occur larger delays while making a decision about the PU. Hence, it is necessary to find out the number of CR users which are exactly contributing for making a final decision about the PU, and these CRs are known as optimal number of CR users (N_{opt}). The expression for N_{opt} can be calculated as follows [27];

$$\Delta Z(N) = Z(N+1) - Z(N) = 0 \tag{5.22}$$

$$\begin{aligned} \Rightarrow &\left[(1-P_f)(1-r)+rP_f\right]^N - \left[(1-P_f)(1-r)+rP_f\right]^{N+1} \\ &+\left[P_m(1-r)+r(1-P_m)\right]^{N+1} - \left[P_m(1-r)+r(1-P_m)\right]^N = 0 \end{aligned} \tag{5.23}$$

after some mathematical computations and using [27, Eq.16], the expression for N_{opt} is obtained as;

$$N_{opt} \cong \left\lceil \frac{\ln f_2(r, P_f, P_m)}{\ln f_1(r, P_f, P_m)} \right\rceil \tag{5.24}$$

$$f_1(r, P_f, P_m) = \frac{P_m(1-r)+r(1-P_m)}{(1-P_f)(1-r)+rP_f} \tag{5.25}$$

$$f_2(r, P_f, P_m) = \frac{2rP_f - r - P_f}{P_m - 2rP_m + r - 1} \tag{5.26}$$

The derived N_{opt} expression remains the same for all fading channels. But, P_m expression varies for different fading channels. Hence, N_{opt} value varies with fading effect. From Eq. (5.24), it is clear that N_{opt} value depends on error probability rate (r) present in the R-channel. There are some special cases to calculate N_{opt} value for various values of r are given in [27] as follows;

Case (i): If R-channel is error-free (r=0), then N_{opt} expression reduces to

$$N_{opt} \cong \left\lceil \frac{\ln \frac{P_f}{1-P_m}}{\ln \frac{1-P_f}{P_m}} \right\rceil \tag{5.27}$$

When P_m and P_f values are equal, then N_{opt} value becomes '1'. It represents that only one CR is enough to minimize the total error value for the proposed network with perfect R-channel.

Case (ii): For r=1, there is a possibility to occur deterministic errors in the R-channel. Then N_{opt} expression reduces to

$$N_{opt} \cong \left\lceil \frac{\ln \frac{P_m}{1-P_f}}{\ln \frac{1-P_m}{P_f}} \right\rceil \tag{5.28}$$

When the deterministic errors are present in R-channel, N_{opt} value becomes '1' when both P_f and P_m values are equal.

Case (iii): For r=0.5, it represents that R-channel has maximum uncertainty.

5.5.2. Calculation of an Optimal Threshold Value (λ_{opt})

Sometimes it is required to optimize the threshold value to decide the PU activity with least value of the threshold. The expression for λ_{opt} can be calculated by differentiating Eq. (5.19) with respect to λ as follows [27];

$$\frac{\partial Z(n)}{\partial \lambda} = -N(2r-1)\left[(1-P_f)(1-r)+rP_f\right]^{N-1}\frac{\partial P_f}{\partial \lambda} + N(1-2r)\left[P_m(1-r)+r(1-P_m)\right]^{N-1}\frac{\partial P_m}{\partial \lambda} \tag{5.29}$$

5.5.3. Calculation of an Optimal Arbitrary Power of Received Signal (p_{opt})

It is also required to optimize the *p*-value to achieve the minimum value of total error rate. The expression for p_{opt} can be calculated by differentiating Eq. (5.19) with respect to *p* as follows [27];

$$\frac{\partial Z(n)}{\partial p} = -N(2r-1)\left[(1-P_f)(1-r)+rP_f\right]^{N-1}\frac{\partial P_f}{\partial p} + N(1-2r)\left[P_m(1-r)+r(1-P_m)\right]^{N-1}\frac{\partial P_m}{\partial p} \quad (5.30)$$

5.6. Optimization of CSS Network Parameters for Different Fusion Rules in Rayleigh Fading Channel

5.6.1. Derivation for Optimal Threshold (λ_{opt}) Expression

An optimum value of threshold (λ_{opt}) is required to decide the existence of PU with a minimum threshold value. For a single antenna case (*M*=1), the closed form of expression for λ_{opt} can be derived by differentiating Eq. (5.8) and Eq. (5.15) w.r.t. λ as;

$$\frac{\partial P_f}{\partial \lambda} + \frac{\partial P_m}{\partial \lambda} = 0 \quad (5.31)$$

$$\frac{\partial P_f}{\partial \lambda} = -\exp\left(-\frac{\lambda^{\frac{2}{p}}}{\sigma_n^2}\right)\frac{2\lambda^{\frac{2}{p}-1}}{p\sigma_n^2} \quad (5.32)$$

$$\frac{\partial P_m}{\partial \lambda} = \exp\left(-\frac{\lambda^{\frac{2}{p}}}{\sigma_n^2(1+\bar{\gamma})}\right)\frac{2\lambda^{\frac{2}{p}-1}}{p\sigma_n^2(1+\bar{\gamma})} \quad (5.33)$$

Substituting Eq. (5.32) and Eq. (5.33) in Eq. (5.31), after simplification, the closed form of expression for λ_{opt} is

$$\lambda_{opt} = \left(\frac{\sigma_n^2 \ln(1+\bar{\gamma})}{\bar{\gamma}/(1+\bar{\gamma})}\right)^{\frac{p}{2}} \quad (5.34)$$

Similarly, the closed form of expression for λ_{opt} using multiple antennas (*M*=3) at each CR is obtained as

$$\lambda_{opt} = \left(\frac{\sigma_n^2 \ln(1+\bar{\gamma})}{2\bar{\gamma}/(1+\bar{\gamma})}\right)^{\frac{p}{2}} \quad (5.35)$$

The procedure for the derivation of λ_{opt} expression is provided in Appendix B.1.

5.6.2. Derivation for Optimal Arbitrary Power of Received Signal (p_{opt}) Expression

It is necessary to optimize the arbitrary power of received signal (p). For a single antenna case (M=1), the closed form of expression for p_{opt} can be derived by differentiating Eq. (5.8) and Eq. (5.15) w.r.t. p as follows;

$$\frac{\partial P_f}{\partial p} + \frac{\partial P_m}{\partial p} = 0 \tag{5.36}$$

$$\frac{\partial P_m}{\partial p} = -\frac{2\log\lambda}{p^2}\left(\frac{\lambda^{\frac{2}{p}}}{2(1+\bar{\gamma})\sigma_n^2}\right)\exp\left(-\frac{\lambda^{\frac{2}{p}}}{(1+\bar{\gamma})\sigma_n^2}\right) \tag{5.37}$$

$$\frac{\partial P_f}{\partial p} = \exp\left(-\frac{\lambda^{\frac{2}{p}}}{\sigma_n^2}\right)\frac{2}{p^2}\frac{\lambda^{\frac{2}{p}}\log\lambda}{\sigma_n^2} \tag{5.38}$$

Substituting Eq. (5.37) and Eq. (5.38) in Eq. (5.36), after simplification, the closed form of expression for p_{opt} is

$$p_{opt} = \frac{2\ln\lambda}{\ln\left(\frac{\sigma_n^2\ln(1+\bar{\gamma})}{\left(\frac{\bar{\gamma}}{1+\bar{\gamma}}\right)}\right)} \tag{5.39}$$

Similarly, the closed form of expression for p_{opt} using multiple antennas (M=3) at each CR is obtained as

$$p_{opt} = \frac{2\ln\lambda}{\ln\left(\frac{2\sigma_n^2\ln(1+\bar{\gamma})}{\left(\frac{\bar{\gamma}}{1+\bar{\gamma}}\right)}\right)} \tag{5.40}$$

The procedure for the derivation of expression for p_{opt} is provided in Appendix B.2.

5.6.3. Optimized Expressions of CSS Network Parameters using OR-Rule

A. Calculation of N_{opt} expression

The closed form of expression for N_{opt} can be obtianed using Eq. (5.18) as

$$\Delta Z(N) = Z(N+1) - Z(N) = 0 \tag{5.41}$$

substituting Eq. (5.20) in Eq. (5.41),

$$1-(1-P_f)^{N+1}-1+(1-P_f)^{N}+P_m{}^{N+1}-P_m{}^{N}=0 \tag{5.42}$$

after simplification of Eq. (5.42), the final expression for N_{opt} is

$$N_{opt}=\left\lceil \frac{\ln\left(\frac{1-P_m}{P_f}\right)}{\ln\left(\frac{1-P_f}{P_m}\right)} \right\rceil \tag{5.43}$$

Eq. (5.43) remains the same for any fading channel when *OR-Rule* is used at FC. The procedure for the derivation of N_{opt} expression is provided in Appendix B.3.

B. Calculation of λ_{opt} expression

The closed form of expression for λ_{opt} can be obtained by differenting Eq. (5.18) w.r.t. λ, then make the sum equal to zero i.e.,

$$\frac{\partial Q_f}{\partial \lambda}+\frac{\partial Q_m}{\partial \lambda}=0 \tag{5.44}$$

substituting Eq. (5.20) in Eq. (5.44),

$$N\left(1-P_f\right)^{N-1}\frac{\partial P_f}{\partial \lambda}+N\left(P_m\right)^{N-1}\frac{\partial P_m}{\partial \lambda}=0 \tag{5.45}$$

where $\partial P_f / \partial \lambda$ and $\partial P_m / \partial \lambda$ are given by Eq. (5.32) and Eq. (5.33), substituting them in Eq. (5.45) gives the final expression for λ_{opt} using single antenna (*M*=1) at each CR and *OR-Rule* at FC is

$$\lambda_{opt}=\left(\frac{\sigma_n^2\left[\left(N-1\right)\ln\left(\frac{1-P_f}{P_m}\right)+\ln\left(1+\bar{\gamma}\right)\right]}{\left(\frac{\bar{\gamma}}{1+\bar{\gamma}}\right)} \right)^{\frac{p}{2}} \tag{5.46}$$

Similarly, the final expression for λ_{opt} using multiple antennas (*M*=3) at each CR and *OR-Rule* at FC is

$$\lambda_{opt}=\left(\frac{\sigma_n^2\left[\left(N-1\right)\ln\left(\frac{1-P_f}{P_m}\right)+\ln\left(1+\bar{\gamma}\right)\right]}{\left(\frac{2\bar{\gamma}}{1+\bar{\gamma}}\right)} \right)^{\frac{p}{2}} \tag{5.47}$$

The procedure for the derivation of λ_{opt} expression is provided in Appendix B.4.

C. Calculation of p_{opt} expression

The closed form of expression for p_{opt} can be obtained by differentiating Eq. (5.18) w.r.t. p and make the sum equal to zero i.e.,

$$\frac{\partial Q_f}{\partial p} + \frac{\partial Q_m}{\partial p} = 0 \tag{5.48}$$

substituting Eq. (5.20) in Eq. (5.48),

$$N\left(1-P_f\right)^{N-1}\frac{\partial P_f}{\partial p} + N\left(P_m\right)^{N-1}\frac{\partial P_m}{\partial p} = 0 \tag{5.49}$$

where $\partial P_m / \partial p$ and $\partial P_f / \partial p$ are given by Eq. (5.37) and Eq. (5.38), substituting them in Eq. (5.49) gives the final expression for p_{opt} using single antenna (M=1) at each CR and *OR-Rule* at FC is

$$p_{opt} = \frac{2\ln\lambda}{\ln\left(\dfrac{\sigma_n^2\left[\left(N-1\right)\ln\left(\dfrac{1-P_f}{P_m}\right)+\ln\left(1+\bar{\gamma}\right)\right]}{\left(\dfrac{\gamma}{1+\gamma}\right)}\right)} \tag{5.50}$$

Similarly, the final expression for p_{opt} using multiple antennas (M=3) at each CR and *OR-Rule* at FC is

$$p_{opt} = \frac{2\ln\lambda}{\ln\left(\dfrac{2\sigma_n^2\left[\left(N-1\right)\ln\left(\dfrac{1-P_f}{P_m}\right)+\ln\left(1+\bar{\gamma}\right)\right]}{\left(\dfrac{\gamma}{1+\gamma}\right)}\right)} \tag{5.51}$$

The procedure for the derivation of p_{opt} expression is provided in Appendix B.5.

5.6.4. Optimized Expressions of CSS Network Parameters using AND-Rule

A. Calculation of N_{opt} expression

The closed form of expression for N_{opt} can be obtianed using Eq. (5.20) as

$$\Delta Z(N) = Z(N+1) - Z(N) = 0 \tag{5.52}$$

substituting Eq. (5.21) in Eq. (5.52),

$$1-(1-P_m)^{N+1}-1+(1-P_m)^N+{P_f}^{N+1}-{P_f}^N=0 \tag{5.53}$$

after simplification of Eq. (5.53), the final expression for N_{opt} is

$$N_{opt}=\left\lceil \frac{\ln\left(\frac{1-P_f}{P_m}\right)}{\ln\left(\frac{1-P_m}{P_f}\right)} \right\rceil \tag{5.54}$$

Eq. (5.54) remains the same for any fading channel when *AND-Rule* is used at FC. The procedure for the derivation of N_{opt} expression is provided in Appendix B.6.

B. Calculation of λ_{opt} expression

The closed form of expression for λ_{opt} can be obtained by differentiating Eq. (5.18) w.r.t. λ, then make the sum equal to zero i.e.,

$$\frac{\partial Q_f}{\partial \lambda}+\frac{\partial Q_m}{\partial \lambda}=0 \tag{5.55}$$

substituting Eq. (5.21) in Eq. (5.55),

$$N\left(P_f\right)^{N-1}\frac{\partial P_f}{\partial \lambda}+N\left(1-P_m\right)^{N-1}\frac{\partial P_m}{\partial \lambda}=0 \tag{5.56}$$

where $\partial P_f / \partial \lambda$ and $\partial P_m / \partial \lambda$ are given in Eq. (5.32) and Eq. (5.33), substitutng them in Eq. (5.56), the final expression for λ_{opt} using single antenna (M=1) at each CR and *AND-Rule* at FC is

$$\lambda_{opt}=\left(\frac{\sigma_n^2\left[(N-1)\ln\left(\frac{P_f}{1-P_m}\right)+\ln\left(1+\bar{\gamma}\right)\right]}{\left(\frac{\bar{\gamma}}{1+\bar{\gamma}}\right)} \right)^{\frac{p}{2}} \tag{5.57}$$

Similarly, the final expression for λ_{opt} using multiple antennas (M=3) at each CR and *AND-Rule* at FC is

$$\lambda_{opt}=\left(\frac{\sigma_n^2\left[(N-1)\ln\left(\frac{P_f}{1-P_m}\right)+\ln\left(1+\bar{\gamma}\right)\right]}{\left(\frac{2\bar{\gamma}}{1+\bar{\gamma}}\right)} \right)^{\frac{p}{2}} \tag{5.58}$$

The procedure for the derivation of λ_{opt} expression is provided in Appendix B.7.

C. Calculation of p_{opt} expression

The closed form of expression for p_{opt} can be obtained by differentiating Eq. (5.18) w.r.t. *p*, and make the sum equal to zero i.e.,

$$\frac{\partial Q_f}{\partial p} + \frac{\partial Q_m}{\partial p} = 0 \tag{5.59}$$

substituting Eq. (5.21) in Eq. (5.59),

$$N\left(P_f\right)^{N-1}\frac{\partial P_f}{\partial p} + N\left(1-P_m\right)^{N-1}\frac{\partial P_m}{\partial p} = 0 \tag{5.60}$$

where $\partial P_m / \partial p$ and $\partial P_f / \partial p$ are given in Eq. (5.37) and Eq. (5.38), substitutng them in Eq. (5.60), the final expression for p_{opt} using single antenna (*M*=1) at each CR and *AND-Rule* at FC is

$$p_{opt} = \frac{2\ln\lambda}{\ln\left(\dfrac{\sigma_n^2\left[\left(N-1\right)\ln\left(\dfrac{P_f}{1-P_m}\right)+\ln\left(1+\bar{\gamma}\right)\right]}{\left(\dfrac{\bar{\gamma}}{1+\bar{\gamma}}\right)}\right)} \tag{5.61}$$

Similarly, the final expression for p_{opt} using multiple antennas (*M*=3) at each CR and *AND-Rule* at FC is

$$p_{opt} = \frac{2\ln\lambda}{\ln\left(\dfrac{2\sigma_n^2\left[\left(N-1\right)\ln\left(\dfrac{P_f}{1-P_m}\right)+\ln\left(1+\bar{\gamma}\right)\right]}{\left(\dfrac{\bar{\gamma}}{1+\bar{\gamma}}\right)}\right)} \tag{5.62}$$

The procedure for the derivation of p_{opt} expression is provided in Appendix B.8.

5.7. Optimization of CSS Network Parameters for Different Fusion Rules in Weibull Fading Channel

5.7.1. Derivation for Optimal Threshold (λ_{opt}) Expression

For a single antenna case (*M*=1), the closed form of expression for λ_{opt} can be derived as follows

$$\frac{\partial P_f}{\partial \lambda} + \frac{\partial P_m}{\partial \lambda} = 0 \tag{5.63}$$

The probability of false alarm expression for Weibull fading channel using multiple antennas at each CR in the proposed CSS network is

$$P_f = 1 - \left[1 - \exp\left(-\left\{ \frac{\lambda^{2/P}\Gamma(\mathrm{P})}{\sigma_n^2} \right\}^C \right) \right]^M \tag{5.64}$$

The missed detection probability expression for Weibull fading channel using multiple antennas at each CR in the proposed CSS network is

$$P_m = \left[1 - \exp\left(-\left\{ \frac{\lambda^{2/P}\Gamma(\mathrm{P})}{\sigma_n^2(1+\bar{\gamma})} \right\}^C \right) \right]^M \tag{5.65}$$

differentiating Eq. (5.64) and Eq. (5.65) w.r.t. λ, expressions for single antenna case are;

$$\frac{\partial P_f}{\partial \lambda} = -\exp\left(-\left\{ \frac{\lambda^{2/p}\Gamma(\mathrm{P})}{\sigma_n^2} \right\}^C \right) C \left\{ \frac{\lambda^{2/p}\Gamma(\mathrm{P})}{\sigma_n^2} \right\}^{C-1} \frac{2\lambda^{(2/p)-1}\Gamma(\mathrm{P})}{p\sigma_n^2} \tag{5.66}$$

$$\frac{\partial P_m}{\partial \lambda} = \exp\left(-\left\{ \frac{\lambda^{2/p}\Gamma(\mathrm{P})}{\sigma_n^2\left(1+\bar{\gamma}\right)} \right\}^C \right) C \left\{ \frac{\lambda^{2/p}\Gamma(\mathrm{P})}{\left(1+\bar{\gamma}\right)\sigma_n^2} \right\}^{C-1} \frac{2\lambda^{(2/p)-1}\Gamma(\mathrm{P})}{p\sigma_n^2\left(1+\bar{\gamma}\right)} \tag{5.67}$$

Substituting Eq. (5.66) and Eq. (5.67) in Eq. (5.63), after simplification, the closed form of expression for λ_{opt} is

$$\lambda_{opt} = \left(\frac{\sigma_n^2}{\Gamma(\mathrm{P})} \left(\frac{C\ln\left(1+\bar{\gamma}\right)}{\left(1 - \left\{ \frac{1}{\left(1+\bar{\gamma}\right)} \right\}^C \right)} \right)^{1/C} \right)^{P/2} \tag{5.68}$$

Similarly, the closed form of expression for λ_{opt} using multiple antennas (M=3) at each CR is obtained as

$$\lambda_{opt} = \left(\frac{\sigma_n^2}{\Gamma(\mathrm{P})} \left(\frac{C\ln\left(1+\bar{\gamma}\right)}{\left(2\left\{ \frac{\bar{\gamma}}{\left(1+\bar{\gamma}\right)} \right\}^C \right)} \right)^{1/C} \right)^{P/2} \tag{5.69}$$

The procedure for the derivation of λ_{opt} expression is provided in Appendix C.1.

5.7.2. Derivation for Optimal Arbitrary Power of Received Signal (p_{opt}) Expression

For a single antenna case (*M*=1), the closed form of expression for p_{opt} can be calculated by differentiating Eq. (5.64) and Eq. (5.65) w.r.t *p* as

$$\frac{\partial P_f}{\partial p}+\frac{\partial P_m}{\partial p}=0 \tag{5.70}$$

$$\frac{\partial P_m}{\partial p}=-\exp\left(-\left\{\frac{\lambda^{2/p}\Gamma(\mathrm{P})}{\sigma_n^2(1+\bar{\gamma})}\right\}^{C}\right)C\left\{\frac{\lambda^{2/p}\Gamma(\mathrm{P})}{\sigma_n^2(1+\bar{\gamma})}\right\}^{C-1}\frac{2}{p^2}\frac{\lambda^{(2/p)}\log\lambda\Gamma(\mathrm{P})}{\sigma_n^2(1+\bar{\gamma})} \tag{5.71}$$

$$\frac{\partial P_f}{\partial p}=\exp\left(-\left\{\frac{\lambda^{2/p}\Gamma(\mathrm{P})}{\sigma_n^2}\right\}^{C}\right)C\left\{\frac{\lambda^{2/p}\Gamma(\mathrm{P})}{\sigma_n^2}\right\}^{C-1}\frac{2}{p^2}\frac{\lambda^{(2/p)}\log\lambda\Gamma(\mathrm{P})}{\sigma_n^2} \tag{5.72}$$

Substituting Eq. (5.71) and Eq. (5.72) in Eq. (5.70), after simplification, the closed form of expression for p_{opt} is

$$p_{opt}=\frac{2\ln\lambda}{\ln\left(\left\{\frac{\mathrm{C}\ln(1+\bar{\gamma})}{\left[1-\left(\frac{1}{1+\bar{\gamma}}\right)^{C}\right]}\right\}^{1/C}\left(\frac{\sigma_n^2}{\Gamma(\mathrm{P})}\right)\right)} \tag{5.73}$$

Similarly, the closed form of expression for p_{opt} using multiple antennas (*M*=3) at each CR is obtained as

$$p_{opt}=\frac{2\ln\lambda}{\ln\left(\left\{\frac{\mathrm{C}\ln(1+\bar{\gamma})}{(0.5)\left[1-\left(\frac{1}{1+\bar{\gamma}}\right)^{C}\right]}\right\}^{1/C}\left(\frac{\sigma_n^2}{\Gamma(\mathrm{P})}\right)\right)} \tag{5.74}$$

The procedure for the derivation of p_{opt} expression is provided in Appendix C.2.

5.7.3. Optimized Expressions of CSS Network Parameters using OR-Rule

A. Calculation of λ_{opt} expression

For a single antenna case (*M*=1), the closed form of expression for λ_{opt} can be calculated using Eq. (5.44), Eq. (5.45), Eq. (5.66), and Eq. (5.67);

after some algebraic simplifications, the final expression for λ_{opt} using single antenna (*M*=1) at each CR and *OR-Rule* at FC is

$$\lambda_{opt} = \left(\frac{\sigma_n^2}{\Gamma(\mathrm{P})} \left(\frac{(N-1)\left(\ln\left(\frac{1-P_f}{P_m} \right) \right) + C\ln\left(1+\bar{\gamma}\right)}{\left(1-\left\{ \frac{1}{\left(1+\bar{\gamma}\right)} \right\}^C \right)} \right)^{1/C} \right)^{P/2} \tag{5.75}$$

Similarly, the final expression for λ_{opt} using multiple antennas (*M*=3) at each CR and *OR-Rule* at FC is

$$\lambda_{opt} = \left(\frac{\sigma_n^2}{\Gamma(\mathrm{P})} \left(\frac{(N-1)\left(\ln\left(\frac{1-P_f}{P_m} \right) \right) + C\ln\left(1+\bar{\gamma}\right)}{\left(2\left\{ \frac{\bar{\gamma}}{\left(1+\bar{\gamma}\right)} \right\}^C \right)} \right)^{1/C} \right)^{P/2} \tag{5.76}$$

The procedure for the derivation of λ_{opt} expression is provided in Appendix C.3.

B. Calculation of p_{opt} expression

For a single antenna case (*M*=1), the closed form of expression for p_{opt} can be calculated using Eq. (5.48), Eq. (5.49), Eq. (5.71), and Eq. (5.72);

after some algebraic simplifications, the final expression for p_{opt} using single antenna (*M*=1) at each CR and *OR-Rule* at FC is

$$p_{opt} = \frac{2\ln\lambda}{\ln\left(\left(\frac{(N-1)\left(\ln\left(\frac{1-P_f}{P_m} \right) \right) + C\ln\left(1+\bar{\gamma}\right)}{\left(1-\left(\frac{1}{1+\bar{\gamma}} \right)^C \right)} \right)^{1/C} \frac{\sigma_n^2}{\Gamma(\mathrm{P})} \right)} \tag{5.77}$$

Similarly, the final expression for p_{opt} using multiple antennas (*M*=3) at each CR and *OR-Rule* at FC is

$$p_{opt} = \frac{2\ln\lambda}{\ln\left(\left(\frac{(N-1)\left(\ln\left(\frac{1-P_f}{P_m}\right)\right)+C\ln\left(1+\bar{\gamma}\right)}{\left((0.5)\left(\frac{\bar{\gamma}}{1+\bar{\gamma}}\right)^{C}\right)}\right)^{1/C}\frac{\sigma_n^2}{\Gamma(\mathrm{P})}\right)} \tag{5.78}$$

The procedure for the derivation of p_{opt} expression is provided in Appendix C.4.

5.7.4. Optimized Expressions of CSS Network Parameters using AND-Rule

A. Calculation of λ_{opt} expression

For a single antenna case (*M*=1), the closed form of expression for λ_{opt} can be calculated using Eq.(5.55), Eq. (5.56), Eq. (5.66), and Eq. (5.67);

after some algebraic simplifications, the final expression for λ_{opt} using single antenna (*M*=1) at each CR and *AND-Rule* at FC is

$$\lambda_{opt} = \left(\frac{\sigma_n^2}{\Gamma(\mathrm{P})}\left(\frac{(N-1)\left(\ln\left(\frac{P_f}{1-P_m}\right)\right)+C\ln\left(1+\bar{\gamma}\right)}{\left(1-\left\{\frac{1}{\left(1+\bar{\gamma}\right)}\right\}^{C}\right)}\right)^{1/C}\right)^{P/2} \tag{5.79}$$

Similarly, the final expression for λ_{opt} using multiple antennas (*M*=3) at each CR and *AND-Rule* at FC is

$$\lambda_{opt} = \left(\frac{\sigma_n^2}{\Gamma(\mathrm{P})}\left(\frac{(N-1)\left(\ln\left(\frac{P_f}{1-P_m}\right)\right)+C\ln\left(1+\bar{\gamma}\right)}{\left(2\left\{\frac{\bar{\gamma}}{\left(1+\bar{\gamma}\right)}\right\}^{C}\right)}\right)^{1/C}\right)^{P/2} \tag{5.80}$$

The procedure for the derivation of λ_{opt} expression is provided in Appendix C.5.

B. Calculation of p_{opt} expression

For a single antenna case (M=1), the closed form of expression for p_{opt} can be calculated using using Eq. (5.59), Eq. (5.60), Eq. (5.71), and Eq. (5.72);
after some algebraic simplifications, the final expression for p_{opt} using single antenna (M=1) at each CR and *AND-Rule* at FC is

$$p_{opt} = \frac{2\ln\lambda}{\ln\left(\left(\frac{(N-1)\left(\ln\left(\frac{P_f}{1-P_m}\right)\right)+C\ln\left(1+\bar{\gamma}\right)}{\left(1-\left(\frac{1}{1+\bar{\gamma}}\right)^{C}\right)}\right)^{1/C}\frac{\sigma_n^2}{\Gamma(\mathrm{P})}\right)} \tag{5.81}$$

Similarly, the final expression for p_{opt} using multiple antennas (M=3) at each CR and *AND-Rule* at FC is

$$p_{opt} = \frac{2\ln\lambda}{\ln\left(\left(\frac{(N-1)\left(\ln\left(\frac{P_f}{1-P_m}\right)\right)+C\ln\left(1+\bar{\gamma}\right)}{\left((0.5)\left(\frac{\bar{\gamma}}{1+\bar{\gamma}}\right)^{C}\right)}\right)^{1/C}\frac{\sigma_n^2}{\Gamma(\mathrm{P})}\right)} \tag{5.82}$$

The procedure for the derivation of λ_{opt} expression is provided in Appendix C.6.

5.8. Optimization of CSS Network Parameters in Non-Fading Environment

A. Calculation of λ_{opt} expression

The expression for λ_{opt} in AWGN channel can be calculated by differentiating Eq. (5.6) and Eq. (5.17) w.r.t. λ;

$$\frac{\partial P_f}{\partial\lambda} = -M\,\frac{2\lambda^{(2-p)/p}}{p}\left[1-\exp\left(-\lambda^{2/p}\Big/\sigma_n^2\right)\right]^{M-1}\exp\left(-\frac{\lambda^{2/p}}{\sigma_n^2}\right) \tag{5.83}$$

$$\frac{\partial P_m}{\partial\lambda} = \frac{M}{\sqrt{\pi}\,p}\left(\frac{\lambda^{(2/p)-1}}{(1+\bar{\gamma})\sigma_n^2}\right)\exp\left(-\frac{\lambda^{2/p}}{2(1+\bar{\gamma})\sigma_n^2}\right)\left[\frac{1}{\sqrt{\pi}}\gamma\left(\frac{1}{2},\frac{\lambda^{2/p}}{2(1+\bar{\gamma})\sigma_n^2}\right)\right]^{M-1} \tag{5.84}$$

Substituting N=1, M=1, p=2, r=0.1, Eq. (5.83), and (5.84) in (5.29), after some algebraic computation and the expression reduces to;

$$\lambda^{2/p} - C_2 \ln\left(\lambda^{2/p}\right) - C_3 = 0 \tag{5.85}$$

where

$$C_2 = -(1+\bar{\gamma})/(1+2\bar{\gamma}) \tag{5.86}$$

$$C_3 = (1+\gamma)\ln\left(\frac{(1/2)^{1/2}}{\sqrt{\pi}(1+\bar{\gamma})^m}\right)\Big/\left(\frac{1}{2}\right) - (1+\bar{\gamma}) \tag{5.87}$$

B. Calculation of p_{opt} expression

The expression for p_{opt} in AWGN channel can be calculated by differentiating Eq. (5.5) and Eq. (5.17) w.r.t. *p*;

$$\frac{\partial P_f}{\partial p} = -\frac{2\lambda^{2/p}}{p^2\sigma_n^2}\ln\lambda M\left(1-\exp\left(-\lambda^{(2/p)}\big/\sigma_n^2\right)\right)^{M-1}\exp\left(-\lambda^{(2/p)}\big/\sigma_n^2\right) \tag{5.88}$$

$$\frac{\partial P_m}{\partial p} = -\frac{M\log\lambda}{\sqrt{\pi}\,p^2}\left(\frac{\lambda^{2/p}}{(1+\bar{\gamma})\sigma_n^2}\right)\exp\left(-\frac{\lambda^{2/p}}{2(1+\bar{\gamma})\sigma_n^2}\right)\left[\frac{1}{\sqrt{\pi}}\gamma\left(\frac{1}{2},\frac{\lambda^{2/p}}{2(1+\bar{\gamma})\sigma_n^2}\right)\right]^{M-1} \tag{5.89}$$

substituting *N*=1, *M*=1, *r*=0.1, Eq. (5.88), and Eq.(5.89) in Eq. (5.30), after some algebraic computation, the final expression for p_{opt} is obtained as:

$$p_{opt} = \frac{2\log\lambda}{\log\left[\left(\frac{\log\sqrt{\pi}+0.5\log\left(\frac{2(1+\bar{\gamma})}{\sigma_n^2}\right)}{\left[1-\frac{1}{2(1+\bar{\gamma})}\right]}\right)\sigma_n^2\right]} \tag{5.90}$$

5.9. Results and Discussions

The simulation results and their discussions are presented in this section. The effect on performance for different values of network parameters such as threshold value (λ), arbitrary power of received signal (*p*), average sensing channel SNR ($\bar{\gamma}$), multiple number of antennas (*M*), number of CR users (*N*), and different fading parameters is discussed when the proposed system is affected by various fading environments. The simulation results are evaluated to find out the detection performance using complementary receiver operating characteristics (CROC), total error rate $(Q_m + Q_f)$ curves, and to calculate the optimal values of network

parameters such as N_{opt}, p_{opt}, and λ_{opt} values for the proposed CSS network using single and multiple antennas at each CR.

Figure 5.3 illustrates the CROC curves for various fading channels which are drawn between P_f and P_m values. The MATLAB based simulation is evaluated for two different values of M (M=1 and M=2), fixed values of $\bar{\gamma}$=10 dB, K=2, and p=3. From Fig.5.3, it can be observed that P_m value decreases as P_f value increases. A similar phenomenon is observed with other parameters also such as M and Rician fading parameter (K). As K value increases, fading effect between the transmitter and receiver decreases, and thereby P_m value decreases. When K value increases from K=0 (Rayleigh) to K=2 (Rician), P_m value decreases by 39.2% at M=2 and it decreases by 15.2% at M=1, P_f=0.1, $\bar{\gamma}$=10 dB and p=3. Finally, our simulation results are perfectly in accordance with Rayleigh channel when Rician fading channel parameter value is chosen as K=0. All the simulation results are drawn with strong support of analytical expressions and simulation results are in perfect accordance with theoretical results.

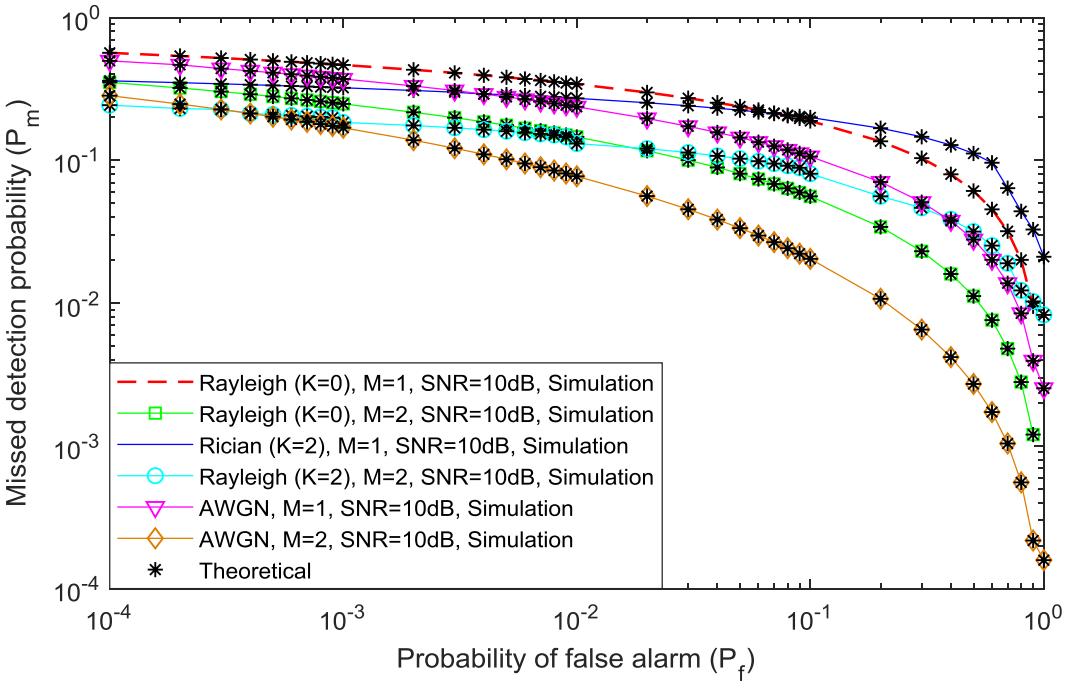

Fig.5.3. CROC graphs for different fading channels.

In Fig.5.4 CROC curves are drawn for various fading channels such as Rayleigh, Weibull, and Hoyt fading channels. The simulation is evaluated for two different values of M (M=1 and M=2), fixed values of $\bar{\gamma}$=10 dB, V=3, q=0.3, and p=3. From Fig.5.4, it can be observed that P_m value decreases as P_f value increases. The similar nature is observed with

other parameters also. As V value increases, fading effect decreases, and thereby P_m value decreases.

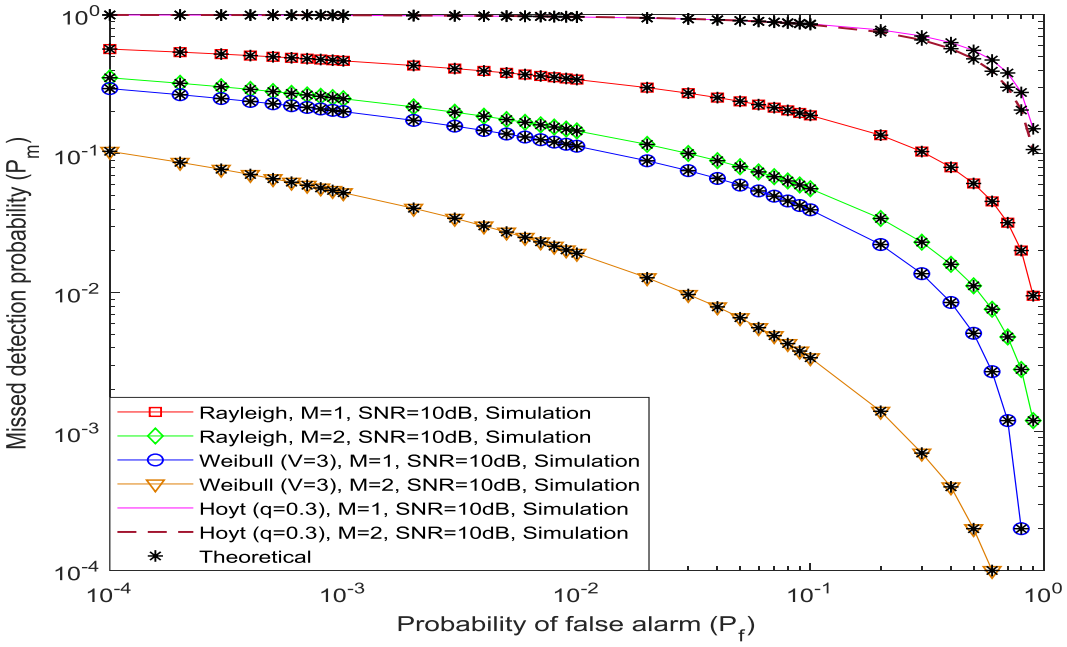

Fig.5.4. CROC graphs for different fading channels.

When V value increases from V=2 (Rayleigh) to V=3 (Weibull), P_m value decreases by 69.2% at M=2 and it decreases by 55.2% at M=1, P_f=0.1, $\bar{\gamma}$=10 dB, and p=3. It can be observed from the simulation that the missed detection probability values are more in Hoyt fading environment and less in Weibull fading environment. Finally, our simulation results are in perfectly in accordance with Rayleigh channel when Weibull fading channel parameter (V) value chosen as V=2.

Figure 5.5 is drawn between N_{opt} and error rate in R-channel (r) using single antenna (M=1) at each CR for different fading environments. The performance is evaluated for various values of p (p=2 and p=3), λ (λ =20 and λ=30) and the performance comparison between CED and IED schemes are also provided in the simulation. As r value increases in R-channel, N_{opt} value decreases because increased value of r makes the R-channel more imperfect and increases the error rate in it, this makes the number of CR users to identify the PU activity decreases. As p value decreases, N_{opt} value increases because the received signal strength decreases at receiver. When p value decreases from p=3 to p=2, N_{opt} value increases from 12 to 33 in Rician fading channel (K=2) and it increases from 15 to 19 in Rayleigh fading channel (K=0) at $\bar{\gamma}$=5 dB, λ=20, and r=0.03.

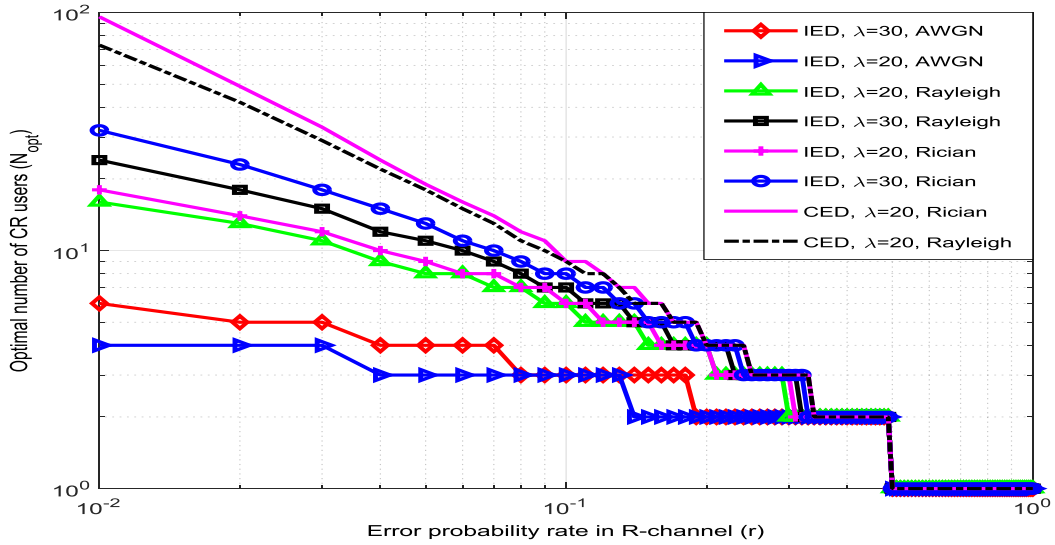

Fig.5.5. N_{opt} versus r graphs for different fading channels using single antenna at each CR.

Similarly, when λ value decreases, N_{opt} value decreases because of decreased P_f value. When λ value decreases from λ = 30 to λ = 20, N_{opt} value decreases from 5 to 4 in AWGN channel, it drops from 15 to 11 in Rayleigh channel, and it falls from 18 to 12 in Rician fading channel (K=2) at p=3, $\bar{\gamma}$=5 dB, and r=0.03. We can conclude from the above simulation that N_{opt} value is less for AWGN environment. The lower values of N_{opt} can be achieved with an IED technique as compared to the CED technique.

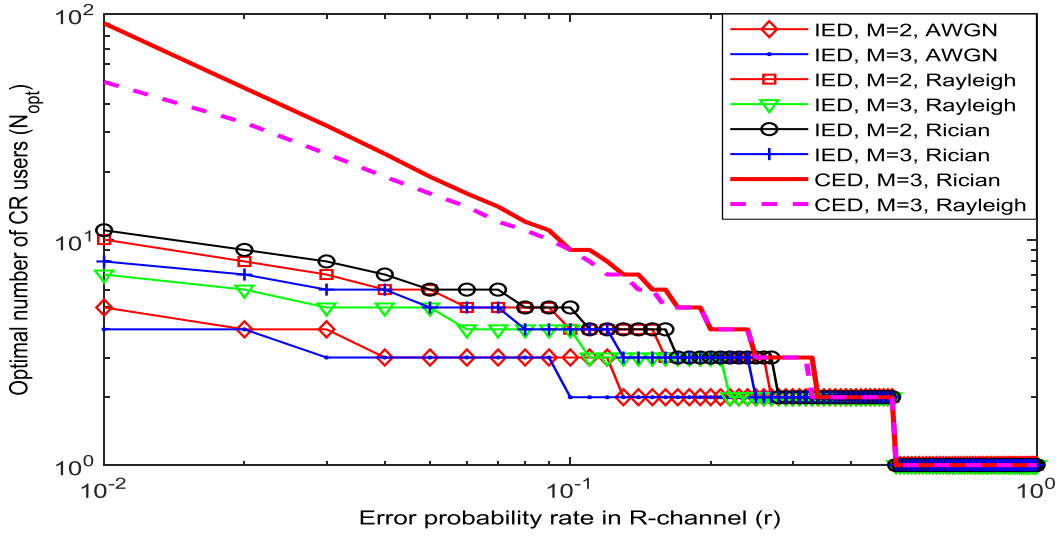

Fig.5.6. N_{opt} versus r graphs for different fading channels using multiple antennas at each CR.

Figure 5.6 is drawn between N_{opt} and r for different fading channels using multiple antennas (M=2 and M=3) at each CR. As M value increases, N_{opt} value decreases compared to single antenna case. When M value increases, diversity order at each CR increases which improves the received signal strength and reduces the noise value present in R-channel, hence N_{opt} value decreases. When M value increases from M=2 to M=3, N_{opt} value reduces from 8 to 6 in Rician channel, it decreases from 7 to 5 in Rayleigh channel, and it falls from 4 to 3 in AWGN channel at λ=20, K=2, p=3, $\bar{\gamma}$=5 dB, and r=0.03. For an instant, at λ=20, M=3, $\bar{\gamma}$=5 dB, r=0.03, as p value increases from p=2 to p=3, N_{opt} value decreases from 32 to 7 in Rician channel and it drops from 24 to 5 in Rayleigh fading channel.

In Fig.5.7, N_{opt} value calculated for various values of r considering single antenna (M=1) at each CR in different fading environments such as (Rayleigh, Hoyt and Weibull fading channel). The performance comparison between different detection schemes (CED and IED), comparison among various fading channels are also provided in Fig.5.7. As p value decreases from p=3 to p=2, N_{opt} value increases from 8 to 18 in Rayleigh fading channel and it increases from 10 to 19 in Weibull fading channel (V=3) respectively at $\bar{\gamma}$=5dB, λ=20, and r=0.05. N_{opt} value is less in Rayleigh fading environment and high in Hoyt fading environment.

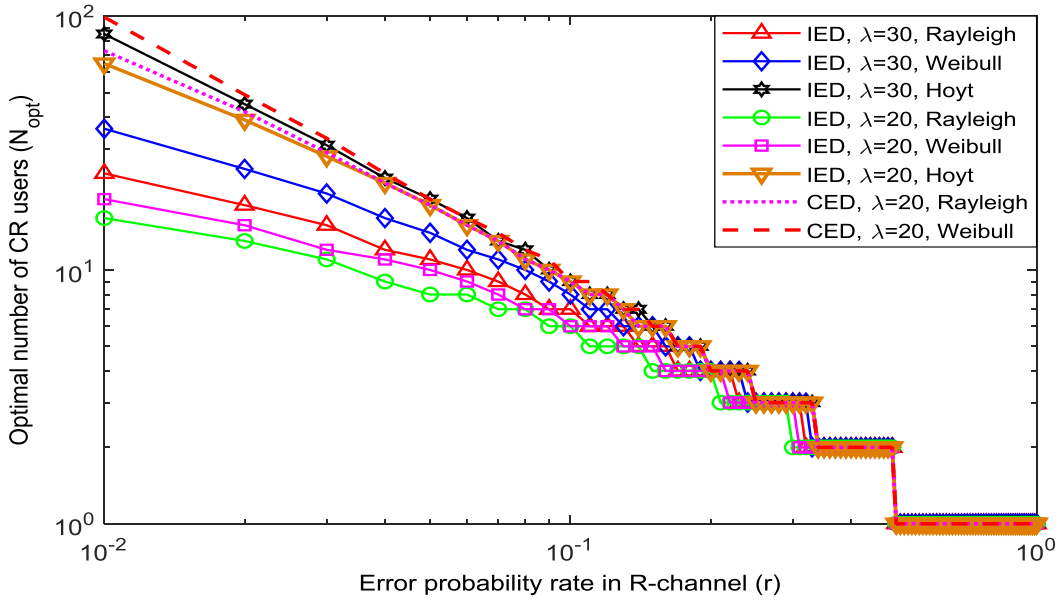

Fig.5.7. N_{opt} versus r graphs for different fading channels using single antenna at each CR.

Similar analysis (N_{opt} vs r) is carried out in Fig.5.8 also considering multiple antennas at each CR (M=2 and M=3) in Rayleigh, Hoyt, and Weibull fading environments. As multiple antennas at each CR increases, N_{opt} value decreases compared to single antenna case.

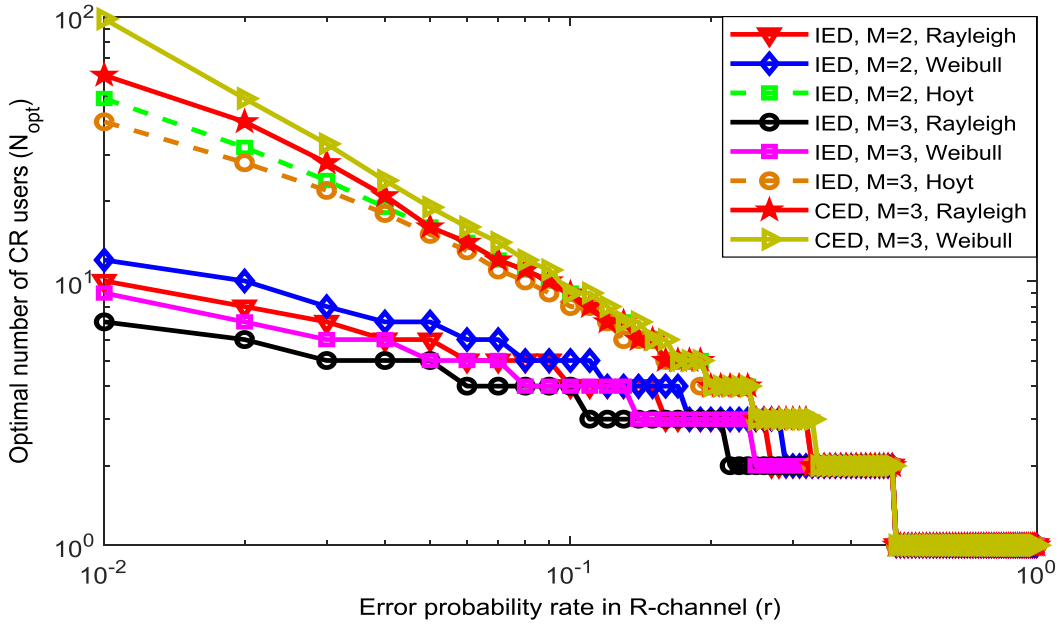

Fig.5.8. N_{opt} versus r graphs for different fading channels using multiple antennas at each CR.

As M value increases from M=2 to M=3, N_{opt} value reduces from 7 to 5 in Rayleigh fading, it decreases from 8 to 6 in Weibull fading (V=3), and it reduces from 15 to 13 in Hoyt fading channel (q=0.2) at λ=20, p=3, $\bar{\gamma}$=5dB, and r=0.05. These N_{opt} values are less compared to a single antenna case provided in Fig.5.7. For a particular value of λ=20, M=3, $\bar{\gamma}$=5dB, r=0.05, if p value increases from p=2 to p=3, N_{opt} value decreases from 33 to 6 in Weibull fading channel (V=3) and it decreases from 24 to 5 in Rayleigh fading channel.

Figure 5.9 is drawn between N_{opt} and λ for various value of p (p=2 and p=3), $\bar{\gamma}$ ($\bar{\gamma}$=5 dB and $\bar{\gamma}$=10 dB), and fixed value of M (M=1). The performance comparison for various fading channels (AWGN, Rayleigh and Rician) is provided in Fig.5.9. As $\bar{\gamma}$ value increases, signal strength increases in S-channel which reduces N_{opt} value. When $\bar{\gamma}$ value increases from $\bar{\gamma}$=5 dB to $\bar{\gamma}$=10 dB, N_{opt} value decreases from 6 to 4 in AWGN channel, it decreases from 16 to 6 in Rayleigh channel and it decreases from 18 to 5 in Rician channel at K=2, p=3, M=1, λ=20, and r=0.01. When p value increases from p=2 to p=3, N_{opt} value decreases from 96 to 18 in Rician channel and it reduces from 73 to 16 in Rayleigh channel at M=1, $\bar{\gamma}$=5dB, r=0.01 and λ =20. Finally, we can conclude from the simulation that N_{opt} value is less for lower thresholds and its value increases with λ. N_{opt} value is minimum with an IED scheme compared to the CED scheme.

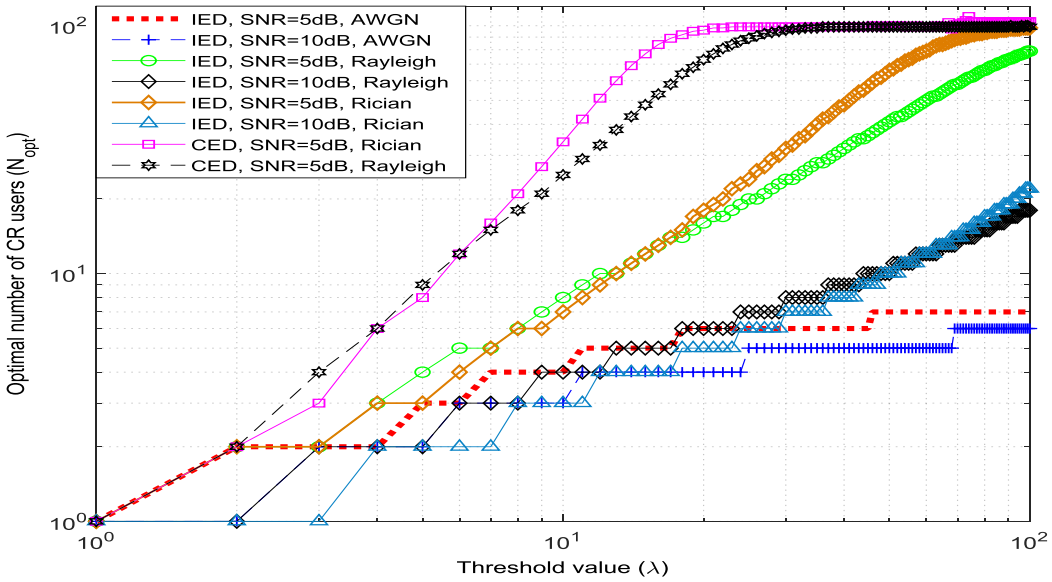

Fig.5.9. N_{opt} versus λ graphs for different fading channels using single antenna at each CR.

Figure 5.10 is drawn between N_{opt} and λ for various values of M namely (M=2 and M=3), fixed values of $\bar{\gamma}$=5 dB, r=0.01, and λ=20. It can be observed from the simulation that N_{opt} value increases with λ value. When p value increases from p=2 to p=3, N_{opt} value decreases from 8 to 4 in Rayleigh fading and it reduces from 10 to 3 in Rician channel at M=3, λ=20, and r=0.01. As M value increases from M=2 to M=3, N_{opt} value decreases from 4 to 3 in AWGN channel, it reduces from 4 to 2 in Rayleigh fading, and it drops from 3 to 2 in Rician channel at λ= 20, K=2, p=3, $\bar{\gamma}$=5 dB, and r=0.01.

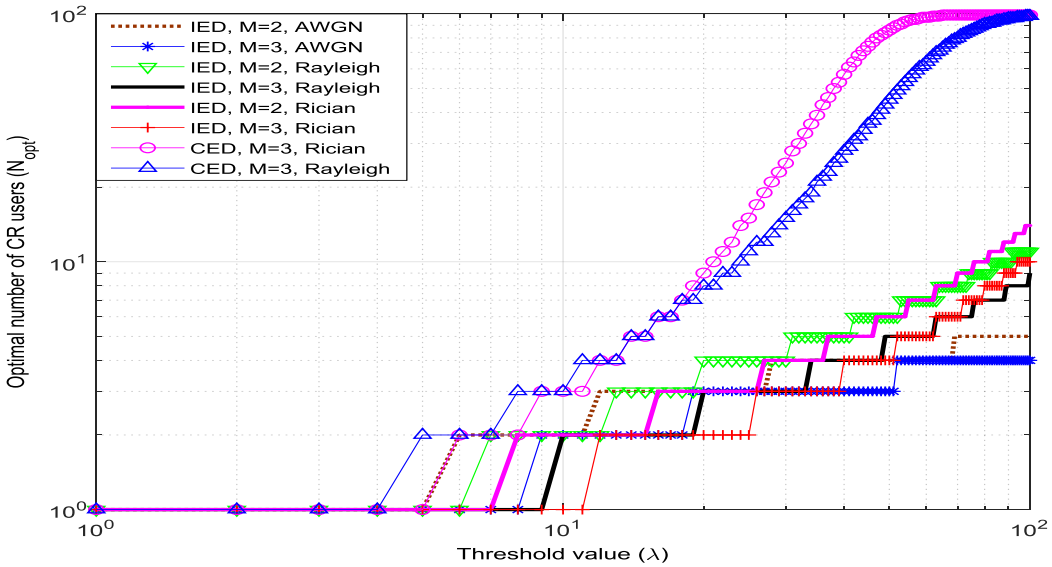

Fig.5.10. N_{opt} versus λ graphs for different fading channels using multiple antennas at each CR.

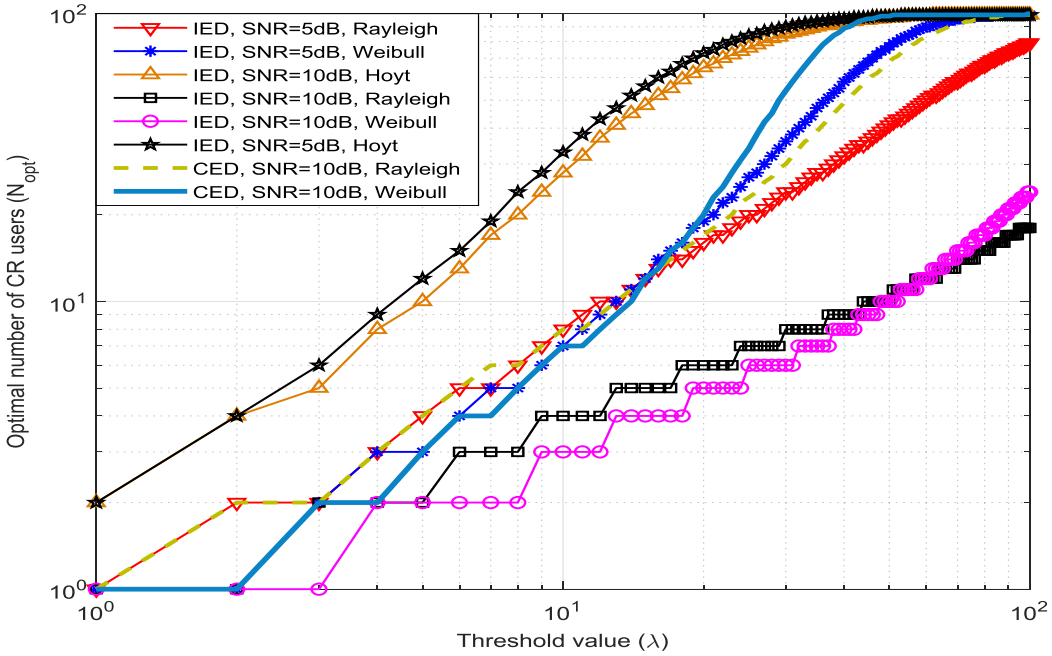

Fig.5.11. N_{opt} versus λ graphs for different fading channels using single antenna at each CR.

In Fig.5.11, performance is evaluated to calculate N_{opt} value for different λ values using single antenna at each CR. The performance comparison for various fading channels (Rayleigh, Weibull and Hoyt) is provided in Fig.5.11. As S-channel SNR value increases from 5dB to 10dB, N_{opt} value decreases from 16 to 6 in Rayleigh fading channel, it reduces from 19 to 5 in Weibull channel, and it decreases by 73 to 65 in Rayleigh fading channel respectively at V=3, q=0.2, p=3, M=1, λ=20, and r=0.01. As p value increases from p=2 to p=3, N_{opt} value decreases from 17 to 6 in Rayleigh fading channel and it decreases from 20 to 5 in Hoyt fading channel at $\bar{\gamma}$=10dB, r=0.01, and λ=20.

Figure 5.12 is also drawn between N_{opt} and λ considering multiple antennas (M=2 and M=3) at each CR. As the number of antennas at each CR increases from M=2 to M=3, N_{opt} value decreases from 4 to 3 in Rayleigh fading channel, it decreases from 3 to 2 in Weibull fading channel, it decreases from 58 to 49 in Hoyt fading channel, and these values are less compared to single antenna case. The simulation parameters used in Fig. 5.11 are λ= 20, K=2, p=3, $\bar{\gamma}$=5dB and 10dB, r=0.01, and M=2 and 3.

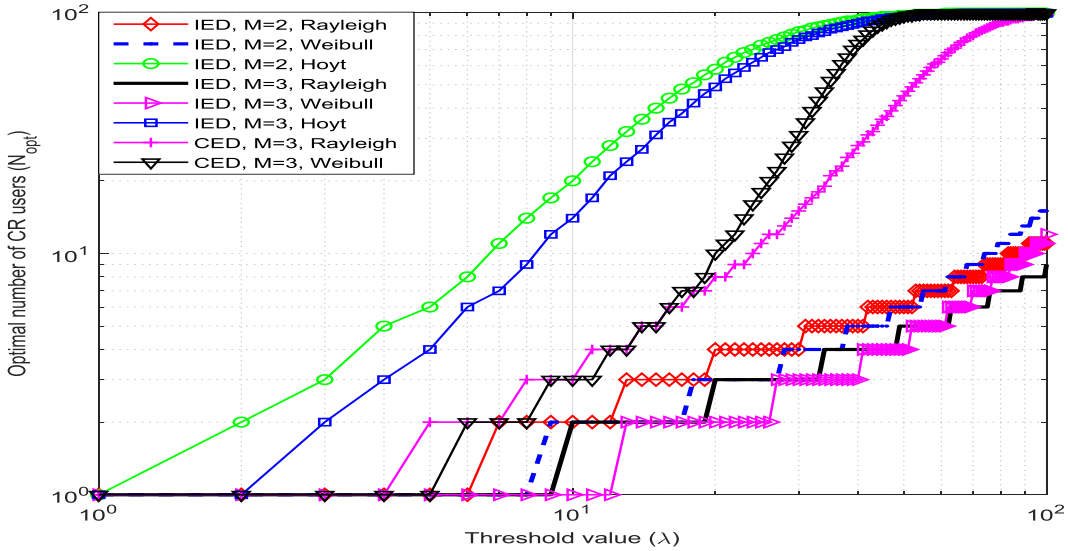

Fig.5.12. N_{opt}versus λ graphs for different fading channels using multiple antennas at each CR.

Figure 5.13 is drawn between total error rate $(Q_m + Q_f)$ and p for various values of M namely (M=1 and M=3), N (N=1 and N=3), fixed values of $\bar{\gamma}$=10 dB, λ=30, and r=0.01 in various fading environments. The performance comparison for different fading channels (AWGN, Rayleigh and Rician) is provided in Fig.5.13 to decide which fading channel achieves the least value of total error rate. It is evident from the Figure that as p value increases, $(Q_m + Q_f)$ value initially decreases up to minimum value then it increases.

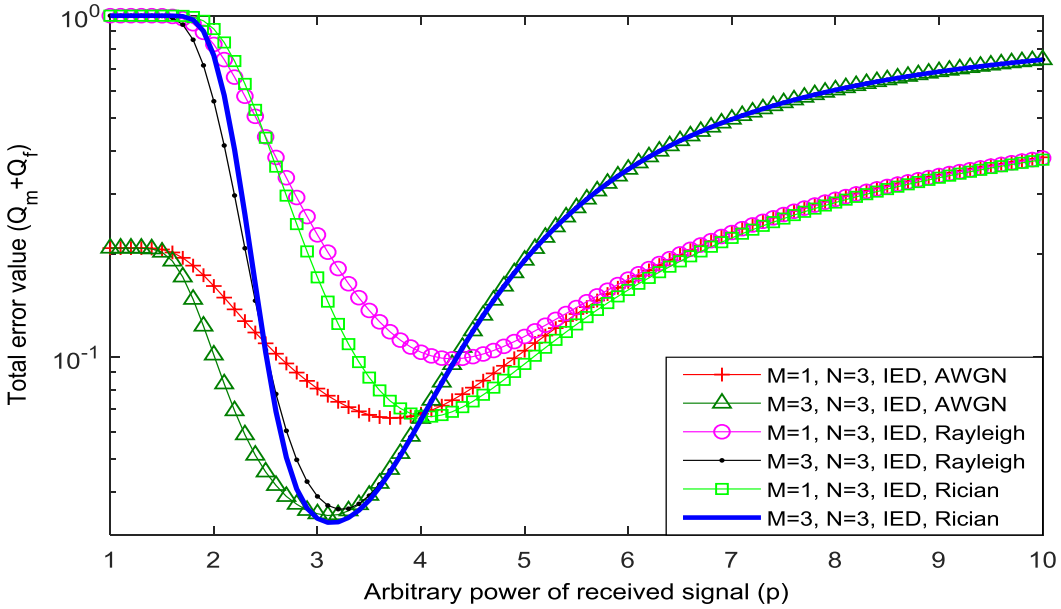

Fig.5.13. $Q_m + Q_f$ versus p graphs for different fading channels.

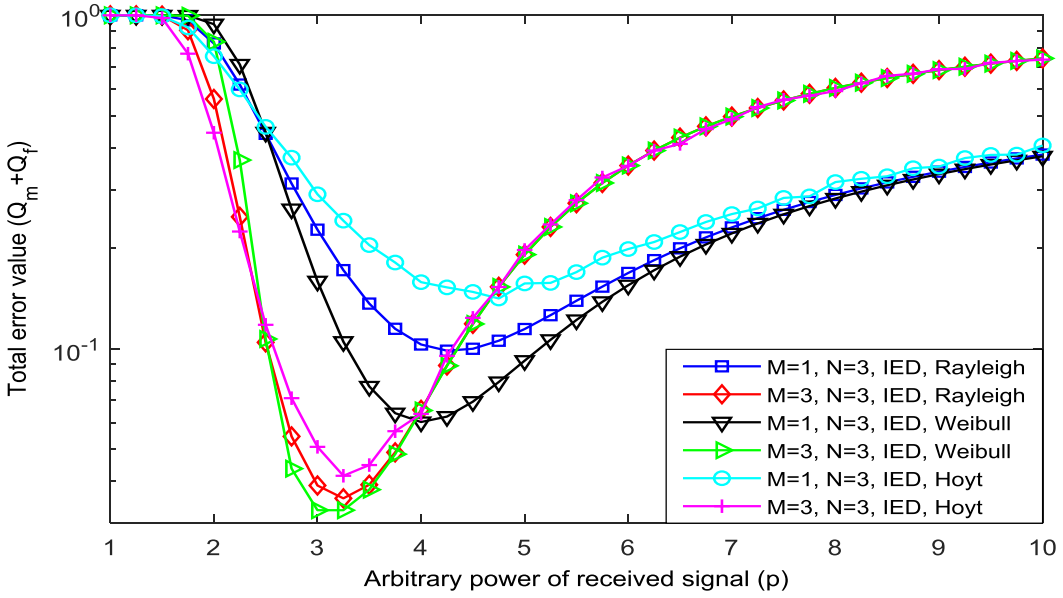

Fig.5.14. $Q_m + Q_f$ versus p graphs for different fading channels.

Similar variation is observed with all other parameters also, and this nature of the curve is due to decrease in λ value for increase in p-value according to $\lambda = \lambda_n \sigma_n^p$. The increased P_f value at each CR increases the Q_f value at FC, thereby it improves the total error value. Including the total error rate performance, an optimum value of p (p_{opt}) is also calculated from fig.5.13. The value of p at which the total error rate is minimum is called as optimum value p. The minimum value of total error rate for single antenna case (M=1) in AWGN channel is 0.0603 at p=3.7, its value for Rayleigh fading is 0.0944 at p=4.3, and its value for Rician fading channel is 0.0743 at p=4, $\bar{\gamma}$=10 dB, λ=30, r=0.01, M=1, and N=3. Similarly, for multiple antenna case (M=3), minimum value of total error for AWGN channel is 0.0312 at p=3.1, it obtained as 0.0347 for Rayleigh channel at p=3.2, and it is obtained as 0.0336 for Rician fading channel at p=3.2 for similar network parameters. From the above lines, we can conclude that total error value is more with single antenna case compared to multiple antenna case. $(Q_m + Q_f)$ value is less in Rician channel compared to Rayleigh channel because it consists of line of sight (LoS) propagation between transmitter and receiver.

The effect of multiple antennas on total error value over various fading channels is provided in Fig.5.14. The minimum value of total error rate for single antenna case in Rayleigh channel is 0.0944 at p=4.3, its value in Weibull fading channel is 0.0661 at p=4, and its value in Hoyt fading channel is 0.1415 at p=4.75, M=1, $\bar{\gamma}$=10dB, λ=30, N=3, and r=0.01. For multiple (M=3) case, $(Q_m + Q_f)$ value reduces to 0.0347 at p=3.2 in Rayleigh fading, it drops to 0.0332

at p=3 in Weibull fading, and it falls to 0.0416 at p=3.25 in Hoyt fading channel for similar network parameters. We can conclude from Fig.5.13 and Fig.5.14 that Weibull fading channel achieves lower a value of total error compared to other fading channels.

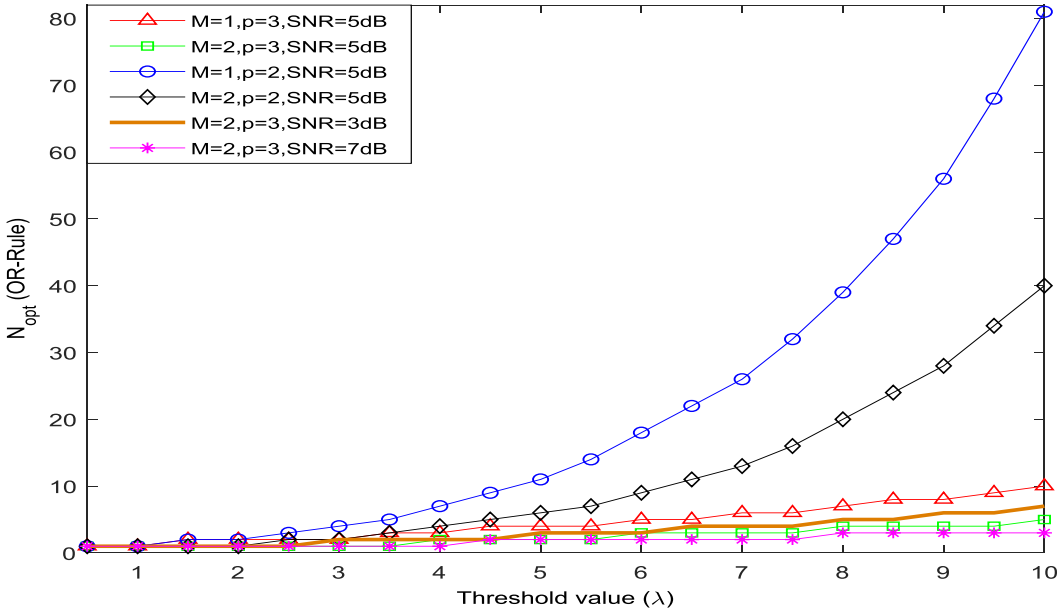

Fig.5.15. N_{opt} versus λ graphs for Rayleigh fading channel using *OR-Rule* at FC.

An optimum value of number of CRs (N_{opt}) is calculated as a function of λ using hard decision fusion (*OR*-rule) at FC over Rayleigh fading effect in Fig.5.15. N_{opt} value is calculated for error free R-channel and for various values of *M*, *p*, and $\bar{\gamma}$. From simulation it is noted that N_{opt} value increases with λ for a given $\bar{\gamma}$, *p*, and *M* values. Since we are using *OR-Rule* at FC, as λ value increases, then FC needs binary decisions from more SUs to reduce the missed detection probability. For a particular case, when $\bar{\gamma}$ value increases from 5 dB to 7 dB, N_{opt} value decreases from 13 to 2 at λ=7, *M*=2, and *p*=3. N_{opt} value is less for lower threshold values, it increases with a threshold value and it also depends on *p*-value. If the detection scheme changes from CED (*p*=2) to IED (*p*=3), N_{opt} value decreases from 26 to 6 for single antenna case, and it decreases from 13 to 4 for multiple antenna case at *M*=2, λ=7, and $\bar{\gamma}$=5dB. Finally, the number of antennas at each CR also affects the N_{opt} value i.e., when *M* value increases from *M*=1 to *M*=2, N_{opt} value decreases by 57.1% at λ=8, *p*=3, and $\bar{\gamma}$=5dB.

In Fig.5.16, the total error rate performance is analyzed as a function of *p* using *OR-Rule* at FC over Rayleigh fading channel. Three values of *N* (*N*=1, *N* =2 and *N*=3), two values

of M (M=1 and M=2), and two values of λ (λ=30 and λ=20) are considered as variable parameters.

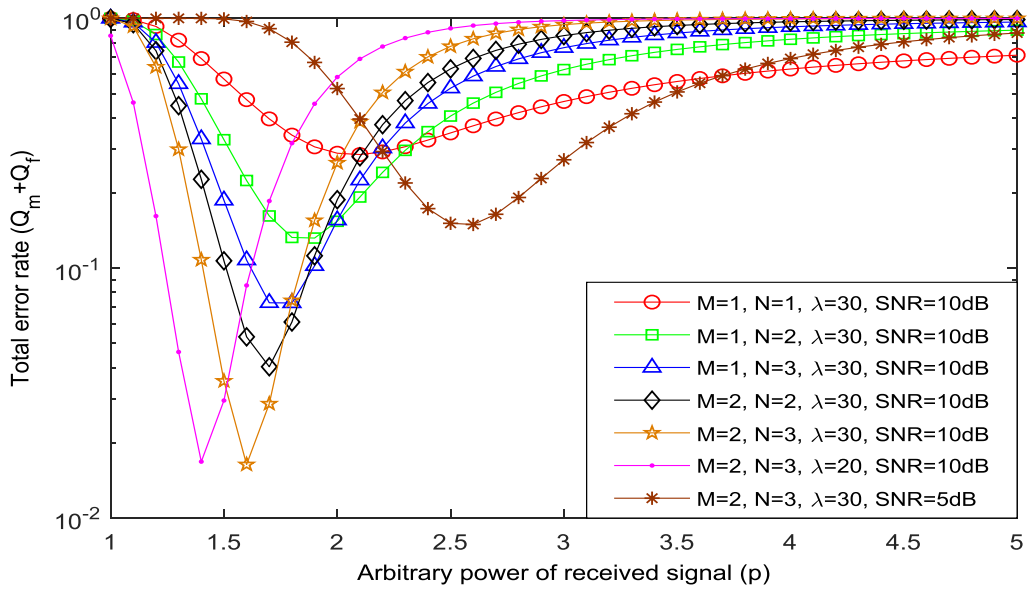

Fig.5.16. $Q_m + Q_f$ versus p graphs for Rayleigh fading channel using *OR-Rule* at FC.

The total error rate performance and p_{opt} values are calculated from Fig.5.16. An optimum value of p also depends on various network parameters. For a particular case, if N value increases from N=1 to N=3, $(Q_m + Q_f)$ value decreases by 28.8% at p=2, M=1, λ=30, and $\bar{\gamma}$=10dB. As N value increases, p_{opt} value decreases and also shifts towards left (moves towards origin). The performance can be improved further by increase in the number of antennas at each CR user. As M value at each CR increases from M=1 to M=2, $(Q_m + Q_f)$ value decreases by 60.5% at p=1.8, λ=30, N=3, and $\bar{\gamma}$=10dB.

In Fig.5.17, $(Q_m + Q_f)$ performance is shown as a function of λ for various values of N, p, $\bar{\gamma}$, and M. The performance is evaluated using *OR-Rule* at FC over Rayleigh fading channel. It can be observed from the simulation that as λ value increases, initially total error rate value decreases up to minimum value and then it increases up to certain point. The nature of the curve remains the same with other parameters also. Including the total error rate and an optimum value of λ (λ_{opt}) is also calculated using this simulation. The value of λ at which the total error is minimum is treated as optimum value of λ. At λ=10, M=1, $\bar{\gamma}$=10dB, and p=3, if N value increases from N=1 to N=3, $(Q_m + Q_f)$ value decreases by 80.3%. As N value increases, λ_{opt} value also increases and the curve moves away from the origin i.e., shifts towards right.

When M value increases from M=1 to M=2, $(Q_m + Q_f)$ value decreases by 51.2% at λ =12, N=3, p=3, and $\bar{\gamma}$=10dB. It can be clearly observed from the simulation that for fixed values of M and N, as p value decreases, total error rate curve shifts towards the origin.

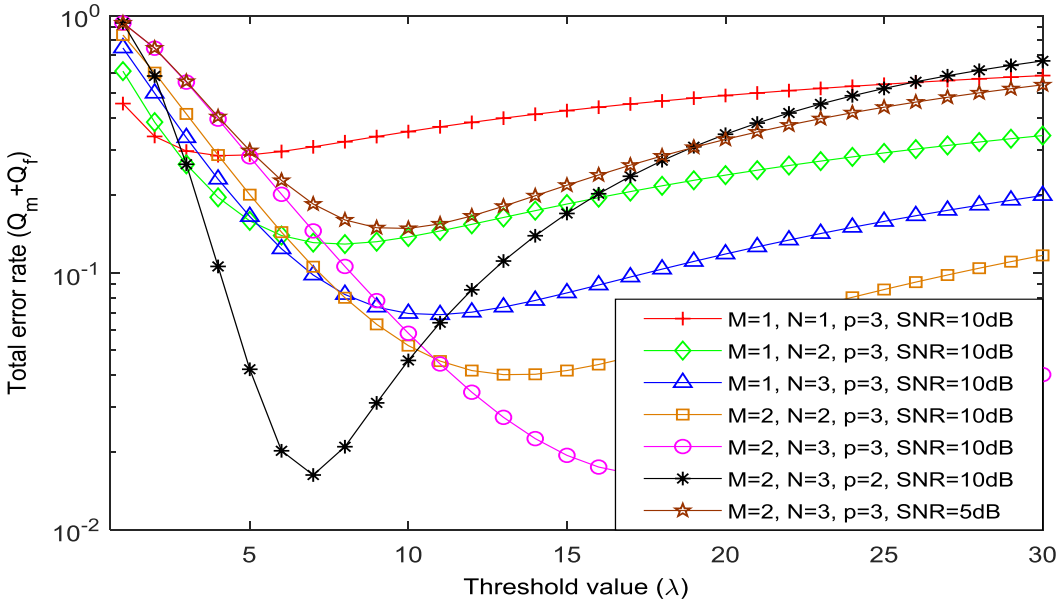

Fig.5.17. $Q_m + Q_f$ versus λ graphs for Rayleigh fading channel using *OR-Rule* at FC.

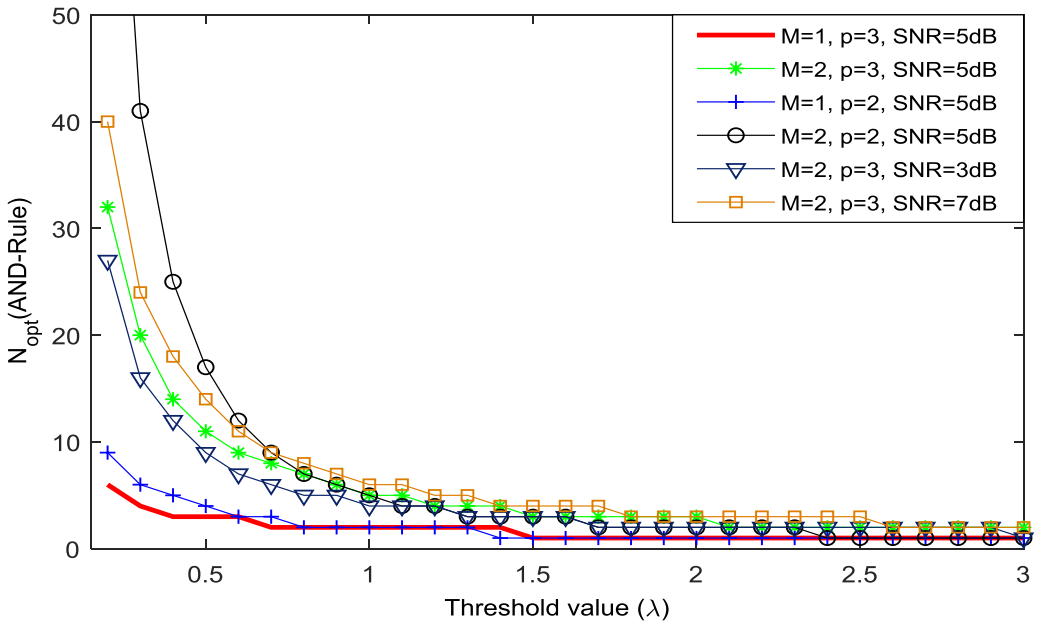

Fig.5.18. N_{opt} versus λ graphs for Rayleigh fading channel using *AND-Rule* at FC.

In Fig.5.18, N_{opt} value is calculated as a function of λ. The performance is evaluated using *AND-Rule* at FC over Rayleigh fading channel for different values of p (p=2 and p=3), M (M=1 and M=2), and $\bar{\gamma}$ ($\bar{\gamma}$=5dB and $\bar{\gamma}$=7dB). N_{opt} value is calculated when S-channel is

affected by Rayleigh fading and R-channel is considered as error free channel. From Fig.5.18, it is clear that N_{opt} value decreases with the increment of λ value using *AND-Rule* at FC and similar nature is observed with other parameters also. As $\bar{\gamma}$ value decreases from 7dB to 5dB, N_{opt} value decreases from 14 to 11 at λ=0.5, *p*=3, and *M*=2. As *p* value increases from *p*=2 to *p*=3, N_{opt} value decreases by 54.5% at λ=0.5, $\bar{\gamma}$=5dB, and *M*=2. Similarly, as *M* value increases from *M*=1 to *M*=2, N_{opt} value decreases from 11 to 3 at λ=0.5, $\bar{\gamma}$=5dB, and *p*=3.

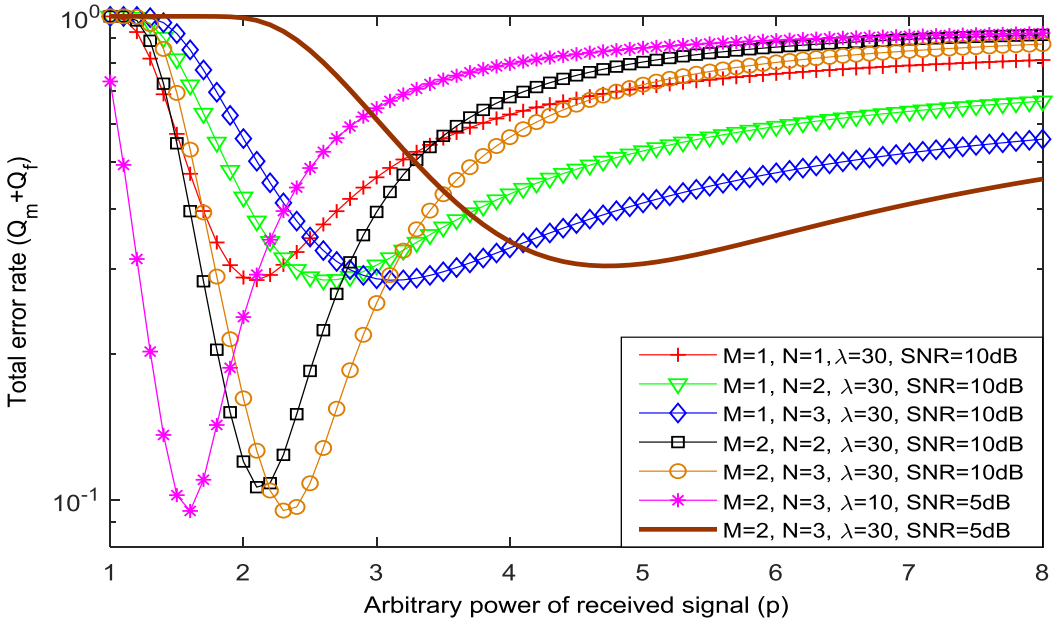

Fig.5.19. $Q_m + Q_f$ versus *p* graphs for Rayleigh fading channel using *AND-Rule* at FC.

Figure 5.19 is drawn between $(Q_m + Q_f)$ and *p* using *AND-Rule* at FC over Rayleigh fading channel. Three values of *N* namely (*N*=1, *N*=2, and *N*=3), two values of *M* (*M*=1 and *M*=2), and two values of λ (λ=30 and λ=20) are used in this simulation. For a particular case, when *N* value increases from *N*=1 to *N*=3, $(Q_m + Q_f)$ value decreases by 47.1% at *p*=4, *M*=1, λ=30, and $\bar{\gamma}$=10 dB. An optimum value of *p* also increases and shifts towards right as *N* value increases. Similarly, when *M* value at each CR increases from *M*=1 to *M*=2, $(Q_m + Q_f)$ value decreases by 69.1% at *p*=2.5, λ=30, *N*=3, and $\bar{\gamma}$=10 dB.

Figure 5.20 is drawn between N_{opt} and λ using *OR-Rule* at FC over Weibull fading channel. N_{opt} value is calculated for error free R-channel, various values of network parameters such as *M*, *p*, $\bar{\gamma}$, and *V*. For a particular case, when $\bar{\gamma}$ value increases from 5dB to 7dB, N_{opt} value decreases by 50.0% at λ=6, *M*=2, *p*=3, and *V*=3. Similarly, as *V* value increases from *V*=2 to *V*=3, N_{opt} value decreases by 28.5% at λ=8, *M*=1, *p*=3, and $\bar{\gamma}$=5dB. If the detection

scheme changes from CED (p=2) to IED (p=3), N_{opt} value decreases by 80.0% at λ=8, M=2, V=3, and $\bar{\gamma}$=5dB. Finally, the number of antennas at each CR also affect the N_{opt} value, as M value increases from M=1 to M=2, N_{opt} value decreases by 50% at λ=7, p=3, V=3, and $\bar{\gamma}$=5dB.

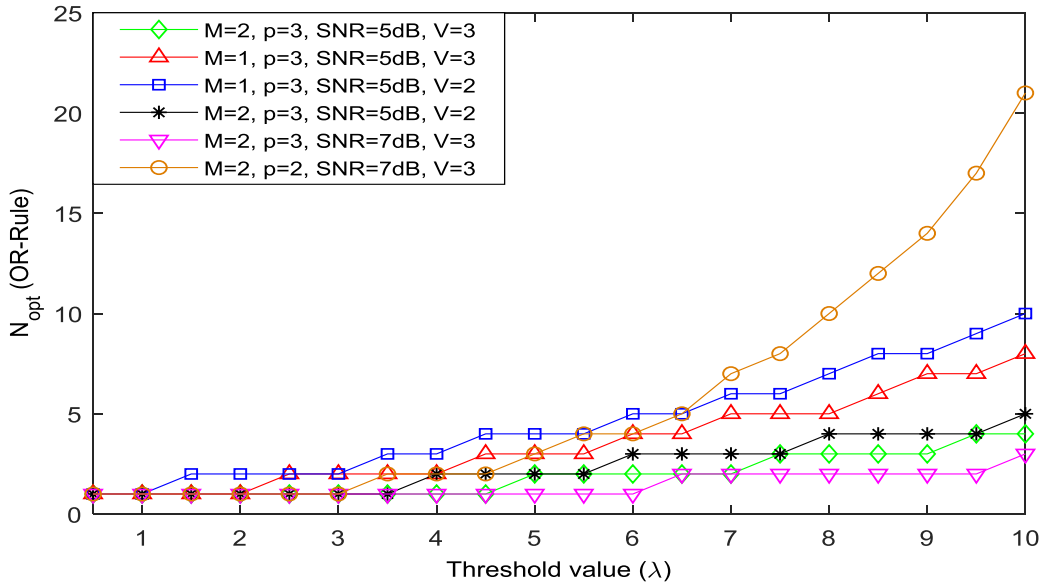

Fig.5.20. N_{opt} versus λ graphs for Weibull fading channel using *OR-Rule* at FC.

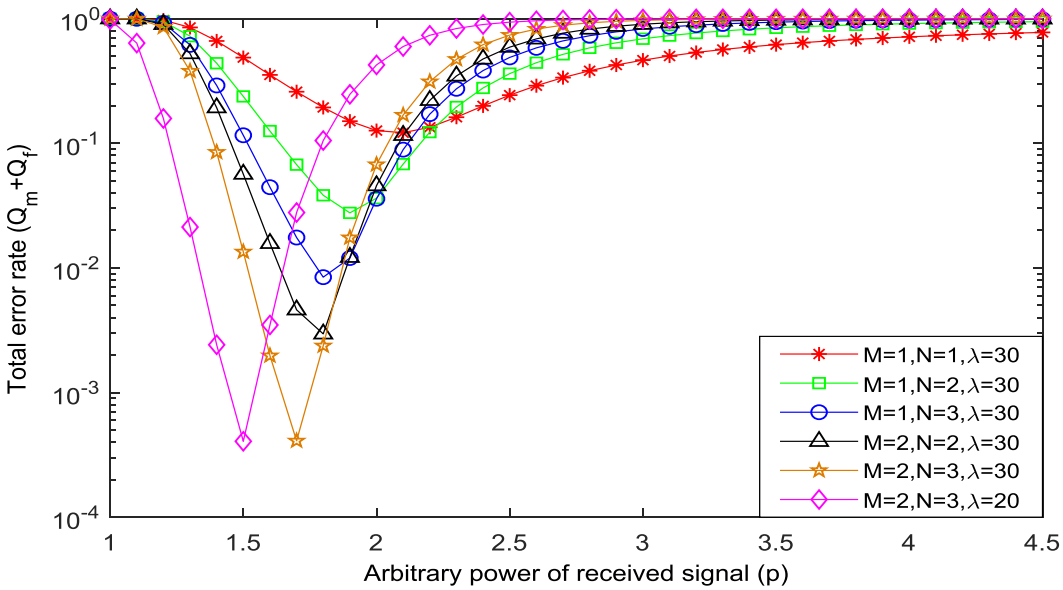

Fig.5.21. $Q_m + Q_f$ versus p graphs for Weibull fading channel using *OR-Rule* at FC.

In Fig.5.21, total error probability performance is analyzed as a function of p using *OR-Rule* at FC over Weibull fading channel. The simulation results are in exact accordance with derived theoretical expressions. Three values of N (N=1, N=2 and N=3), two values of M (M=1

and *M*=2), and two values of λ (λ=30 and λ=20) are considered as simulation parameters. For a particular case, at *p*=3, *M*=1, λ=30, and $\bar{\gamma}$=10dB, if *N* value increases from *N*=1 to *N*=3, $(Q_m + Q_f)$ value decreases by 26.8%. As *M* value increases from *M*=1 to *M*=2, $(Q_m + Q_f)$ value decreases by 55.9% at *p*=3, λ=30, *N*=2, and $\bar{\gamma}$=10dB.

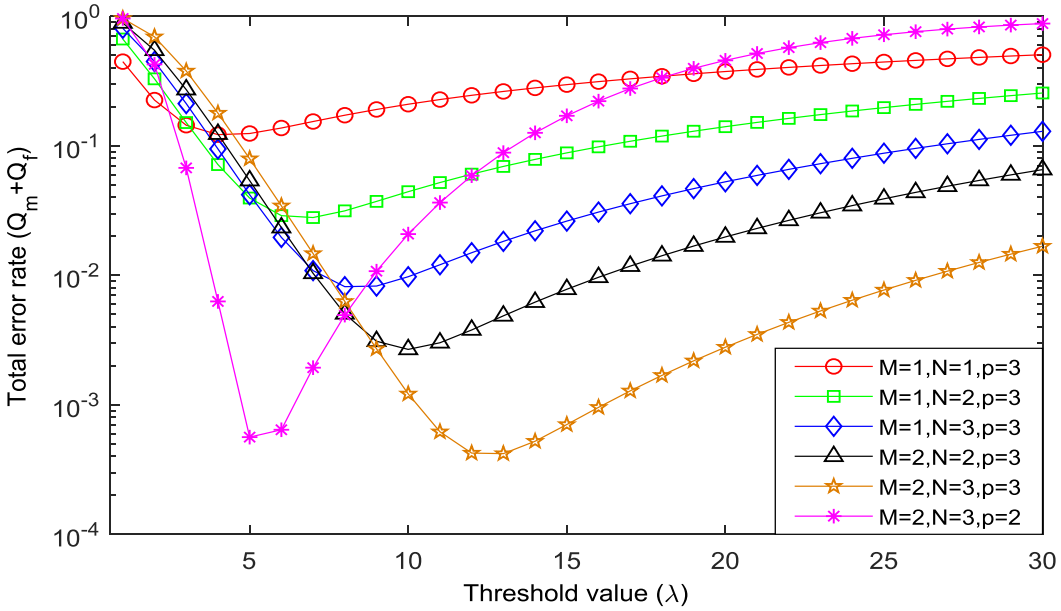

Fig.5.22. $Q_m + Q_f$ versus λ graphs for Weibull fading channel using *OR-Rule* at FC.

In Fig.5.22, $(Q_m + Q_f)$ performance is shown as a function of λ for various values of *N*, *p*, and *M* using *OR-Rule* at FC over Weibull fading channel. As *N* value increases from *N*=1 to *N*=3, $(Q_m + Q_f)$ value decreases by 95.3% at λ=10, *M*=1, *V*=3, $\bar{\gamma}$=10 dB and *p*=3. When *M* value increases from *M*=1 to *M*=2, $(Q_m + Q_f)$ value decreases by 87.5% at λ=10, *N*=3, *p*=3, *V*=3, and $\bar{\gamma}$=10dB. It can be clearly observed from the simulation that for fixed values of *M* and *N*, as λ value increases, the total error rate curve shifts towards right i.e. moves away from the origin.

In Fig.5.23, N_{opt} value is calculated as a function of λ using *AND-Rule* at FC over Weibull fading channel. The performance is evaluated for different values of *p* namely (*p*=2 and *p*=3), *V* namely (*V*=2 and *V*=3), *M* namely (*M*=1 and *M*=2), and $\bar{\gamma}$ namely ($\bar{\gamma}$=5dB and $\bar{\gamma}$=7dB) in Weibull fading channel. As $\bar{\gamma}$ value decreases from 7dB to 5dB, N_{opt} value decreases from 29 to 23 at λ=0.6, *p*=3, *M*=2 and *V*=3. As fading factor value increases from *V*=2 to *V*=3, N_{opt} value increases from 11 to 31 at λ=0.5, $\bar{\gamma}$=5dB, *p*=3, and *M*=2. If the number of antennas at each CR increases from *M*=1 to *M*=2, there is a significant improvement in N_{opt} value from 6 to 31 at λ=0.5, $\bar{\gamma}$=5dB, *p*=3, and *V*=3.

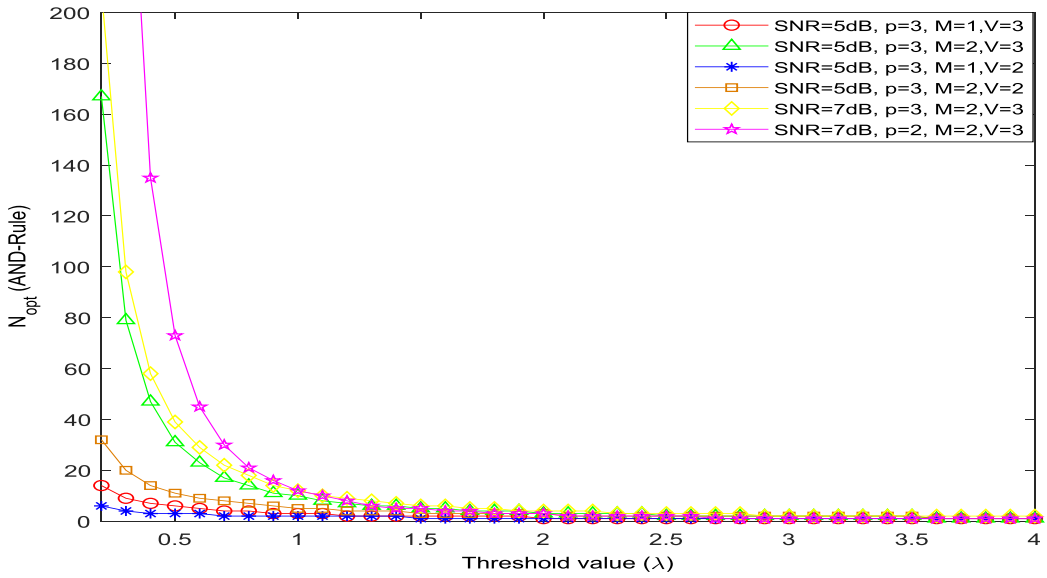

Fig.5.23. N_{opt} versus λ graphs for Weibull fading channel using *AND-Rule* at FC.

Finally, we can conclude that two different fusion rules are operated individually at FC namely *OR-Rule* and *AND-Rule*. N_{opt} value is high at lower values of λ using *AND-Rule* at FC and its value is high at higher values of λ using *OR-Rule* at FC.

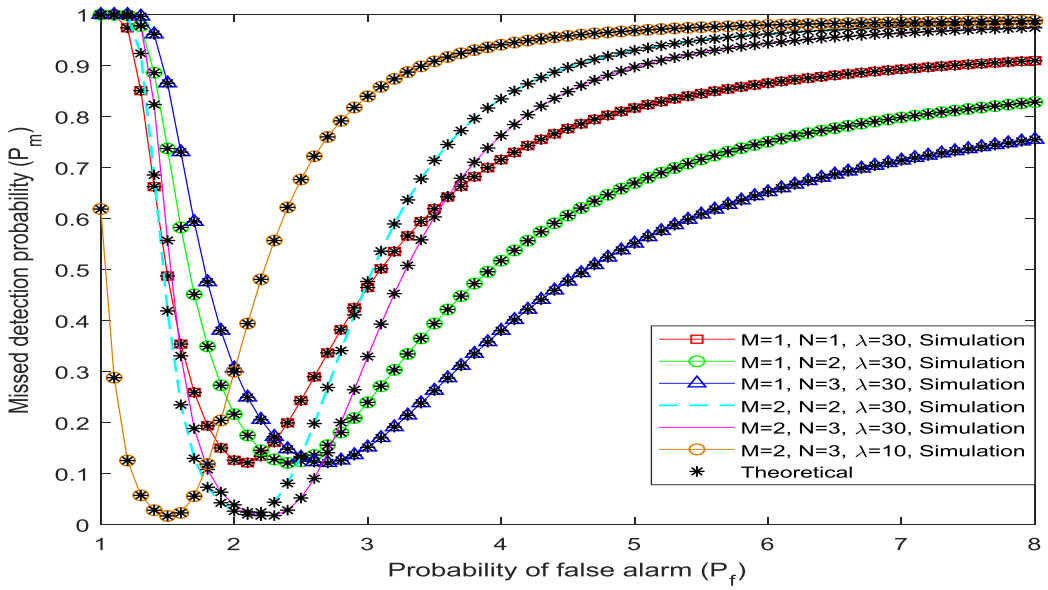

Fig.5.24. $Q_m + Q_f$ versus p graphs for Weibull fading channel using *AND-Rule* at FC.

Figure 5.24 is drawn between $(Q_m + Q_f)$ and p using *AND-Rule* at FC over Weibull fading channel. This simulation is drawn with the strong support of theoretical expressions. Three values of N namely (N=1, N=2 and N=3), two values of M (M=1 and M=2), and two values of λ (λ=30 and λ=20) are used to simulate Fig.5.24. For a particular case, when N value

increases from N=1 to N=3, $(Q_m + Q_f)$ value decreases by 68.1% at p=4, M=1, λ=30, and $\bar{\gamma}$=10dB. Similarly, when M value at each CR increases from M=1 to M=2, $(Q_m + Q_f)$ value decreases by 60.8% at p=3, λ=30, N=3, and $\bar{\gamma}$=10dB.

It is evident from the Fig.5.24 that the total error probability value initially decreases with increases in the p value and increases next with further increases in the value of p. Similar variation is observed with all other network parameters also. This nature of the curve is due to increase in the value of p, the detection threshold value according to $\lambda = \lambda_n \sigma_n^p$ decreases so that there is a chance of getting higher probabilities of false alarm at a CR user (P_f) and at FC (Q_f), which leads to increase in the total error probability. Similarly, when the number of CR users in the network increases, and considering AND logic fusion at FC, the probability of false alarm value increases which in turn increases in total error probability. It can be seen from Fig. 5.24 that there exists an optimum value of p for which the total error probability is minimum. This optimum value of p depends on value of λ, M and N i.e., it is different for different values of λ, M, and N. Finally, dip shows the optimum value of respective network parameter in the simulation.

In chapter-5, we have evaluated the closed form of optimal expressions for CSS network parameters such as optimal number of CR users (N_{opt}), optimal value of threshold value (λ_{opt}), optimal value of arbitrary the power of received signal (p_{opt}) are derived in various fading environments. We have derived the novel expressions of missed detection probability (P_m) considering multiple antennas (M) at each CR for different fading channels. The simulations are drawn to find out the optimal values of network parameters and to calculate the minimum value of total error rate for various fading channels. The performance is evaluated using multiple antennas and an IED scheme at each CR in the proposed CSS network when it is affected by various fading environments. Most of the MATLAB figures are drawn with the support of analytical results and some are drawn with the support of simulations such as CROC curves for different fading environments. For an example, modified modified Fig. 5.3, Fig.5.4, and Fig.5.24 shows that our simulations results are perfectly in accordance with theoretical results.

Optimized network parameters	N_{opt}			p_{opt}			λ_{opt}			$Q_m + Q_f$		
Number of antennas	*M*=1	*M*=2	*M*=3	*M*=1	*M*=2	*M*=3	*M*=1	*M*=2	*M*=3	*M*=1	*M*=2	*M*=3
Rayleigh fading (Existing)	11	7	5	4.3	4	3.2	32	28	24	0.0985	0.0671	0.0357
Rician fading (Proposed)	12	8	6	4	3.5	3.1	27	25	21	0.0667	0.0523	0.0296
Weibull fading (Proposed)	16	11	9	3.5	2.9	2.5	19	18	15	0.0403	0.0358	0.0201
Hoyt fading (Proposed)	29	15	13	4.75	4.2	3.25	35	32	28	0.1415	0.0823	0.0416

Table 5.1. Optimized values of CSS network parameters over various fading channels.

Table 5.1 shows the optimized CSS network parameter values for different fading channels. The optimum values are calculated using the multiple antennas and an IED scheme at each CR in the proposed CSS network over various fading channels. From the Table 5.1, we can conclude that as the number of antennas at each CR are increases, an optimum value of CSS network parameters is decreases because of the diversity order at each CR is increases. From the eq. (5.24), we can claim that for a particular value of probability of false alarm, probability of missed detection and for given error rates, it gives an optimum value of number of CR users (N_{opt}). This N_{opt} value also depends on number of antennas used at each CR, as the number of antennas at each CR is increases, N_{opt} value is decreases. Similarly, we have derived the closed form of optimized mathematical expressions such as arbitrary power of the received signal (p_{opt}) and threshold value (λ_{opt}) for different fusion rules (OR-Rule and AND-Rule), different values of number of antennas at each CR (*M*=1, *M*=2 and *M*=3), different number of CR users in the network (*N*=1, *N*=2 and *N*=3). The closed form of optimal expressions for λ_{opt} and p_{opt} are provided in the section 5.6, section 5.7 and section 5.8 respectively. Finally, for an optimal values of N_{opt}, λ_{opt} and p_{opt}, we have calculated total error value (Q_m+Q_f) also for different fading environments. For these optimal values of network parameters, we have achieved the lower value of total error rates, so for what values of total error value is minimum those values are treated as optimal values of CSS network

parameters. We have calculated the closed form of an optimal expressions up to number of antennas M=3 because after that system complexity increases, calculation of mathematical expression becomes more complex, and after M=3 there is not much improvement in the optimum values. Finally, we can conclude that total error value is minimum in Weibull fading and its value is more in Hoyt fading channel.

5.10. Conclusions

In this chapter, we have proposed the cooperative spectrum sensing (CSS) network which is equipped with multiple antennas and an improved energy detector (IED) scheme as detection technique at each cognitive radio (CR) and the performance is evaluated over various fading channels. Selection combining (SC) scheme is used at each CR, it receives the binary decisions of the primary user (PU) from an IED technique using multiple antennas and selects better detection value of PU. The sensing information about the PU is passed to the fusion center (FC) through reporting channel (R-channel). Final decision is made at FC using different fusion rules (*OR-Rule, AND-Rule*). We have derived the novel expressions of missed detection probability using multiple antennas and an IED scheme at each CR for different fading channels.

The performance is analyzed with the help of complementary receiver operating characteristics (CROC) and total error rate curves for the proposed CSS network. Finally, we have also derived the closed form of optimal expressions for various CSS network parameters such as an optimum number of CRs, the optimum value of the arbitrary power of received signal, and the optimum value of detection threshold to obtain the optimal performance of CSS network. Our simulation results are perfectly in accordance with analytical results. The simulation results depends on various values of network parameters such as average sensing channel SNR ($\bar{\gamma}$), multiple antennas (M) at each CR, detection threshold value (λ), arbitrary power of the received siganl (p), and number of CR users (N). The performance is evaluated using single and multiple antennas at each CR for various fading channels and comparison between them also provided. The performance comparison between CED and IED schemes are also provided. Finally, we can conclude that detection performance is improved by considering multiple antennas and an IED scheme at each CR in the CSS network.

CHAPTER-6

Average Channel Throughput and Network Utility Function Analysis using CSS Network

6.1. Introduction

This chapter describes the performance evaluation of average channel throughput and network utility function analysis using the proposed CSS network. Cognitive radio technique introduces the concept of spectrum reuse with the help of secondary users. These secondary users are allowed to utilize the radio spectrum without interfering in the primary user's operation. But, in realistic environment detection of the primary user is not accurate due to multipath fading and shadowing effects. This issue can be resolved by taking the cooperation of multiple secondary users in the network. The sensing performance can be improved by increasing the sensing duration, but it reduces the data transmission rate which further reduces the throughput value of the network [101]. There will be an always trade-off between sensing time and throughput of the network [30]. The average channel throughput value can be improved when the sensing and transmission are performed simultaneously [102]. The average channel throughput (C_{avg}) performance is evaluated and improved using the proposed CSS network over Rayleigh and Weibull fading channels. It is not always true that increased number of CR users in the network will improve the throughput of the network. So, an optimal number of secondary users should be calculated to maximize the average channel throughput for different fusion rules. Similarly, network utility function (NUF) analysis is also necessary to improve the detection probability of primary user and to an efficient utilization of radio spectrum [31]. The performance of NUF is also described in detail using the fusion rules at FC in the proposed CSS network.

6.2. System Model

Figure 6.1 shows the proposed model of CSS network with *N* number of SUs, an FC, and a PU. The channel present between PU and SUs is called as sensing channel (S-channel), in this channel each CR senses and stores the information about the PU. The sensing information associated with each CR is transferred to the FC through the reporting channel (R-channel) and S-channel is assumed as an error-free channel. The R-channel lies between SUs and FC in the proposed network and error rate (p_e) is considered in it. Complete information from all CRs are collected at FC, and the final decision is made at FC using fusion rules such as $k=1+n$ and $k=N-n$, where *k*-is selected number of CRs, *N*-is total number of available CRs, and *n*-is positive integer ($n=2$ is assumed in simulations). Each CR uses an IED scheme and selection combining (SC) diversity technique to get the binary decision about the PU [28].

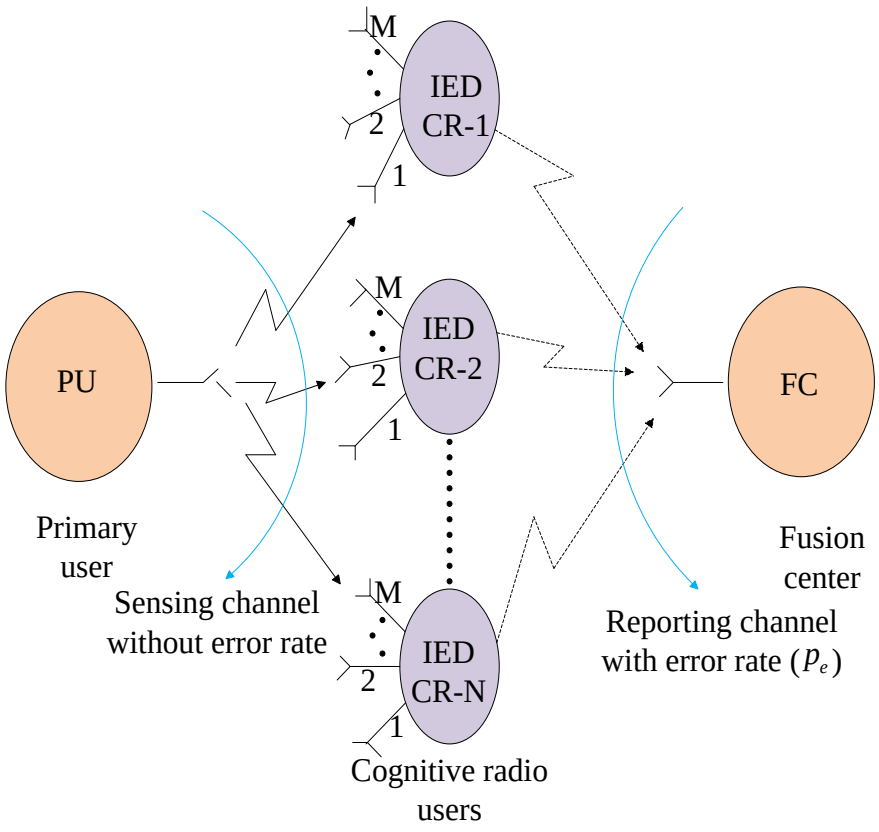

Fig.6.1. Proposed model of cooperative spectrum sensing network.

Two hypotheses are defined in the literature to decide the absence and presence of PU as H_0 and H_1 respectively. The received signal at *j*-th CR can be written as [10];

$$y_j(t) = \begin{cases} n_j(t) & : H_0 \\ h_j * s(t) + n_j(t) & : H_1 \end{cases} \tag{6.1}$$

In the above expression, $s(t)$ represents the received signal at the input of IED and $n_j(t)$ is the noise value at *j*-th CR. AWGN noise (Additive white Gaussian noise) is considered in the network which is uniformly distributed over each CR. h_j is the fading coefficient which occurs due to fading effect in the channel.

The expression for *i*-th antenna to make a local decision about the PU is given by [18]

$$W_i = y_i^{\,p} \qquad p > 0 \tag{6.2}$$

For an IED scheme, *p*-value should be more than 2, i.e., (*p*> 2) to achieve better detection probability than CED scheme.

Each CR uses an IED technique to get the decision statistics from all (*i* = 1….*M*) antennas. With the help of selection combining (SC), the largest value of w_i can be selected from all available w_i values and it is denoted as *Z*. The final decision about the PU is obtained by comparing *Z* value with detection threshold (λ) is calculated as [28];

$$\begin{aligned} Z \geq \lambda \quad & : H_1 \\ \&\ \ \mathrm{Z} < \lambda \quad & : H_0 \end{aligned} \tag{6.3}$$

Where λ can be obtained from the expression

$$\lambda = \lambda_n \sigma_n^p \tag{6.4}$$

where λ_n represents the normalized detection threshold value and σ_n^2 is the noise power for *p*=2.

6.3. Calculation of Missed Detection Probability (P_m) Expression

In this section, missed detection probability (P_m) expression for Rayleigh and Weibull fading channels are calculated using multiple antenna and an IED scheme at each CR in CSS network.

6.3.1. Missed Detection Probability Expression in Rayleigh Fading Channel

The missed detection probability expression for Rayleigh fading channel can be calculated using the PDF given in [28] as;

$$f_{y_i|\mathrm{H}_1}(\mathrm{y}) = \frac{2y^{\frac{2-p}{p}}}{p(\mathrm{E_s}\,\sigma_h^2 + \sigma_n^2)} \exp\left(-\frac{y^{2/p}}{(\mathrm{E_s}\,\sigma_h^2 + \sigma_n^2)} \right) \tag{6.5}$$

Steps involved in the calculation of P_m expression for Rayleigh fading channel are provided in [28]. Finally, P_m expression for Rayleigh fading channel with an IED scheme and single antennas at each CR is given in [28] as;

$$P_m = \left(1 - \exp\left(-\lambda^{2/p} / (1+\bar{\gamma})\sigma_n^2\right)\right) \tag{6.6}$$

where $\bar{\gamma} = E_s\sigma_h^2 / \sigma_n^2$ is S-channel SNR.

The detection probability (P_d) can be calculated as

$$P_d = 1 - P_m \tag{6.7}$$

The closed form of P_m expression for Rayleigh fading channel using an IED scheme with multiple antennas (*M*) at each CR is [28]

$$P_m = \left(1 - \exp\left(-\lambda^{2/p} / (1+\bar{\gamma})\sigma_n^2\right)\right)^M \tag{6.8}$$

The expression for P_m is different for different fading channels because it depends upon S-channel SNR value whereas the probability of false alarm (P_f) expression remains the same for various fading channels [10]. The expression for P_f using an IED scheme using multiple antennas (*M*), selection combining (SC) diversity scheme at each CR is given in [28] as;

$$P_f = 1 - \left(1 - \exp\left(-\lambda^{2/p} / \sigma_n^2\right)\right)^M \tag{6.9}$$

6.3.2. Missed Detection Probability Expression in Weibull Fading Channel

The missed detection probability expression for Weibull fading channel can be derived with the help of PDF given in [112] as;

$$f_{w_i|\mathrm{H}_1}(\mathrm{y}) = \frac{2y^{(2/p)-1}C}{p}\left[\frac{\Gamma(P)}{(E_s\sigma_h^2+\sigma_n^2)}\right]^C \left(\mathrm{y}^{2/p}\right)^{\mathrm{C}-1} \exp\left(-\left\{\frac{\mathrm{y}^{2/p}\Gamma(P)}{(E_s\sigma_h^2+\sigma_n^2)}\right\}^C\right) \tag{6.10}$$

where $C = V/2$, $P = 1 + 1/C$, and V –is Weibull fading parameter.

The missed detection probability expression for Weibull fading channel with an IED scheme and single antennas at each CR is derived by us using the steps given in [28] as;

$$P_m = \left[1 - \exp\left(-\left\{ \frac{\lambda^{2/p}\Gamma(P)}{\sigma_n^2(1+\bar{\gamma})} \right\}^C \right) \right] \tag{6.11}$$

where $\bar{\gamma} = E_s\sigma_h^2 / \sigma_n^2$ is S-channel SNR.

The missed detection probability expression for Weibull fading channel using an IED scheme and multiple antennas (*M*) at each CR is derived as;

$$P_m = \left[1 - \exp\left(-\left\{ \frac{\lambda^{2/p}\Gamma(P)}{\sigma_n^2(1+\bar{\gamma})} \right\}^C \right) \right]^M \tag{6.12}$$

6.4. Fusion Rules

As we discussed above, the information from *i*-th CR in the form of one-bit decision (μ_i) is transfered to FC over an erroneous reporting channel. The information from all CRs (*N*) are collected at FC and compared with an integer value of detection threshold (λ) to make a final deccision about PU. The final decision can be made at FC using the following expression;

$$k \text{ out of } N \text{ rule} = \begin{cases} H_1 & if \ \sum_{i=1}^{k} \mu_i \geq \lambda, \\ H_0 & if \ \sum_{i=1}^{k} \mu_i < \lambda \end{cases} \tag{6.13}$$

For *k*=1, the above expression represents the expression for *OR-Rule* and for *k*=*N*, it indicates the expression for *AND-Rule*. In this chapter, we are evaluating the performances using *k*=1+*n* and *k*=*N*-*n* fusion rules at FC. The value of *n* can be chosen from $0 \leq n < N$ (*n*=2 is chosen in simulation).

Let P_{de} and P_{fe} be the effective probability of detection and effective probability of false alarm of a secondary user over erroneous reporting channel as seen by the FC and is given by [102];

$$P_{fe} = P_f\left(1 - p_e\right) + p_e\left(1 - P_f\right) \tag{6.14}$$

$$P_{de} = P_d\left(1 - p_e\right) + p_e\left(1 - P_d\right) \tag{6.15}$$

The information associated with each CR is transferred to FC through R-channel in the form of binary decisions (either 0 or 1). The following expressions with an error rate in an erroneous R-channel are used to make a final decision about the PU [102];

$$P_{F,k} = \sum_{l=k}^{N} \binom{N}{l} P_{fe}{}^{l} \left(1 - P_{fe}\right)^{N-l}$$

$$= 1 - \sum_{l=0}^{k-1} \binom{N}{l} P_{fe}{}^{l} \left(1 - P_{fe}\right)^{N-l} \tag{6.16}$$

$$P_{\mathrm{D},k} = \sum_{l=k}^{N} \binom{N}{l} p_{de}{}^{l} \left(1 - p_{de}\right)^{N-l}$$

$$= 1 - \sum_{l=0}^{k-1} \binom{N}{l} p_{de}{}^{l} \left(1 - p_{de}\right)^{N-l} \tag{6.17}$$

6.5. Average Channel Throughput

Generally, average channel throughput can be defined as it is the rate of successful information (message) is delivered over a communication channel. The units of average channel throughput is bits per seconds (bits/seconds). If the information is in the packets then units of average channel throughput is packets per seconds (packets/seconds). Average channel throughput (C_{avg}) value can be calculated for the proposed CSS network by using the following expressions given in [102, 119] as;

$$C_{avg,k}(N) = \varphi_0 + \varphi_1 P_{D,k}(N) - \varphi_2 P_{\mathrm{F},k}(N) \tag{6.18}$$

where $$\varphi_0 = P_1\left(\tilde{C}_p + \tilde{C}_s\right) + P_0 C_s \tag{6.19}$$

$$\varphi_1 = P_1\left(C_p - \tilde{C}_p + \tilde{C}_s\right) \tag{6.20}$$

$$\varphi_2 = P_0 C_s \tag{6.21}$$

In the above expressions $\tilde{C}_s$, C_s are the throughputs of the secondary system in the presence and absence of PU respectively. $\tilde{C}_p$, C_p are the throughputs of the primary system in the presence and absence of SU respectively. P_1 and P_0 are the probabilities of PU when it is in active and inactive state. Sum of these two probabilities should be equal to one ($P_0 + P_1 = 1$).

The final expression for average channel throughput using different fusion rules (k=1+n and k=N-n) at FC are given in [102] as;

$$C_{avg,1+n}(N) = \varphi_0 + \varphi_1 P_{D,1+n}(N) - \varphi_2 P_{F,1+n}(N) \tag{6.22}$$

$$C_{avg,N-n}(N) = \varphi_0 + \varphi_1 P_{D,N-n}(N) - \varphi_2 P_{F,N-n}(N) \tag{6.23}$$

6.5.1. Calculation of an Optimal Number of SUs using k=1+n Fusion Rule

Average channel throughput value can be improved with the increase in the number of SUs (N). As the number of SUs increased in the network, they may produce larger delays in deciding the activity of PU. Hence, it is necessary to calculate the optimal number of SUs (N^*) which exactly contribute towards the improvement of average channel throughput performance.

The final expression for an optimal number of SUs (N^*) to maximize the average channel throughput using k=1+n fusion rule at FC for the proposed CSS network is given as [102];

$$N_{1+n}^* = \left\lceil \frac{\ln(\varphi_1/\varphi_2) + (n+1)\alpha}{\beta} + n \right\rceil \tag{6.24}$$

$$\alpha = \ln\frac{1-p_{me}}{p_{fe}}, \quad \beta = \ln\frac{1-p_{fe}}{p_{me}} \tag{6.25}$$

For n=0 in Eq. (6.24), the optimal number of SUs expression is obtained when hard decision logic called *OR-Rule* is used at FC. The expression for an optimal number of SUs to maximize the channel throughput using *OR-Rule* is

$$N_{OR}^* = \left\lceil \frac{\ln(\varphi_1/\varphi_2) + \alpha}{\beta} \right\rceil \tag{6.26}$$

6.5.2. Calculation of an Optimal Number of SUs using k=N-n Fusion Rule

An optimal value of SUs (N^*) to maximize the C_{avg} value using k=N-n fusion rule at FC for the proposed CSS network is given as [102];

$$N_{M-n}^* = \left\lceil \frac{(n+1)\beta - \ln(\varphi_1/\varphi_2)}{\alpha} + n \right\rceil \tag{6.27}$$

For n=0 in Eq. (6.27), N^* expression is obtained when hard decision logic called *AND-Rule* is used at FC. The expression for N^* to maximize the channel throughput using *AND-Rule* is

$$N_{AND}^{*} = \left\lceil \frac{\beta - \ln(\varphi_1/\varphi_2)}{\alpha} \right\rceil \tag{6.28}$$

The expressions for α and β are given in Eq. (6.25). With the help of above expressions, simulation results are plotted to calculate the optimal number of SUs using k=1+n and k=N-n fusion rules at FC and using single and multiple antennas at each CR in the proposed CSS network.

6.6. Network Utility Function

The closed form of expression to maximize the network utility function (NUF) for the proposed CSS network is [31]

$$J(N) = u_1\left(\left(1 - P_{F,k}(N)\right)p(H_0) + P_{m,k}(N)\,p(H_1)\right) - u_2 P_{m,k}(N)\,p(H_1) - u_3 N \tag{6.29}$$

The above mentioned final NUF expression is a combination of three parts, in which the first part gives information regarding the amount of spectrum usage. When PUs have not identified accurately, interference problem of SUs with PUs can occur which is represented by second part of above equation. Finally, the third part gives information about the utilization of resources in the network. μ_1, μ_2, and μ_3 are the cost functions. $p(H_0)$ and $p(H_1)$ are the probabilities of inactive and active states of PU. The network utility function performance increases with the cooperation of SUs in the proposed system.

6.7. Results and Discussions

In this section, simulation results and their discussions are provided. With the help of simulation results, the average channel throughput (C_{avg}) and network utility function (NUF) performances are evaluated. The proposed CSS network consists of an IED scheme, multiple antennas (M), selection combining technique at each CR, and the error rate is considered in R-channel. An error rate (p_e) in R-channel, pre-defined detection threshold (λ), multiple antennas (M) at each CR, and the number of SUs (N) in the network are treated as simulation parameters to get the performances for different fusion rules (k=1+n and k=N-n) at FC over Rayleigh and Weibull fading channels.

Figure 6.2 is drawn between C_{avg} and λ using k=1+n fusion rule at FC. The performance is evaluated using an IED scheme with a single antenna at each CR over Rayleigh fading channel. Two different values of N namely N=3 and N=4, two values of S-channel SNRs namely $\bar{\gamma}$=5dB and $\bar{\gamma}$=10dB, and the error rates in R-channel p_e=0 and p_e=0.2 are chosen as variable parameters in this simulation. The performance comparison between perfect (error free R-channel) and imperfect R-channel (error rate present in R-channel) is provided to show the effect of an error rate on average channel throughput value.

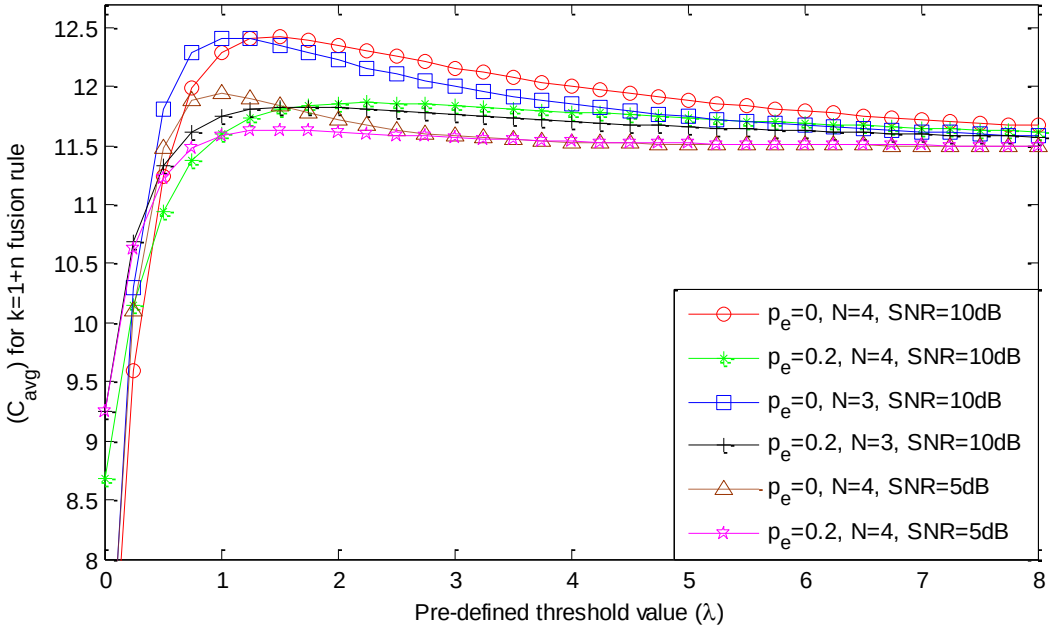

Fig.6.2. C_{avg} versus λ with a single antenna at each CR using k=1+n fusion rule at FC.

It can be observed from Fig.6.2 that throughput value is maximum with error-free R-channel and performance decreases as the error rate increases in R-channel. As the error rate increases from p_e=0 to p_e=0.2 in R-channel, C_{avg} value decreases by 2.63% at λ=3, N=4, M=1, and $\bar{\gamma}$=10dB. It can also observed from the simulation that initially throughput value increases at lower values of λ and it reaches the maximum point after that it decreases at higher values of λ. C_{avg} value increases with the cooperation of multiple numbers of SUs in the network using k=1+n fusion rule. As N value increases from N=3 to N=4, C_{avg} value increases by 1.31% at λ=3, M=1, and $\bar{\gamma}$=10dB.

In Fig.6.3, performance is drawn between C_{avg} and λ using k=1+n fusion rule at FC and multiple antennas at each CR over Rayleigh fading. The throughput value increases with multiple antennas compared to a single antenna. When the number of antennas at each CR are

increases from M=1 to M=2, C_{avg} value increases by 3.56% with perfect R-channel (p_e=0) and it increases by 1.3% with imperfect R-channel with an error rate of p_e=0.2, λ=3, N=3, and $\bar{\gamma}$=10dB. As the S-channel SNR value increases from $\bar{\gamma}$=5dB to $\bar{\gamma}$=10dB, C_{avg} value increases by 1.87% at p_e=0.2, λ=3, N=3, and M=2. Simulation parameters that are used in Fig.6.2 and Fig.6.3 are k=1+n (n=2) fusion rule, C_s=10, $\tilde{C}_s$ =5, C_p=20, $\tilde{C}_p$ = 10. From the above lines, we can conclude that the number of SUs (N), multiple antennas (M) at each CR, S-channel SNR, and the error rate play a significant role in analyzing the performance of average channel throughput value.

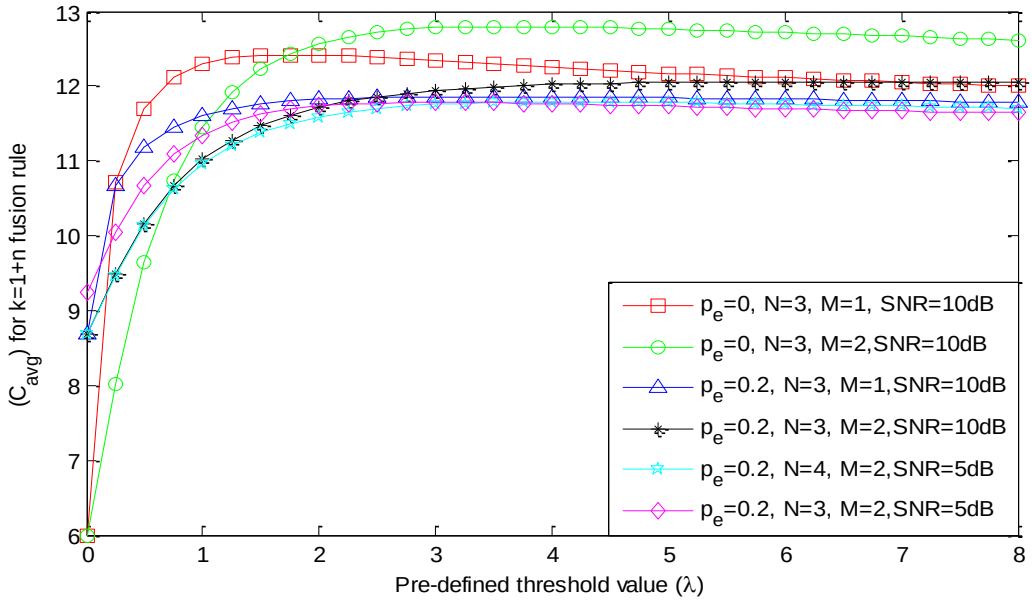

Fig.6.3. C_{avg} versus λ with multiple antennas at each CR using k=1+n fusion rule at FC.

In Fig.6.4, the analysis of C_{avg} is explained for various values of λ using k=N-n fusion rule at FC with a single antenna (M=1) at each CR over Rayleigh fading. Using k=N-n fusion rule at FC, throughput value decreases as the number of SUs and the error rate in R-channel increases. When the error rate increases in R-channel from p_e=0 to p_e=0.2, C_{avg} value decreases by 3.96% at λ=2, N=3, M=1, and $\bar{\gamma}$=10dB. For higher values of detection threshold, C_{avg} value decreases with the increament of number SUs in the network. Similarly, for lower values of λ, C_{avg} value increases with increase in number of SUs. For a particular case, when N value increases from N=3 to N=4, C_{avg} value decreases by 1.3% with perfect R-channel and it decreases by 0.67% with imperfect channel at p_e= 0.2, λ=3, M=1, and $\bar{\gamma}$ =10dB. As S-channel SNR decreases from $\bar{\gamma}$ =10dB to $\bar{\gamma}$ =5dB, C_{avg} value decreases by 4.02% with perfect R-channel and it decreases by 2.11% with imperfect

channel respectively at p_e= 0.2, λ=3, and *M*=1.

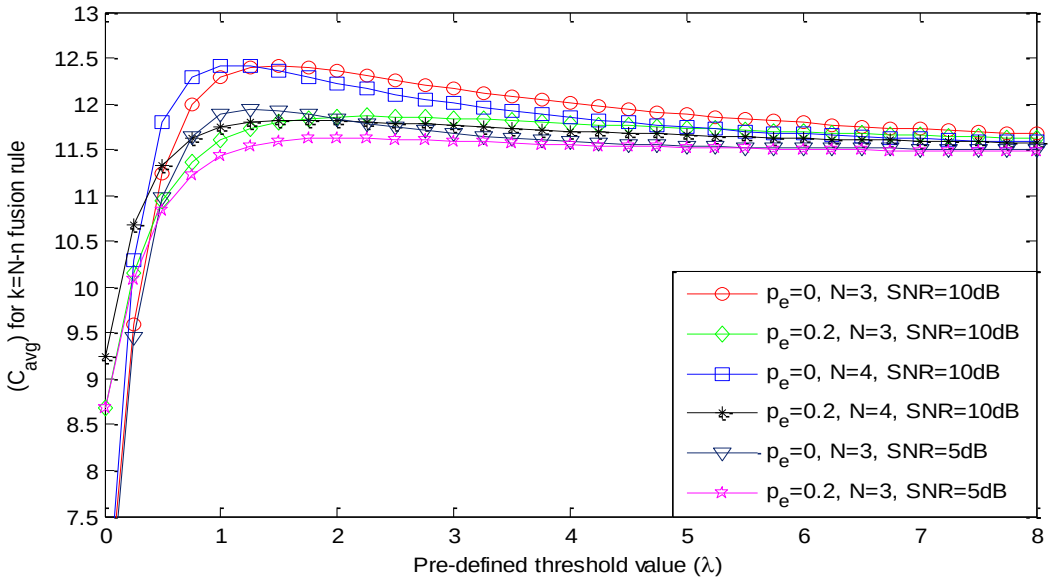

Fig.6.4. C_{avg} versus λ with a single antenna at each CR using *k*=*N*-*n* fusion rule at FC.

In Fig.6.5, performance is analyzed between C_{avg} and λ considering multiple antennas at each CR using *k*=*N*-*n* fusion rule at FC over Rayleigh fading. For an instant, when *M* value increases from *M*=1 to *M*=2, C_{avg} value increases by 4.45% with perfect R-channel and it increases by 1.34% with imperfect R-channel at p_e=0.2, λ=4, *N*=3, and $\bar{\gamma}$ =10dB. From the literature, it is clear that using multiple antennas at each CR improves the performance which has been proved using simulations.

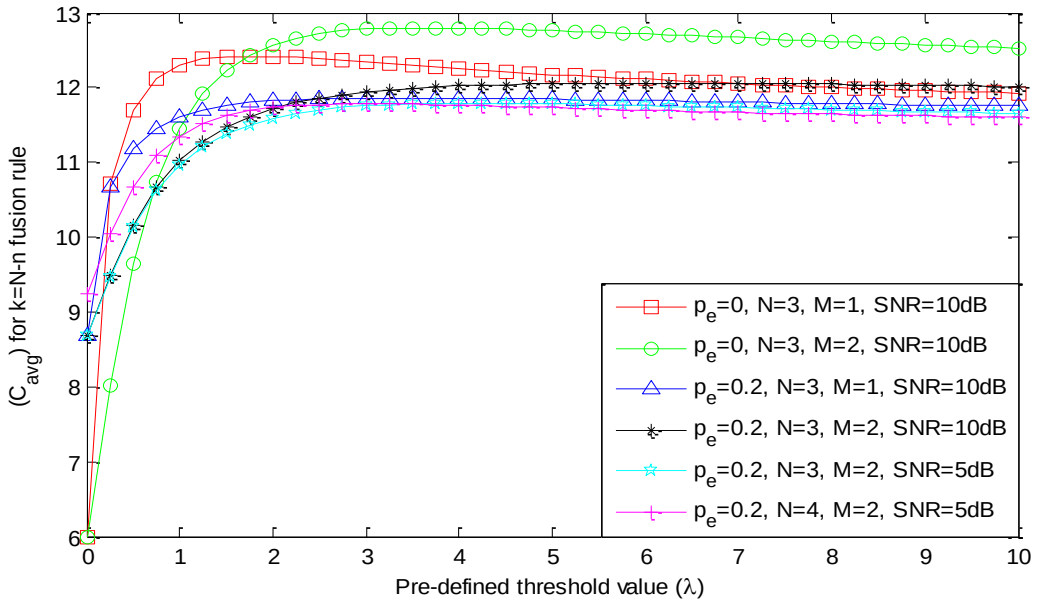

Fig.6.5. C_{avg} versus λ with multiple antennas at each CR using *k*=*N*-*n* fusion rule at FC.

Figure 6.6 shows the calculation of an optimal number of SUs (N^*) for various values of pre-defined threshold (λ) using k=1+n fusion rule at FC. The performance is analyzed by considering single antenna at each CR over Rayleigh fading channel. The performance comparison between error free and error rate present in R-channel is provided using MATLAB simulation. N^* value drastically decreases by introducing the error rate in R-channel. As p_e value increases from p_e=0 to p_e=0.01, N^* value decreases from 16 to 13 at λ=12 and k=3. Hence, error rate plays a significant role in deciding the optimal number of SUs. It can be observed from simulation that as k value increases, N^* value increases due to the cooperation among the CR users. When k value increases from k=1 to k=3, N^* value increases from 4 to 16 with perfect R-channel and it increases from 4 to 13 with imperfect R-channel at λ=12 and p_e=0.01. Finally, we can conclude that for lower values of λ, N^* value is very low and it increases with λ using k=1+n fusion rule at FC.

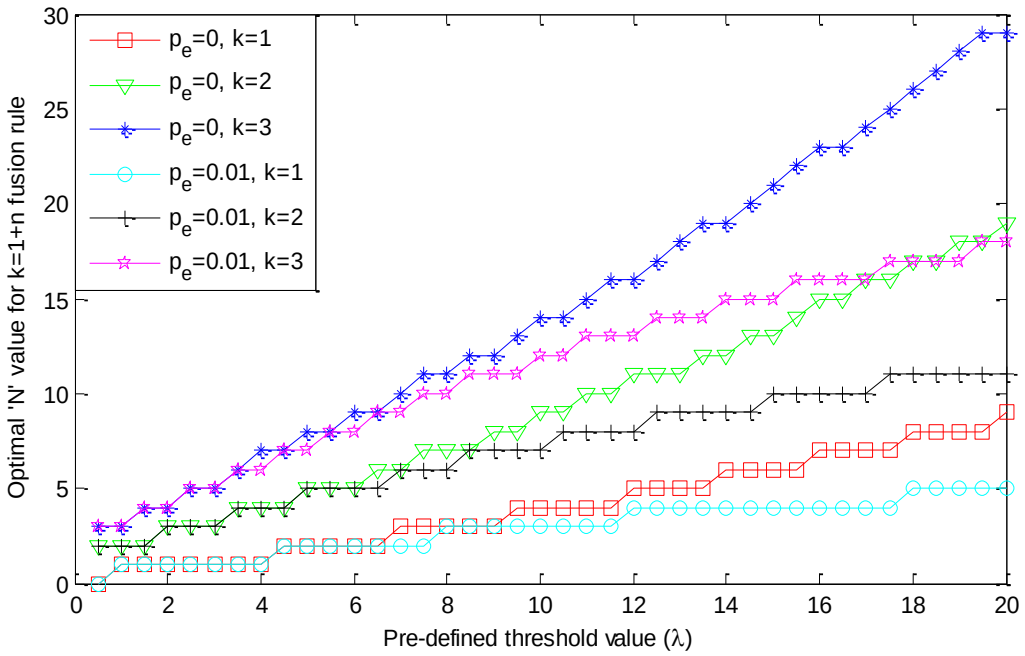

Fig.6.6. N^* versus λ with a single antenna at each CR using k=1+n fusion rule at FC.

N^* versus λ analysis is carried out in Fig.6.7 using k=1+n fusion rule at FC. The main difference between these two graphs (Fig.6.6 and Fig.6.7) is that the earlier one is drawn for a single antenna case and the later one is drawn for multiple antennas case. Using multiple antennas at each CR, N^* value decreases compared to a single antenna case. As M value increases from M=1 to M=2, N^* value drops from 11 to 6 with error free R-channel and it decreases from 8 to 5 with imperfect channel at p_e=0.01, λ=12, p=3, and k=2. Though multiple antennas at each CR are present due to the error rate in R-channel, N^* value reduces. As p_e

value increases from p_e= 0 to p_e=0.01, N^* value decreases from 6 to 5 at λ=12, k=2, M=2, and p=3. Due to the error rate in R-channel, the number of local sensing results received at FC reduces, hence N^* value decreases.

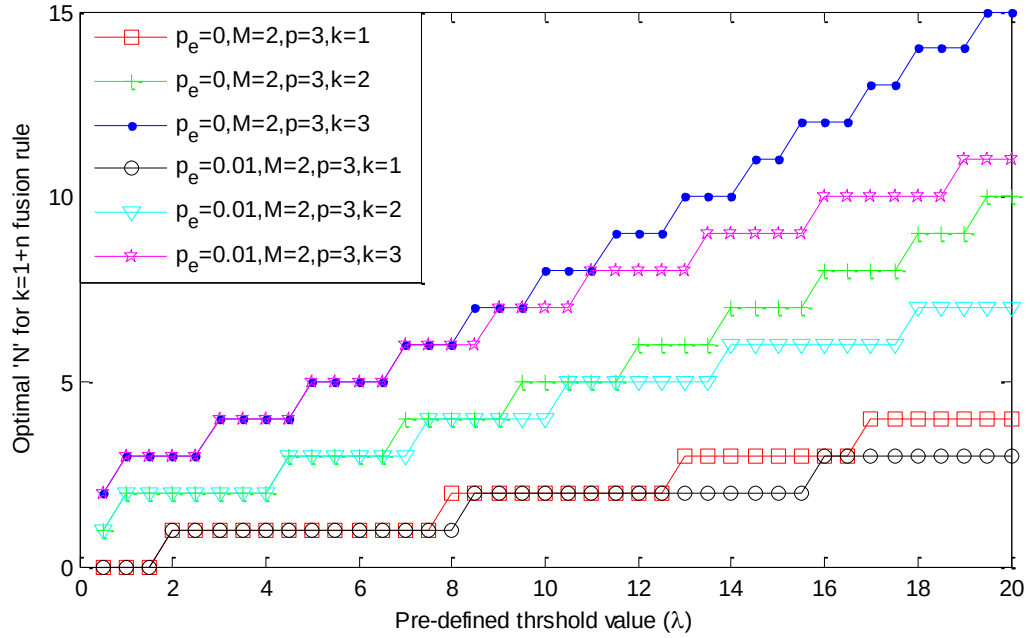

Fig.6.7. N^* versus λ with multiple antennas at each CR using k=1+n fusion rule at FC.

Figure 6.8 and Figure 6.9 are the plots drawn between N^* and λ using k=N-n fusion rule at FC using single and multiple antennas at each CR over Rayleigh fading. The performance comparison between error free and error rate present in R-channel is provided using MATLAB simulations. N^* value is more with error free R-channel and it decreases with the increment of error rate in R-channel. It can be observed from the simulation that as k value increases, N^* value increases in both cases. As k value increases from k=1 to k=3, N^* value increases from 2 to 5 with a single antenna at each CR (M=1) and it increases from 5 to 14 with multiple antennas at each CR (M=2) at λ=2 and p_e=0. Similarly, as the error rate increases from p_e=0 to p_e=0.01, N^* value decreases from 10 to 9 for a single antenna case and it decreases from 14 to 13 for multiple antennas case at λ=2, p=3, and k=3. For higher values of λ, N^* value is almost constant, it means that there is no improvement in the optimum number of SUs for higher values of λ. On the other hand, N^* value is high for lower values of λ. For k=N-n fusion rule, N^* value decreases with the increment of threshold value.

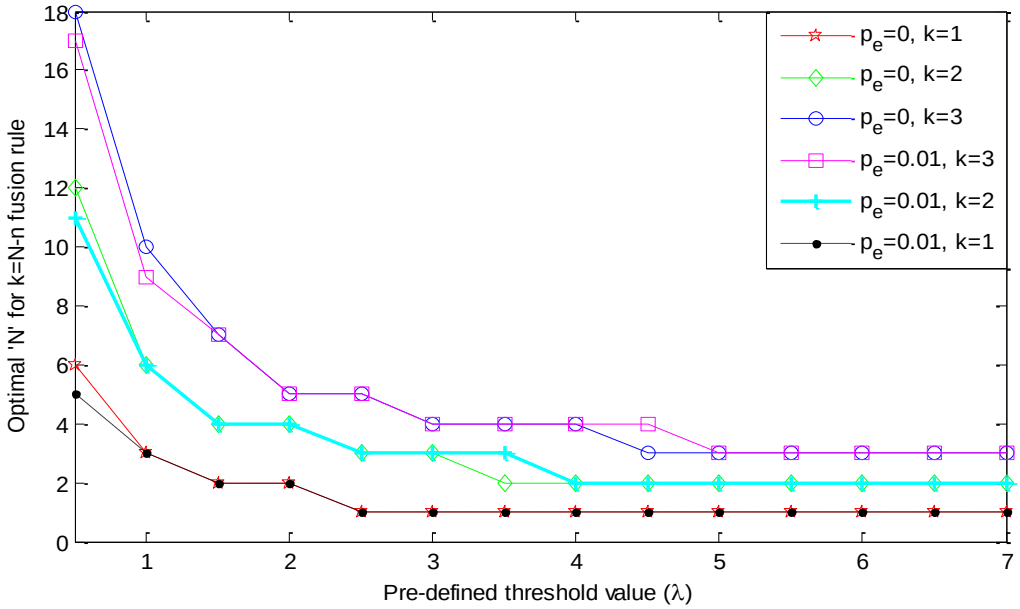

Fig.6.8. N^* versus λ with a single antenna at each CR using *k*=*N*-*n* fusion rule at FC.

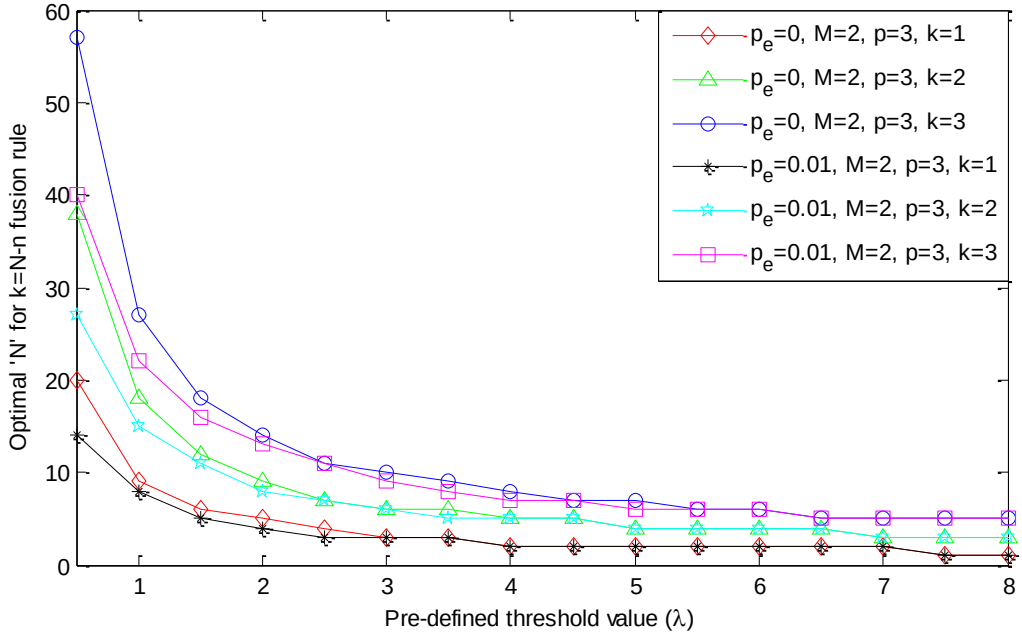

Fig.6.9. N^* versus λ with multiple antennas at each CR using *k*=*N*-*n* fusion rule at FC.

The main difference in the performance of C_{avg} value using *k*=1+*n* rule and *k*=*N*-*n* fusion rules at FC is that it increases with the cooperation of CR users using *k*=1+*n* fusion rule and it decreases using *k*=*N*-*n* fusion rule at FC.

In Fig.6.10, the performance of network utility function (NUF) is evaluated for various values of λ with a single antenna at each CR using *k*=1+*n* fusion rule at FC. NUF performance

is evaluated using an IED scheme over Rayleigh fading channel for error free and error present in R-channel. As the error rate increases in R-channel, NUF value decreases and its value maximum with error free channel. As the error rate increases from p_e=0 to p_e=0.05, NUF value decreases by 48.9% at λ=2, N=3, and $\bar{\gamma}$=10dB. NUF value increases with the increase in number of SUs in the network using k=1+n fusion rule at FC.

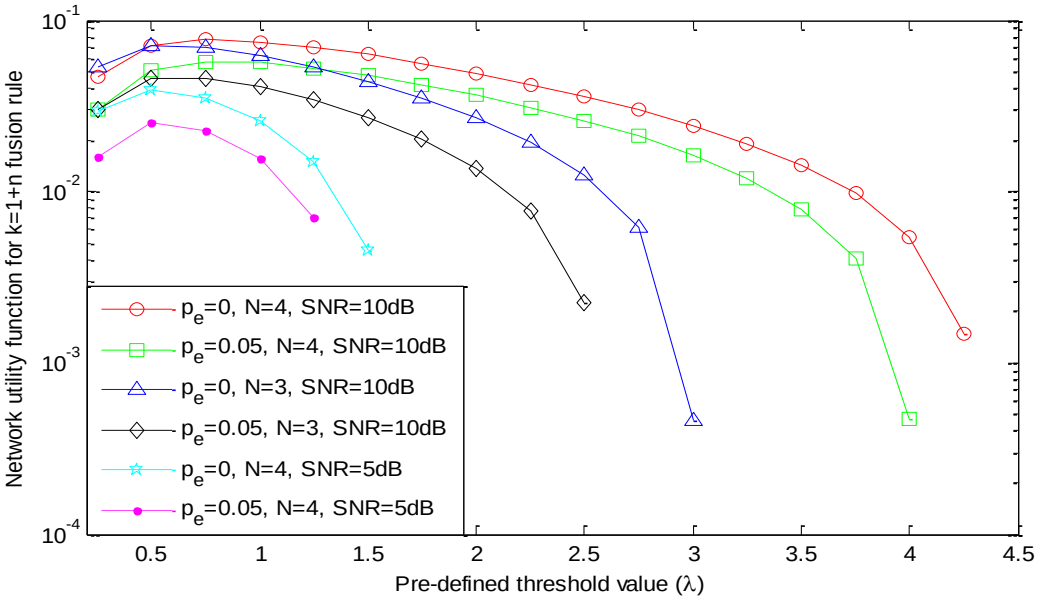

Fig.6.10. NUF versus λ with a single antenna at each CR using k=1+n fusion rule at FC.

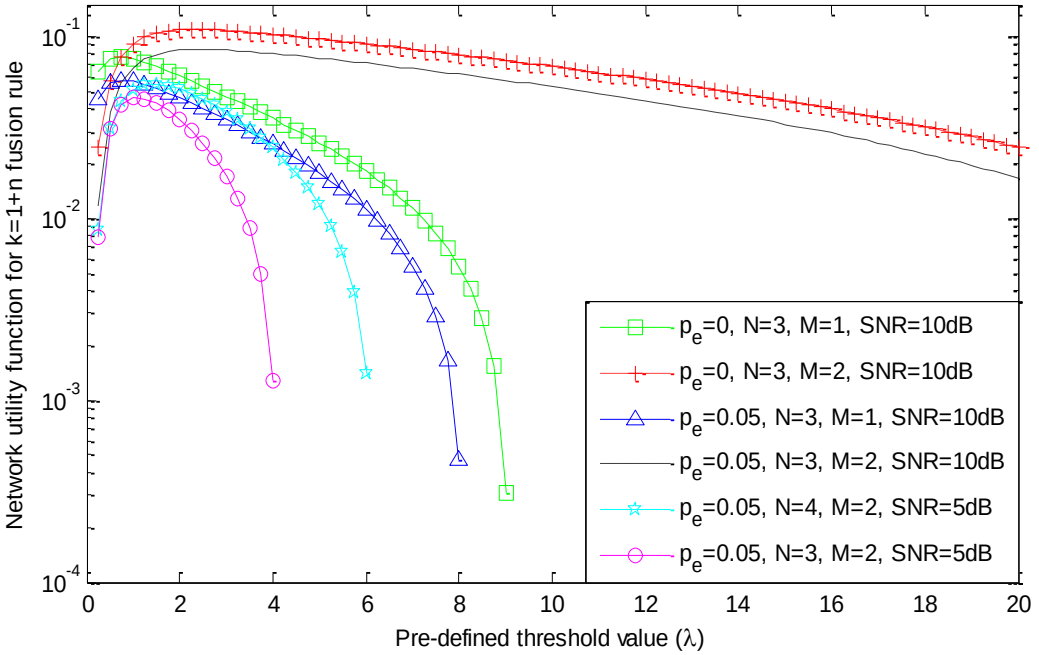

Fig.6.11. NUF versus λ with multiple antennas at each CR using k=1+n fusion rule at FC.

As N value increases from N=3 to N=4, NUF value increases by 81.8% with perfect R-channel and it increases by 76.8% with imperfect R-channel at p_e=0.05, λ=1.5, and M=1. Finally, S-channel SNR also plays a significant role in describing NUF performance. As S-channel SNR value increases, NUF value increases because of reduction in noise value. As S-channel SNR value increases from 5dB to 10 dB, NUF value increases by 262.3% with perfect R-channel and it increases by 193.2% with imperfect channel at λ=1.5, M=1, N=4, and p_e=0.05 using k=1+n fusion rule at FC. Simulation parameters used in this simulation are μ_1=0.2, μ_2=0.8, μ_3=0.005, $p(H_0)$=0.7, and $p(H_1)$=0.3.

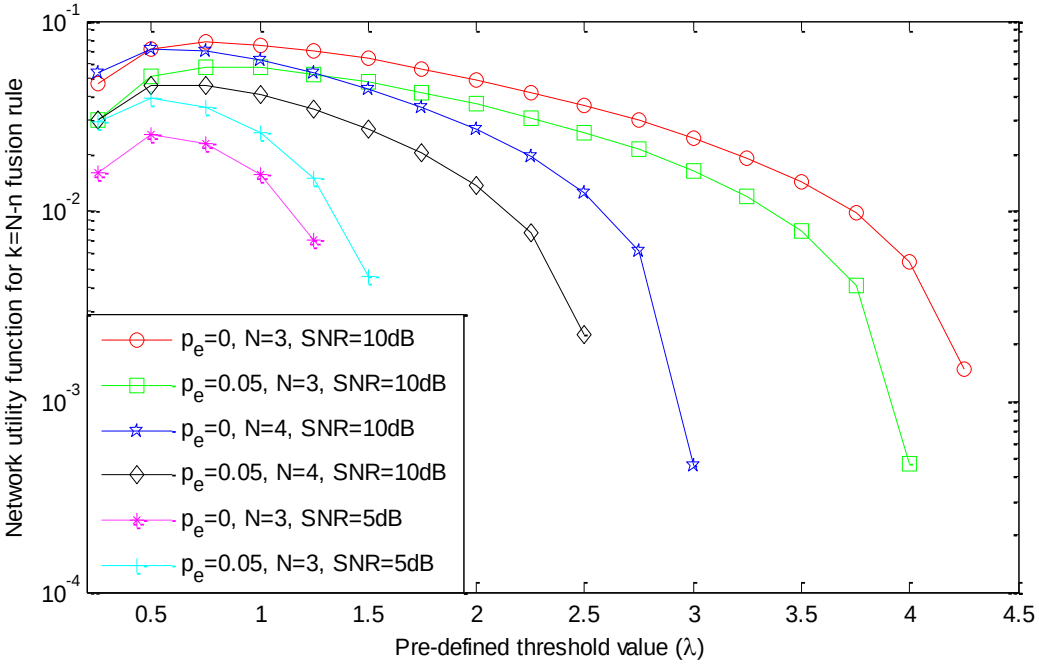

Fig.6.12. NUF versus λ with a single antenna at each CR using k=N-n fusion rule at FC.

The effect on NUF performance for different values of λ using k=N-n fusion rule at FC is shown in Fig.6.12 and Fig.6.13 respectively. NUF analysis is evaluated for a single antenna case in Fig.6.12 and for multiple antennas case in Fig.6.13 using simulations. NUF value decreases with the increase in number of SUs in CSS network using k=N-n fusion rule at FC. When N value increases from N=3 to N=4, NUF value decreases by 30.2% with perfect R-channel and it decreases by 43.2% with imperfect R-channel at λ=1.5 and M=1. Similarly, when M value increases from M=1 to M=2, NUF value increases by 66.3% with perfect R-channel and it increases by 68.7% with imperfect R-channel at λ=1.5 and N=3. As the error rate value increases from p_e=0 to p_e=0.05, NUF value decreases by 24.3% for a single antenna case and it decreases by 23.1% for multiple antennas case at N=3 and λ=1.5.

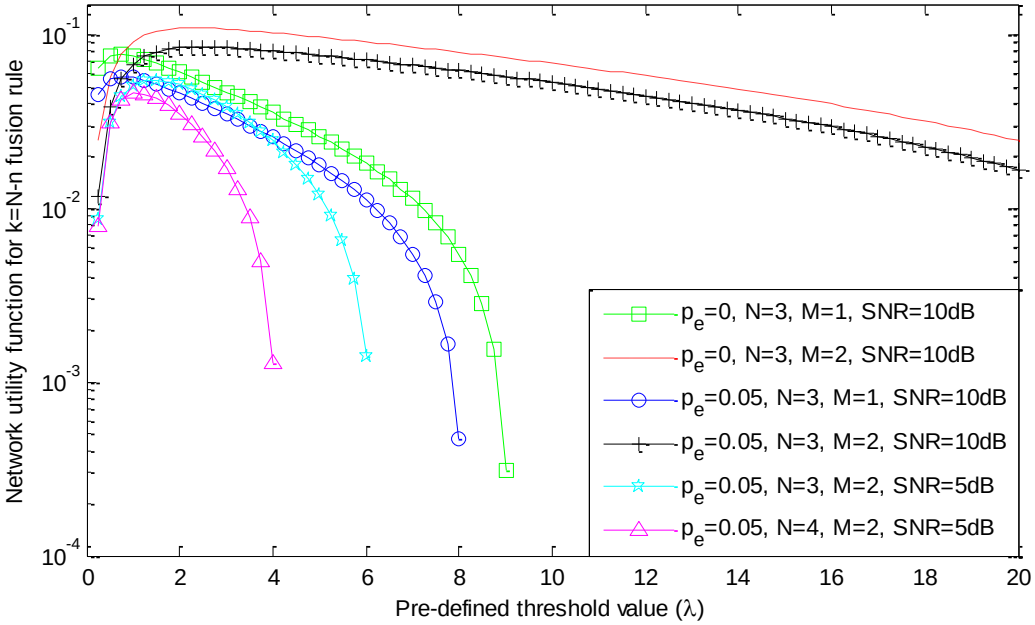

Fig.6.13. NUF versus λ with multiple antennas at each CR using *k*=*N*-*n* fusion rule at FC.

Till now, we have analyzed the performance of C_{avg} and NUF analysis in Rayleigh fading channel using the proposed CSS network. Similar analysis is carried out with the help of simulations from Fig.6.14 to Fig.6.21 over Weibull fading channel.

Figure 6.14 is a plot drawn between C_{avg} and λ using *k*=1+*n* fusion rule at FC. The performance is evaluated using an IED scheme in the proposed CSS network over Weibull fading channel for different values of *N* namely (*N*=3, *N*=4, and *N*=5), *M* namely (*M*=1 and *M*=2), and error rates (p_e=0 and p_e=0.2) in R-channel. The performance comparison between perfect and imperfect R-channel is provided to show the effect of an error rate on C_{avg}. It can be observed from Fig.6.14 that the throughput value is maximum with error free R-channel and performance decreases as the error rate increases in R-channel. As p_e value increases from p_e=0 to p_e=0.2, C_{avg} value decreases by 6.1% at *M*=2, *N*=3, $\bar{\gamma}$=10dB, and λ=8. It is also observed that the throughput value initially increases at lower values of detection threshold, reaches to the maximum, and then decreases at higher values of detection thresholds. As *N* value increases from *N*=3 to *N*=5, C_{avg} value increases by 1.8% for a single antenna case and it increases by 3.2% for multiple antenna case at λ=6, p_e=0.2, and $\bar{\gamma}$=10dB. Finally, throughput value also depends on multiple antennas that are used at each CR. If the number of antennas at each CR increases from *M*=1 to *M*=2, C_{avg} value increases by 2.43% at λ=6, *N*=4, p_e=0.2, and

$\bar{\gamma}$=10dB. This graph is simulated for the network parameters such as $\bar{\gamma}$=10dB, p_e= 0 and 0.2, k=1+n (n=2) fusion rule, C_s=10, $\tilde{C}_s$ =5, C_p=20, $\tilde{C}_p$ =10, M=1 and 2, and N=3, 4, and 5.

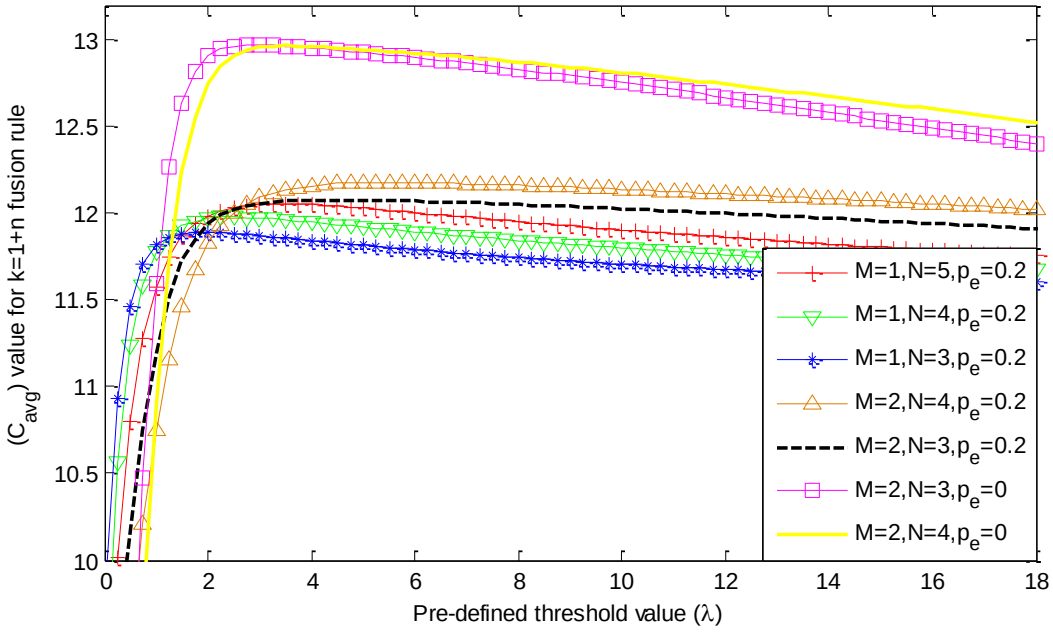

Fig.6.14. C_{avg} versus λ using k=1+n rule at FC.

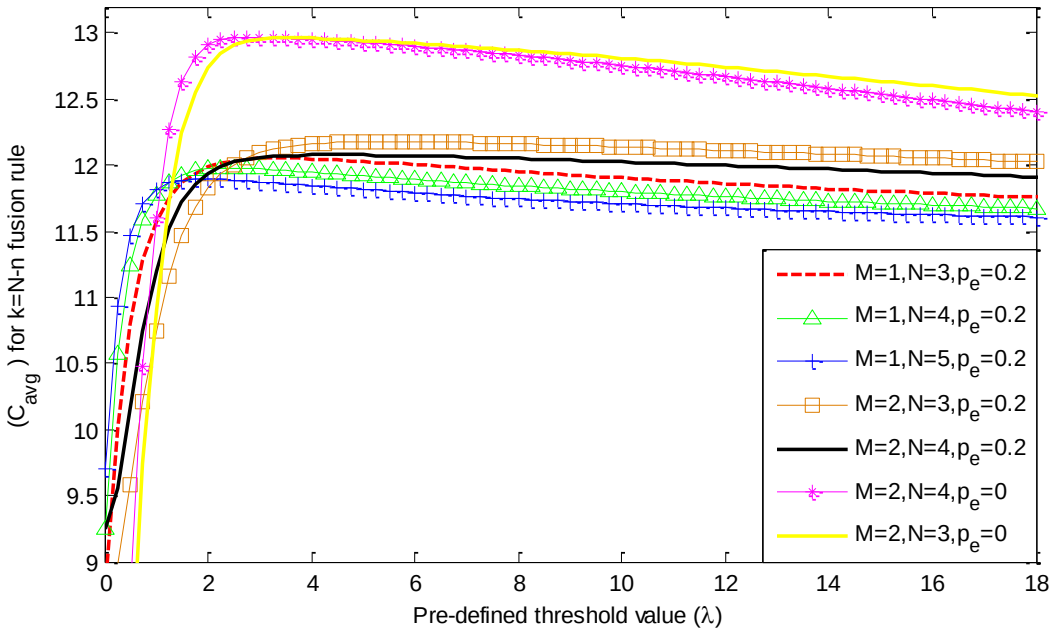

Fig.6.15. C_{avg} versus λ using k=N-n rule at FC.

Figure 6.15 is drawn between C_{avg} and λ using k=N-n fusion rule at FC. The performance comparison between perfect and imperfect R-channel, performance comparison

between single and multiple antennas at each CR are provided in the simulations. As p_e value increases from p_e=0 to p_e=0.2, C_{avg} value decreases by 5.7% at M=2, N=3, $\bar{\gamma}$=10dB, and λ=6. C_{avg}value decreases with the cooperation of multiple numbers of SUs using k=N-n fusion rule. As N value increases from N=3 to N=5, C_{avg} value decreases by 1.75% for single antenna case and it decreases by 0.9% for multiple antenna case at λ=8, p_e=0.2, $\bar{\gamma}$=10dB. Finally, if the number of antennas at each CR increases from M=1 to M=2, C_{avg} value increases by 1.77% at N=4, p_e=0.2, λ=8, and $\bar{\gamma}$=10dB.

Figure 6.16 is drawn between N^* and λ using k=1+n fusion rule at FC over Weibull fading channel. The performance is analyzed by using single antenna at each CR. In Fig.6.16, the performance comparison between error free and error rate present in R-channel is provided using MATLAB simulation. N^* value drastically decreases by introducing the error rate in R-channel. As p_e value increases from p_e=0 to p_e=0.01, N^* value decreases from 24 to 12 at λ=12 and k=3. It can be observed from the simulation that as k value increases, N^* value increases due to the cooperation among the CR users. When k value increases from k=1 to k=3, N^* value increases from 7 to 24 with perfect R-channel and it increases from 3 to 12 with imperfect R-channel at λ=12.

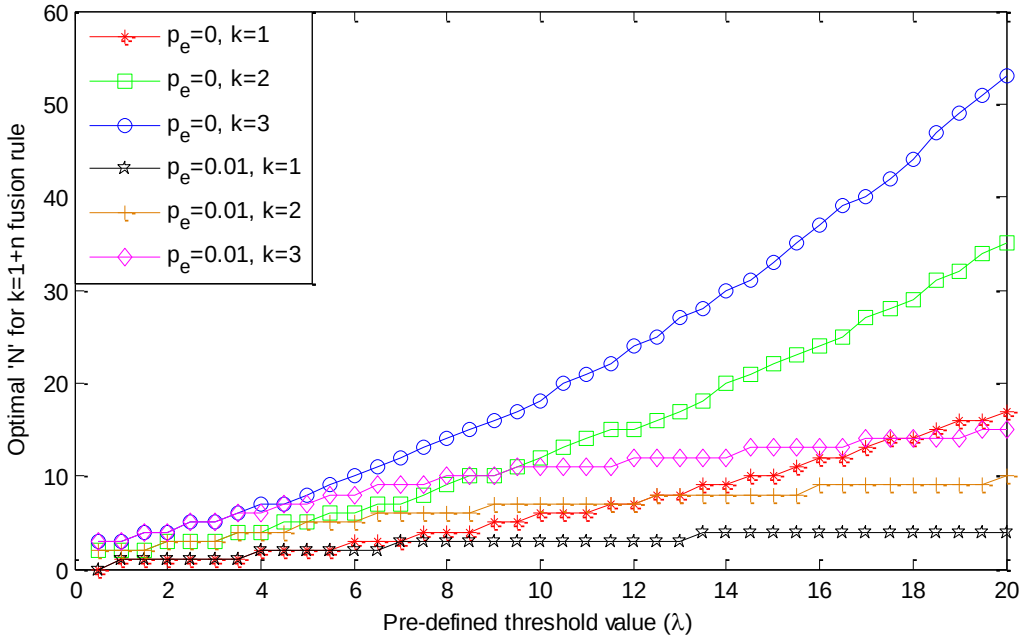

Fig.6.16. N^* versus λ with a single antenna at each CR using k=1+n fusion rule at FC.

Figure 6.17 is drawn between N^* and λ using multiple antennas at each CR and k=1+n fusion rule at FC over Weibull fading channel. Using multiple antennas at each CR, N^* value

decreases compared to a single antenna case because the increased number of antennas improves the diversity order. As M value increases from M=1 to M=2, N^* value drops from 24 to 13 with error free R-channel and it decreases from 12 to 7 with imperfect R-channel at λ=12, p=3, and k=3. As p_e value increases from p_e= 0 to p_e=0.01, N^* value decreases from 13 to 7 at λ=12, k=3, M=2, and p=3.

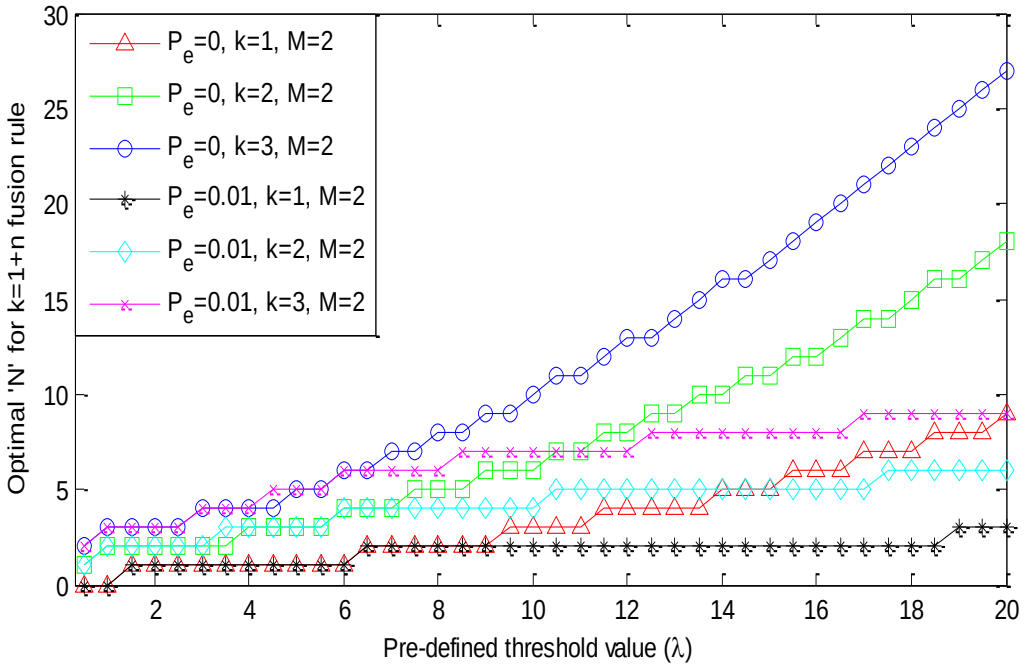

Fig.6.17. N^* versus λ with multiple antennas at each CR using k=1+n fusion rule at FC.

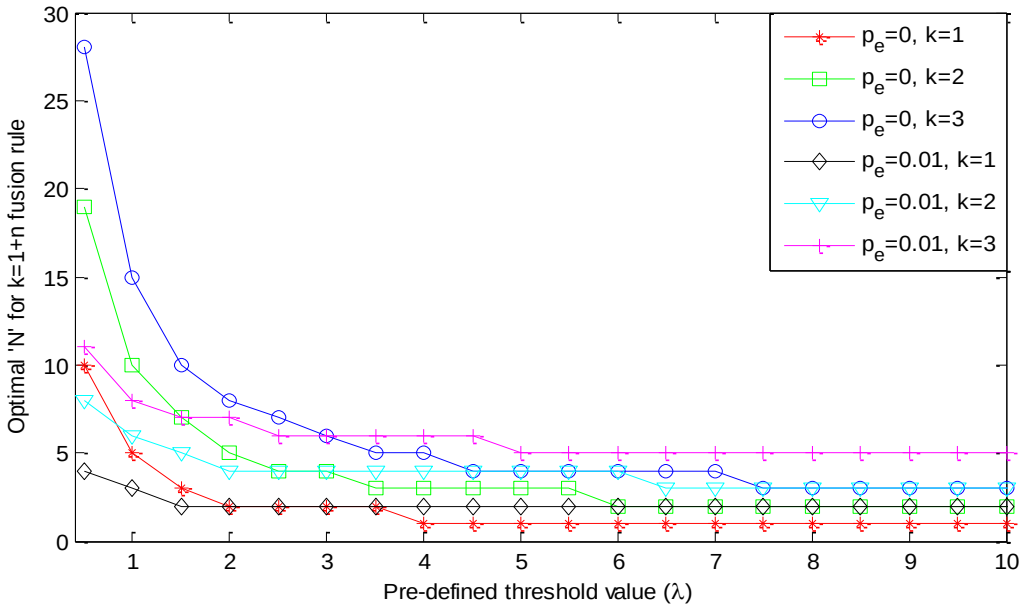

Fig.6.18. N^* versus λ with a single antenna at each CR using k=N-n fusion rule at FC.

Figure 6.18 and Figure 6.19 are the plots drawn between N^* and λ using k=N-n fusion rule at FC, considering single and multiple antennas at each CR respectively over Weibull fading channel. The performance comparison between error free and error rate present in R-channel is provided using MATLAB simulations. It is observed that N^* value is more with error free R-channel and it decreases with the increase in the error rate in R-channel.

It can be observed from the simulation that as k value increases, N^* value increases in both the cases. As k value increases from k=1 to k=3, N^* value increases from 2 to 8 for a single antenna case and it increases from 6 to 18 for multiple antennas case with perfect R-channel at λ=2. Similarly, as the error rate increases from p_e=0 to p_e=0.01, N^* value decreases from 8 to 7 for a single antenna case and it decreases from 18 to 14 for multiple antennas case at λ=2, p=3, and k=3. For k=N-n fusion rule, N^* value decreases with increase in threshold value.

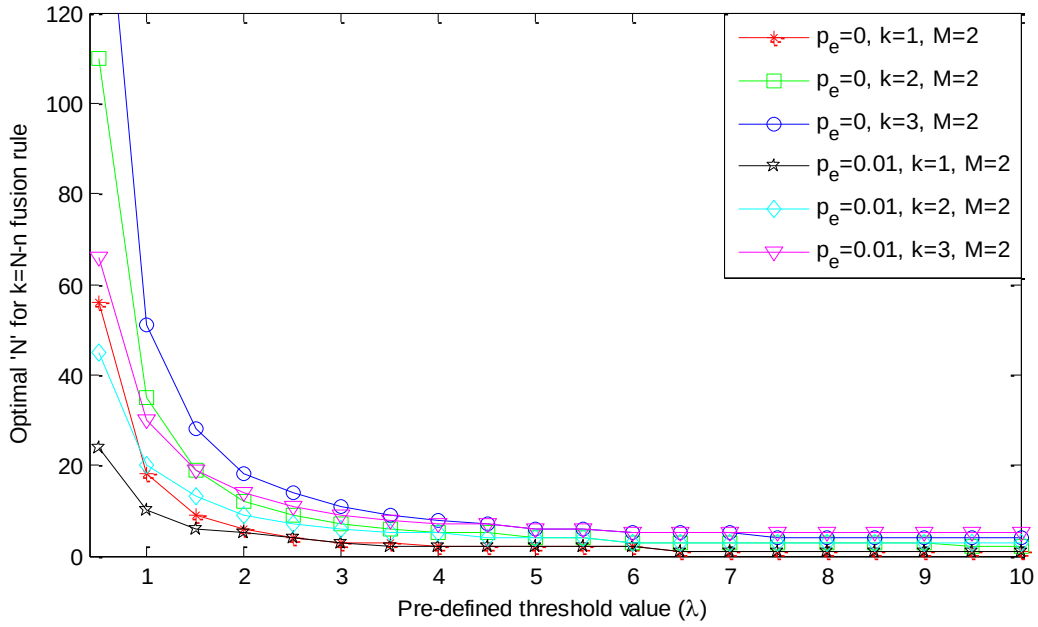

Fig.6.19. N^* versus λ with multiple antennas at each CR using k=N-n fusion rule at FC.

Figure 6.20 is drawn between NUF and λ using k=1+n fusion rule at FC. NUF performance is evaluated using the proposed CSS network over Weibull fading channel with an error rate (p_e) in R-channel. As the error rate increases in the R-channel, NUF value decreases, and its value maximum with error free R-channel. As p_e value increases from p_e=0 to p_e=0.05, NUF value decreases by 16.3% at λ=4, M=2, N=4, p=3, and $\bar{\gamma}$=10dB. As the cooperation among the CR users increases, NUF value also increases using k=1+n fusion rule at FC. When the number of SUs increases from N=3 to N=4, NUF value increases by 75.8% at M=1 and it increases by 16.4% at M=2, p_e=0.05, λ=4, and $\bar{\gamma}$ =10dB. As M value increases from

M=1 to M=2, NUF value increases by 123.7% at N=4, p_e=0.05, λ=4, and $\bar{\gamma}$=10dB. Figure 6.20 is obtained for various values of M (namely M=1 and M=2), N (namely N=3, N=4 and N=5), p_e (namely p_e=0 and p_e=0.05), fixed values of $P(H_1)$=0.3, $P(H_0)$=0.7, μ_1=0.2, μ_2=0.8, μ_3=0.005, and $\bar{\gamma}$=10dB.

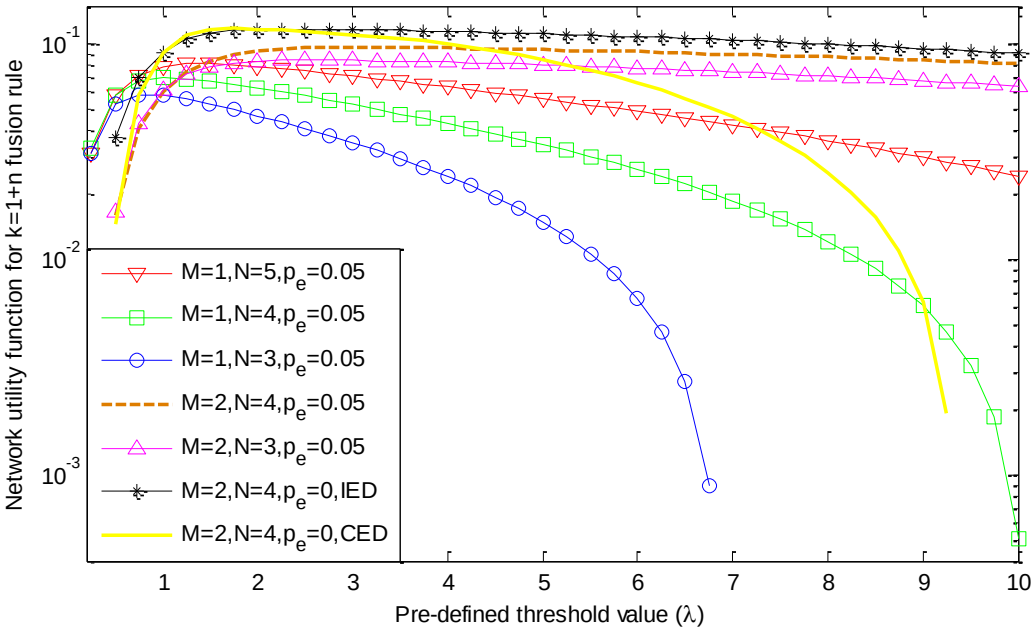

Fig.6.20. NUF versus λ graphs using k=1+n rule at FC.

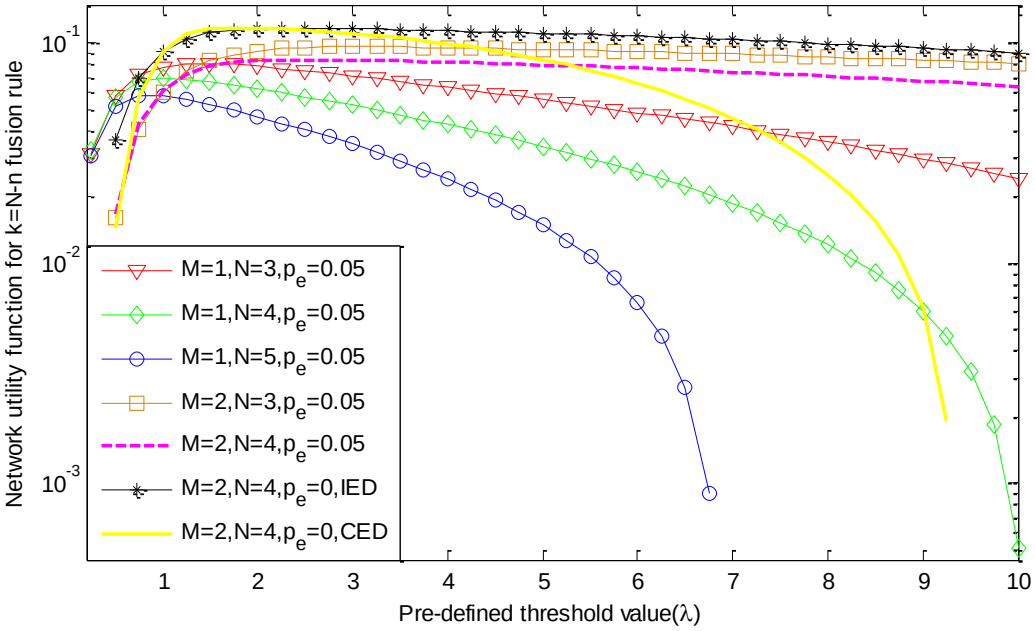

Fig.6.21. NUF versus λ graphs using k=N-n rule at FC.

Figure 6.21 is drawn between NUF and λ using *k*=*N*-*n* fusion rule at FC over Weibull fading channel. The performance comparison between perfect and imperfect R-channel is provided using the simulation. As p_e value increases from p_e=0 to p_e=0.05, NUF value decreases by 28.1% at λ=3, *M*=2, *N*=4, *p*=3, and $\bar{\gamma}$=10dB. When *N* value increases from *N*=3 to *N*=4, NUF value decreases by 32.2% for a single antenna case and it decreases by 14.1% at *M*=2, p_e=0.05, λ=3, and $\bar{\gamma}$=10dB. Similarly, when *M* value decreases from *M*=2 to *M*=1, NUF value decreases by 33.9% at *N*=3, p_e=0.05, λ=4, and $\bar{\gamma}$=10dB. Finally, NUF value also depends upon arbitrary power of received signal (*p*). From the graph it can be observed that NUF value increases with an IED scheme (*p*=3) at each CR compared to the CED scheme (*p*=2) at each CR in the proposed CSS network.

Fusion rule	Variable Parameter	Threshold value	Affected parameter	Increment or Decrement in % in Rayleigh fading	Increment or Decrement in % in Weibull fading
k=1+*n*, p_e=0, *M*=1	*N*=3 to *N*=4	λ=3	C_{avg}	1.4% (increases)	1.6% (increases)
k=1+*n*, p_e=0=0.2, *M*=1	*N*=3 to *N*=4	λ=3	C_{avg}	0.68% (increases)	0.8% (increases)
k=1+*n*, *N*=3, *M*=1	p_e=0 to p_e=0.2	λ=3	C_{avg}	2.10% (decreases)	3.21% (decreases)
k=1+*n*, p_e=0, *N*=3	*M*=1 to *M*=2	λ=3	C_{avg}	3.56% (increases)	4.12% (increases)
k=1+*n*, p_e=0.2, *N*=3	*M*=1 to *M*=2	λ=3	C_{avg}	1.77% (increases)	2.37% (increases)
k=1+*n*, *N*=3, *M*=2	p_e=0 to p_e=0.2	λ=3	C_{avg}	6.57% (decreases)	6.94% (decreases)
k=*N*-*n*, p_e=0, *M*=1	*N*=3 to *N*=4	λ=3	C_{avg}	1.52% (decreases)	1.2% (decreases)
k=*N*-*n*, p_e=0.2, *M*=1	*N*=3 to *N*=4	λ=3	C_{avg}	0.76% (decreases)	0.74% (decreases)
k=*N*-*n*, *N*=3, *M*=1	p_e=0 to p_e=0.2	λ=3	C_{avg}	2.63% (decreases)	2.13% (decreases)
k=*N*-*n*, p_e=0, *N*=3	*M*=1 to *M*=2	λ=3	C_{avg}	4.40% (decreases)	3.62% (decreases)
k=*N*-*n*, p_e=0.2, *N*=3	*M*=1 to *M*=2	λ=3	C_{avg}	1.97% (decreases)	1.74% (decreases)
k=*N*-*n*, *N*=3, *M*=2	p_e=0 to p_e=0.2	λ=3	C_{avg}	7.27% (decreases)	5.07% (decreases)
k=1+*n*, p_e=0, *M*=1	*k*=1 to *k*=3	λ=12	M^*	5 to 16 (increases)	7 to 24 (increases)

$k=1+n$, $p_e=0.01$, $M=1$	$k=1$ to $k=3$	$\lambda=12$	M^*	4 to 13 (increases)	3 to 12 (increases)
$k=1+n$, $k=2$, $M=1$	$p_e=0$ to $p_e=0.01$	$\lambda=12$	M^*	11 to 8 (decreases)	15 to 7 (decreases)
$k=1+n$, $p_e=0$, $k=2$	$M=1$ to $M=2$	$\lambda=12$	M^*	11 to 6 (decreases)	15 to 8 (decreases)
$k=1+n$, $p_e=0.01$, $k=2$	$M=1$ to $M=2$	$\lambda=12$	M^*	8 to 5 (decreases)	7 to 5 (decreases)
$k=1+n$, $k=2$, $M=2$	$p_e=0$ to $p_e=0.01$	$\lambda=12$	M^*	6 to 5 (decreases)	8 to 5 (decreases)
$k=N-n$, $p_e=0$, $M=1$	$k=1$ to $k=3$	$\lambda=1$	M^*	3 to 10 (increases)	5 to 15 (increases)
$k=N-n$, $p_e=0.01$, $M=1$	$k=1$ to $k=3$	$\lambda=1$	M^*	3 to 9 (increases)	3 to 8 (increases)
$k= N-n$, $k=3$, $M=1$	$p_e=0$ to $p_e=0.01$	$\lambda=1$	M^*	10 to 9 (decreases)	10 to 6 (decreases)
$k=N-n$, $p_e=0$, $k=2$	$M=1$ to $M=2$	$\lambda=1$	M^*	6 to 18 (increases)	10 to35 (increases)
$k=N-n$, $p_e=0.01$, $k=2$	$M=1$ to $M=2$	$\lambda=1$	M^*	6 to 15 (increases)	6 to 20 (increases)
$k=N-n$, $k=2$, $M=2$	$p_e=0$ to $p_e=0.01$	$\lambda=1$	M^*	18 to15(decreases)	35 to 20 (decreases)
$k=1+n$, $p_e=0$, $M=1$	$N=3$ to $N=4$	$\lambda=1.5$	NUF	76.2% (increases)	84.1% (increases)
$k=1+n$, $p_e=0.05$, $M=1$	$N=3$ to $N=4$	$\lambda=1.5$	NUF	43.2% (increases)	53.4% (increases)
$k=1+n$, $M=3$, $M=1$	$p_e=0$ to $p_e=0.05$	$\lambda=1.5$	NUF	38.4% (decreases)	43.2% (decreases)
$k=1+n$, $p_e=0$, $N=3$	$M=1$ to $M=2$	$\lambda=1.5$	NUF	55.2% (increases)	61.4% (increases)
$k=1+n$, $p_e=0.05$, $N=3$	$M=1$ to $M=2$	$\lambda=1.5$	NUF	52.6% (increases)	64.7% (increases)
$k=1+n$, $N=3$, $M=2$	$p_e=0$ to $p_e=0.05$	$\lambda=1.5$	NUF	23.7% (decreases)	31.2% (decreases)
$k=N-n$, $p_e=0$, $M=1$	$N=3$ to $N=4$	$\lambda=1.5$	NUF	30.2% (decreases)	17.2% (decreases)
$k=N-n$, $p_e=0.05$, $M=1$	$N=3$ to $N=4$	$\lambda=1.5$	NUF	43.2% (decreases)	14.5% (decreases)
$k=N-n$, $N=3$, $M=1$	$p_e=0$ to $p_e=0.05$	$\lambda=1.5$	NUF	24.3% (decreases)	18.3% (decreases)
$k=N-n$, $p_e=0$, $N=3$	$M=1$ to $M=2$	$\lambda=1.5$	NUF	66.3% (increases)	66.3% (increases)
$k=N-n$, $p_e=0.05$, $N=3$	$M=1$ to $M=2$	$\lambda=1.5$	NUF	68.7% (increases)	11.7% (increases)
$k=N-n$, $N=3$, $M=2$	$p_e=0$ to $p_e=0.05$	$\lambda=1.5$	NUF	23.1% (decreases)	15.1% (decreases)

Table 6.1. C_{avg} and NUF performances for various network parameters of proposed CSS network over Rayleigh fading channel and Weibull fading channel.

Table 6.1 and Table 6.2 shows the simulated values for average channel throughput, an optimal number of CR users, and NUF. All the above-tabulated values are calculated with the help of MATLAB simulation results which are simulated with the strong support of analytical

expressions. All these values are calculated using different fusion rules (k=1+n and k=N-n) at FC over Rayleigh and Weibull fading channels. From the tables, it is clear that average channel throughput and network utility function values are increases by using k=1+n fusion rule at FC and decreases by using k=N-n fusion rule at FC with the increasing of number of SUs (N). Finally, the performance is degraded when the error rate is introduced in reporting channel.

6.8. Conclusions

The average channel throughput (C_{avg}) and network utility network utility function (NUF) performances are evaluated using the proposed CSS network over Rayleigh and Weibull fading channels. The proposed CSS network consist of multiple antennas at each CR, selection combining scheme and an improved energy detector are used at each CR. The final decision about the primary user can be made at FC using different fusion rules such as k=1+n and k=N-n rules. An optimal number CRs are calculated to maximize the average channel throughput value for different fusion rules. The simulation results depend upon various values of system parameters such as average sensing channel SNR ($\bar{\gamma}$), multiple antennas (M) at each CR, detection threshold value (λ), arbitrary power of received signal (p), Weibull fading parameter (V), and number of CR users (N). Finally, we can conclude that C_{avg} and NUF performances are improved by using multiple antennas and an IED detection scheme at each CR.

Chapter-7

Conclusions and Future Scope

7.1. Conclusions

Radio spectrum is a precious resource that available in nature which should be utilized properly to meet the present requirements and to avoid spectrum scarcity. Currently, most of the studies are carried out to identify the effective ways for efficient utilization of radio spectrum. Cognitive radio (CR) network is considered as an important technology for efficient utilization of radio spectrum. The concept of spectrum sensing is used to monitor the radio spectrum continuously and to identify the vacant bands. But, detection performance using spectrum sensing technique is limited due to shadowing, multipath fading effect, and time-varying nature of wireless channels present in the environment. Though the fading effect is present in the network, detection probability can be improved using the cooperative spectrum sensing (CSS) network with the cooperation of multiple CRs.

The main aim of our thesis is to evaluate the detection probability and to improve the spectral efficiency using the cooperative spectrum sensing network over a various fading channels with the help of different techniques. We have provided a rigorous analytical framework for the analysis of conventional energy detector (CED) and an improved energy detector (IED) based cooperative spectrum sensing in cognitive radio networks.

Chapter 3 brings to light the observation that the detection performance is degraded due to multipath fading and shadowing effects present in the nature. Soft data fusion rules called diversity techniques are used to boost up the detection performance. In this chapter, detection performance is evaluated and improved by using diversity techniques in CSS network. Various diversity techniques (SC, SLS, SLC, MRC, and EGC) are used in CSS network to improve the detection probability of PU over different fading channels (Rayleigh, Rician, Nakagami-*m*,

Weibull, and Hoyt fading). The performance is analyzed using the conventional energy detection technique and single antenna at each CR in CSS network over various fading channels. The performance comparison among various diversity techniques over different fading channels is provided using MATLAB simulations. All the MATLAB simulations are drawn with the support of analytical expressions. Finally, the performance is described using the simulations which are drawn between average sensing channel SNR versus detection probability curves and complementary receiver operating characteristic (CROC) curves.

In chapter 4, censoring schemes are used to eliminate the heavily faded radio links of reporting channel in CSS network when it is affected by various fading environments. The detection probability is improved and system complexity is reduced using the censoring schemes in CSS networks. Rank based and Threshold based censoring schemes are used individually in reporting channel of CSS network when it is influenced by various fading environments. The final decision about the primary user is taken at fusion center using majority logic and MRC Rule respectively. The performance comparison between perfect and imperfect channel estimations are provided using simulation results.

Though the conventional energy detection technique and a single antenna at each CR in CSS network are used to improve the detection probability of PU but, its performance is limited. So, we have proposed the CSS network which is equipped with multiple antennas at each CR, selection combining scheme is used to select the maximum value of antenna, and an improved energy detector (IED) scheme is employed as a detection technique. With our proposed CSS network, detection performance is vastly improved. In chapter 5, we have optimized the performance of proposed CSS network by optimizing its network parameters over various fading channels. We have derived the closed form of expressions for missed detection probability in various fading channels. The optimized expressions for number of CR users (N_{opt}), arbitrary power of received signal (p_{opt}), and threshold value (λ_{opt}) over various fading channels are also derived. The performance is analyzed using CROC curves and total error rate curves which are drawn with the strong support of analytical expressions.

In chapter 6, an average channel throughput and network utility function (NUF) performances is evaluated over Rayleigh and Weibull fading channels. The performance is analyzed using the proposed CSS network which is equipped with multiple antennas at each CR and an IED scheme is employed as a detection technique. The final decision about the primary user is taken at FC using different fusion rules such as k=1+n and k=N-n. The channel

throughput and NUF performances are evaluated using single and multiple antennas at each CR and the performance comparison between them also provided with the help of simulations. The optimal number of CR users are calculated to maximize the average channel throughput using $k=1+n$ and $k=N-n$ fusion rules in Rayleigh and Weibull fading environments.

The proposed CSS network, system models of CED and IED schemes, and the performance metrics introduced by this thesis are because of low complexity and wide suitability for various fading conditions. All our simulations results are perfectly in accordance with analytical results. Our proposed networks, detection models, methodologies, and results are helpful to improve the detection probability of PU, to achieve optimal performance, and to improve the spectral efficiency.

7.2. Future Scope

In this thesis, we have used several techniques to improve the detection probability and to improve the spectral efficiency using CSS network. However, there are still some open problems that warrant further consideration in future work. For example, though using the CED scheme, we are able to identify the vacant bands present in the spectrum. The performance can be further improved by using other detection techniques such as Matched filter detection technique, Cyclostationary detection technique, and Eigenvalue detection technique can be utilized to improve the detection probability at lower values of sensing channel SNRs. However, in practice, detection performance is degraded even if cooperative spectrum sensing schemes are adopted because of fading and shadowing effects. In our research work, we have used single stage spectrum sensing technique and the detection performance can be further improve by implementing two-stage spectrum sensing scheme in the cognitive radio networks. In two-stage spectrum sensing scheme, two different detection schemes are used at two different levels so that the detection performance can be improved.

Instead of using hard decision rules and soft data fusion rules individually at FC, if hybrid methods (combining both hard and soft data schemes) are used at FC it will further improve the detection performance of PU. This hybrid technique can be applied to all the objectives mentioned in this thesis. In this thesis, we have examined the performance of cooperative spectrum sensing network for limited fading channels only. It will be interesting to study the performance using other fading channels also such as kappa-mu, eta-mu, and kappa-mu extreme fading channels.

Finally, energy detection based spectrum sensing and cooperative spectrum sensing networks can be implemented in real-time scenario.

References

[1] Federal Communications Commission. Spectrum policy task force. ET Docket 02-135, November 2002. [Online]. Available: https://www.fcc.gov/document/spectrum-policy-task-force.

[2] I. F. Akyildiz, W.-Y. Lee, M. C. Vuran and Mohanty, "Next generation/dynamic spectrum access/cognitive radio wireless networks: A survey," *Elsevier Comput. Networks*, vol. 50, no.13, pp. 2127–2159, May 2006.

[3] S. Haykin, "Cognitive radio: brain-empowered wireless communications," *IEEE J. Selected Areas Commun.*, vol. 23, no. 2, pp. 201–220, Feb. 2005.

[4] Q. Zha and B. M. Sadler, "A survey of dynamic spectrum access," *IEEE Signal Processing Mag.*, vol. 24, no. 3, pp. 79–89, May 2007.

[5] J. Mitola, III, "Cognitive radio for flexible mobile multimedia communications," in *Proc. IEEE Int. Workshop Mobile Multimedia Communications*, pp. 3–10, Nov. 1999.

[6] R. W. Brodersen, A. Wolisz, D. Cabric, S. M. Mishra and D. Willkomm, "Corvus: A cognitive radio approach for usage of virtual unlicensed spectrum," White Paper, 2004.

[7] D. Cabric, S. M.Mishra and R. W. Brodersen, "Implementation issues in spectrum sensing for cognitive radios," *in Proc. of Asilomar Conference on Signals, Systems and Computers*, pp.772-776, November 2004.

[8] J. Ma, G. Y. Li and B. H. Juang, "Signal processing in cognitive radio," in *Proc. of IEEE*, Vol.97, no. 5, pp. 805–823, May 2009.

[9] Yucek and Arslan, "Survey of spectrum sensing algorithms for cognitive radio applications," *IEEE Commun. Surveys Tutorials*, vol.11, no. 1, pp. 116–130, Quarter 2009.

[10] F.F. Digham, S. Alouini, and M.K. Simon, "On the energy detection of unknown signals over fading channels," *Proceedings of IEEE International Conference on Communications (ICC)*, Alaska, USA, pp.3575-3579, 2003.

[11] F. F. Digham, M.-S. Alouini and M. K. Simon, "On the energy detection of unknown signal over fading channels," *Communication, IEEE Transactions on*, vol.55, no.1, pp.21–24, 2007.

[12] S.Herath, N. Rajatheva, and Tellambura, "Energy detection of unknown signals in fading and diversity reception," *IEEE Trans. Comm.,* vol. 59, no. 9, pp. 2443-2453, 2011.

[13] G. Ganesan and Y. Li, "Cooperative spectrum sensing in cognitive radio, part I: Two user networks," *IEEE Trans. Wireless Commun.,* vol. 6, no. 6, pp. 2204–2213, June 2007.

[14] G. Ganesan and Y. Li, "Cooperative spectrum sensing for cognitive radio networks," *In Proc. of IEEE Symp. New Frontiers in Dynamic Spectrum Access Networks (DySPAN),* Baltimore, USA, pp.137-143, 2005.

[15] G. Ghasemi and E.S. Sousa, "Collaborative spectrum sensing for opportunistic access in Fading environments," *In Proc. of First IEEE International Symposium on New Frontier in Dynamic Spectrum Access Network* Baltimore, USA, pp.131-136, November 2005.

[16] K. B. Letaief and W. Zhang, "Cooperative communications for cognitive radio networks," In *Proc. of IEEE,* vol. 97, no. 5, pp. 878–893, May 2009.

[17] M. Lopez and F. Casadeval, "Improved energy detection spectrum sensing for cognitive radio," *IET Commun.,* vol. 6, issue. 8, pp.785-796.

[18] Y. Chen, "Improved energy detector for random signals in Gaussian noise," *in IEEE Transaction Wireless. Comm.,* vol. 9, no. 2, pp. 558-563, 2005.

[19] O. Olabiyi and A. Annamalai, "Further results on energy detection of random signals in Gaussian noise," *in Proceedings of ICCVE,* pp. 14-19, 2013.

[20] W. Han, J. Li, Z. Li, J. Si and Y. Zhang, "Efficient soft decision fusion rule in Cooperative spectrum sensing," *IEEE Transactions on Signal Processing,* Vol. 61, no. 18, pp.1931-1943.

[21] Y. Zhao, G. Kang, J. Wang, X. Lin and Y. Liu, "A soft fusion scheme for cooperative spectrum sensing based on the log-likelihood ratio," *In Proc. of IEEE 24th International symposium on Personal Indoor and Mobile Radio Communications (PIMRC).*

[22] S. Nallagonda, B. kumar, S. D. Roy and S. Kundu, "Performance of cooperative spectrum with soft data fusion schemes in fading channels," *In Proceedings of the India Conference,* IIT Kanpur, pp.1-5, 2013.

[23] C. Kundu, S. Kundu, G. Ferrari and R. Raheli, "Distributed detection with censoring of sensor in Rayleigh faded channel," *In Proc. of Third international conference on comm. systems and networks (COMSNETS),* Bangalore, India, 2013.

[24] S. Nallagonda, S.D.Roy, S. Kundu, G. Ferrari and Raheli, "Cooperative spectrum sensing with censoring of cognitive radios in fading channel under majority logic fusion," In F. Bader and M. G.Di Benedetto (Eds.), Cognitive communications and cooperative Het Net coexistence, Springer International Publishing, pp. 133-161.

[25] S. Nallagonda, S.D. Roy and S. Kundu, "Performance evaluation of cooperative spectrum sensing with censoring of cognitive radios in Rayleigh fading channel," *Wireless personal Communications*, vol. 70, no.4, pp. 1409–1424, 2013.

[26] W. Zhang, R. Mallik and K. Letief, "Optimization of cooperative spectrum sensing with energy detection in cognitive radio networks," *in IEEE Transactions on wireless comms.*, vol. 8, no.12, pp. 5761-5766, 2011.

[27] A. Singh, M. R. Bhatnagar and R Mallik, "Optimization of cooperative spectrum sensing with an improved energy detector over imperfect reporting channel," *in Proceedings of IEEE* Vehicular Technology Conference (VTC Fall), 2011.

[28] Singh, M. R. Bhatnagar and R.K. Mallik, "Cooperative spectrum sensing in multiple antenna based cognitive radio network using an improved energy detector," *in IEEE Communication Letters*, vol. 16, no.1, pp. 64-67, 2012.

[29] S. Q. Liu and B. J. Hu, "Cooperative spectrum sensing based on improved energy detector for cognitive radios," *in Proceedings of IEEE International conference ICSPCC,* Guilin, pp. 1-4, 2014.

[30] Y.C.Liang, Y. Zeng, E. Peh and A. Hoang, "Sensing-throughput tradeoff for cognitive radio networks", *In Wireless Comms, IEEE Transactions on*, vol. 7, no. 4, pp.1326-1337, 2008.

[31] Suwen Wu, Z. Ming and Jinkang Zhu, "Optimal number of secondary users through maximizing utility in cooperative spectrum sensing," *In IEEE Vehicular Technology conference (VTC Fall)*, pp.634-639, 2009.

[32] "United States frequency allocations: The radio spectrum," Oct. 2003. [Online]. Available: http://www.ntia.doc.gov/osmhome/allochrt.pdf.

[33] J. Wang, M. Ghosh, and K. Challapali, "Emerging cognitive radio applications: A survey," *IEEE Commun. Mag.*, vol. 49, no. 3, pp. 74–81, Mar. 2011.

[34] P. Pawelczak, K. Nolan, L. Doyle, S. W. Oh, and D. Cabric, "Cognitive radio: Ten years of experimentation and development," *IEEE Commun. Mag.*, vol. 49, no.3, pp. 90–100, 2011.

[35] J. Mitola and G. Maguire, “Cognitive radio: Making software radios more personal,” in *IEEE Personal Communications*, Vol. 6, No. 4, pp.13–18, 1999.

[36] B. Wang and K. J. R. Liu, “Advances in cognitive radio networks: A survey,” *IEEE J. Sel. Topics Signal Process.*, vol. 5, no. 1, pp. 5–23, Feb. 2011.

[37] Y. Zeng, Y.-C. Liang, A. T. Hoang, and R. Zhang, “A review on spectrum sensing in cognitive radio: challenges and solutions,” *EURASIP J. Advances in Signal Process.*, 2010.

[38] Y. C. Liang, K. Chen, and P. Mahonen, “Cognitive radio networking and communications: An overview,” *IEEE Trans. Veh. Technol.*, vol. 60, no. 7, pp. 3386–3407, Sep. 2011.

[39] I.F. Akyildiz, B.F. Lo, and R. Balakrishnan, “Cooperative spectrum sensing in cognitive radio networks: a survey,” *Physical Communication (Elsevier) Journal*, vol. 4, no.1, pp. 40-62, 2011.

[40] J. Proakis and D. Manolakis, *Digital Signal Processsing*. Prentice Hall, 1996.

[41] Liangping, Yingxue Li and Demir.A, “Matched filtering assisted energy detection for sensing weak primary user signals”, *IEEE International Conference on Acoustics, speech and signal Processing (ICASSP)*, pp. 3149 – 3152, 2012.

[42] W. Gardner, “Signal interception: a unifying theoretical framework for feature detection,” *in IEEE Transactions on Communications*, vol. 36, no.8, pp. 897–906, 1988.

[43] A. Fehske, J. Gaeddert and J. Reed, “A new approach to signal classification using spectral correlation and neural networks,” *In Proc. of IEEE DySPAN*, pp. 144–150, 2005.

[44] A. Goldsmith, *Wireless communications*. Cambridge university press, 2005.

[45] FCC, ET Docket No 03-237 Notice of inquiry and notice of proposed Rulemaking, Nov.2003.

[46] P. J. Kolodzy, “Interference temperature: a metric for dynamic spectrum utilization,” *In Proc. of International Journal of Network Management*, vol. 16, no. 2, pp. 103–113, 2006.

[47] C. Cordeiro, K. Challapali, D. Birru, and S. S. N., “IEEE 802.22: An introduction to the first wireless standard based on cognitive radios,” *Journal of Commun. (JCM)*, vol.1, no.1, pp. 38-47, Apr. 2006.

[48] S. J. Shellhamer, “Spectrum sensing in IEEE 802.22,” *in Proc. of first IAPR workshop on Cognitive Information Processing*, June 2008.

[49] C. Stevenson, G. Chouinard, Z. Lei, W. Hu, S. Shellhammer and W. Caldwell, “IEEE 802.22: The first cognitive radio wireless regional area network standard,” *IEEE comm., Mag.*, vol. 47, no. 1, pp. 130–138, Jan. 2009.

[50] M. Naraghi-Pour and T. Ikuma, “Autocorrelation-based spectrum sensing for cognitive radios,” *Vehicular Technology, IEEE Transactions on*, vol. 59, no. 2, pp. 718–733, 2010.

[51] Y. Zeng, Y. Liang, A. Hoang and R. Zhang, “A review on spectrum sensing for cognitive radio: Challenges and solutions,” *EURASIP J. Appl. Signal Process. (USA)*, 2010.

[52] B. Razavi, “Cognitive radio design challenges and techniques,” *IEEE Journal Solid-State Circuits*, vol. 45, no. 8, pp. 1542–1553, Aug. 2010.

[53] R. Prasad, P. Pawelczak, J. Hoffmeyer and H. Berger, “Cognitive functionality in next generation wireless networks: standardization efforts,” *IEEE Commun. Mag.*, vol. 46, no. 4, pp. 72-78, Apr. 2008.

[54] H. Urkowitz, “Energy detection of unknown deterministic signals,” *Proc. IEEE*, vol. 55, no.4, pp. 523-531, 1967.

[55] R. Fan and Jiang, “Optimal multi-channel cooperative sensing in cognitive radio networks,” *IEEE Trans. Wireless Commun.*, vol. 9, no. 3, pp. 1128–1138, Mar. 2010.

[56] I.E.Atawi, “Spectrum-sensing in cognitive radio networks over composite multipath shadowed fading channels”, *in Proc. of Computers and Electrical Engineering*, vol. 52, pp.337-348, January 2016.

[57] A. Ghasemi and E. S. Sousa, “Spectrum sensing in cognitive radio networks: Requirements, challenges and design trade-offs,” *IEEE Commun. Mag.*, vol. 46, no. 4, pp. 32–39, Apr. 2008.

[58] S. M. Mishra, A. Sahai and R. W. Brodersen, “Cooperative sensing among cognitive radios,” in *Proc. IEEE Int. Conf. Commun. (ICC)*, pp.1658–1663, June 2006.

[59] Y. Zeng, Y.-C. Liang, A. T. Hoang, and E. C. Y. Peh, “Reliability of spectrum sensing under noise and interference uncertainty,” in *Proc. IEEE Int. Conf. Commun. (ICC)*, pp.1–5, June 2009.

[60] G. Ganesan and Y. G. Li, "Cooperative spectrum sensing in cognitive radio networks," in *Proc. of 1st IEEE Int. Symp. New Frontiers Dynamic Spectrum. Access Netw. (DySPAN)*, November 2005, pp. 137–143.

[61] G. Ganesan and Y.G. Li, "Agility improvement through cooperative diversity in cognitive radio," in *Proc. of IEEE Global Telecommun. Conf. (GLOBECOM)*, pp. 2505–2509, Dec. 2005.

[62] P. Sadhukhan, N. Kumar and M.R. Bhatnagar, "Improved energy detector based spectrum sensing for cognitive radio: an experimental study," *in Proc. of IEEE India conference on (INDICON)*, Mumbai, India, pp. 1-5, 2013.

[63] T. Rappaport, *Wireless communications: principles and practice*. Publishing house of elects. Industry, 2004.

[64] M. K. Simon and M.-S. Alouini, *Digital communication over fading channels*. John Wiley and Sons, NJ, US, 2nd edition, Dec. 2004.

[65] V. Erceg, L. J. Greenstein, S. Y. Tjandra and et.al., "An empirically based path loss model for wireless channels in suburban environments," *In Selected Areas in Communications, IEEE Journal on*, vol. 17, no. 7, pp. 1205–1211, 1999.

[66] S. Nallagonda, A. Chandra, S.D. Roy, S. Kundu, P. Kukolev and A. Prokes, "Detection performance of cooperative spectrum sensing with hard decision fusion in fading channels," *International Journal of Electronics (Taylor and Francis)*, vol. 103, no. 2, pp.297–321, February 2016.

[67] A.Chandra, C.Bose and M.Kr. Bose, "Performance of Non-coherent MFSK with selection and switched diversity over Hoyt fading channel," *Wireless personal communication*, vol. 68, no. 2, pp. 379-399, Jan. 2013.

[68] Spyros Kyperountas, Neiyer Correal, Qicai Shi and Zhuan Ye, "Performance analysis of cooperative spectrum sensing in Suzuki fading channels," *in Proc. of IEEE International Conference on Cognitive Radio Oriented Wireless Networks and Communications (CrownCom'07),* pp. 428-432, June 2008.

[69] S. Nallagonda, S. D. Roy and S. Kundu, "Performance of cooperative spectrum sensing in fading channels," *Proceedings of the 1st International conference on Recent Advances in Information Technology RAIT-2012*, Dhanbad, India, March 2012.

[70] J. Duan and Y. Li, "Performance analysis of cooperative spectrum sensing in different fading channels," in *Proceedings of the 2nd International Conference on Computer Engineering and Technology (ICCET '10)*, Chengdu, China, pp. 364–368, June 2010.

[71] D. Cabric, "Addressing feasibility of cognitive radios," *IEEE Signal Process. Mag.*, vol. 25, no. 6, pp. 85–93, Nov. 2008.

[72] C. Tellambura, H. Jiang and S. Atapattu. *Energy detection for spectrum sensing in cognitive radio*, Springer, February 2014.

[73] G. L. Stuber, *Principles of Mobile Communications*. Norwell, MA: Kluwer Academic Publishers, 1996.

[74] Hikmat Y. Darawsheh and Ali Jamoos, "Performance analysis of energy detector over α-μ fading Channels with Selection Combining", *In Wireless Personal Communication*, Vol. 77, no. 2, pp.1507-1517, July 2014.

[75] Niu, R., Chen, B. and Varshney, P.K, "Decision fusion rules in wireless sensor networks using fading statistics," *In Proceedings of the 37th Annual Conference on Information Sciences and Systems (CISS'03)*, 2003.

[76] J. Ma, G. Zhao and Y. Li, "Soft combination and detection for cooperative spectrum sensing in cognitive radio networks," *IEEE Trans. Wireless Communication*, vol. 7, no.11, pp. 4502–4507, 2008.

[77] S. Chaudhari, J. Lunden and V. Koivunen, "Cooperative sensing with imperfect reporting Channels Hard Decisions or Soft Decisions," *IEEE Transactions on Signal Processing*, 2012.

[78] S. Chaudhari and V. Koivunen, "Impact of reporting-channel coding on the performance of distributed sequential sensing," In *Proceedings of IEEE 14th Workshop on Signal Processing Advances in Wireless Communications (SPAWC)*, 2013.

[79] S. Chaudhari, J. Lunden and V.Koivunen, "Effects of quantization and channel errors on sequential detection in cognitive radios," *In 46th Annual Conference on Information and Systems (CISS)*, 2012.

[80] W. Han, J. Li, Z. Li, J. Si and Y. Zhang, "Efficient soft decision fusion rule in cooperative spectrum sensing," *IEEE Transactions on Signal Processing*, vol. *61*, no.8, pp.1931-1943.

[81] C. Altay, H. B. Yilmaz and T. Tugcu, "Cooperative sensing analysis under imperfect reporting Channel," In *Proceedings of IEEE Symposium on Computers and Comm.*, 2012.

[82] A. Ghasemi and E.S. Sousa, "Opportunistic spectrum access in fading channels through collaborative sensing," *IEEE Journal in selected. Areas of communication*, vol. 2, no. 2, pp. 71–82, 2007.

[83] Y. Zou, Y. Yao and B. Zheng, "A selective-relay based cooperative spectrum sensing scheme without dedicated reporting channels in cognitive radio networks," *In IEEE Transactions on Wireless Communications*, vol. *10*, no.4, pp.1188–1198.

[84] G. Ferrari and R. Pagliari, "Decentralized binary detection with noisy communication links," *Transactions on Aerospace Electronic Systems*, vol. 42, no. 4, pp. 1554–1563, 2012.

[85] S. Nallagonda, S.D. Roy, S. Kundu, G. Ferrari and R. Raheli, "Cooperative spectrum sensing with censoring of cognitive radios in Rayleigh fading under majority logic fusion," *in Proceedings of the National Conference on Communications*, IIT Delhi, pp. 1-5, 2012.

[86] C. Sun, W. Zhang and K.B. Letaief, "Cooperative spectrum sensing for cognitive radios under bandwidth constraints," In *IEEE Wireless Communication and Networking Conf*erence *(WCNC 2007)*, pp. 1–5, 2007.

[87] Ferrari and Pagliari, "Decentralized detection in sensor networks with noisy communication links," *in Proc. Tyrrhenian Int. Workshop on Digital Commun. (TIWDC'05)*, Sorrento, Italy, June 2005.

[88] B. Chen, R. Jiang, T. Kasetkasem and P. Varshney, "Channel aware decision fusion in wireless sensor networks," *IEEE Transactions on Signal Processing*, vol. *52*, pp. 3454–3458, 2011.

[89] C. Rago, P. Willett and Y. Bar-Shalom, "Censoring sensors: A low-communication rate scheme for distributed detection," *in IEEE Transactions on Aerospace and Electronic System*, vol.17, pp. 554–567, 1996.

[90] Appadwedula, V.V. Veeravalli and D.L. Jones, "Energy-efficient detection in sensor networks," *IEEE Journal on Selected Areas in Communications*, vol. 23, no. 4, pp. 693–702, 2005.

[91] H.R. Ahmadi and A. Vosoughi, "Channel aware sensor selection in distributed detection Systems," *In IEEE 10th workshop on volume signal Processing advances in wireless Comm., SPAWC.2009*, pp. 71–75, 2009.

[92] H. Ahmadi and A. Vosoughi, "Impact of channel estimation error on decentralized detection in bandwidth constrained wireless sensor networks," *In Proceedings on IEEE MILCOM 2008*, pp. 1–7, 2008.

[93] C. Kundu, S. Kundu, G. Ferrari, and R. Raheli "Distributed detection using MRC with censored sensors and Rayleigh faded communications," *In IEEE international symposium on information theory (ISIT2011)*, Russia: Saint-Petersburg, pp. 2163–2167, 2011.

[94] S. Nallagonda, S.D. Roy, S. Kundu, G. Ferrari and R. Raheli, "Performance of MRC fusion based cooperative spectrum sensing with censoring of cognitive radios in Rayleigh fading channel," *In Proc.WCMC Conference*, Sardinia, Italy: Academic Press, pp. 30-35, 2013.

[95] J. Lunden, V. Koivunen, A. Huttunen and H.V. Poor, "Censoring for collaborative spectrum sensing in cognitive radios," *In Proceedings of the 41st Asilomar Conference on Signals, Systems, and Computers, Pacific Grove*, USA: CA, pp. 772–776, 2007.

[96] Z. Quan, S. Cui and A. H. Sayed, "Optimal linear cooperation for spectrum sensing in cognitive radio networks," *IEEE J. Sel. Topics Signal Process.*, vol. 2, no. 1, pp. 28-40, Feb. 2008.

[97] E. Peh, Y.C. Liang, Y. L. Guan and Y. Zeng, "Optimization of cooperative sensing in cognitive radio networks," in *Proc. IEEE Int. Wireless Commun. Networking Conf.*, Hong Kong, Mar. 2007, pp. 27-32.

[98] W. Zhang, R. K. Mallik and K. B. Leraief, "Cooperative spectrum sensing optimization in cognitive radio networks," *in Proc. of IEEE ICC*, pp. 3411–3415, May 2008.

[99] Y. Chen, "Improved energy detector for random signals in Gaussian noise," *in IEEE Transactions on Wireless. Commun.*, vol. 9, no. 2, pp. 558–563, Feb. 2010.

[100] A. Singh, M. R. Bhatnagar and R. K. Mallik, "Cooperative spectrum sensing with an improved energy detector in cognitive radio network," in *Proc. of National Conference Communication,* 2011.

[101] S. Stotas and A. Nallanathan, "On the throughput and spectrum sensing enhancement of the opportunistic spectrum access cognitive radio network," *Wireless Communications, IEEE Transactions on*, vol. 11, no.1, pp. 97–107, 2012.

[102] N. R. Bhanavathu and M. Z. A. Khan, "On throughput maximization of cognitive radio using cooperative spectrum sensing over erroneous control channel," *IEEE conference on communication NCC*, pp.1-6, 2016.

[103] S. Maleki, and S. Chepuri, "Optimal hard fusion strategies for cognitive radio networks," *in Wireless Communications and Networking Conference (WCNC-11), IEEE*, pp. 1926–1931, March 2011.

[104] M. Mashreghi and B. Abolhassani, "Optimum number of secondary users and optimum fusion rule in cooperative spectrum sensing to maximize channel throughput," *in Proc. Telecommun., (IST), 5th IEEE International Symposium on*, pp. 1–6, Dec 2010.

[105] N. R. Banavathu and M. Z. A. Khan, "Optimal n-out-of- k voting rule for cooperative spectrum sensing with energy detector over erroneous control channel," *in Proc. IEEE 81st Vehicular Technology Conference (VTC Spring)*, pp. 1–5, May 2015.

[106] Z. Quan, S. Cui and A. Sayed, "Optimal linear cooperation for spectrum sensing in cognitive radio networks," *in Proc. IEEE Jrnl of Selected Topics in Signal processing, Processing*, vol. 2, no.1, pp. 28-40, 2008.

[107] A.H. Nuttall, "Some integrals involving the QM function," *in IEEE Transactions on information theory*, vol. 21, no. 1, pp. 95–96, 1975.

[108] I.S. Gradshteyn and I.M. Ryzhik. *Table of integrals, series, and products.* 5th edition London: Academic Press, 1994.

[109] Y. Liu, D. Yuan, M. Jiang, W. Fan, G. Jin and F. Li, "Analysis of square law combining scheme for cognitive radios over Nakagami channels," in *Proc. of IEEE GLOBECOM*, pp. 1-5, 2009.

[110] S. Nallagonda, V. C. Sekhar, A. Chandra, S.D.Roy and S. Kundu, "Detection performance of soft data fusion in Rician fading channel for cognitive radio network," In *Proceedings of 18th International Symposium on WPMC*, Hyderabad, India, pp. 1–5, December 2015.

[111] H. Sun, A. Nallanathan, J. Jiang and C. Wang, "Cooperative spectrum sensing with diversity reception in cognitive radios," *6th International ICST Conference on comm., and Networking in China (CHINACOM)*, Harbin, China, p. 216–220, August 2011.

[112] S. Nallagonda, A. Chandra, S.D. Roy and S. Kundu, "Analytical performance of soft data fusion-aided spectrum sensing in hybrid terrestrial-satellite networks," *Int. Journal Satellite Commun. Network.*, vol.35, pp. 461–480, November 2016.

[113] Y. L. Foo, "Performance of cooperative spectrum sensing under Rician and Nakagami fading," *Wireless Personal Communications*, vol. 70, pp. 1541-1551, 2013.

[114] Warit Prawatmuang, *Cooperative spectrum sensing for cognitive radio.* PhD Thesis, The University of Manchester, September 2013.

[115] I.S. Gradshteyn and I.M. Ryzhik. *Table of Integrals, Series and Products*, 7th edition, Academic Press/ Elsevier: San Diego, CA, USA, March 2007.

[116] N.C. Sagias, G. Karagianidis and G. Tombras, "Error-rate analysis of switched diversity receivers in Weibull fading," *in IET Electron. Letters*, vol. 20, pp. 1472 – 1474, Dec 2004.

[117] P.C. Sofotasios, M.K. Fikadu, K. Ho-Van and M. Valkama, "Energy detection sensing of unknown signals over Weibull fading conditions," *in Proceedings of International Conference on Advanced Technologies for Communications (ATC)*, pp. 414-419, 2013.

[118] D. Teguig, B.Scheers and V.Le Nir, "Data fusion schemes for cooperative spectrum sensing in cognitive radio networks," *In Commun. and Info. Systems Conf., Military (MCC)*, pp. 1–7, October 2012.

[119] H. Hu, H.Zhang, H.Yu and Y.Chen "Energy efficient design of channel sensing in cognitive radio networks," *in Computers and Electrical Engineering*, vol.42, pp.207-220, February 2015.

List of Publications

International Journals

1. M.Ranjeeth and S.Anuradha, "The Effect of Weibull Fading Channel on Cooperative Spectrum Sensing Network Using an Improved Energy Detector," ***Telecommunications Systems,*** **Springer**, pp.1-28, Oct-2017. **(SCI)**

2. M.Ranjeeth and S.Anuradha, "Throughput Analysis in Proposed Cooperative Spectrum Sensing Network with an Improved Energy Detector scheme over Rayleigh Fading Channel," ***Int. Journal of Electronics and Communications,*** **AEU Journal**, **Elsevier**, vol.83, pp.416-426, Jan-2018. **(SCI)**

3. M.Ranjeeth, S.Anuradha, and N.Srinivas, "Performance Analysis of Cooperative Spectrum Sensing Network Using Optimization Technique in Different fading channels," ***Wireless Personal Communications,*** **Springer**, Vol. 97, no.2, pp. 2887–2909, Nov-2017. **(SCI)**

4. M.Ranjeeth and S.Anuradha, "Threshold based censoring of Cognitive Radios in Rician Fading Channel," ***Wireless Personal Communications***, **Springer**, Vol.93, no.2. pp. 409-430, June-2016. **(SCI)**

5. M.Ranjeeth and S.Anuradha, "Optimization Analysis of Improved Energy Detection Based Cooperative Spectrum Sensing in Nakagami-*m* and Weibull Fading Channels," ***Journal of engineering science and technology review***, Vol.10, no. 2, pp.114-121, June-2017. **(Scopus)**

6. M.Ranjeeth and S.Anuradha, "Maximization of Network Utility Function in Cooperative Spectrum Sensing using Energy Detection Scheme," ***Indian Journal of Science and Technology***, Vol. 9 (SI), pp.1-4, Dec-2016. **(Scopus)**

7. M.Ranjeeth and S.Anuradha, "Performance of Nakagami-*m* Fading Channel over Energy Detection Based Spectrum Sensing," *In proc.* of ***World Academy of Science, Engineering Technology (WASET), International Journal of Electrical, computers, Electronics and Communication Engineering***, Vol. 8, no.10, 2014, pp.1598-1602. **(Scopus)**

International Conferences

1. M.Ranjeeth and S.Anuradha, "Network Utility Function Performance Analysis Using Cooperative Spectrum Sensing Network over Fading Channels," ***14th International INDICON conference***, IIT-Roorkee, Dec.15-17, 2017. **(IEEE)**

2. M.Ranjeeth and S.Anuradha,"Threshold Based Censoring of CRs in Fading Channel with perfect channel estimation," ***11th International conference on CROWNCOM***, Grenoble, France, pp. 220-231, May 30-June 1, 2016. **(Springer)**

3. M.Ranjeeth and S.Anuradha "Rank based Censoring of Cognitive Radios with Cooperative Spectrum Sensing under Hoyt Fading Channel" ***Int. Conf. on iCATccT***, BIET, Bengaluru, Oct 29-31, 2015 **(IEEE)**

4. M.Ranjeeth and S.Anuradha, "Cooperative Spectrum Sensing with Square Law Combining Diversity Reception," ***Third International Conf. on Signal processing, Communication and Networking***, ICSCN, March 2015. **(IEEE)**

5. M.Ranjeeth and S.Anuradha, "Performance of Fading Channels on Energy Detection Based Spectrum Sensing," ***2nd Int. Conf. on CNT***, pp.361-370, October 17-18, 2014. (**Elsevier**)

6. M.Ranjeeth and S.Anuradha, "Throughput Analysis in Cooperative Spectrum Sensing Network using an Improved Energy Detector," ***17th International Conference on Wireless Telecommunications Symposisum***, Phoenix, Arizona, USA, April 18-20, 2018. (**Accepted**)

Citations

1. S.A. Juboori and X. Fernando, "Correlated multichannel spectrum sensing cognitive radio system with selection combining," *In proceedings of Global Communication Conference (GLOBECOM)*, Washington, DC, USA, 4-8 December, 2016.

2. Pappu Kumar Verma , Sanjay Kumar Soni and Priyanka Jain, "On the performance of energy detection-based CR with SC diversity over IG channel," *In proceedings of International Journal of Electronics*, Taylor and Francis Publications, DOI: 10.1080/00207217.2017.1330425, 2017.

3. L. Gahane, P.K.Sharma, and N. Varshney, "An improved energy detector for mobile cognitive users over generalized fading channels," *In proceedings of IEEE Transactions on communications*, DOI 10.1109/TCOMM.2017. 2754250.

4. A.T. Mohammad "Performance evaluation and comparison of different transmitter detection techniques for application in cognitive radio," *In proceedings of International Journal of Networks and Communications*, vol.5, no.5, pp.83-96, 2015.

5. F.G. Mengistu and A.T. Mohammad "Performance comparison of the standard transmitter energy detector and an enhanced energy detector techniques," *In proceedings of International Journal of Networks and Communications*, vol.6, no.3, pp.39-48, 2016.

6. Ansar Ul Haq, *Multiband energy spectrum sensing in cooperative-cognitive network*, MS EE Theses, Bahria University DSpace digital repository.

7. Kandunuri Kalyani and Y. Rakesh Kumar, "Energy detection spectrum sensing technique in cognitive radio over fading channels models," *In proceedings of International Journal of Engineering Technology Science and Research (JETSR)*, ISSN 2394–3386 Vol. 4, Issue 7, July 2017.

8. Sonia Ben Aissa, Moez Hizem, and Ridha Bouallegue, "Performance of fading channels on asynchronous ofdm based cognitive radio networks," *In proceedings of International Journal of Wireless and Mobile Networks (IJWMN)*, Vol.9, No.4, August 2017.

9. Buthaina Mosa and Aya Falah Algamluoli, "Performance of energy detector for cognitive radio system over AWGN and Rayleigh channel," *In proceedings of International Journal of Computer Applications*, ISSN 0975 – 8887, Vol. 167, No.3, June 2017.

Appendix-A

A.1. Derivation of Missed Detection Probability (P_m) Expression for AWGN channel

The probability density function (PDF) expression for AWGN channel when signal is present, is given in [100, 64] as;

$$f_{y_i|H_1}(y) = \frac{2y^{\frac{1-p}{p}}}{p\sqrt{2\pi(E_s\sigma_h^2+\sigma_n^2)}}\exp\left(-\frac{y^{2/p}}{2(E_s\sigma_h^2+\sigma_n^2)}\right) \tag{A.1}$$

the closed form of P_m expression for AWGN channel can be calculated as [10, 28];

$$P_m = pr(y<\lambda\,|\,H_1) = \int_0^{\lambda} f_{w_i|H_1}(y)dy \tag{A.2}$$

$$\Rightarrow \int_0^{\lambda} \frac{2y^{\frac{1-p}{p}}}{p\sqrt{2\pi(E_s\sigma_h^2+\sigma_n^2)}}\exp\left(-\frac{y^{2/p}}{2(E_s\sigma_h^2+\sigma_n^2)}\right)dy,$$

$$\Rightarrow \frac{y^{1/p}}{\sqrt{2(E_s\sigma_h^2+\sigma_n^2)}} = \sqrt{t}\ ,\ \Rightarrow \frac{y^{(1-p)/p}}{p\sqrt{2(E_s\sigma_h^2+\sigma_n^2)}}dy = \frac{dt}{2\sqrt{t}}$$

$$\Rightarrow \frac{1}{\sqrt{\pi}}\int_0^{\left(\frac{\lambda^{2/p}}{2(E_s\sigma_h^2+\sigma_n^2)}\right)} t^{-\frac{1}{2}}\exp(-t)dt,$$

$$P_m = \frac{1}{\sqrt{\pi}}\gamma\left(\frac{1}{2}, \frac{\lambda^{2/p}}{2(E_s\sigma_h^2+\sigma_n^2)}\right) \tag{A.3}$$

where $\gamma(,)$ is an incomplete gamma function.

We have considered that each CR is having multiple antennas and selection combining (SC) scheme is used to select the maximum value of antenna among all antennas (M).

SC diversity scheme is used at each CR to select the maximum value of decision statistics available at each antenna [28] is

$$Z = \Pr[\max(W_1, W_2, W_3 ... W_M)] \tag{A.4}$$

Under hypothesis H_1, using SC diversity scheme missed detection probability can be calculated as;

$$P_m = \Pr[\max(W_1, W_2, W_3 ... W_M) \le |\, H_1] \tag{A.5}$$

Having multiple antennas and using SC diversity scheme at each CR, P_m expression for AWGN channel is obtained as;

$$P_m = \frac{1}{\sqrt{\pi}}\left[\gamma\left(\frac{1}{2}, \frac{\lambda^{2/p}}{2(E_s\sigma_h^2+\sigma_n^2)}\right)\right]^M \tag{A.6}$$

A.2. Derivation of P_m Expression for Rayleigh Fading Channel

The PDF expression for Rayleigh fading channel when signal is present, is given in [28] as;

$$f_{y_i|H_1}(y) = \frac{2y^{\frac{2-p}{p}}}{p(E_s\sigma_h^2+\sigma_n^2)}\exp\left(-\frac{y^{2/p}}{(E_s\sigma_h^2+\sigma_n^2)}\right) \tag{A.7}$$

the closed form of P_m expression for Rayleigh fading channel can be derived by substituting Eq. (A.7) in Eq. (A.2);

$$\Rightarrow \int_0^{\lambda} \frac{2y^{\frac{2-p}{p}}}{p(E_s\sigma_h^2+\sigma_n^2)}\exp\left(-\frac{y^{2/p}}{(E_s\sigma_h^2+\sigma_n^2)}\right)dy,$$

$$\Rightarrow \int_0^{\left(\frac{\lambda^{2/p}}{(E_s\sigma_h^2+\sigma_n^2)}\right)} \exp(-t)dt,$$

$$P_m = \left(1-\exp\left(-\lambda^{2/p}/(1+\bar{\gamma})\sigma_n^2\right)\right) \tag{A.8}$$

where $\bar{\gamma} = E_s\sigma_h^2/\sigma_n^2$ is S-channel SNR.

Having multiple antennas and using SC diversity scheme at each CR, P_m expression for Rayleigh fading channel is

$$P_m = \left(1-\exp\left(-\lambda^{2/p}/(1+\bar{\gamma})\sigma_n^2\right)\right)^M \tag{A.9}$$

A.3. Derivation of P_m Expression for Rician Fading Channel

The PDF expression for Rician fading channel when signal is present, is given in [11] as;

$$f_{w_i|H_1}(y) = \frac{2y^{(2/p)-1}(K+1)}{p(E_s\sigma_h^2+\sigma_n^2)}\exp\left(-K-\frac{(K+1)y^{2/p}}{(E_s\sigma_h^2+\sigma_n^2)}\right)I_0\left(2\sqrt{\frac{K(1+K)y^{2/p}}{(E_s\sigma_h^2+\sigma_n^2)}}\right) \tag{A.10}$$

the closed form of P_m expression for Rician fading channel can be obtained by substituting Eq. (A.10) in Eq. (A.2);

$$\Rightarrow \int_0^{\lambda} \frac{2y^{(2/p)-1}(\mathrm{K}+1)}{p(E_s\sigma_h^2+\sigma_n^2)} \exp\left(-K-\frac{(\mathrm{K}+1)\,\mathrm{y}^{2/p}}{(E_s\sigma_h^2+\sigma_n^2)}\right) I_0\left(2\sqrt{\frac{K(1+\mathrm{K})\,\mathrm{y}^{2/p}}{(E_s\sigma_h^2+\sigma_n^2)}}\right) dy,$$

$$\Rightarrow \int_0^{\left(\frac{(1+K)\lambda^{2/p}}{(E_s\sigma_h^2+\sigma_n^2)}\right)} \exp(-t)\exp(-K) I_0(2\sqrt{K\lambda})\, dt,$$

$$P_m = \left[1-Q\left(\sqrt{2K}, \lambda^{1/P}\sqrt{\frac{2(1+K)}{\sigma_n^2(1+\bar{\gamma})}}\right)\right] \tag{A.11}$$

Having multiple antennas and using SC diversity scheme at each CR, P_m expression for Rician fading channel is

$$P_m = \left[1-Q\left(\sqrt{2K}, \lambda^{1/P}\sqrt{\frac{2(1+K)}{\sigma_n^2(1+\bar{\gamma})}}\right)\right]^M \tag{A.12}$$

A.4. Derivation of P_m Expression for Weibull Fading Channel

The PDF expression for Weibull fading channel when signal is present, is given in [64] as;

$$f_{w_i|\mathrm{H}_1}(\mathrm{y}) = \frac{2y^{(2/p)-1}C}{p}\left[\frac{\Gamma(\mathrm{P})}{(E_s\sigma_h^2+\sigma_n^2)}\right]\left(\mathrm{y}^{2/p}\right)^{\mathrm{C}-1} \exp\left(-\left\{\frac{\mathrm{y}^{2/p}\Gamma(\mathrm{P})}{(E_s\sigma_h^2+\sigma_n^2)}\right\}^C\right) \tag{A.13}$$

where $C = V/2$ and $P = 1 + 1/C$, V – is Weibull fading parameter.

the closed form of P_m expression for Weibull fading channel can be obtained by substituting Eq. (A.13) in Eq. (A.2);

$$\Rightarrow \int_0^{\lambda} \frac{2y^{(2/p)-1}C}{p}\left[\frac{\Gamma(\mathrm{P})}{(E_s\sigma_h^2+\sigma_n^2)}\right]\left(\mathrm{y}^{2/p}\right)^{\mathrm{C}-1} \exp\left(-\left\{\frac{\mathrm{y}^{2/p}\Gamma(\mathrm{P})}{(E_s\sigma_h^2+\sigma_n^2)}\right\}^C\right) dy$$

$$\Rightarrow \int_0^{\left(\frac{\Gamma(\mathrm{P})\lambda^{2/p}}{(E_s\sigma_h^2+\sigma_n^2)}\right)} \exp(-\mathrm{t})\, \mathrm{dt},$$

$$P_m = \left[1-\exp\left(-\left\{\frac{\lambda^{2/P}\Gamma(\mathrm{P})}{\sigma_n^2(1+\bar{\gamma})}\right\}^C\right)\right] \tag{A.14}$$

Having multiple antennas and using SC diversity scheme at each CR, P_m expression for Weibull fading channel is

$$P_m = \left[1 - \exp\left(-\left\{\frac{\lambda^{2/P}\Gamma(P)}{\sigma_n^2(1+\bar{\gamma})}\right\}^C\right)\right]^M \quad \text{(A.15)}$$

A.5. Derivation of P_m Expression for Hoyt Fading Channel

The PDF expression for Hoyt fading channel when signal is present, is given in [64] as;

$$f_{y_i|H_1}(y) = \frac{y^{2/p-1}}{p\sigma_1\sigma_2}\exp\left(-\left(\frac{y^{2/p}}{4}\right)\left(\frac{1}{\sigma_2^2}+\frac{1}{\sigma_1^2}\right)\right) I_0\left(\left(\frac{y^{2/p}}{4}\right)\left(\frac{1}{\sigma_2^2}-\frac{1}{\sigma_1^2}\right)\right) \quad \text{(A.16)}$$

where $\sigma_I = \sqrt{\frac{\Omega q^2}{1+q^2}}$, $\sigma_q = \sqrt{\frac{\Omega}{1+q^2}}$, and q is Hoyt fading parameter that ranges from 0 to 1.

The closed form of P_m expression for Hoyt fading channel can be obtained by substituting Eq. (A.16) in Eq. (A.2);

$$= \int_0^{\lambda} \frac{y^{2/p-1}}{p\sigma_1\sigma_2}\exp\left(-\left(\frac{y^{2/p}}{4}\right)\left(\frac{1}{\sigma_2^2}+\frac{1}{\sigma_1^2}\right)\right) I_0\left(\left(\frac{y^{2/p}}{4}\right)\left(\frac{1}{\sigma_2^2}-\frac{1}{\sigma_1^2}\right)\right) dy \quad \text{(A.17)}$$

The expression for P_m in Hoyt fading channel can be calculated from CDF expression, it is given in [67] as;

$$F_{Z|H_1}(z) = \frac{1}{16}\left[1+\exp(-Az^{2/p})\,I_0(Bz^{2/p}) - 2Q(u_1, v_1)\right] \quad \text{(A.18)}$$

$A = \left(\frac{1}{4}\right)\left(\frac{1}{\sigma_2^2}+\frac{1}{\sigma_1^2}\right)$, $B = \left(\frac{1}{4}\right)\left(\frac{1}{\sigma_2^2}-\frac{1}{\sigma_1^2}\right)$, $u_1 = \sqrt{\left(A-\sqrt{A^2-B^2}\right)z^{2/p}}$, $V_1 = \sqrt{\left(A+\sqrt{A^2-B^2}\right)z^{2/p}}$.

Having multiple antennas and using SC diversity scheme at each CR, P_m expression for Hoyt fading channel is

$$P_m = \frac{1}{16}\left[1+\exp(-Az^{2/p})\,I_0(Bz^{2/p}) - 2Q(u_1, v_1)\right]^M \quad \text{(A.19)}$$

Appendix-B

B.1. Optimization of Threshold Value (λ_{opt}) in Rayleigh Fading Channel

For a single antenna case (M=1), the closed form of expression for λ_{opt} can be derived by differentiating Eq. (5.8) and Eq. (5.15) w.r.t. λ as;

$$\frac{\partial P_f}{\partial \lambda} + \frac{\partial P_m}{\partial \lambda} = 0 \tag{B.1}$$

substituting Eq. (5.32) and Eq. (5.33) in Eq. (B.1) gives;

$$\Rightarrow -\exp\left(-\frac{\lambda^{\frac{2}{p}}}{\sigma_n^2}\right)\frac{2\lambda^{\frac{2}{p}-1}}{p\sigma_n^2} + \exp\left(-\frac{\lambda^{\frac{2}{p}}}{\sigma_n^2\left(1+\bar{\gamma}\right)}\right)\frac{2\lambda^{\frac{2}{p}-1}}{p\sigma_n^2\left(1+\bar{\gamma}\right)} = 0 \tag{B.2}$$

applying *logarithm* on both sides to Eq. (B.2);

$$\Rightarrow \left(\frac{\lambda^{\frac{2}{p}}}{\sigma_n^2}\right) = \left(\frac{\lambda^{\frac{2}{p}}}{\sigma_n^2\left(1+\bar{\gamma}\right)}\right) + \ln\left(1+\bar{\gamma}\right) \tag{B.3}$$

after simplification, the closed form of expression for λ_{opt} is

$$\lambda_{opt} = \left(\frac{\sigma_n^2 \ln\left(1+\bar{\gamma}\right)}{\bar{\gamma}/(1+\bar{\gamma})}\right)^{\frac{p}{2}} \tag{B.4}$$

Similarly, for multiple antennas case: $\partial P_f / \partial \lambda$ and $\partial P_m / \partial \lambda$ are given by;

$$\frac{\partial P_f}{\partial \lambda} = -M\,\frac{2\lambda^{(2-\mathrm{p})/p}}{p}\left[1-\exp\left(-\lambda^{2/p}/\sigma_n^2\right)\right]^{M-1}\exp\left(-\frac{\lambda^{2/p}}{\sigma_n^2}\right) \tag{B.5}$$

$$\frac{\partial P_m}{\partial \lambda} = M\,\frac{2\lambda^{(2-\mathrm{p})/p}}{p\left(1+\bar{\gamma}\right)}\left[1-\exp\left(-\lambda^{2/p}/\sigma_n^2\left(1+\bar{\gamma}\right)\right)\right]^{M-1}\exp\left(-\frac{\lambda^{2/p}}{\sigma_n^2\left(1+\bar{\gamma}\right)}\right) \tag{B.6}$$

The expression for λ_{opt} using multiple antennas (M=3) can be calculated by substituting Eq. (B.5) and Eq. (B.6) in Eq. (B.1);

$$\Rightarrow -\frac{6\lambda^{(2-\mathrm{p})/p}}{p}\left[1-\exp\left(-\lambda^{2/p}/\sigma_n^2\right)\right]^2\exp\left(-\frac{\lambda^{2/p}}{\sigma_n^2}\right) + \frac{6\lambda^{(2-\mathrm{p})/p}}{p\left(1+\bar{\gamma}\right)}\left[1-\exp\left(-\lambda^{2/p}/\sigma_n^2\left(1+\bar{\gamma}\right)\right)\right]^2\exp\left(-\frac{\lambda^{2/p}}{\sigma_n^2\left(1+\bar{\gamma}\right)}\right) = 0$$

$$\Rightarrow \left[1-\exp\left(-\lambda^{2/p}/\sigma_n^2\right)\right]^2\exp\left(-\frac{\lambda^{2/p}}{\sigma_n^2}\right) = \frac{1}{\left(1+\bar{\gamma}\right)}\left[1-\exp\left(-\lambda^{2/p}/\sigma_n^2\left(1+\bar{\gamma}\right)\right)\right]^2\exp\left(-\frac{\lambda^{2/p}}{\sigma_n^2\left(1+\bar{\gamma}\right)}\right),$$

applying *logarithm* on both sides and after simplification, the closed form of expression for λ_{opt} using multiple antennas (M=3) at each CR is

$$\lambda_{opt} = \left(\frac{\sigma_n^2 \ln(1+\bar{\gamma})}{2\bar{\gamma}/(1+\bar{\gamma})} \right)^{\frac{p}{2}} \tag{B.7}$$

B.2. Optimization of Arbitrary Power of Received Signal (p_{opt}) in Rayleigh Fading Channel

For a single antenna case (M=1), the closed form of expression for p_{opt} can be derived by differentiating Eq. (5.8) and Eq. (5.15) w.r.t. p as;

$$\frac{\partial P_f}{\partial p} + \frac{\partial P_m}{\partial p} = 0 \tag{B.8}$$

substituting Eq. (5.37) and Eq. (5.38) in Eq. (B.8);

$$\Rightarrow -\frac{2\log\lambda}{p^2}\left(\frac{\lambda^{\frac{2}{p}}}{2(1+\bar{\gamma})\sigma_n^2} \right)\exp\left(-\frac{\lambda^{\frac{2}{p}}}{(1+\bar{\gamma})\sigma_n^2} \right) + \exp\left(-\frac{\lambda^{\frac{2}{p}}}{\sigma_n^2} \right)\frac{2}{p^2}\frac{\lambda^{\frac{2}{p}}\log\lambda}{\sigma_n^2} = 0,$$

$$\Rightarrow \left(\frac{1}{(1+\bar{\gamma})} \right)\exp\left(-\frac{\lambda^{\frac{2}{p}}}{(1+\bar{\gamma})\sigma_n^2} \right) = \exp\left(-\frac{\lambda^{\frac{2}{p}}}{\sigma_n^2} \right),$$

$$\Rightarrow \left(\frac{\lambda^{\frac{2}{p}}}{\sigma_n^2} \right) = \left(\frac{\lambda^{\frac{2}{p}}}{\sigma_n^2(1+\bar{\gamma})} \right) + \ln(1+\bar{\gamma}),$$

after simplification, the closed form of expression for p_{opt} is

$$p_{opt} = \frac{2\ln\lambda}{\ln\left(\frac{\sigma_n^2 \ln(1+\bar{\gamma})}{\left(\frac{\bar{\gamma}}{1+\bar{\gamma}} \right)} \right)} \tag{B.9}$$

Similarly, for multiple antennas case: $\partial P_f / \partial p$ and $\partial P_m / \partial p$ are given by;

$$\frac{\partial P_f}{\partial p} = M\,\frac{2\lambda^{2/p} log\lambda}{p^2\sigma_n^2}\left[1-\exp\left(-\lambda^{2/p}/\sigma_n^2 \right) \right]^{M-1}\exp\left(-\frac{\lambda^{2/p}}{\sigma_n^2} \right) \tag{B.10}$$

$$\frac{\partial P_m}{\partial p} = -M\,\frac{2\lambda^{2/p} log\lambda}{p^2\sigma_n^2\left(1+\bar{\gamma}\right)}\left[1-\exp\left(-\lambda^{2/p}\Big/\sigma_n^2\left(1+\bar{\gamma}\right)\right)\right]^{M-1}\exp\left(-\frac{\lambda^{2/p}}{\sigma_n^2\left(1+\bar{\gamma}\right)}\right) \tag{B.11}$$

The expression for p_{opt} using multiple antennas (M=3) at each CR can be calculated by substituting Eq. (B.10) and Eq. (B.11) in Eq. (B.1);

$$\Rightarrow -\frac{6\lambda^{(2-p)/p}}{p}\left[1-\exp\left(-\lambda^{2/p}\Big/\sigma_n^2\right)\right]^2\exp\left(-\frac{\lambda^{2/p}}{\sigma_n^2}\right)+\frac{6\lambda^{(2-p)/p}}{p\left(1+\bar{\gamma}\right)}\left[1-\exp\left(-\lambda^{2/p}\Big/\sigma_n^2\left(1+\bar{\gamma}\right)\right)\right]^2\exp\left(-\frac{\lambda^{2/p}}{\sigma_n^2\left(1+\bar{\gamma}\right)}\right)=0$$

$$\Rightarrow\left[1-\exp\left(-\lambda^{2/p}\Big/\sigma_n^2\right)\right]^2\exp\left(-\frac{\lambda^{2/p}}{\sigma_n^2}\right)=\left[1-\exp\left(-\lambda^{2/p}\Big/\sigma_n^2\left(1+\bar{\gamma}\right)\right)\right]^2\exp\left(-\frac{\lambda^{2/p}}{\sigma_n^2\left(1+\bar{\gamma}\right)}\right),$$

applying *logarithm* on both sides and after simplification, the closed form of expression for λ_{opt} using multiple antennas (M=3) at each CR is

$$p_{opt} = \frac{2\ln\lambda}{\ln\left(\dfrac{2\sigma_n^2\ln\left(1+\bar{\gamma}\right)}{\left(\dfrac{\bar{\gamma}}{1+\bar{\gamma}}\right)}\right)} \tag{B.12}$$

B.3. Optimization of Number of CRs (N_{opt}) in Rayleigh Fading using OR-Rule at FC

The closed form of expression for N_{opt} using OR-Rule at FC can be calculated using Eq. (5.18) as follows;

$$\text{Total error rate: } Z(\mathrm{N}) = Q_m + Q_f \tag{B.13}$$

$$\Delta Z(N) = Z(N+1) - Z(N)$$

$$\Rightarrow 1-[(1-P_f)]^{N+1}-1+[(1-P_f)]^N+[P_m]^{N+1}-[P_m]^N=0,$$

$$\Rightarrow [P_m]^{N+1}-[(1-P_f)]^{N+1}-[P_m]^N+[(1-P_f)]^N=0,$$

$$\Rightarrow 1-\left((1-P_f)\Big/P_m\right)^{N+1}-\left(1\Big/(P_m)\right)+\frac{1}{(P_m)}\left((1-P_f)\Big/P_m\right)^N=0,$$

$$\Rightarrow 1-\left(1\Big/(P_m)\right)=\left((1-P_f)\Big/P_m\right)^{N+1}-\frac{1}{(P_m)}\left((1-P_f)\Big/P_m\right)^N,$$

after simplification, the above expression reduces to

$$\Rightarrow \left(\left(1-P_m\right) \Big/ P_f \right) = \left(\left(1-P_f\right) \Big/ P_m \right)^N ,$$

applying *logarithm* on both sides, the closed form of expression for N_{opt} using OR-Rule at FC is

$$N_{opt} = \left\lceil \frac{\ln\left(\frac{1-P_m}{P_f}\right)}{\ln\left(\frac{1-P_f}{P_m}\right)} \right\rceil \tag{B.14}$$

B.4. Optimization of Threshold Value (λ_{opt}) in Rayleigh Fading using OR-Rule at FC

The closed form of expression for λ_{opt} using OR-Rule at FC can be calculated using Eq. (5.44) and Eq. (5.20) as follows;

$$\frac{\partial Q_m}{\partial \lambda} + \frac{\partial Q_f}{\partial \lambda} = 0 \tag{B.15}$$

$$N\left(1-P_f\right)^{N-1} \frac{\partial P_f}{\partial \lambda} + N\left(P_m\right)^{N-1} \frac{\partial P_m}{\partial \lambda} = 0 \tag{B.16}$$

for a single antenna case (M=1), $\partial P_f \big/ \partial \lambda$ and $\partial P_m \big/ \partial \lambda$ expressions are given by Eq.(5.32) and Eq.(5.33), substituting them in Eq. (B.16);

$$\Rightarrow N\left(1-P_f\right)^{N-1} \left(-\exp\left(-\frac{\lambda^{2/p}}{\sigma_n^2} \right) \frac{2\lambda^{(2/p)-1}}{p\sigma_n^2} \right) + N\left(P_m\right)^{N-1} \left(\exp\left(-\frac{\lambda^{2/p}}{\sigma_n^2\left(1+\bar{\gamma}\right)} \right) \frac{2\lambda^{(2/p)-1}}{p\sigma_n^2\left(1+\bar{\gamma}\right)} \right) = 0 ,$$

$$\Rightarrow \left(1-P_f\right)^{N-1} \left(\exp\left(-\frac{\lambda^{2/p}}{\sigma_n^2} \right) \right) = \left(P_m\right)^{N-1} \left(\exp\left(-\frac{\lambda^{2/p}}{\sigma_n^2\left(1+\bar{\gamma}\right)} \right) \right) \left(\frac{1}{1+\bar{\gamma}} \right),$$

applying *logarithm* on both sides and solving algebraic expressions, the closed form of expression for λ_{opt} using single antenna and multiple number of CRs in CSS network is

$$\lambda_{opt} = \left(\left((N-1)\left(\ln\left(\frac{1-P_f}{P_m} \right) \right) + \ln\left(1+\bar{\gamma} \right) \right) \sigma_n^2 \Big/ \left(\frac{\bar{\gamma}}{1+\bar{\gamma}} \right) \right)^{p/2} \tag{B.17}$$

Similarly, using multiple antennas (M=3) at each CR and multiple number of SUs (N) in the proposed CSS network, the expression for λ_{opt} can be calculated using Eq. (B.5) and Eq.(B.6), substituting them in Eq. (B.16) as follows;

$$\Rightarrow N\left(1-P_f\right)^{N-1} - \frac{6\lambda^{(2-p)/p}}{p}\left[1-\exp\left(-\lambda^{2/p}\Big/\sigma_n^2\right)\right]^2 \exp\left(-\frac{\lambda^{2/p}}{\sigma_n^2}\right) +$$

$$N\left(P_m\right)^{N-1}\frac{6\lambda^{(2-p)/p}}{p\left(1+\bar{\gamma}\right)}\left[1-\exp\left(-\lambda^{2/p}\Big/\sigma_n^2\left(1+\bar{\gamma}\right)\right)\right]^2 \exp\left(-\frac{\lambda^{2/p}}{\sigma_n^2\left(1+\bar{\gamma}\right)}\right) = 0$$

applying *logarithm* on both sides and solving algebraic expressions, the closed form of expression for λ_{opt} using multiple antennas and multiple number of CRs in CSS network is

$$\lambda_{opt} = \left(\left((N-1)\left(\ln\left(\frac{1-P_f}{P_m} \right) \right) + \ln\left(1+\bar{\gamma} \right) \right) \sigma_n^2 \Big/ \left(\frac{2\bar{\gamma}}{1+\bar{\gamma}} \right) \right)^{p/2} \tag{B.18}$$

B.5. Optimization of Arbitrary Power of Received Signal (p_{opt}) in Rayleigh Fading using OR-Rule at FC

The closed form of expression for p_{opt} using OR-Rule at FC can be calculated using Eq. (5.48) as follows;

$$\frac{\partial Q_m}{\partial p} + \frac{\partial Q_f}{\partial p} = 0 \tag{B.19}$$

$$N\left(1-P_f\right)^{N-1}\frac{\partial P_f}{\partial p} + \left(P_m\right)^{N-1}\frac{\partial P_m}{\partial p} = 0 \tag{B.20}$$

for a single antenna case (M=1), $\partial P_f / \partial p$ and $\partial P_m / \partial p$ expressions are given by Eq.(5.37) and Eq. (5.38), substituting them in Eq.(B.20);

$$\Rightarrow N\left(1-P_f\right)^{N-1}\left(\exp\left(-\frac{\lambda^{2/p}}{\sigma_n^2}\right)\frac{2}{p^2}\frac{\lambda^{(2/p)}\log\lambda}{\sigma_n^2}\right)+N\left(P_m\right)^{N-1}\left(-\exp\left(-\frac{\lambda^{2/p}}{\sigma_n^2(1+\bar{\gamma})}\right)\frac{2}{p^2}\frac{\lambda^{(2/p)}\log\lambda}{\sigma_n^2(1+\bar{\gamma})}\right)=0$$

after some algebraic simplifications, above Eq. reduces to

$$\Rightarrow\left(1-P_f\right)^{N-1}\left(\exp\left(-\frac{\lambda^{2/p}}{\sigma_n^2}\right)\right)=\left(P_m\right)^{N-1}\left(\exp\left(-\left\{\frac{\lambda^{2/p}}{\sigma_n^2\left(1+\bar{\gamma}\right)}\right\}\right)\right)\left(\frac{1}{1+\bar{\gamma}}\right),$$

$$\Rightarrow\frac{\lambda^{2/p}}{\sigma_n^2}=\frac{\left(N-1\right)\left(\ln\left(\frac{1-P_f}{P_m}\right)\right)+\ln\left(1+\bar{\gamma}\right)}{\left(\frac{\bar{\gamma}}{1+\bar{\gamma}}\right)},$$

applying *logarithm* on both sides, after simplification, the closed form of expression for p_{opt} using single antenna at each CR and multiple number of CRs in CSS network is

$$p_{opt}=\frac{2\ln\lambda}{\ln\left(\frac{\left(\left(N-1\right)\left(\ln\left(\frac{1-P_f}{P_m}\right)\right)+\ln\left(1+\bar{\gamma}\right)\right)\sigma_n^2}{\left(\frac{\bar{\gamma}}{1+\bar{\gamma}}\right)}\right)} \tag{B.21}$$

Similarly, using multiple antennas (*M*=3) at each CR and multiple number of SUs (*N*) in the proposed CSS network, the expression for p_{opt} can be calculated using Eq. (B.10) and Eq.(B.11), substituting them in Eq. (B.20) as follows;

$$\Rightarrow N\left(1-P_f\right)^{N-1}\left(-M\left[1-\exp\left(-\frac{\lambda^{2/p}}{\sigma_n^2}\right)\right]^{M-1}\exp\left(-\frac{\lambda^{2/p}}{\sigma_n^2}\right)\frac{2}{p^2}\frac{\lambda^{(2/p)}\log\lambda}{\sigma_n^2}\right)$$

$$+N\left(P_m\right)^{N-1}\left(-M\left[1-\exp\left(-\left\{\frac{\lambda^{2/p}}{\sigma_n^2(1+\bar{\gamma})}\right\}\right)\right]^{M-1}\exp\left(-\frac{\lambda^{2/p}}{\sigma_n^2(1+\bar{\gamma})}\right)\frac{2}{p^2}\frac{\lambda^{(2/p)}\log\lambda}{\sigma_n^2(1+\bar{\gamma})}\right)=0,$$

applying *logarithm* on both sides and solving algebraic expressions, the closed form of expression for p_{opt} using multiple antennas (*M*=3) and multiple number of CRs in CSS network is

$$p_{opt} = \frac{2\ln\lambda}{\ln\left(\frac{\left((N-1)\left(\ln\left(\frac{1-P_f}{P_m}\right)\right)+\ln\left(1+\bar{\gamma}\right)\right)\sigma_n^2}{\left(\frac{\bar{\gamma}}{1+\bar{\gamma}}\right)(0.5)}\right)} \tag{B.22}$$

B.6. Optimization of Number of CRs (N_{opt}) in Rayleigh Fading using AND-Rule at FC

The closed form of expression for N_{opt} using AND-Rule at FC can be calculated using Eq. (5.18) as follows;

$$\text{Total error rate: } Z(\mathrm{N}) = Q_m + Q_f$$

$$\Delta Z(N) = Z(N+1) - Z(N)$$

$$\Rightarrow 1-[(1-P_m)]^{N+1} - 1 + [(1-P_m)]^N + [P_f]^{N+1} - [P_f]^N = 0$$

$$\Rightarrow [P_f]^{N+1} - [(1-P_m)]^{N+1} - [P_f]^N + [(1-P_m)]^N = 0,$$

$$\Rightarrow 1 - \left(\frac{(1-P_m)}{P_f}\right)^{N+1} - \left(\frac{1}{(P_f)}\right) + \frac{1}{(P_f)}\left(\frac{(1-P_m)}{P_f}\right)^N = 0,$$

$$\Rightarrow \left(\frac{(1-P_m)}{P_f}\right) = \left(\frac{(1-P_f)}{P_m}\right)^N,$$

applying *logarithm* on both sides, the closed form of expression for N_{opt} using AND-Rule at FC is

$$N_{opt} = \left\lceil \frac{\ln\left(\frac{1-P_f}{P_m}\right)}{\ln\left(\frac{1-P_m}{P_f}\right)} \right\rceil \tag{B.23}$$

B.7. Optimization of Threshold Value (λ_{opt}) in Rayleigh Fading using AND-Rule at FC

The closed form of expression for λ_{opt} using AND-Rule at FC can be calculated using Eq. (5.44) and Eq. (5.21) as follows;

$$\frac{\partial Q_m}{\partial \lambda} + \frac{\partial Q_f}{\partial \lambda} = 0 \tag{B.24}$$

$$N\left(P_f\right)^{N-1}\frac{\partial P_f}{\partial \lambda} + N\left(1-P_m\right)^{N-1}\frac{\partial P_m}{\partial \lambda} = 0 \tag{B.25}$$

for a single antenna case (M=1), $\partial P_f / \partial \lambda$ and $\partial P_m / \partial \lambda$ expressions are given by Eq.(5.32) and Eq.(5.33), substituting them in Eq. (B.25);

$$\Rightarrow N\left(P_f\right)^{N-1}\left(-\exp\left(-\frac{\lambda^{2/p}}{\sigma_n^2}\right)\frac{2\lambda^{(2/p)-1}}{p\sigma_n^2}\right) + N\left(1-P_m\right)^{N-1}\left(\exp\left(-\frac{\lambda^{2/p}}{\sigma_n^2\left(1+\bar{\gamma}\right)}\right)\frac{2\lambda^{(2/p)-1}}{p\sigma_n^2\left(1+\bar{\gamma}\right)}\right) = 0$$

applying *logarithm* on both sides and solving algebraic expressions, the closed form of expression for λ_{opt} using single antenna and multiple number of CRs in CSS network is

$$\lambda_{opt} = \left(\left(\left(N-1\right)\left(\ln\left(\frac{P_f}{1-P_m}\right)\right) + \ln\left(1+\bar{\gamma}\right)\right)\sigma_n^2 \Big/ \left(\frac{\bar{\gamma}}{1+\bar{\gamma}}\right)\right)^{p/2} \tag{B.26}$$

Similarly, using multiple antennas (M=3) at each CR and multiple number of SUs (N) in the proposed CSS network, the expression for λ_{opt} can be calculated using Eq. (B.5) and Eq.(B.6), substituting them in Eq. (B.25) as follows;

$$\Rightarrow N\left(P_f\right)^{N-1} - \frac{6\lambda^{(2-p)/p}}{p}\left[1-\exp\left(-\lambda^{2/p}/\sigma_n^2\right)\right]^2\exp\left(-\frac{\lambda^{2/p}}{\sigma_n^2}\right) +$$

$$N\left(1-P_m\right)^{N-1}\frac{6\lambda^{(2-p)/p}}{p\left(1+\bar{\gamma}\right)}\left[1-\exp\left(-\lambda^{2/p}\Big/\sigma_n^2\left(1+\bar{\gamma}\right)\right)\right]^2\exp\left(-\frac{\lambda^{2/p}}{\sigma_n^2\left(1+\bar{\gamma}\right)}\right) = 0$$

applying *logarithm* on both sides and solving algebraic expressions, the closed form of expression for λ_{opt} using multiple antennas (M=3) and multiple number of CRs in CSS network is

$$\lambda_{opt} = \left(\left((N-1)\left(\ln\left(\frac{P_f}{1-P_m} \right) \right) + \ln\left(1+\bar{\gamma} \right) \right) \sigma_n^2 \Big/ \left(\frac{\bar{2\gamma}}{1+\bar{\gamma}} \right) \right)^{p/2} \tag{B.27}$$

B.8. Optimization of Arbitrary Power of Received Signal (p_{opt}) in Rayleigh Fading using AND-Rule at FC

The closed form of expression for p_{opt} using AND-Rule at FC can be calculated using Eq. (5.48) as follows;

$$\frac{\partial Q_m}{\partial p} + \frac{\partial Q_f}{\partial p} = 0 \tag{B.28}$$

$$N\left(P_f\right)^{N-1} \frac{\partial P_f}{\partial p} + \left(1-P_m\right)^{N-1} \frac{\partial P_m}{\partial p} = 0 \tag{B.29}$$

for a single antenna case (M=1), $\partial P_m / \partial p$ and $\partial P_f / \partial p$ expressions are given by Eq.(5.37) and Eq. (5.38), substituting them in Eq.(B.29):

$$\Rightarrow N\left(P_f\right)^{N-1}\left(\exp\left(-\frac{\lambda^{2/p}}{\sigma_n^2} \right) \frac{2}{p^2} \frac{\lambda^{(2/p)} \log\lambda}{\sigma_n^2} \right) + N\left(1-P_m\right)^{N-1}\left(-\exp\left(-\frac{\lambda^{2/p}}{\sigma_n^2(1+\bar{\gamma})} \right) \frac{2}{p^2} \frac{\lambda^{(2/p)} \log\lambda}{\sigma_n^2(1+\bar{\gamma})} \right) = 0$$

$$\Rightarrow \left(P_f\right)^{N-1}\left(\exp\left(-\frac{\lambda^{2/p}}{\sigma_n^2} \right) \right) = \left(1-P_m\right)^{N-1}\left(\exp\left(-\left\{ \frac{\lambda^{2/p}}{\sigma_n^2\left(1+\bar{\gamma}\right)} \right\} \right) \right)\left(\frac{1}{1+\bar{\gamma}} \right),$$

$$\Rightarrow \frac{\lambda^{2/p}}{\sigma_n^2} = \frac{(N-1)\left(\ln\left(\frac{P_f}{1-P_m} \right) \right) + \ln\left(1+\bar{\gamma} \right)}{\left(\frac{\bar{\gamma}}{1+\bar{\gamma}} \right)},$$

applying *logarithm* on both sides and solving algebraic expressions, the closed form of expression for p_{opt} using single antenna and multiple number of CRs in CSS network is

$$p_{opt} = \frac{2\ln\lambda}{\ln\left(\frac{\left((N-1)\left(\ln\left(\frac{P_f}{1-P_m}\right)\right)+\ln\left(1+\bar{\gamma}\right)\right)\sigma_n^2}{\left(\frac{\bar{\gamma}}{1+\bar{\gamma}}\right)}\right)} \tag{B.30}$$

Similarly, using multiple antennas (M=3) at each CR and multiple number of SUs (N) in the proposed CSS network, the expression for p_{opt} can be obtained using Eq.(B.10) and Eq.(B.11), substituting them in Eq. (B.29) as follows;

$$\Rightarrow N\left(P_f\right)^{N-1}\left(-M\left[1-\exp\left(-\frac{\lambda^{2/p}}{\sigma_n^2}\right)\right]^{M-1}\exp\left(-\frac{\lambda^{2/p}}{\sigma_n^2}\right)\frac{2}{p^2}\frac{\lambda^{(2/p)}\log\lambda}{\sigma_n^2}\right)$$

$$+N\left(1-P_m\right)^{N-1}\left(-M\left[1-\exp\left(-\left\{\frac{\lambda^{2/p}}{\sigma_n^2(1+\bar{\gamma})}\right\}\right)\right]^{M-1}\exp\left(-\frac{\lambda^{2/p}}{\sigma_n^2(1+\bar{\gamma})}\right)\frac{2}{p^2}\frac{\lambda^{(2/p)}\log\lambda}{\sigma_n^2(1+\bar{\gamma})}\right)=0$$

applying *logarithm* on both sides and solving algebraic expressions, the closed form of expression for p_{opt} using multiple antennas (M=3) and multiple number of CRs in CSS network is

$$p_{opt} = \frac{2\ln\lambda}{\ln\left(\frac{\left((N-1)\left(\ln\left(\frac{P_f}{1-P_m}\right)\right)+\ln\left(1+\bar{\gamma}\right)\right)\sigma_n^2}{\left(\frac{\bar{\gamma}}{1+\bar{\gamma}}\right)(0.5)}\right)} \tag{B.31}$$

Appendix-C

C.1. Optimization of threshold value (λ_{opt}) in Weibull fading channel

For a single antenna case (M=1), the closed form of expression for λ_{opt} can be derived by using Eq. (5.63);

$$\frac{\partial P_f}{\partial\lambda}+\frac{\partial P_m}{\partial\lambda}=0 \tag{C.1}$$

substituting Eq. (5.66) and Eq. (5.67) in Eq. (C.1) gives;

$$\Rightarrow -\exp\left(-\left\{\frac{\lambda^{2/p}\Gamma(\mathrm{P})}{\sigma_n^2}\right\}^C\right)C\left\{\frac{\lambda^{2/p}\Gamma(\mathrm{P})}{\sigma_n^2}\right\}^{C-1}\frac{2\lambda^{(2/p)-1}\Gamma(\mathrm{P})}{p\sigma_n^2}+\exp\left(-\left\{\frac{\lambda^{2/p}\Gamma(\mathrm{P})}{\sigma_n^2\left(1+\bar{\gamma}\right)}\right\}^C\right)C\left\{\frac{\lambda^{2/p}\Gamma(\mathrm{P})}{\left(1+\bar{\gamma}\right)\sigma_n^2}\right\}^{C-1}\frac{2\lambda^{(2/p)-1}\Gamma(\mathrm{P})}{p\sigma_n^2\left(1+\bar{\gamma}\right)}=0$$

$$\Rightarrow \exp\left(-\left\{\frac{\lambda^{2/p}\Gamma(\mathrm{P})}{\sigma_n^2}\right\}^C\right)=\exp\left(-\left\{\frac{\lambda^{2/p}\Gamma(\mathrm{P})}{\sigma_n^2\left(1+\bar{\gamma}\right)}\right\}^C\right)\left\{\frac{1}{\left(1+\bar{\gamma}\right)}\right\}^C,$$

$$\Rightarrow \left(\left\{\frac{\lambda^{2/p}\Gamma(\mathrm{P})}{\sigma_n^2}\right\}^C\right)\left(1-\left\{\frac{1}{\left(1+\bar{\gamma}\right)}\right\}^C\right)=C\ln\left(1+\bar{\gamma}\right),$$

$$\Rightarrow \left(\left\{\frac{\lambda^{2/p}\Gamma(\mathrm{P})}{\sigma_n^2}\right\}^C\right)=C\ln\left(1+\bar{\gamma}\right)\Big/\left(1-\left\{\frac{1}{\left(1+\bar{\gamma}\right)}\right\}^C\right),$$

$$\lambda_{opt}=\left(\frac{\sigma_n^2}{\Gamma(\mathrm{P})}\left(C\ln\left(1+\bar{\gamma}\right)\Big/\left(1-\left\{\frac{1}{\left(1+\bar{\gamma}\right)}\right\}^C\right)\right)^{1/C}\right)^{P/2} \tag{C.2}$$

Similarly, the closed form of expression for λ_{opt} with multiple antennas (M=3) at each CR can be calculated as;

$$\Rightarrow -\frac{6\lambda^{(2-\mathrm{p})/p}\Gamma(P)}{p\sigma_n^2}\left[1-\exp\left(-\left\{\lambda^{2/p}\Gamma(P)\Big/\sigma_n^2\right\}^C\right)\right]^2\exp\left(-\left\{\lambda^{2/p}\Gamma(P)\Big/\sigma_n^2\right\}^C\right)C\left\{\lambda^{2/p}\Gamma(P)\Big/\sigma_n^2\right\}^{C-1}$$

$$+\frac{6\lambda^{(2-\mathrm{p})/p}\Gamma(P)}{p\sigma_n^2(1+\bar{\gamma})}\left[1-\exp\left(-\left\{\lambda^{2/p}\Gamma(P)\Big/\sigma_n^2(1+\bar{\gamma})\right\}^C\right)\right]^2\exp\left(-\left\{\lambda^{2/p}\Gamma(P)\Big/\sigma_n^2(1+\bar{\gamma})\right\}^C\right)C\left\{\lambda^{2/p}\Gamma(P)\Big/(1+\bar{\gamma})\sigma_n^2\right\}^{C-1}=0$$

$$\Rightarrow \left[1-\exp\left(-\left\{\lambda^{2/p}\Gamma(P)\Big/\sigma_n^2\right\}^C\right)\right]^2 \exp\left(-\left\{\lambda^{2/p}\Gamma(P)\Big/\sigma_n^2\right\}^C\right)$$

$$= \left[1-\exp\left(-\left\{\lambda^{2/p}\Gamma(P)\Big/\sigma_n^2(1+\bar{\gamma})\right\}^C\right)\right]^2 \exp\left(-\left\{\lambda^{2/p}\Gamma(P)\Big/\sigma_n^2(1+\bar{\gamma})\right\}^C\right)\left\{1\Big/(1+\bar{\gamma})\right\}^C ,$$

$$\lambda_{opt} = \left(\frac{\sigma_n^2}{\Gamma(\mathrm{P})}\left(C\ln\left(1+\bar{\gamma}\right)\Big/\left(2\left\{\frac{\bar{\gamma}}{\left(1+\bar{\gamma}\right)}\right\}^C\right)\right)^{1/C}\right)^{P/2} \tag{C.3}$$

C.2. Optimization of Arbitrary Power of Received Signal (p_{opt}) in Weibull Fading Channel

For a single antenna case (M=1), the closed form of expression for p_{opt} can be obtained by using Eq. (5.70) as;

$$\frac{\partial P_f}{\partial p} + \frac{\partial P_m}{\partial p} = 0 \tag{C.4}$$

substituting Eq. (5.71) and Eq. (5.72) in Eq. (C.4) gives;

$$\Rightarrow -\exp\left(-\left\{\frac{\lambda^{2/p}\Gamma(\mathrm{P})}{\sigma_n^2(1+\bar{\gamma})}\right\}^C\right) C\left\{\frac{\lambda^{2/p}\Gamma(\mathrm{P})}{\sigma_n^2(1+\bar{\gamma})}\right\}^{C-1} \frac{2}{p^2}\frac{\lambda^{(2/p)}\log\lambda\Gamma(\mathrm{P})}{\sigma_n^2(1+\bar{\gamma})}$$

$$+M\exp\left(-\left\{\frac{\lambda^{2/p}\Gamma(\mathrm{P})}{\sigma_n^2}\right\}^C\right) C\left\{\frac{\lambda^{2/p}\Gamma(\mathrm{P})}{\sigma_n^2}\right\}^{C-1} \frac{2}{p^2}\frac{\lambda^{(2/p)}\log\lambda\Gamma(\mathrm{P})}{\sigma_n^2} = 0 ,$$

$$\Rightarrow \exp\left(-\left\{\frac{\lambda^{2/p}\Gamma(\mathrm{P})}{\sigma_n^2}\right\}^C\right) = \exp\left(-\left\{\frac{\lambda^{2/p}\Gamma(\mathrm{P})}{\sigma_n^2(1+\bar{\gamma})}\right\}^C\right)\left\{\frac{1}{(1+\bar{\gamma})}\right\}^C$$

$$\Rightarrow \left\{\frac{\lambda^{2/p}\Gamma(\mathrm{P})}{\sigma_n^2}\right\}^C\left(1-\left(\frac{1}{(1+\bar{\gamma})}\right)^C\right) = C\log\left(1+\bar{\gamma}\right),$$

$$p_{opt} = \frac{2\ln\lambda}{\ln\left(\left\{\frac{C\ln\left(1+\bar{\gamma}\right)}{\left[1-\left(\frac{1}{1+\bar{\gamma}}\right)^{C}\right]}\right\}^{1/C}\left(\frac{\sigma_n^2}{\Gamma(P)}\right)\right)} \tag{C.5}$$

Similarly, the closed form of expression for p_{opt} with multiple antennas (M=3) at each CR can be calculated as;

$$\Rightarrow -\left[1-\exp\left(-\left\{\frac{\lambda^{2/p}\Gamma(P)}{\sigma_n^2(1+\bar{\gamma})}\right\}^{C}\right)\right]^2 \exp\left(-\left\{\frac{\lambda^{2/p}\Gamma(P)}{\sigma_n^2(1+\bar{\gamma})}\right\}^{C}\right) C\left\{\frac{\lambda^{2/p}\Gamma(P)}{\sigma_n^2(1+\bar{\gamma})}\right\}^{C-1} \frac{6}{p^2}\frac{\lambda^{(2/p)}\log\lambda\Gamma(P)}{\sigma_n^2(1+\bar{\gamma})}$$

$$+\left[1-\exp\left(-\left\{\frac{\lambda^{2/p}\Gamma(P)}{\sigma_n^2}\right\}^{C}\right)\right]^2 \exp\left(-\left\{\frac{\lambda^{2/p}\Gamma(P)}{\sigma_n^2}\right\}^{C}\right) C\left\{\frac{\lambda^{2/p}\Gamma(P)}{\sigma_n^2}\right\}^{C-1} \frac{6}{p^2}\frac{\lambda^{(2/p)}\log\lambda\Gamma(P)}{\sigma_n^2} = 0 \quad ,$$

$$\Rightarrow \left[1-\exp\left(-\left\{\frac{\lambda^{2/p}\Gamma(P)}{\sigma_n^2(1+\bar{\gamma})}\right\}^{C}\right)\right]^2 \exp\left(-\left\{\frac{\lambda^{2/p}\Gamma(P)}{\sigma_n^2(1+\bar{\gamma})}\right\}^{C}\right)\left\{\frac{1}{(1+\bar{\gamma})}\right\}^{C}$$

$$= \left[1-\exp\left(-\left\{\frac{\lambda^{2/p}\Gamma(P)}{\sigma_n^2}\right\}^{C}\right)\right]^2 \exp\left(-\left\{\frac{\lambda^{2/p}\Gamma(P)}{\sigma_n^2}\right\}^{C}\right) \quad ,$$

$$p_{opt} = \frac{2\ln\lambda}{\ln\left(\left\{\frac{C\ln\left(1+\bar{\gamma}\right)}{(0.5)\left[1-\left(\frac{1}{1+\bar{\gamma}}\right)^{C}\right]}\right\}^{1/C}\left(\frac{\sigma_n^2}{\Gamma(P)}\right)\right)} \tag{C.6}$$

C.3. Optimization of Threshold Value (λ_{opt}) in Weibull Fading using OR-Rule at FC

The closed form of expression for λ_{opt} value can be obtained by using Eq.(5.45)

$$\Rightarrow N\left(1-P_f\right)^{N-1}\frac{\partial P_f}{\partial\lambda} + N\left(P_m\right)^{N-1}\frac{\partial P_m}{\partial\lambda} = 0 \tag{C.7}$$

expressions for $\partial P_f / \partial \lambda$ and $\partial P_m / \partial \lambda$ are given by Eq.(5.66) and Eq.(5.67), substituting them in Eq.(C.7) gives;

$$\Rightarrow N\left(1-P_f\right)^{N-1}\left(-\exp\left(-\left\{\frac{\lambda^{2/p}\Gamma(\mathrm{P})}{\sigma_n^2}\right\}^{C}\right)C\left\{\frac{\lambda^{2/p}\Gamma(\mathrm{P})}{\sigma_n^2}\right\}^{C-1}\frac{2\lambda^{\left(2/p\right)-1}\Gamma(\mathrm{P})}{p\sigma_n^2}\right)$$

$$+N\left(P_m\right)^{N-1}\left(\exp\left(-\left\{\frac{\lambda^{2/p}\Gamma(\mathrm{P})}{\sigma_n^2\left(1+\bar{\gamma}\right)}\right\}^{C}\right)C\left\{\frac{\lambda^{2/p}\Gamma(\mathrm{P})}{\left(1+\bar{\gamma}\right)\sigma_n^2}\right\}^{C-1}\frac{2\lambda^{\left(2/p\right)-1}\Gamma(\mathrm{P})}{p\sigma_n^2\left(1+\bar{\gamma}\right)}\right)=0,$$

$$\Rightarrow\left(1-P_f\right)^{N-1}\left(\exp\left(-\left\{\frac{\lambda^{2/p}\Gamma(\mathrm{P})}{\sigma_n^2}\right\}^{C}\right)\right)=\left(P_m\right)^{N-1}\left(\exp\left(-\left\{\frac{\lambda^{2/p}\Gamma(\mathrm{P})}{\sigma_n^2\left(1+\bar{\gamma}\right)}\right\}^{C}\right)\right)\left(\frac{1}{1+\bar{\gamma}}\right)^{C},$$

applying *logarithm* on both sides and solving algebraic expressions, the closed form of expression for λ_{opt} using single antenna and multiple number of CRs in CSS network is

$$\lambda_{opt}=\left(\frac{\sigma_n^2}{\Gamma(\mathrm{P})}\left(\left(N-1\right)\left(\ln\left(\frac{1-P_f}{P_m}\right)\right)+C\ln\left(1+\bar{\gamma}\right)\Big/\left(1-\left\{\frac{1}{\left(1+\bar{\gamma}\right)}\right\}^{C}\right)\right)^{1/C}\right)^{P/2} \tag{C.8}$$

Similarly, using multiple antennas (M=3) at each CR and multiple number of SUs (N) in the proposed CSS network, the closed form of expression for λ_{opt} is

$$\lambda_{opt}=\left(\frac{\sigma_n^2}{\Gamma(\mathrm{P})}\left(\left(N-1\right)\left(\ln\left(\frac{1-P_f}{P_m}\right)\right)+C\ln\left(1+\bar{\gamma}\right)\Big/\left(2\left\{\frac{\bar{\gamma}}{\left(1+\bar{\gamma}\right)}\right\}^{C}\right)\right)^{1/C}\right)^{P/2} \tag{C.9}$$

C.4. Optimization of Arbitrary Power of Received Signal (p_{opt}) in Weibull Fading using OR-Rule at FC

The closed form of expression for p_{opt} can be calculated by using Eq. (5.49);

$$\Rightarrow N\left(1-P_f\right)^{N-1}\frac{\partial P_f}{\partial p}+\left(P_m\right)^{N-1}\frac{\partial P_m}{\partial p}=0 \tag{C.10}$$

expressions for $\partial P_f / \partial p$ and $\partial P_m / \partial p$ are given by Eq.(5.71) and Eq.(5.72), substituting them in Eq. (C.10);

$$\Rightarrow N\left(1-P_f\right)^{N-1}\left(-M\left[1-\exp\left(-\left\{\frac{\lambda^{2/p}\Gamma(\mathrm{P})}{\sigma_n^2}\right\}^C\right)\right]^{M-1}\exp\left(-\left\{\frac{\lambda^{2/p}\Gamma(\mathrm{P})}{\sigma_n^2}\right\}^C\right)C\left\{\frac{\lambda^{2/p}\Gamma(\mathrm{P})}{\sigma_n^2}\right\}^{C-1}\frac{2}{p^2}\frac{\lambda^{(2/p)}\log\lambda\Gamma(\mathrm{P})}{\sigma_n^2}\right)$$

$$+N\left(P_m\right)^{N-1}\left(-M\left[1-\exp\left(-\left\{\frac{\lambda^{2/p}\Gamma(\mathrm{P})}{\sigma_n^2(1+\bar{\gamma})}\right\}^C\right)\right]^{M-1}\exp\left(-\left\{\frac{\lambda^{2/p}\Gamma(\mathrm{P})}{\sigma_n^2(1+\bar{\gamma})}\right\}^C\right)C\left\{\frac{\lambda^{2/p}\Gamma(\mathrm{P})}{\sigma_n^2(1+\bar{\gamma})}\right\}^{C-1}\frac{2}{p^2}\frac{\lambda^{(2/p)}\log\lambda\Gamma(\mathrm{P})}{\sigma_n^2(1+\bar{\gamma})}\right)=0$$

substituting *M*=1 in above Eq.and after some algebraic simplifications, above Eq. reduces to:

$$\Rightarrow\left(1-P_f\right)^{N-1}\left(\exp\left(-\left\{\frac{\lambda^{2/p}\Gamma(\mathrm{P})}{\sigma_n^2}\right\}^C\right)\right)=\left(P_m\right)^{N-1}\left(\exp\left(-\left\{\frac{\lambda^{2/p}\Gamma(\mathrm{P})}{\sigma_n^2\left(1+\bar{\gamma}\right)}\right\}^C\right)\right)\left(\frac{1}{1+\bar{\gamma}}\right)^C,$$

$$\Rightarrow\frac{\lambda^{2/p}\Gamma(\mathrm{P})}{\sigma_n^2}=\frac{\left(N-1\right)\left(\ln\left(\frac{1-P_f}{P_m}\right)\right)+C\ln\left(1+\bar{\gamma}\right)}{\left(1-\left(\frac{1}{1+\bar{\gamma}}\right)^C\right)},$$

applying *logarithm* on both sides and after simplification, the closed form of expression for an optimum value of *p* with a single antenna at each SU, multiple number of SUs (*N*), and using *OR-Rule* at FC in the proposed CSS network is

$$p_{opt}=\frac{2\ln\lambda}{\ln\left(\left(\frac{\left(N-1\right)\left(\ln\left(\frac{1-P_f}{P_m}\right)\right)+C\ln\left(1+\bar{\gamma}\right)}{\left(1-\left(\frac{1}{1+\bar{\gamma}}\right)^C\right)}\right)^{1/C}\frac{\sigma_n^2}{\Gamma(\mathrm{P})}\right)} \tag{C.11}$$

Similarly, using multiple antennas (*M*=3) at each CR and multiple number of SUs (*N*) in the proposed CSS network, the closed form of expression for p_{opt} is

$$p_{opt} = \frac{2\ln\lambda}{\ln\left(\left(\frac{(N-1)\left(\ln\left(\frac{1-P_f}{P_m}\right)\right)+C\ln\left(1+\bar{\gamma}\right)}{\left((0.5)\left(\frac{\bar{\gamma}}{1+\bar{\gamma}}\right)^{C}\right)}\right)^{1/C}\frac{\sigma_n^2}{\Gamma(\mathrm{P})}\right)} \tag{C.12}$$

C.5. Optimization of Threshold Value (λ_{opt}) in Weibull Fading using AND-Rule at FC

The closed form of expression for λ_{opt} value can be obtained by using Eq.(5.56);

$$\Rightarrow N\left(P_f\right)^{N-1}\frac{\partial P_f}{\partial\lambda}+N\left(1-P_m\right)^{N-1}\frac{\partial P_m}{\partial\lambda}=0 \tag{C.13}$$

expressions for $\partial P_f/\partial\lambda$ and $\partial P_f/\partial\lambda$ are given by Eq.(5.66) and Eq.(5.67), substituting them in Eq.(C.13) gives;

$$\begin{aligned}
&\Rightarrow N\left(P_f\right)^{N-1}\left(-\exp\left(-\left\{\frac{\lambda^{2/p}\Gamma(\mathrm{P})}{\sigma_n^2}\right\}^{C}\right)C\left\{\frac{\lambda^{2/p}\Gamma(\mathrm{P})}{\sigma_n^2}\right\}^{C-1}\frac{2\lambda^{(2/p)-1}\Gamma(\mathrm{P})}{p\sigma_n^2}\right)\\
&+N\left(1-P_m\right)^{N-1}\left(\exp\left(-\left\{\frac{\lambda^{2/p}\Gamma(\mathrm{P})}{\sigma_n^2\left(1+\bar{\gamma}\right)}\right\}^{C}\right)C\left\{\frac{\lambda^{2/p}\Gamma(\mathrm{P})}{\left(1+\bar{\gamma}\right)\sigma_n^2}\right\}^{C-1}\frac{2\lambda^{(2/p)-1}\Gamma(\mathrm{P})}{p\sigma_n^2\left(1+\bar{\gamma}\right)}\right)=0\\
&\Rightarrow\left(P_f\right)^{N-1}\left(\exp\left(-\left\{\frac{\lambda^{2/p}\Gamma(\mathrm{P})}{\sigma_n^2}\right\}^{C}\right)\right)=\left(1-P_m\right)^{N-1}\left(\exp\left(-\left\{\frac{\lambda^{2/p}\Gamma(\mathrm{P})}{\sigma_n^2\left(1+\bar{\gamma}\right)}\right\}^{C}\right)\right)\left(\frac{1}{1+\bar{\gamma}}\right)^{C},
\end{aligned} \tag{C.14}$$

applying *logarithm* on both sides and solving algebraic expressions, an optimum value of λ with a single antenna at each SU, multiple number of SUs (*N*), and using AND-Rule at FC in the proposed CSS network is

$$\lambda_{opt} = \left(\frac{\sigma_n^2}{\Gamma(\mathrm{P})} \left(\frac{(N-1)\left(\ln\left(\frac{P_f}{1-P_m} \right) \right) + C\ln\left(1+\bar{\gamma}\right)}{\left(1 - \left\{ \frac{1}{\left(1+\bar{\gamma}\right)} \right\}^C \right)} \right)^{1/C} \right)^{P/2} \tag{C.15}$$

Similarly, using multiple antennas (M=3) at each CR and multiple number of SUs (N) in the proposed CSS network, the expression for λ_{opt} is

$$\lambda_{opt} = \left(\frac{\sigma_n^2}{\Gamma(\mathrm{P})} \left(\frac{(N-1)\left(\ln\left(\frac{P_f}{1-P_m} \right) \right) + C\ln\left(1+\bar{\gamma}\right)}{\left(2\left\{ \frac{\bar{\gamma}}{\left(1+\bar{\gamma}\right)} \right\}^C \right)} \right)^{1/C} \right)^{P/2} \tag{C.16}$$

C.6. Optimization of Arbitrary Power of Received Signal (p_{opt}) in Weibull Fading using AND-Rule at FC

The closed form of expression for p_{opt} can be calculated by using Eq. (5.60);

$$\Rightarrow N\left(P_f\right)^{N-1}\frac{\partial P_f}{\partial p} + \left(1-P_m\right)^{N-1}\frac{\partial P_m}{\partial p} = 0 \tag{C.17}$$

expressions for $\partial P_m / \partial p$ and $\partial P_f / \partial p$ are given by Eq.(5.71) and Eq.(5.72), substituting them in Eq. (C.17);

$$\Rightarrow N\left(P_f\right)^{N-1}\left(-M\left[1-\exp\left(-\left\{ \frac{\lambda^{2/p}\Gamma(\mathrm{P})}{\sigma_n^2} \right\}^C \right) \right]^{M-1} \exp\left(-\left\{ \frac{\lambda^{2/p}\Gamma(\mathrm{P})}{\sigma_n^2} \right\}^C \right) C\left\{ \frac{\lambda^{2/p}\Gamma(\mathrm{P})}{\sigma_n^2} \right\}^{C-1} \frac{2}{p^2}\frac{\lambda^{(2/p)}\log\lambda\Gamma(\mathrm{P})}{\sigma_n^2} \right)$$

$$+N\left(1-P_m\right)^{N-1}\left(-M\left[1-\exp\left(-\left\{ \frac{\lambda^{2/p}\Gamma(\mathrm{P})}{\sigma_n^2(1+\bar{\gamma})} \right\}^C \right) \right]^{M-1} \exp\left(-\left\{ \frac{\lambda^{2/p}\Gamma(\mathrm{P})}{\sigma_n^2(1+\bar{\gamma})} \right\}^C \right) C\left\{ \frac{\lambda^{2/p}\Gamma(\mathrm{P})}{\sigma_n^2(1+\bar{\gamma})} \right\}^{C-1} \frac{2}{p^2}\frac{\lambda^{(2/p)}\log\lambda\Gamma(\mathrm{P})}{\sigma_n^2(1+\bar{\gamma})} \right) = 0$$

$$\Rightarrow \left(P_f\right)^{N-1}\left(\exp\left(-\left\{ \frac{\lambda^{2/p}\Gamma(\mathrm{P})}{\sigma_n^2} \right\}^C \right) \right) = \left(1-P_m\right)^{N-1}\left(\exp\left(-\left\{ \frac{\lambda^{2/p}\Gamma(\mathrm{P})}{\sigma_n^2\left(1+\bar{\gamma}\right)} \right\}^C \right) \right)\left(\frac{1}{1+\bar{\gamma}} \right)^C,$$

applying *logarithm* on both sides and solving algebraic expressions, an optimum value of *p* is

$$p_{opt} = \frac{2\ln\lambda}{\ln\left(\left(\frac{(N-1)\left(\ln\left(\frac{P_f}{1-P_m}\right)\right)+C\ln\left(1+\bar{\gamma}\right)}{\left(1-\left(\frac{1}{1+\bar{\gamma}}\right)^{C}\right)}\right)^{1/C}\frac{\sigma_n^2}{\Gamma(\mathrm{P})}\right)} \tag{C.18}$$

Similarly, using multiple antennas (*M*=3) at each CR and multiple number of SUs (*N*) in the proposed CSS network, the expression for p_{opt} is

$$p_{opt} = \frac{2\ln\lambda}{\ln\left(\left(\frac{(N-1)\left(\ln\left(\frac{P_f}{1-P_m}\right)\right)+C\ln\left(1+\bar{\gamma}\right)}{\left((0.5)\left(\frac{\bar{\gamma}}{1+\bar{\gamma}}\right)^{C}\right)}\right)^{1/C}\frac{\sigma_n^2}{\Gamma(\mathrm{P})}\right)} \tag{C.19}$$